THE INFLUENCE OF AGE AND TYPE 2 DIABETES ON CARDIOPROTECTIVE INTERVENTIONS AGAINST MYOCARDIAL ISCHAEMIA-REPERFUSION INJURY

Thesis submitted by

Hannah Jayne Whittington

BSc (Hons)

For the degree of

Doctor of Philosophy

Institute of Cardiovascular Sciences

University College London

The Hatter Cardiovascular Institute
University College London Hospital and Medical School
67 Chenies Mews, UCL
London, WC1E 6HX

June 2013

This thesis is dedicated to

my loving Nan.

DECLARATION

I, Hannah Jayne Whittington confirm that the work presented in this thesis is my own. Where information has been derived from other sources, I confirm that this has been indicated in the thesis.

Miss Hannah Whittington

ABSTRACT

The background of the thesis is based on the conflicting results between bench and bedside regarding the susceptibility to myocardial infarction with old age and diabetes. In laboratories all over the world, strategies have been developed to protect the myocardium from this insult, including the use of ischaemic conditioning (short periods of ischaemia and reperfusion prior to or following lethal ischaemia) or the use of a variety of pharmacological agents.

However, surprisingly, translating these effective cardioprotective treatments into the clinic has proved problematic. The main issue seems to be the fact that the experimental investigations have mainly used young, healthy animals while the human patients present often with a number of other risk factors, or comorbidities, such as type 2 diabetes and old age.

Therefore the aim of this thesis was to investigate the susceptibility to ischaemia-reperfusion injury and the proficiency of cardioprotective strategies to protect the heart in the setting of ageing and type 2 diabetes.

Utilizing a model of type 2 diabetes, the Goto-Kakizaki rat and its normoglycaemic control Wistar rat, within the range of 3 to 18 months of age, the Langendorff isolated heart model and in vivo coronary artery occlusion and reperfusion were employed to investigate the susceptibility to ischaemia-reperfusion injury. Mechanical or pharmacological cardioprotective strategies were also investigated in this setting and the mechanisms of the failed cardioprotection were examined further using in vitro techniques focusing on known pro survival signalling pathways within the myocardium.

The ageing diabetic heart demonstrated an increased vulnerability to injury and was less amenable to protection by ischaemic conditioning. Pharmacological agents namely, metformin and sitagliptin appear to differentially protect the diabetic and non-diabetic heart, and this could be due to the underlying intracellular changes associated with ageing and diabetes.

ACKNOWLEDGEMENTS

My sincerest thanks and appreciation go to Professor Yellon who provided me with the opportunity to undertake a PhD in his laboratory group. His continuous enthusiasm and support towards my PhD project have been invaluable.

I would like to thank my primary supervisor Dr Mihaela Mocanu for her invaluable support, guidance and encouragement. I thoroughly enjoyed my time working with her, not only did she motivate me to work hard but also to enjoy the experience, one I will always look back on fondly.

To the staff at the central biological services unit, in particular, Louise Casson, for their assistance in maintaining the ageing rat colonies and providing me with vital technical support throughout my projects.

Additionally, I would like to express my appreciation and thanks to other members of the Hatter Cardiovascular Institute. Particularly, Dr Derek Hausenloy, my tertiary supervisor, for support and providing me with numerous opportunities throughout my studies, and to Dr Andrew Hall for always being available to help with 'technical difficulties'. Thanks to Rachel for the many laughs, support and friendship. Lastly, to all of the other current and past Hatter fellows, especially Andy, Claire, Niall, Ging and Jose for making this experience an enjoyable one.

Finally, I would like to thank my parents, family and friends for their support and encouragement throughout my studies. In particular, Andy for providing me with an escape from all things science, keeping me sane and encouraging me to be the best that I can be.

LIST OF PUBLICATIONS

Whittington HJ, Harding I, Stephenson CIM, Bell R, Hausenloy DJ, Mocanu MM, Yellon DM. Cardioprotection in the aging, diabetic heart: the loss of protective Akt signaling. *Cardiovasc Res.* 2013 May 30. [Epub ahead of print]

Whittington,HJ, Hall,AR, McLaughlin,CP, Hausenloy,DJ, Yellon,DM, Mocanu,MM: Chronic Metformin Associated Cardioprotection Against Infarction: Not Just a Glucose Lowering Phenomenon. *Cardiovasc Drugs Ther*. 2013 Feb;27(1):5-16.

Whittington,HJ, Babu,GG, Mocanu,MM, Yellon,DM, Hausenloy,DJ: The diabetic heart: too sweet for its own good? *Cardiol Res Pract* 2012:845698, 2012

In Submission

Hausenloy,DJ*, **Whittington,HJ*,** Wynne, AM, Begum, SS, Theodorou, L, Riksen, N, Carr, RD, Mocanu, MM, Yellon, DM: Dipeptidyl peptidase-4 inhibitors and GLP-1 reduce myocardial infarct sizein a glucose-dependent manner. In submission to PLOS ONE. * Joint first author.

CONTENTS

DECLARATION 3

ABSTRACT 4

ACKNOWLEDGEMENTS 5

LIST OF PUBLICATIONS 6

CONTENTS 7

LIST OF FIGURES 11

LIST OF TABLES 16

LIST OF ABBREVIATIONS 17

1. INTRODUCTION 25

1.1 Myocardial ischaemia-reperfusion injury 26

1.1.1 Overview of the cardiovascular system 26

1.1.2 Myocardial Infarction 34

1.2 Mitochondria and ischaemia-reperfusion injury 38

1.2.1 Mitochondria 38

1.2.2 PGC-1α 46

1.3 Cell death pathways 53

1.3.1 Necrosis 53

1.3.2 Apoptosis 53

1.3.3 Other forms of cell death 55

1.4 Protecting the heart against ischaemia-reperfusion injury 56

1.4.1 Ischaemic Preconditioning 56

1.4.2 Protective effect of IPC at reperfusion 60

1.4.3 Clinically relevant conditioning strategies 61

1.5 Diabetic heart and Ischaemia-reperfusion Injury 62

1.5.1 Diabetes Mellitus 62

1.5.2 The diabetic heart 66

1.5.3 Susceptibility of the diabetic heart to ischaemia-reperfusion injury 71

1.5.4 Protecting the diabetic heart against ischaemia-reperfusion injury 80

1.6 Ageing heart and ischaemia-reperfusion injury 91

1.6.1 Ageing and the cardiovascular system 91

1.6.2 Ischaemia-reperfusion injury in the aged heart 96

1.6.3 Protection against infarction in the aged heart 98
1.7 Ageing and diabetes in myocardial ischaemia-reperfusion injury 102
1.7.1 Hypotheses and aims 102
2. GENERAL METHODS 104
2.1 Animals 105
2.1.1 Animal models of Diabetes 105
2.1.2 Biological parameters 108
2.2 Assessment of Infarction using ex vivo and in vivo models 108
2.2.1 Langendorff model of retroperfused isolated heart 108
2.2.2 In vivo coronary artery occlusion/2 hour reperfusion (non-recovery model) 118
2.2.3 In vivo coronary artery occlusion/reperfusion (recovery model) 120
2.2.4 Infarct size determination 121
2.3 Characterisation of the Langendorff isolated heart model 124
2.3.1 Introduction 124
2.3.2 Experimental protocol 124
2.3.3 Infarct size in Sprague Dawley rats: reperfusion time and assessment of ischaemic preconditioning 126
2.4 Isolated adult cardiomyocytes 128
2.4.1 Introduction 128
2.4.2 Standard Isolation protocol 128
2.4.3 Isolation of cardiomyocytes from old, diabetic rat hearts 130
2.5 Western Blot Analysis to detect protein expression or activation status 131
2.5.1 Introduction 131
2.5.2 Extraction and quantification of protein samples 132
2.5.3 Gel electrophoresis 134
2.5.4 Transfer of proteins from the gel to a membrane support 135
2.5.5 Membrane blocking and antibody incubation 136
2.5.6 Protein detection using enhanced chemiluminescence (ECL) 136
2.6 Immunoprecipitation 137
2.6.1 Preparation of lysates from heart tissue 137
2.6.2 Immunoprecipitation 138
2.7 Biochemical assays 139
2.7.1 Measurements of intracellular ATP in heart tissue 139
2.7.2 Measurement of free radicals in heart tissue 141
2.8 Electron Microscopy imaging of mitochondria 142
2.8.1 Sample collection and preparation 142
2.8.2 Assessment of structure and organisation of mitochondria 142

2.9 Statistical Analysis 142

3. ISCHAEMIA-REPERFUSION INJURY IN AGEING AND DIABETIC HEARTS 143

3.1 Susceptibility to infarction in ageing and diabetes 144

3.1.1 Introduction: The old diabetic heart and myocardial infarction 144

3.1.2 Hypothesis and aim 144

3.1.3 Experimental Protocols 145

3.1.4 Results 146

3.1.5 Summary of results 160

3.2 Is ischaemic preconditioning possible in the aged, diabetic heart? 161

3.2.1 Introduction 161

3.2.2 Hypothesis and aim 161

3.2.3 Experimental protocols 162

3.2.4 Results 162

3.2.5 Summary of Results 169

3.3 Signalling defects in the ageing and diabetic heart 170

3.3.1 Introduction 170

3.3.2 Hypothesis and aim 172

3.3.3 Experimental Protocols 172

3.3.4 Results 174

3.3.5 Summary of Results 182

3.4 Discussion 182

3.4.1 Relevance of study 182

3.4.2 The activation of Akt in the myocardium – a double edged sword? 183

3.4.3 Is there a link between chronic Akt activation, PGC-1α and antioxidant defence? 184

3.4.4 Is IPC possible in the aged, diabetic heart? 186

3.5 Conclusion 187

4. PHARMACOLOGICAL CARDIOPROTECTION AGAINST ISCHAEMIA-REPERFUSION INJURY IN AGEING AND DIABETES 189

4.1 The effect of chronic metformin treatment in aged, diabetic rats 190

4.1.1 Background 190

4.1.2 Hypothesis 192

4.1.3 Experimental Protocols 193

4.1.4 Results 198

4.1.5 Summary and Discussion 215

4.1.6 Conclusion 221

4.2 Sitagliptin and cardioprotection 223
4.2.1 Background 223
4.2.2 Hypothesis 225
4.2.3 Experimental Protocols 225
4.2.4 Results 226
4.2.5 Summary and Discussion 229
4.3 Conclusion 232
5. OVERALL DISCUSSIONS 233
5.1 General conclusions 234
5.2 Limitations 235
5.3 Future directions 237

LIST OF FIGURES

Figure 1.1: Typical ECG trace with accompanying changes in the electrical activity and ventricular movements with the heart during contraction. 27

Figure 1.2: Diagrammatic representation of the main vessels that constitute the coronary circulation within the heart. 28

Figure 1.3: The glycolytic pathway 29

Figure 1.4: The fate of glucose is dependent on the availability of oxygen 30

Figure 1.5: Fatty acids as a substrate for energy production 30

Figure 1.6: Ischaemic injury 35

Figure 1.7: Reperfusion injury. 36

Figure 1.8: The control of mitochondrial biogenesis. 39

Figure 1.9: The Krebs cycle. 40

Figure 1.10: Oxidative Phosphorylation. 41

Figure 1.11: Structure of the mitochondrial permeability transition pore (mPTP). 46

Figure 1.12: PGC-1α coactivation of transcription factors. 48

Figure 1.13: The key functional domains involved in the interaction of PGC-1α with transcription factors 49

Figure 1.14: Transcriptional targets of PGC-1α. 49

Figure 1.15: Post translational modifications of PGC-1α 51

Figure 1.16: Apoptotic cell death pathways. 55

Figure 1.17: Activation of the PI3K/Akt pathway. 58

Figure 1.18: Downstream targets of Akt-P 59

Figure 1.19: The cellular mechanisms involved in ischaemic preconditioning 60

Figure 1.20: Blood glucose regulation. 63

Figure 1.21: Regulation of circulating blood glucose. 64

Figure 1.22: The generation of superoxide and reactive oxygen species. 67

Figure 1.23: Energy metabolism in the diabetic heart. 71

Figure 1.24: Possible intracellular changes within the diabetic heart. 74

Figure 1.25: Structure, function and activation of AMPK. 84

Figure 1.26: The incretin effect. 88

Figure 1.27: Targets for dipeptidyl peptidase-4 (DPP-4) degradation. 89

Figure 1.28: Molecular and cellular changes in ageing cardiomyocytes 96

Figure 1.29: The main processes that are suggested to contribute to enhanced damage caused by ischaemia-reperfusion injury in the ageing heart. 97

Figure 1.30: Cardioprotection in the ageing heart. 101

Figure 2.1: Schematic representation of retrograde perfusion of the heart. 109

Figure 2.2: Constant pressure Langendorff system controlled by Peristaltic pump.... 111

Figure 2.3: Reference points used to ensure suture is placed surrounding the left anterior descending coronary artery (LAD) 115

Figure 2.4: Surgical steps for In vivo coronary artery occlusion/ reperfusion model. . 119

Figure 2.5: Typical ECG changes during ischaemia-reperfusion model. 120

Figure 2.6: Evans blue staining at the end of reperfusion..... 122

Figure 2.7: Heart slicing and infarct staining. 123

Figure 2.8: Langendorff experimental protocols. 125

Figure 2.9: Area at risk (AAR) in isolated Sprague-Dawley rat hearts subjected to ischaemia-reperfusion protocols. 127

Figure 2.10: Comparison of reperfusion times in isolated hearts isolated from Sprague-Dawley rats subjected to either sham or control protocols. 127

Figure 2.11: Comparison of reperfusion times in isolated hearts from Sprague-Dawley rats subjected to control or ischaemic preconditioning (IPC) protocols..... 128

Figure 2.12: Typical protein standard curve using a BCA assay 133

Figure 2.13: Illustration of immunoprecipitation process..... 139

Figure 2.14: Illustration of reaction of luciferase in presence of ATP 140

Figure 2.15: Typical ATP standard curve 140

Figure 2.16: Illustration of how fluorescence is produced in response to reactive oxygen/nitrogen species 141

Figure 3.1: Scheme of Langendorff experiments performed. 146

Figure 3.2: Blood Glucose and HbA1c levels in ageing and diabetic rats. 147

Figure 3.3: Heart to body weight ratio in ageing diabetic and non-diabetic rats. 148

Figure 3.4: Cardiac function assessment in the diabetic heart subjected to 20 min ischaemia/ 60 min reperfusion. 150

Figure 3.5: Cardiac function assessment in the diabetic heart subjected to 35 min ischaemia/ 60 min reperfusion. 152

Figure 3.6: Cardiac function assessment in the non-diabetic heart subjected to 20 min ischaemia/ 60 min reperfusion. 153

Figure 3.7: Cardiac function assessment in the non-diabetic heart subjected to 35 min ischaemia/ 60 min reperfusion. 155

Figure 3.8: Comparison of RPP in the diabetic versus non-diabetic heart. 156

Figure 3.9: Comparison of RPP in the diabetic and non-diabetic heart subjected to either 20 min or 35 min ischaemia followed by reperfusion. 157

Figure 3.10: The variations in susceptibility to ischaemia with age and diabetes (GK rats). 159

Figure 3.11: The variations in the susceptibility to ischaemia with age (Wistar rats).. 159

Figure 3.12: Scheme of Langendorff experiments performed. 162

Figure 3.13: Recovery of function following ischaemia-reperfusion 163

Figure 3.14: Recovery of function following ischaemia-reperfusion in the non-diabetic heart. 164

Figure 3.15: Recovery of function following ischaemia-reperfusion in the diabetic heart. 165

Figure 3.16: Recovery of function following IPC prior to ischaemia-reperfusion in the non-diabetic heart 166

Figure 3.17: Recovery of function following IPC prior to ischaemia-reperfusion in the diabetic heart. 167

Figure 3.18: The effectiveness of Ischaemic Preconditioning (IPC) on infarct size reduction in the setting of ageing in normoglycaemic Wistar hearts. 168

Figure 3.19: The effectiveness of Ischaemic Preconditioning (IPC) on infarct size in the setting of ageing and type 2 diabetes. 169

Figure 3.20: Scheme of collection of samples using the Langendorff apparatus. 173

Figure 3.21: Phosphorylation of Akt in the diabetic heart. 174

Figure 3.22: Phosphorylation of Akt in the non-diabetic heart. 175

Figure 3.23: PGC-1α expression in the diabetic heart. 176

Figure 3.24: PGC-1α expression in the non-diabetic heart. 176

Figure 3.25: Catalase expression in the diabetic GK heart. 177

Figure 3.26: Oxidative stress levels in the ageing, diabetic heart. 178

Figure 3.27: Catalase expression in the non-diabetic Wistar heart. 178

Figure 3.28: Oxidative stress levels in the ageing, non-diabetic heart. 179

Figure 3.29: Mitochondrial appearance and organisation in the aged and diabetic heart. 180

Figure 3.30: Phosphorylation of Akt following IPC in young and old diabetic rat hearts. 181

Figure 3.31: Phosphorylation of Akt following IPC in young and old non-diabetic rat hearts. 181

Figure 3.32: Possible consequences of the chronically activated RISK kinase Akt, in the aged, diabetic heart. 188

Figure 4.1: Experimental groups and Langendorff experimental protocol. 194

Figure 4.2: Treatment scheme for HL-1 cells. 196

Figure 4.3: Treatment scheme for HL-1 cells. 197

Figure 4.4: Treatment organisation for isolated cardiomyocytes. 198

Figure 4.5: The effect of chronic metformin treatment on infarct size in the Wistar and GK rat. 201

Figure 4.6: Cardiac function assessment following chronic metformin treatment in the Wistar (non-diabetic) and Goto-Kakizaki (GK, diabetic) heart. 202

Figure 4.7: The effect of chronic metformin treatment on AMPK expression and phosphorylation. 203

Figure 4.8: The effect of chronic metformin treatment on Akt expression and phosphorylation. 204

Figure 4.9: The effect of chronic metformin treatment on PGC-1α expression in the diabetic heart. 205

Figure 4.10: The effect of chronic metformin treatment on Mfn-2 expression in the diabetic heart. 206

Figure 4.11: The effect of metformin treatment on mitochondrial appearance in the diabetic heart. 207

Figure 4.12: The effect of metformin treatment on the subcellular localisation of PGC-1α. 208

Figure 4.13: The effect of chronic metformin treatment on basal ATP levels in the diabetic Goto-Kakizaki (GK) rat heart. 209

Figure 4.14: Characterisation of the effectiveness of Compound C in blocking the action of metformin on AMPK activation in HL-1 cells. 210

Figure 4.15: Characterisation of the effectiveness of Compound C in blocking the action of metformin on ACC activation in HL-1 cells. 210

Figure 4.16: AMPK activation following 16 hours metformin treatment in HL-1 cells. 211

Figure 4.17: PGC-1α expression following 16 hours metformin treatment in HL-1 cells. 211

Figure 4.18: Mfn-2 expression following 16 hours metformin treatment in HL-1 cells. 212

Figure 4.19: Plating of isolated cardiomyocytes. 212

Figure 4.20: AMPK activation following 16 hours metformin treatment in isolated cardiomyocytes from the 12 month diabetic GK hearts. 213

Figure 4.21: PGC-1α expression following 16 hours metformin treatment in isolated cardiomyocytes from the 12 month diabetic GK hearts. 214

Figure 4.22: Assessment of Mfn-2 expression following 16 hours metformin treatment in isolated 12 month diabetic GK cardiomyocytes. 215

Figure 4.23: The effect of chronic metformin treatment in type 2 diabetic rats. 222

Figure 4.24: The influence of glucose levels on sitagliptin induced cardioprotection in the isolated heart. 224

Figure 4.25: The influence of glucose levels on GLP-1 induced cardioprotection in the isolated heart. 224

Figure 4.26: The effect of different concentrations of glucose on infarct size. 225

Figure 4.27: Basal blood glucose levels in non-diabetic and diabetic rats. 227

Figure 4.28: Summary of blood glucose measured before and after administration of sitagliptin or control. 228

Figure 4.29: The effect of Sitagliptin treatment on infarct size in the young Wistar, and middle-aged Wistar and GK rats. 229

LIST OF TABLES

Table 1.1: Studies indicating the diabetic heart is more sensitive to ischaemic injury compared to normoglycaemic controls..... 76

Table 1.2: Studies indicating the diabetic heart is less sensitive to ischaemic injury compared to normoglycaemic controls..... 78

Table 1.3: Studies indicating no difference in the sensitivity of the diabetic heart to ischaemic injury compared to normoglycaemic controls..... 80

Table 1.4: The life expectancy of laboratory animals 98

Table 2.1: The rat's age in months and its relationship with human age in years 107

Table 2.2: Krebs and Henseleit (KHB) physiological salt solution composition..... 112

Table 2.3: Exclusion criteria for rat Langendorff experiments..... 117

Table 2.4: Advantages and disadvantages of the Langendorff isolated heart preparation 118

Table 2.5: Composition of the stock perfusion solution required for isolation of cardiomyocytes..... 129

Table 2.6: Additional components to be added to each specific stock perfusion solution on day of isolation..... 129

Table 2.7: Additional components to be added to stock perfusion solution on day of isolation 131

Table 2.8: The adjustment of samples to give equal protein concentrations within in sample..... 133

Table 2.9: Composition of SDS-PAGE gels 135

Table 2.10: Lysis buffer compositions..... 138

Table 3.1: Summary of biological parameters. 148

Table 4.1: Summary of metformin treatment in Goto-Kakizaki rats. 199

Table 4.2: Summary of metformin treatment in Goto-Kakizaki rats. 200

Table 4.3: The effect of sitagliptin treatment on body weight..... 227

LIST OF ABBREVIATIONS

°C - degrees Celsius

µl - microliter

$^{\bullet}O_2^-$ - superoxide

$^{\bullet}OH^-$ - hydroxyl radical

ΔpH - proton electrochemical gradient

$\Delta\psi_m$ - membrane potential

AAR - area-at-risk

ACC - acetyl-coenzyme A carboxylase

ACE-I - angiotensin-converting enzyme inhibitors

ADP - adenosine diphosphate

AGE - advanced glycation end-product

AICAR - 5-aminoimidazole-4-carboxamide-1-b-d-ribofuranoside

Akt - protein kinase B

AMI - acute myocardial infarction

AMP - adenosine monophosphate

AMPD - adenosine monophosphate deaminase

AMPK - adenosine monophosphate kinase

ANOVA - analysis of variance

ANP - atrial natriuretic peptide

ANT - adenine nucleotide translocase

Apaf-1 - apoptotic protease activating factor-1

AT1 - Angiotensin II receptor type 1

ATP - adenosine triphosphate

AV Node - Atrio-Ventricular node

BAD - BCL-2 associated death promoter

BAK - BCL-2 antagonist protein

BAX - BCL-2 associated X protein

BCA - bicinchoninic acid

BCL-2 - B cell lymphoma 2

BCL-xL - B cell lymphoma-extra large

BH_4 - tetrahydrobiopterin

BID - BH3 interacting-domain death agonist

BK - bradykinin

BK-2R - bradykinin 2 receptor

BNP - B-type natriuretic peptide

BSA - bovine serum albumin

Bz - benzodiazepine

Ca^{2+} - calcium ion

CABG - coronary artery bypass grafting

CaMKK - calmodulin dependent protein kinase kinase

cAMP - cyclic adenosine monophosphate

CF - coronary flow

CHD - coronary heart disease

CK-MB - creatine kinase myocardial band

CL - cardiolipin

Clk-2 - CDC-like kinase 2

CNS - central nervous system

CO_2 - Carbon dioxide

CoA - coenzyme A

CPT-1 - carnitine palmitoyl transferase 1

CPT-2 - carnitine palmitoyl transferase 2

CREB - cAMP response element binding protein

CsA - cyclosporin A

Cu^{2+} - copper ion

CuSOD - copper superoxide dismutase

CV - Cardiovascular

CVD - cardiovascular disease

Cx43 - connexion 43

CypD - cyclophillin D

Cyt c - cytochrome c

DCFH-DiOxyQ - dichlorodihydrofluorescin DiOxyQ

DIL - death-inducing ligands

DIO - diet-induced obesity rat

DISC - death inducing signalling complex

DNA - deoxyribonucleic acid

DPP-4 - dipeptidyl peptidase-4 enzyme

$DPP\text{-}4^{-/-}$ - dipeptidyl peptidase-4 knock out

DRP-1 - dynamin-related protein 1

ECG - electrocardiogram

ECL - enhanced chemiluminescence

EM - electron microscope/microscopy

eNOS - endothelial nitric oxide synthase

EPO - erythropoietin

ER - endoplasmic reticulum

ERK1/2 - extracellular signal related kinases 1 and 2

ERRs - estrogen-related receptors

ERR-α - estrogen-related receptor-alpha

ERR-γ - estrogen-related receptor-gamma

ETC - electron transport chain

F_0F_1ATP synthase - complex V of the electron transport chain

FAD^+ - flavin adenine dinucleotide (oxidised form)

FADH/$FADH_2$ - flavin adenine dinucleotide (reduced form)

FAO- fatty acid oxidation

FAT/CD36 - fatty acid translocase/transporters

FoxO1 - forkhead box class-O1

FOXO3a - forkhead box class-O3a

g - grams

GABA - gamma-aminobutyric acid

$GABA_A$ R - gamma-aminobutyric acidA receptor

GCN5 - histone acetyltransferase KAT2A

GFAT - glutamine:fructose 6-phosphate amidotransferase

GIP - glucose-dependent insulinotropic polypeptide

GK - Goto-Kakizaki

GLP-1 - glucagon-like peptide-1

GLP-1 (7-36) - isoform of glucagon-like peptide-1

GLP-1 (9-36) - metabolite of GLP-1 (7-36)

GLP-1(7-37) - isoform of glucagon-like peptide-1

GLUT-1 - glucose transporter-1

GLUT-1 TG - glucose transporter-1 transgenic mice

GLUT-2 - glucose transporter 2

GLUT-4 - glucose transporter 4

GPCR - G protein coupled receptor

GPx - gluthathione peroxidase

GSH - gluthathione

GSK-3 - glycogen synthase kinase 3

GSK-3β - glycogen synthase kinase-3β

GTP - guanosine triphosphate

h - hours

H^+ - hydrogen ion/proton

H_2O - water

H_2O_2 - hydrogen peroxide

HAT - histone acetyletransferase

HbA1c - glycated haemoglobin A

HDAC - class II histone deactylases

HDL - high density lipoprotein

HFD - high-fat diet induced insulin resistance syndrome rat

hfis1 - human mitochondrial fission protein 1

HIF-1α - hypoxic inducible factor-1α

HK - hexokinase

HMG-CoA - 3-hydroxy-3-methylglutaryl-coenzyme A

HR - heart rate

HRP - horse radish peroxidase

HW/BW% - heart weight to body weight percentage

I.P. - intraperitoneal

I/R% - infarct to risk zone ratio

IFM - interfibrillar mitochondria

IGF-1 - insulin-like growth factor 1

IHD - ischaemic heart disease

IL-6 - interleukin-6

IMAC - inner membrane anion channel

IMM - inner mitochondrial membrane

IP - immunoprecipitation

IPC - ischaemic preconditioning

IPost - ischaemic post conditioning

IR - ischaemia-reperfusion

IRI - ischaemia-reperfusion injury

IRS - insulin receptors

IU - international units

JAK - janus kinase

K^+ - potassium channel

K_{ATP} channel - ATP-sensitive K+ channel

KC - Krebs cycle

K_{Ca} - calcium gated potassium channel

kg - kilograms

KHB - Krebs Henseleit Buffer

L - litre

LAD - left anterior descending coronary artery

LDL - low density lipoprotein

LKB-1 - tumour repressor protein (also known as STK11)

LVDP - left ventricular developed pressure

LVEDP - left ventricular end diastolic pressure

LVEF - left ventricular ejection fraction

LVH - left ventricular hypertrophy

M - molar

MAPK - mitogen-activated protein kinase

MCP-1 - monocyte chemoattractant protein-1

MEF-2 - myocyte enhancing factor-2

MEK1/2 - mitogen-activated protein kinase 1/2

Mfn1/2 - mitofusin 1/2

Mg - milligrams

Mg^{2+} - magnesium

MHC - myosin heavy chain

MI - myocardial infarction

Min - minute

mM - millimolar

mm/Hg - millimeter of mercury

mmol/L - millimole per litre

mmol/mol - millimole per mole

MnSOD - manganese superoxide dismutase

MOA - monoamine oxidase

MOMP - mitochondrial outer membrane permeabilisation

MPG - N-2-mercaptopropionyl glycine

mPTP - mitochondrial permeability transition pore

mtDNA - mitochondrial DNA

MVO - microvascular obstruction

n - number of subjects/samples

Na^+/HCO_3 - symporter- sodium/hydrogen carbonate symporter

Na^+/K^+-ATPase - sodium/potassium ATPase

Na^+ - sodium ion

NAD^+ - nicotinamide adenine nucleotide (oxidised form)

NADH - nicotinamide adenine nucleotide (reduced form)

NADPH - nicotinamide adenine dinucleotide phosphate

NAM - Nicotinamide

Nampt - nicotinamide phosphoribosyltransferase

NCX - sodium/calcium exchanger

NFκB - nuclear factor κ B

NO - nitric oxide

NOD - non-obese diabetic mice

NPY - neuropeptide Y

NR - nuclear receptor

Nrfs - nuclear respiratory factors

NS - non significant

NTFs - nuclear transcription factors

O_2 - Oxygen

O-GlcNAcylation - O-linked N-acetyl-glucosamine glycosylation

OGT - O-linked N-acetylglucosamine

OLETF - Otsuka Long Evans Tokushima Fatty rat

OMM - outer mitochondrial membrane

$ONOO^-$ - peroxynitrite

Opa1 - optic atrophy protein 1

P - phosphate

P160MBP - p160 myb binding protein

$p47^{phox}$ - subunit of NAPDH oxidase

p53 - protein 53/tumour protein 53

$p66^{shc}$ - 66kDa isoform of the growth factor adapter Shc

p85 - protein 85

PBS - phosphate buffered saline

PCI - percutaneous coronary intervention

PDK-1 - phosphoinositide-dependent protein kinase-1

PGC-1 – PPARγ coactivator-1

PGC-1α - peroxisome proliferator –activated receptor γ co-activator 1 α

PGC-1β - peroxisome proliferator –activated receptor γ co-activator 1 β

P_i - inorganic phosphate

PI3K - phosphatidylinositol-3-kinase

PIP_2 - phosphatidylinositol-3,4-biphosphate

PIP_3 - phosphatidylinositol-3,4,5-triphosphate

PKA - protein kinase A

PKC - protein kinase C

PKC-β - protein kinase C –β isoform

PKCε - protein kinase C epsilon

PKG - protein kinase G

PPARα - peroxisome proliferator-activated receptor alpha

PPARβ - peroxisome proliferator-activated receptor beta

PPARγ - peroxisome proliferator-activated receptor gamma

PPIase - prolyl isomerase

PRC - PGC-1-related coactivator

PRMT-1 - protein arginine N-methyltransferase 1

PTEN - Protein phosphatase and tensin homolog deleted on chromosome 10

PVDF - polyvinylidene fluoride

RIC - remote ischaemic conditioning

RIPA - RadioImmunoPrecipitation Assay

RISK - reperfusion injury salvage kinase

RNS - reactive nitrogen species

ROS - reactive oxygen species

Rpm - revolutions per minute

RPP - rate pressure product

RTKs - receptor tyrosine kinases

SA Node - Sinoatrial node

SAFE - survival activating factor enhancement

SD - Sprague dawley rat

SDF-1α - stromal cell-derived factor 1α

SDS-PAGE - sodium dodecyl sulphate polyacrylamide gel electrophoresis

SEM - standard error of the mean

SERCA - Calcium sarcoplasmic reticulum pump

SIRT-1 - silence information regulator of transcription -type 1

SOD - superoxide dismutase

SR - sarcoplasmic reticulum

SRC-1 - steroid receptor co-activator-1

SSM - subsarcolemmal mitochondria

STAT3 - signal transducer and activator of transcription 3

STZ - streptozotocin

SWOP - second window of cardioprotection

T2D - type 2 diabetes

Tfam - mitochondrial transcription factor A

TNF - tumor necrosis factor

TRAIL - TNF-related apoptosis-inducing ligands

TRAP/DRIP - thyroid hormone receptor-associated protein/vitamin D receptor-interacting protein

TSPO - translocator protein

TTC - triphenyltetrazolium chloride

UCP - uncoupling protein

UKPDS - United Kingdom Prospective Diabetes Study

VDAC - voltage-dependent anion channel

VEGF - vascular endothelial growth factor

ZDF - zucker diabetic fatty

ZnSOD - zinc superoxide dismutase

1. INTRODUCTION

1.1 Myocardial ischaemia-reperfusion injury

1.1.1 Overview of the cardiovascular system

The cardiovascular (CV) system is highly adapted to efficiently transport vital nutrients and remove metabolic waste in order to ensure the viability of tissues. Hence, any disruption to this process can lead to detrimental outcomes. The heart is a very specialized muscle, with high energy demands necessary for its continuous activity. To appreciate the consequences of a malfunctioned cardiovascular system, it is important to highlight some crucial aspects of the intricate regulation required for an accurate cardiovascular physiology.

1.1.1.1 The control of myocardial contraction

Specialised cells within cardiac muscle initiate an electrical signal in the Sinoatrial (SA) node located in the intra-atrial septum, which propagates through the atrial walls triggering synchronous atrial contraction. Subsequently, electrical activity diffuses to the Atrio-Ventricular (AV) node, through the bundle of HIS and Purkinje fibres, causing simultaneous ventricular contraction and cardiac systole. Contraction of the right ventricle propels deoxygenated blood under low pressure via the pulmonary circulation to the lungs. Whereas, concurrent contraction of the left ventricle promotes a high pressure movement of oxygenated blood through the systemic circulation to peripheral tissues. Following ventricular contraction, both the atrial and ventricular chambers relax and enter cardiac diastole, whereby venous blood enters the right atrium via the superior and inferior vena cava and flows through the tricuspid valve into the right ventricle. Blood entering the left atrium via the pulmonary veins, passes through the mitral valve into the left ventricle [1].

The electrical activity of the heart is visualised by healthcare professionals by an electrocardiogram (ECG) and a typical ECG is shown in Figure 1.1. Many clinical problems can often be detected by specific irregularities in ECG.

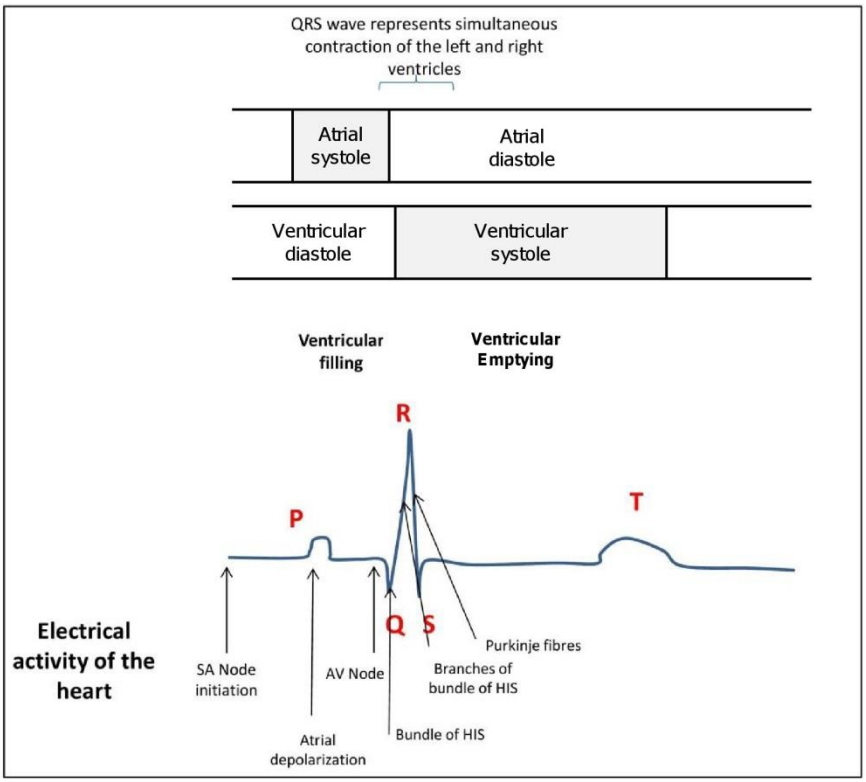

Figure 1.1: Typical ECG trace with accompanying changes in the electrical activity and ventricular movements with the heart during contraction

A complex vascular system ensures that the heart's very high energy demands are met. Coronary arteries provide oxygenated blood to, and coronary veins remove deoxygenated from, the myocardium. The major vessels of the coronary circulation include the left main coronary artery that divides into the left anterior descending coronary artery (LAD) and circumflex branch, and the right main coronary artery. Both vessels originate at the coronary ostia located at the base of the aorta behind the aortic valve leaflets. Blood flow is distributed via these vessels to different regions of the heart, with the left main coronary artery and subsequently the LAD providing blood to the left ventricle (Figure 1.2). The specialised anatomy of the coronary circulation means that each region of the heart is only supplied by one artery, therefore blockade of an artery and subsequent ischaemia can be extremely detrimental. The cardiac veins redistribute deoxygenated blood to the right atrium through the coronary sinus and contain valves to ensure the unidirectional flow of blood. The main coronary veins are the coronary sinus, the anterior interventricular veins, left marginal veins, posterior veins of the left ventricle, and the posterior interventricular veins [1].

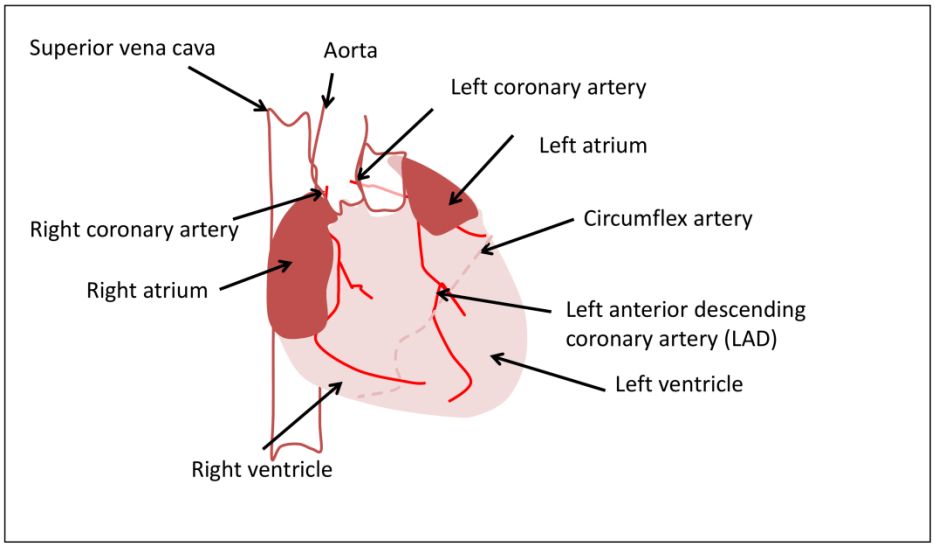

Figure 1.2: Diagrammatic representation of the main vessels that constitute the coronary circulation within the heart. The left anterior descending coronary artery (LAD) supplies the left ventricle with blood.

1.1.1.2 Cardiac energy metabolism

Production and utilization of adenosine triphosphate (ATP) is obligatory for ion homeostasis, contraction of sarcomeres, and to maintain basal metabolic processes within the heart[2]. The ratio between production and utilization is exquisitely regulated to ensure myocardial metabolism is modulated to meet the demand of ATP required. The majority of ATP, approximately 95% is produced via oxidative phosphorylation in the mitochondria, with the remaining 5% derived from glycolysis and ATP formation from the Krebs cycle. These processes are described in more detail later.

Energy metabolism is intricately controlled. The conversion of glucose into pyruvate via a set of cytosolic enzymes constitutes the glycolytic pathway (Figure 1.3). The eventual fate of pyruvate is dependent on the availability of O_2. In the absence of O_2, one glucose molecule is converted into two pyruvate molecules yielding 2 ATP molecules and lactic acid. However, in the presence of O_2, the pyruvate formed in glycolysis can be transferred into the mitochondria and interact with coenzyme A (CoA) to form acetyl CoA and CO_2 (Figure 1.4).

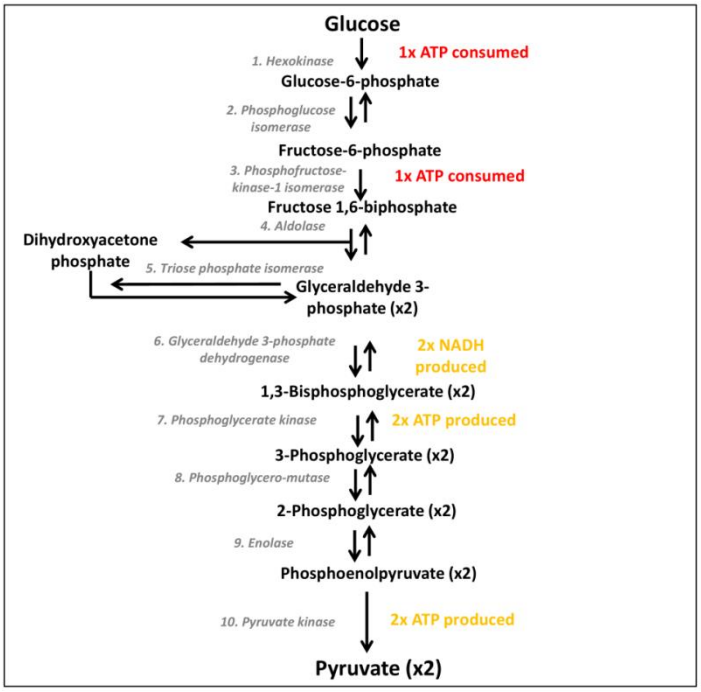

Figure 1.3: The glycolytic pathway. One molecule of glucose is converted to two molecules of pyruvate via a 10 enzyme catalysed steps. Two molecules of ATP are produced per glucose molecule.

Fatty acids released into the blood stream from triacylglycerol fat stores are taken up and utilized by the heart as the main source of ATP. Fatty acids enter a cell via fatty acid protein transporters on the cell surface namely fatty acid translocase (FAT/CD36). Once inside the cytosol, a CoA group is added to the free fatty acid by fatty acyl-CoA synthase to form a fatty acyl CoA molecule. Fatty acyl CoA molecules cannot pass through the inner mitochondrial membrane so it is transformed by carnitine palmitoyl transferase 1 (CPT-1) to acylcarnitine. An exchange transporter protein located on the inner mitochondrial membrane exchanges cartinine for acylcarnitine allowing entry into the mitochondria. Acylcarnitine reacts with CoA via carnitine palmitoyl transferase 2 (CPT-2), reforming as a fatty acyl CoA molecule in the mitochondria[3]. Each molecule of fatty acyl CoA enters the fatty acid β-oxidation pathway to form acetyl CoA and a shortened acyl CoA molecule. Oxidation of a fatty acyl CoA molecule is repeated until an even number of carbon atoms are completely converted to acetyl CoA. For example, an 18-carbon free fatty acid would yield nine molecules of acetyl CoA (Figure 1.5).

Acetyl CoA derived from either a carbohydrate or fatty acid source enter the Krebs cycle and generate electrons for entry into the electron transport chain (ETC), stimulating oxidative phosphorylation within the mitochondria. The structure and importance of energy production from within the mitochondria is discussed in further detail later.

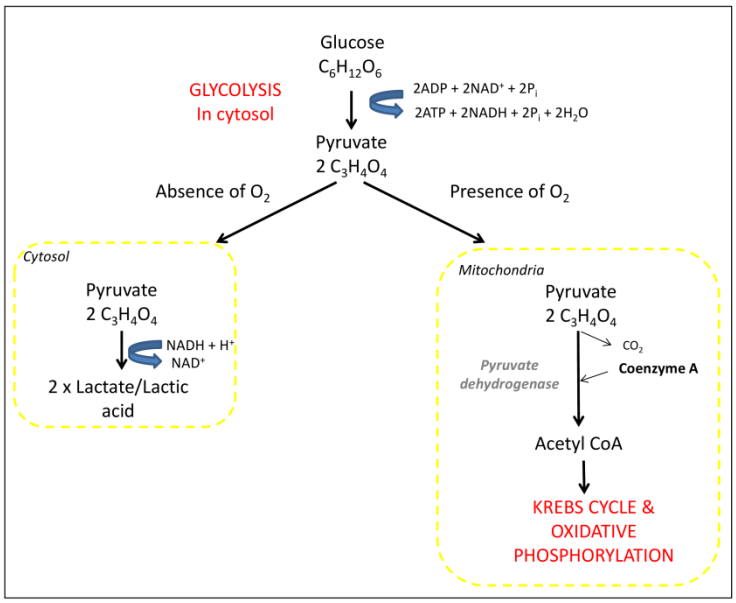

Figure 1.4: The fate of glucose is dependent on the availability of oxygen. One molecule of glucose is converted into two molecules of pyruvate via glycolysis in the cytosol. In the absence of oxygen, pyruvate is converted into lactate. In the presence of oxygen, pyruvate enters the mitochondria and is converted by pyruvate dehydrogenase and reacts with Coenzyme A to form acetyl CoA. Acetyl CoA can enter the Krebs cycle and provides the substrates for oxidative phosphorylation.

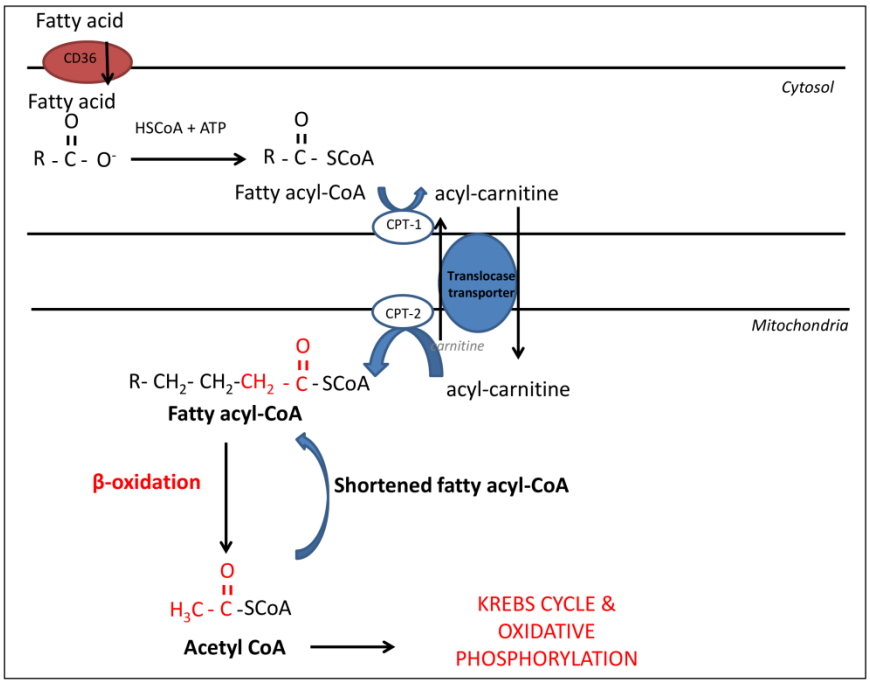

Figure 1.5: Fatty acids as a substrate for energy production. Circulating free fatty acids enter the cytosol via fatty acid transporters on the cell surface. Fatty acids are converted to fatty acyl-CoA and transformed into acyl-carnitine by carnitine palmitoyl transferase 1 (CPT-1), transferred across the membrane and converted into fatty acyl-CoA by carnitine palmitoyl transferase 2 (CPT-2). Each fatty acyl-CoA molecule undergoes β-oxidation forming acetyl CoA. Acetyl CoA can enter the Krebs cycle and provides the substrates for oxidative phosphorylation.

1.1.1.3 Cardiovascular disease

The term cardiovascular disease (CVD) spans all diseases of the heart and circulatory system. There are four main types of atherosclerotic CVD: coronary heart disease, stroke, peripheral arterial disease and aortic disease. All four have a general common phenotype whereby blood flow is reduced to the heart, brain or peripheral organs usually via an obstruction in the vasculature. This obstruction can be caused by the formation of a blood clot within a blood vessel known as thrombosis or the accumulation of fatty deposits inside an artery, causing narrowing and hardening of that vessel, known as atherosclerosis. Other CVDs include congenital heart disease, rheumatic heart disease, cardiomyopathies and cardiac arrhythmias[4].

Coronary heart disease (CHD) also known as ischaemic heart disease (IHD), is a debilitating and life threatening illness, that has become one of the leading causes of death in the UK. IHD is characterized by a reduction in blood supply to the heart muscle leading to a decreased delivery of vital components such as oxygen and nutrients to the tissue. This reduction in blood flow is attributed to a blockade in the coronary arteries of the heart, which carry oxygen-rich blood to the muscle. These blockages are plaques that have built up inside coronary arteries and can consist of numerous factors including fat and cholesterol along with other substances present in the blood. Without sufficient oxygen delivered to the heart, the muscle cells become ischaemic, eventually leading to cell death. This phenomenon is known as myocardial infarction (MI)[4]. The inability of the myocardium, which is an irreversibly differentiated tissue, to repair itself leads to an infiltration of inflammatory mediators. Lymphocytes, neutrophils and macrophages remove and replace dead cardiomyocytes with collagen deposits which lead to scar formation. Cardiac muscle efficiency is therefore compromised and can progress into heart failure[5].

Atherosclerotic plaques can take numerous years to develop and often go unnoticed until it is too late. The rate at which they develop often depend on lifestyle choices (smoking, exercise) but also can be influenced by a person's inherited genetic background. There are many so called risk factors that have been shown to increase a person's susceptibility to IHD, these include: obesity, hypertension and diabetes. Patients that present in the clinic with either acute or chronic myocardial infarction (MI) often have a plethora of these risk factors. My PhD thesis focuses on two associated risk factors: **ageing** and **type 2 diabetes.**

1.1.1.3.1 Myocardial infarction: contribution of ischaemia-reperfusion injury

As described, MI is caused by the prevention of blood flow to an area of the heart, therefore the best treatment strategy is to remove the impediment so that the blood flow is restored to the ischaemic area. In clinical settings, after an acute MI (AMI), reperfusion of the myocardium is performed using thrombolytic therapy or primary percutaneous coronary intervention (PCI). Complete reperfusion of the myocardium is likely to be achieved, however death rates and incidence of cardiac heart failure after an AMI remain at 10% and 25% [6], respectively. These data suggest that paradoxically, the return in blood flow could cause damage[7]. This phenomenon is known as ischaemia-reperfusion injury (IRI).

Since first being described by Jennings et al, 1960 [8] there has been vast efforts in targeting cellular damage caused by ischaemia-reperfusion injury. There are four different types of injury caused to the heart by reperfusion leading to cardiac dysfunction: myocardial stunning, microvascular obstruction, arrhythmias and lethal myocardial reperfusion injury[7].

Myocardial stunning refers to the mechanical dysfunction following acute non-lethal ischaemia-reperfusion, with no irreversible damage and eventual full functional recovery [9]. Interestingly, even though stunning is a form of reperfusion injury, the intensity of ischaemia is thought to prime the myocardium for the development of such injury. In this regard, reduction in the severity of ischaemia would be effective in limiting post-ischaemic dysfunction. Two interacting pathways have been described regarding the mechanism of reperfusion induced myocardial stunning: the oxyradical hypothesis and the calcium hypothesis [9]. These hypotheses combine to form a central concept that reperfusion of the myocardium initiates a generation of oxygen-derived free radicals and Ca^{2+} overload causing detrimental effects to the contractile apparatus of the cardiomyocyte. The generation of ROS can also simultaneously escalate Ca^{2+} overload by impairing the activity of the Ca^{2+} regulated ATPase and subsequently hindering Ca^{2+} transport in the sarcoplasmic reticulum. This results in a reduced sequestration of Ca^{2+} and increased cytosolic Ca^{2+}. Furthermore, ROS-induced sarcolemmal damage promotes a non-selective permeability of the membrane and successively results in injurious Ca^{2+} and Na^{+} overload[9]. Numerous investigations have uniformly demonstrated a protective effect of antioxidants against reperfusion induced myocardial stunning[9].

Obstruction in the coronary microvasculature can lead to little or no blood flow reaching the ischaemic myocardium upon initiation of reperfusion, this known as the no

reflow phenomenon [10]. It was first described by Krug et al, 1966 as the 'inability to reperfuse a previously ischaemic region'[11]. Microvascular obstruction (MVO) (also known as the no reflow phenomenon) can result from the deposit or accumulation of fatty materials within the microvasculature. Micro-embolization of constituents from atherosclerotic plaques or platelet micro-thrombi and also neutrophil plugging can form blockages preventing the return of blood flow to an ischaemic area[12]. Endothelial cell and cardiomyocyte swelling can also cause compression on external capillaries resulting in impaired vasodilation and contribute to MVO.

Reperfusion arrhythmias occur upon revascularization of the acutely ischaemic myocardium [13], these arrhythmias occur only in salvaged myocardium and cannot arise from dead cells. Upon restoration of blood flow there is a reinstatement of ATP, generation of free radicals and an adjustment in the resting membrane potential due to alterations of the inward and outward ion flux. These changes have been suggested to contribute to these rhythm disturbances. Interestingly, it has been shown using experimental animal models that as the duration of ischaemia increases, so does the incidence of reperfusion arrhythmias[13]. However, the occurrence of reperfusion arrhythmias follows a bell-shaped curve, with the peak incidence arising when the myocardium is subjected to approximately 10 minutes of ischaemia[13]. Arrhythmias that develop within 30 minutes of experimental coronary artery occlusion follow a bimodal distribution and can be classed into (1) immediate or phase 1a ventricular arrhythmias or (2) delayed or phase 1b arrhythmias. The most common are ventricular premature beats, non-sustained ventricular tachycardia, non-sustained ventricular fibrillation and an accelerated idioventricular rhythm. These type of arrhythmias usually self-terminate or can be easily treated[14]. However, sustained ventricular tachycardia or fibrillation that is not effectively managed by anti-arrhythmic drugs or ended by a defibrillator can result in sudden cardiac death[15].

Lethal ischaemia-reperfusion injury can add to the demise of cardiomyocytes during ischaemia-reperfusion, both processes can contribute to eventual infarction of the myocardium. The following section focusses on this phenomenon, the cellular mechanisms that contribute to myocardial infarction and how these can be targeted to limit the damage caused by ischaemia-reperfusion injury.

1.1.2 Myocardial Infarction

1.1.2.1 Infarction and ischaemic injury

The heart is a highly energetic organ, dependent on substrate utilization to produce and use adenosine triphosphate (ATP). As previously mentioned, under normal conditions, about 95% of ATP is produced via oxidative phosphorylation in the mitochondria using fatty acids as the main energy substrate, with the remaining 5% originating from glycolysis. For ATP to be produced, cells require oxygen. Coronary artery blockade or occlusion during ischaemia prevents the delivery of oxygen to the cells, leading to impairment of energy metabolism. Under ischaemic conditions, energy metabolism is shifted to anaerobic glycolysis to provide ATP. This causes the reduction of pyruvate to lactate increasing the release of protons (H^+) and inorganic phosphate, creating an acidic intracellular environment.

A reduced production of ATP leads to numerous downstream effects within the myocardium, including deleterious accumulation of ions. Sarcoplasmic reticulum (SR) Ca^{2+} uptake mechanisms are impaired, resulting in an increased intracellular accumulation of Ca^{2+}. Prolonged ischaemia also reduces intracellular Mg^{2+}, an essential cofactor needed to activate the Na^+/K^+-ATPase system. A combined reduction of both ATP and Mg^{2+} alter the activity of the Na^+/K^+-ATPase of the sarcolemma resulting in an accumulation of Na^+ in the cytosol. Increased H^+ ions also contribute to the accumulation of Na^+ via up regulation of the Na^+/H^+ exchanger. Na^+ overload is exacerbated by inhibition of the Na^+ pump caused by ATP depletion. The cell attempts to counteract the accumulation of Na^+ by reversing the usual movement of ions through the Na^+/Ca^{2+} exchanger to remove Na^+ from the cell at the consequence of accumulating more cytosolic Ca^{2+}. Excess cytosolic Ca^{2+} is transported into the mitochondria by the mitochondrial Ca^{2+} uniporter causing an increase in the activation of Ca^{2+}-dependent dehydrogenase enzymes. A subsequent decline in the generation of NADH results in a reduced availability of electrons to enter the electron transport chain (ETC). As a consequence, mitochondrial membrane potential subsides due to the limitation of the proton gradient. The proton-translocating F_0F_1ATP synthase, which normally produces ATP, becomes an F_0F_1ATPase, consuming ATP to pump H^+ from the matrix into the intermembrane space[16, 17].

As the severity of the ischaemic insult progresses, the accumulation of intracellular of solutes causes osmotic swelling. This eventually results in sarcolemmal disruption and will trigger necrotic cell death pathways (Figure 1.6).

The ultrastructural changes which occur in the myocardium can be rectified with reperfusion of the ischaemic region if reperfusion is rapidly reinstated. Ischaemic times of greater than 20 min produce more pronounced tissue injury, and ultimately if not prevented end in cardiomyocyte death. Area at risk of the myocardium[18, 19], ischaemic duration[18, 19], volume of collateral blood flow[18] and temperature[20] are all factors that have been suggested to contribute to myocardial infarction in experimental models.

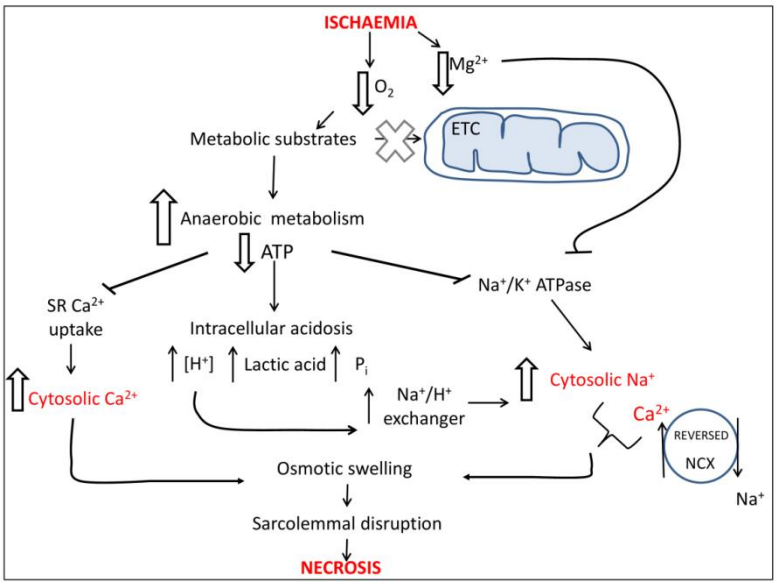

Figure 1.6: Ischaemic injury. Cessation of blood flow during ischaemia decreases the delivery of oxygen to the ischaemic area. The decrease in the availability of oxygen results in the reliance on anaerobic metabolism yielding in a decreased production of ATP. Consequently, the cellular environment becomes acidic and ion transport is affected. These changes lead to an increase in cytosolic calcium and sodium driving osmotic swelling and necrotic cell death.

1.1.2.2 Infarction and reperfusion injury

Upon reperfusion of the ischaemic myocardium, restoration of oxygen and hence increased ATP production lead to a metabolic and biochemical shift to counteract aforementioned ischaemia-induced changes. Paradoxically, reperfusion salvages myocardium but also induces some cell death due to rapid metabolic changes. Numerous endogenous factors contribute to lethal reperfusion injury. These include an increase in oxidative stress via the production of reactive oxygen species (ROS), restoration of intracellular calcium and pH and triggering of inflammatory mechanisms; all of which interact with each other to mediate opening of the mitochondrial permeability transition pore (PTP), leading to eventual cardiomyocyte death, summarised in Figure 1.7.

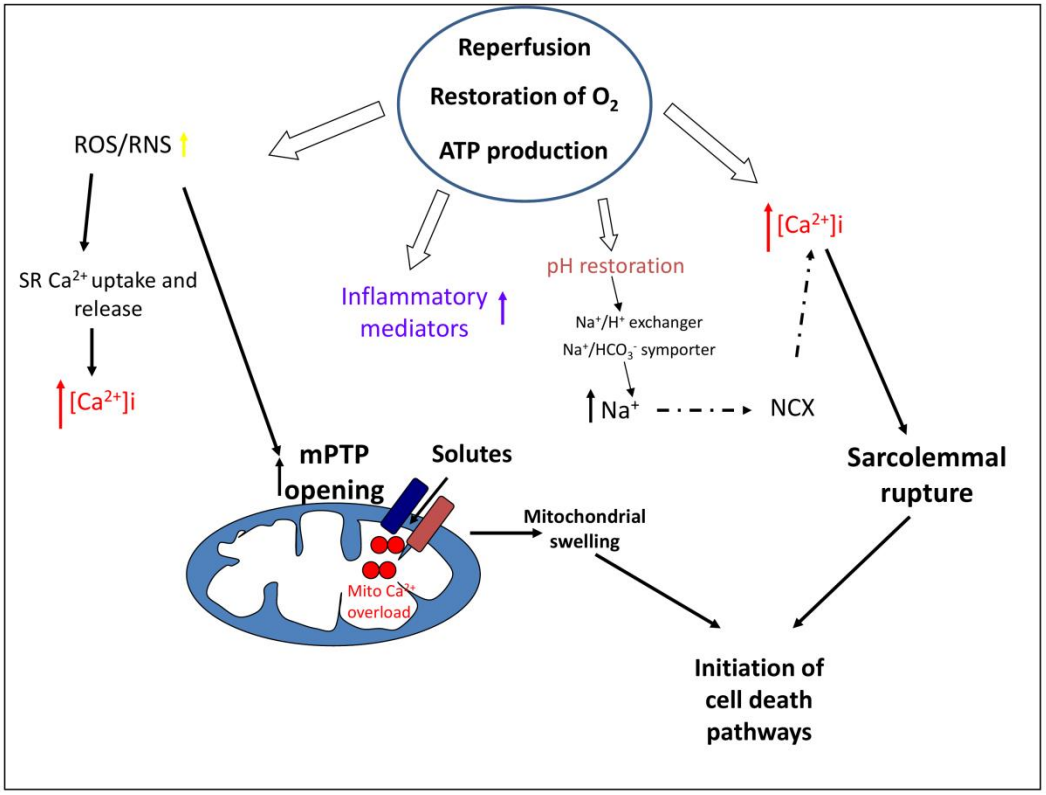

Figure 1.7: Reperfusion injury.. Upon reperfusion of the ischaemic myocardium there is a rapid restoration of oxygen and subsequently the production of ATP is restored. These changes result in an increase in reactive oxygen and nitrogen species (ROS/RNS), inflammatory mediators, intracellular calcium and the restoration of pH. Subsequently, the mitochondrial permeability transition pore (mPTP) opens allowing the entry of solutes into the mitochondrial matrix, resulting in mitochondrial swelling. Cytosolic Ca2+ overload can also lead to the rupture of the sarcolemmal membrane. These processes initiate cell death pathways.

1.1.2.2.1 Oxygen paradox

On rapid re-oxygenation of the ischaemic myocardium an 'oxygen paradox' occurs, whereby oxidative stress caused by an imbalance of pro-oxidative enzymes and anti-oxidative enzymes, leads to further deleterious effects on the myocardium than that caused by ischaemia alone [21]. Hearse et al, demonstrated in the isolated rat heart that hypoxia followed by re-oxygenation elicited more damage than hypoxia alone, causing myofibrillar hypercontracture and sarcolemmal disruption [21]. As aerobic metabolism is restored upon re-oxygenation, reactive oxygen species (ROS) are generated from within the mitochondria [22] and from endothelial cells via xanthine oxidase [23]. As reperfusion persists, neutrophils can also produce ROS via NADPH oxidases [23]. Experimental investigations have highlighted such a vital role for the oxygen paradox in the damage produced by reperfusion, numerous studies utilizing antioxidant agents at the onset of reperfusion have noted a reduction in infarct size. However, development of clinical strategies to target oxidative stress within the myocardium has been disappointing [24]. Vitally, oxidative stress reduces the

bioavailability of nitric oxide (NO) [25], an intracellular signalling molecule that has important innate cardioprotective interactions such as inhibition of neutrophil accumulation, inactivation of superoxide's and improvement of coronary blood flow [26].

1.1.2.2.2 Intracellular calcium overload

An increase in oxygen availability and restoration of aerobic glycolysis promote a rapid increase in intracellular Ca^{2+}, together causing re-energization of the cell. The return of ATP levels promote activation of ATP-controlled ion pumps, the Na^+/K^+ pump is reactivated generating a Na^+ gradient that favours the forward movement of the Na^+/Ca^{2+} exchanger, decreasing cytoplasmic Ca^{2+} concentration. The Ca^{2+}-sarcoplasmic reticulum pump (SERCA) sequesters Ca^{2+} in the sarcoplasmic reticulum (SR) leading to overload and subsequent release of Ca^{2+}. This continuous cycling of Ca^{2+} uptake and release by the SR, and the preceding oxidative stress-induced dysfunction of the SR and sarcolemma membrane damage, contributes to cytosolic Ca^{2+} overload initiating myofibrillar activation and hypercontracture.

1.1.2.2.3 Restoration of physiological pH

Rapid normalization of cellular pH upon reperfusion can also contribute to further Ca^{2+} overload within the cell. The ischaemia-induced acidic pH of the cell reduces its contractility; upon reperfusion there is a rapid normalisation of pH within the interstitial space with the cytoplasm remaining acidic. This creates a proton gradient to extrude H^+ ions from the cell via the Na^+/H^+ exchanger and the Na^+/HCO_3^- symporter. These actions promote hypercontracture via a net influx of Na^+ driving further over load of cellular Ca^{2+}. Interestingly, in vitro studies have shown that maintenance of an acidic extracellular environment during the first few minutes of reperfusion elicits cardioprotective effects on the myocardium, however this effect was lost if the acidosis persisted beyond 3 minutes [27]. Lactate produced during anaerobic glycolysis and other cellular debris' are washed-out upon reperfusion creating an osmotic gradient between the intracellular and extracellular space favouring water to enter the cell. The accumulation of water and cytosolic overload of Na^+ activating the Na^+/H^+ exchanger leads to intracellular pressure increases and stretch in the sarcolemma. This mechanical stretch and hence hypercontracture of the cell leads to eventual cell rupture.

1.2 Mitochondria and ischaemia-reperfusion injury

1.2.1 Mitochondria

1.2.1.1 Mitochondrial morphology

Mitochondria are dynamic organelles that can interact with other mitochondria, alter their appearance and change their morphology. They can undergo a process called fission to generate fragmented mitochondria or alternatively endure a fusion process creating an interconnected, elongated phenotype. Efficient regulation of both fission and fusion of mitochondria by specific proteins have been implicated in a number of biological processes. These processes include cell division, autophagy, apoptosis and metabolism[28].

The aforementioned deleterious effects of reperfusion can impact on the mitochondria not only via signalling to the mPTP, but can also lead to morphological changes [29]. These changes are determined by the redistribution of mitochondrial DNA and other constituents that maintain mitochondrial structure and function forming networks of elongated or fragmented mitochondria. The equilibrium between fission and fusion is a dynamic, cycling process that is controlled by distinct proteins. Fission is controlled by the GTPase molecule, dynamin-related protein 1 (Drp-1) that is recruited from the cytosol to the mitochondria and interacts with the OMM protein human mitochondrial fission protein 1 (hFis1) [30, 31]. Mitochondrial fusion is controlled by 3 dynamin-related GTPases, mitofusin (Mfn) 1 and 2 within the OMM and optic atrophy protein 1 (Opa1) within the IMM[32, 33]. Alongside the involvement of Mfn2 in promoting mitochondrial fusion, Mfn2 can tether the mitochondria to the endoplasmic reticulum (ER) [34]. This results in an increased mitochondrial accumulation of cytotoxic Ca^{2+} that is released from the ER which may influence mPTP opening [34]. The relationship between cell death and mitochondrial dynamics is still not completely understood. Ong et al, 2010 demonstrated that inhibiting mitochondrial fission decreased cardiomyocyte death following ischaemia/reperfusion and that HL-1 cells overexpressing mitofusin proteins were protected against this insult [35]. However, it has been suggested that fused mitochondria are more sensitive to cell death increasing mPTP opening [36], Mfn-2 deficient mice are protected against reperfusion injury [37] and Mfn1 deficient mice are protected against ROS-induced mitochondrial dysfunction [38].

1.2.1.2 Mitochondrial biogenesis

Mitochondrial biogenesis can be defined as the process that leads to the growth and division of pre-existing mitochondria[39]. Compromised mitochondrial biogenesis and

hence function can be influenced by environmental stresses and has been linked to numerous diseases[40], especially between metabolic and cardiovascular diseases. It is also suggested that the transcriptional control of mitochondrial biogenesis coordinates with fission and fusion mechanisms within the mitochondria[39] (Figure 1.8).

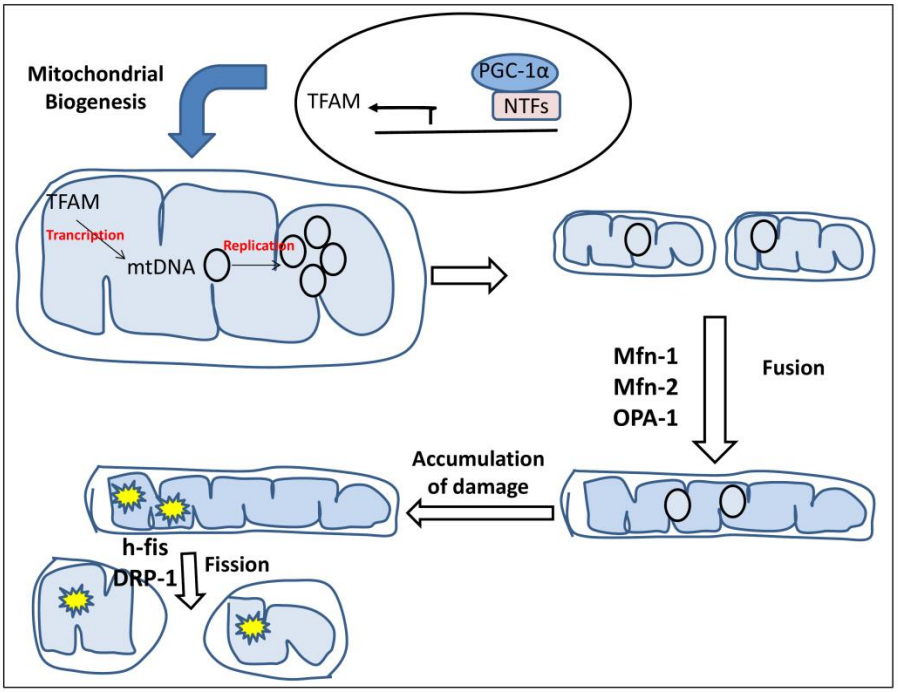

Figure 1.8: The control of mitochondrial biogenesis. The co-activator PGC-1α binds to transcription factors to drive the transcription of genes involved in the regulation of mitochondrial biogenesis. PGC-1α increases the transcription of mitochondrial transcription factor A (Tfam) which results in mitochondrial DNA transcription and replication. These newly formed mitochondria can fuse together forming an extended network of mitochondrion, this process of elongation is coordinated by fusion proteins: mitofusin-1 (Mfn-1), mitofusin-2 (Mfn-2) and optic atrophy protein 1 (OPA-1). Damaged sections of fused mitochondria can be removed by fission proteins (h-fis and DRP-1) ensuring correctly functioning mitochondria remain.

At the nuclear level, there are numerous transcriptional proteins that are involved in regulating mitochondrial biogenesis including mitochondrial transcription factor A (Tfam), nuclear respiratory factors (Nrfs) and peroxisome proliferator-activated receptor gamma co-activator (PGC-1α) [41, 42]. Since its original discovery[43], PGC-1α has emerged as a master regulator of mitochondrial biogenesis implemented in maintaining optimum metabolic equilibrium[44].

1.2.1.3 The physiological role of cardiac mitochondria

Mitochondria are specialized, dynamic organelles located in the cytoplasm of the cell; they play an essential role in cell life and death. They are considered the 'biochemical powerhouse' of the cell, playing a crucial role in many metabolic processes leading to ATP production. They also contribute to cellular stress responses [45], cell death [46],

cellular Ca^{2+} homeostasis [47] and are implicated in pathologies such as ageing [48] and diabetes [49].

1.2.1.4 Cardiac energy metabolism in the mitochondria

Glucose and fatty acids are sequentially oxidised to form a common intermediate acetyl CoA in the mitochondria. The β-oxidation of fatty acids generates the electron carriers NADH and FADH. Upon entry into the Krebs cycle, acetyl CoA is further oxidised producing more NADH and $FADH_2$. Cytosolic NADH generated during glycolysis cannot enter the mitochondria directly. The malate-aspartate shuttle indirectly transfers electrons from NADH in the cytosol across the impermeable inner mitochondrial membrane (IMM) to NADH in the mitochondrial matrix. Generation of NADH/FADH/$FADH_2$ is summarised in Figure 1.9.

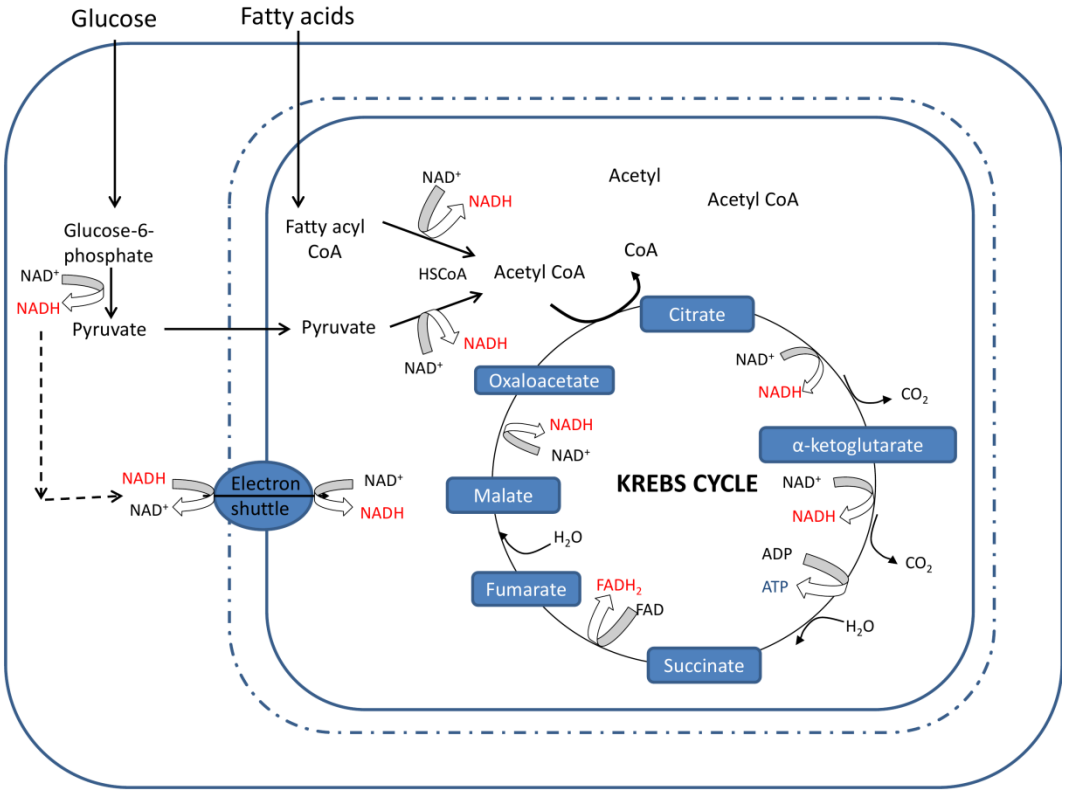

Figure 1.9: The Krebs cycle. Glycolytic and β-oxidation pathways lead to the production of acetyl CoA for entry into the Krebs cycle. The electron carrier, NADH that is generated in the cytosol is shuttled into the mitochondrial matrix, with the remaining NADH generated within the mitochondria throughout β-oxidation and at several points of the Krebs cycle. An alternative electron carrier $FADH_2$ is also generated as a result of the conversion of succinate to fumarate.

NADH initiates the electron transport chain (ETC) by feeding electrons to complex I (NADH-ubiquinone oxidoreductase/dehydrogenase) and subsequently transferring electrons to ubiquinone (coenzyme Q). Ubiquinone is a lipid-soluble mobile electron carrier that transfers electrons from complex I to complex III (cytochrome bc1).

In the terminal redox reaction, complex III reduces an associated electron carrier, cytochrome c and electrons are transferred into complex IV (cytochrome c oxidase). These step-wise redox reactions at complexes I, III and IV are coupled to the active pumping of hydrogen ions out of the mitochondrial matrix into the intermembrane space. This establishes a large proton-motive force across the inner membrane. Membrane bound complex II (succinate dehydrogenase) of the ETC does not contribute to this proton-motive force. Complex II directly reduces succinate to fumarate, as part of the Krebs cycle, generating the electron donor $FADH_2$. Complex II donates the electrons generated from $FADH_2$ directly to Ubiquinone promoting direct passage of electrons through complex's III and IV. The proton-motive force created by the accumulation of H^+ produces a large driving force consisting of a membrane potential ($\Delta\psi_m$ ~ -200mV) and a proton gradient (ΔpH) which is used by ATP synthase (F_1−F_0 ATPase) to phosphorylate ADP to ATP [50]. ATP is exported to the cytosol via adenine nucleotide translocase (ANT) and used for numerous cellular processes. An overview of oxidative phosphorylation is summarised in Figure 1.10.

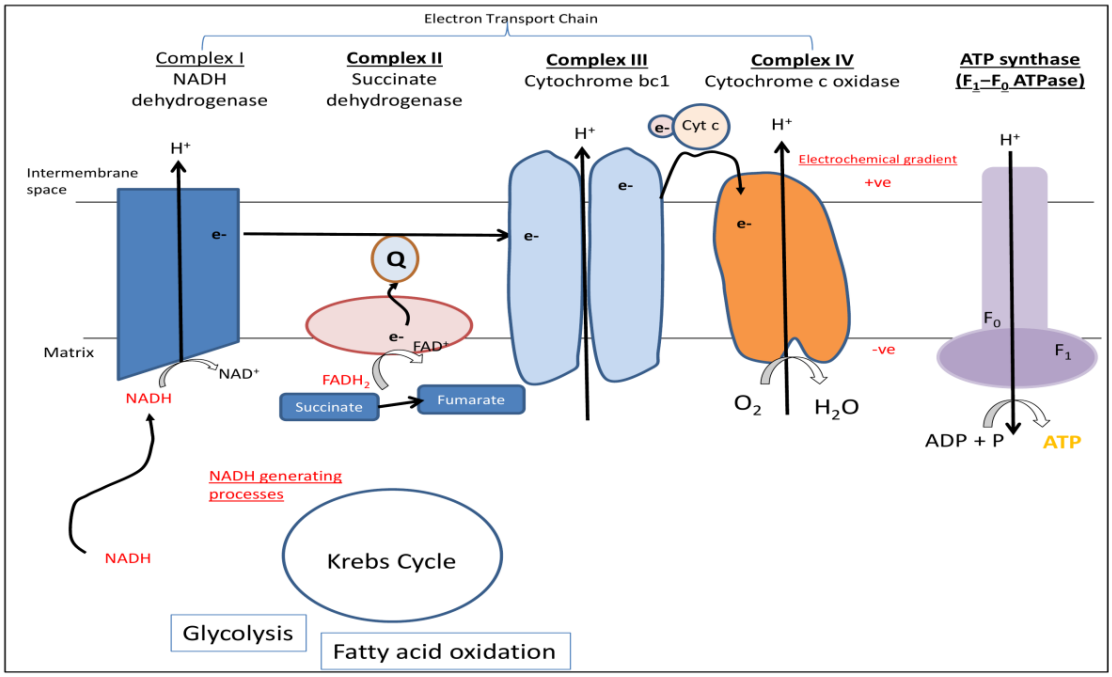

Figure 1.10: Oxidative Phosphorylation. Electron carriers generated during glycolysis, β-oxidation and the Krebs cycle feed electrons to complex I of the electron transport chain (ETC). Electrons (e^-) are shuttled from complex I to complex III through ubiquinone (coenzyme Q) and then via cytochrome c to complex IV. The movement of e^- generate a proton (H^+) gradient across the membrane resulting in activation of the ATP synthase and generation of ATP. Complex II of the ETC does not contribute directly to the proton gradient. However, the conversion of succinate to fumarate during the Krebs cycle can directly provide the electrons to the ETC via $FADH_2$.

Alternatively, movement of electrons and proton influx into the mitochondrial matrix can occur independently of phosphorylating ADP. This process is called uncoupled oxidative phosphorylation. This results from damage to the ATP-synthase or an increased permeability to the IMM allowing passive movement of protons. This 'proton leak' is facilitated by IMM proteins such as uncoupling proteins (UCPs)[51], adenine nucleotide translocases (ANTs)[52]and also cytochrome c[53]. Energy derived from proton leak is dissipated as heat.

1.2.1.5 Mitochondrial ion transport

Mitochondria possess a smooth outer mitochondrial membrane and a convoluted inner membrane forming tubular structures called cristae. These membranes define two distinct spaces in the mitochondrion, the intermembrane space between the inner and outer membrane, and the mitochondrial matrix within the inner membrane. The outer mitochondrial membrane (OMM) is a phospholipid bilayer containing numerous proteins called porins and channels that allow movement of molecules up to 10KDa between the mitochondria and the cytosol. An extensively studied outer mitochondrial membrane channel is the voltage-dependent anion channel (VDAC). VDAC is located between the outer and inner mitochondrial membrane. It provides the principal route of entry and exit of ions and metabolites across the outer membrane[54].

The inner mitochondrial membrane (IMM) is the major permeability barrier between the cytosol and the mitochondrial matrix, this membrane is freely permeable to only O_2, CO_2 and H_2O. The diverse permeable nature of the IMM and OMM enable the complexes of the ETC to promote a proton gradient across the IMM. This electrochemical gradient forms the basis of the mitochondrial membrane potential (ψ_m) and is a crucial determinant of ion transport across the IMM.

Various transport proteins including ion channels are located in the highly complex cristae-containing membrane allowing passage to otherwise impermeable molecules. These channels compromise approximately 80% of the IMM. The IMM also hosts complexes of the respiratory chain, ATP synthase and various enzymes[55].

There are several modes of ion transport present in the IMM, these include symporters, uniporters and antiporters[54]. Symporters can simultaneously transport multiple ions or metabolites in the same direction across the membrane. Antiporters exchange ions across different sides of the membrane, with or without an electrochemical gradient and uniporters allow the flow of ions electrophoretically down their electrochemical gradient[54]. The IMM has numerous well-characterised cation-

permeable channels. These include the mitochondrial Ca^{2+} uniporter and ryanodine receptors and also potassium channels, the mitochondrial K_{ATP} and K_{Ca} channels. Ca^{2+} can freely pass through the OMM but in order to enter the mitochondrial matrix, it must pass through the mitochondrial Ca^{2+} uniporter located on the IMM. This highly Ca^{2+}-selective, low conductance ion channel[56] provides the primary route for Ca^{2+} uptake into the mitochondrial matrix. An increased uptake of Ca^{2+} into the matrix is important for maintained production of ATP during oxidative phosphorylation[57]. Efficient control of mitochondrial K^+ flux is important to counterbalance the activity of the mitochondrial uniporter[58].

However, less information is known about the existence and expression of anion permeable IMM ion channels. Early studies provided evidence for an inner membrane anion channel (IMAC). These channels are controlled by protons, Mg^{2+}, temperature and pH but their exact physiological role is still largely unknown[59].

Tightly regulated mitochondrial ion flux limits unnecessary energy wastage and prevents mitochondrial swelling and eventual rupture of the OMM[58]. Rupture of the OMM can result in non-functional and deleterious mitochondria. Channel opening in response to energy dissipation will increase flux through the ETC. If this is not efficiently compensated for by an increased production of substrates, oxidation status and subsequent changes in levels of reactive oxygen species occur. Hence, mitochondrial ion channels can also act as redox regulators which will impact on intracellular signalling cascades such as the transcription and translation of proteins and also cell death pathways[60].

During normal physiological conditions, maintaining mitochondrial function, metabolism, structure and ion transport are crucial for numerous critical cellular functions. The recovery of pH, oxidative stress and Ca^{2+} overload already described during reperfusion, can impact on the functional capacity and activity of the mitochondria. Reperfusion increases the open probability of the mitochondrial permeability transition pore (mPTP). The mPTP is the major end-effector of ischaemia-reperfusion injury, contributing to cardiomyocyte hypercontracture and cell death.

1.2.1.6 Mitochondria permeability transition pore (mPTP)

It was originally thought that mitochondrial swelling in response to high levels of Ca^{2+} was the result of non-specific permeabilisation of the inner membrane of the mitochondria. Work throughout the late 1970s proved otherwise, with the identification of a non-specific channel that allowed passage of molecules up to 1.5 kDa in presence

of high Ca^{2+} [61]. This was explored further into the late 1980s, whereby Crompton et al demonstrated that both Ca^{2+} and oxidative stress synergistically promote reversible opening of an inner membrane pore in isolated rat heart mitochondria[62]. This non-selective membrane channel, is now commonly known as mitochondrial permeability transition pore (mPTP) [63]. The mPTP is a responsive channel, which opens and closes according to the cellular environment for example pH.

The structure of the mPTP is still not completely defined and is a matter of intense debate[64]. It became generally accepted that the mPTP comprised of a complex of proteins spanning the inner and outer mitochondrial membranes [63]. It was originally defined as an outer mitochondrial membrane protein voltage-dependent anion channel (VDAC), mitochondrial adenine nucleotide translocator (ANT) and hexokinase. This was extended to include outer membrane TSPO and Bcl-2 family members. In response to cellular stress such as high Ca^{2+}, cyclophillin D (CypD) was proposed to bind ANT initiating a tunnel-like structure, allowing passage of water and solutes from the cytosol into the mitochondria[65]. Activation of the mPTP was strongly inhibited by CypD receptor blocker cyclosporine A (CsA)[60]. However, Kokoszka et al, 2004 questioned this notion. They demonstrated that mitochondria lacking ANT protein still contained a Ca^{2+}-dependent pore. Moreover, this pore could be triggered by thiol oxidants and inhibited by CsA. These findings suggested that ANT therefore was not an obligatory binding partner of CypD or the site of contact for oxidants[66]. The existence of VDAC as a component of the mPTP was also scrutinised, Krauskopf et al, 2006 performed a detailed comparison of the mPTP in mitochondria from wild type and $VDAC1^{-/-}$ mice and demonstrated VDAC1 was fully dispensable for mPTP regulation and opening. In further support of this, Baines et al, 2007 demonstrated all three isoforms of VDAC were not components of the mPTP [67]. The outer membrane protein translocator protein (TSPO) also appears dispensable, TSPO ligands did not affect activity of the large conductance mPTP[68]. Based on the genetic and pharmacological evidence available it seems likely none of the original channel-forming proteins are in fact necessary for the formation of the mPTP.

CypD is located in the mitochondria and possesses prolyl isomerase (PPIase) activity. Genetic ablation studies firmly support a modulatory role for this protein in the control of mPTP opening[69]. Post translational modifications of CypD such as phosphorylation, acetylation and nitrosylation also affect the open probability of the mPTP[70]. Interestingly, CypD can intereact with numerous proteins, raising the possibility of other potential mPTP components. CypD has been shown to interact with Bcl-2[71], p53[72], ERK-2/GSK-3[73] and also the F_0F_1 ATP synthase[74]. A very recent

publication by Giorgio et al, 2013 has defined the binding site of CypD on the F_0F_1-ATP synthase as the OSCP subunit. Inhibition of the F_0F_1 ATPase with benzodiazepine (Bz)-423, sensitised the mPTP to Ca^{2+} and this effect was blunted by P_i induced CypD binding. They further suggest that the F_0F_1 ATP synthase dimerises to form the mPTP, which is sensitive to classical triggers and inhibitors of the previously defined large conductance channel. Interestingly, they find F_0F_1 ATP synthase monomers lack any channel activity[75]. Interestingly, in this proposed model of the mPTP, pore opening was sensitive to Ca^{2+} and P_i in the absence of CypD. The authors suggest that the binding of CypD to this dimerised channel sensitises the opening of the mPTP thereby opening in response to lower Ca^{2+} concentrations. Further investigations are required to fully define the mPTP and the interaction with the outer mitochondrial membrane[76]. Figure 1.11 shows the classical and newly hypothesised structure of the mPTP.

Upon reperfusion of the ischaemic myocardium, the generation of ROS, overload of Ca^{2+} and restoration of pH influence the open probability of the mPTP. Opening of the mPTP immediately depolarizes the membrane potential ($\Delta\psi_m$), causing dissipation of the proton motive force required to maintain successful oxidative phosphorylation and hence ATP production, leading to bioenergetic failure of the cardiomyocyte [63]. Not only does a cessation of ATP production occur but the reverse mode of the ATPase synthase is activated to try and restore the proton gradient by consuming ATP [50]. Secondly, small molecules pass through the pore leading to accumulation of ions and cofactors within the mitochondria. This causes a metabolic imbalance between the cytosol and the membrane favouring the release of accumulated Ca^{2+} and eventual mitochondrial swelling. Swelling of the mitochondria can occur with or without rupture of the inner mitochondrial membrane. Pressure mounts within the mitochondria leading to eventual rupture of the outer membrane causing the release of pro apoptotic proteins and hence the initiation of cell death pathways[77].

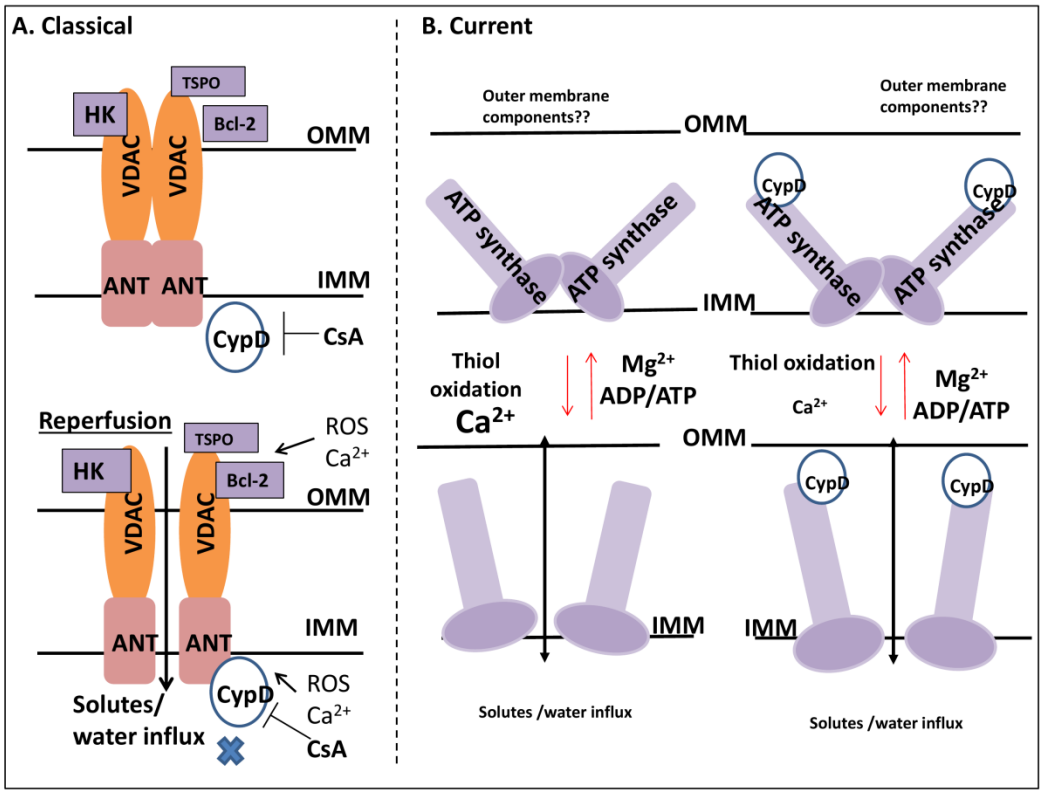

Figure 1.11: Structure of the mitochondrial permeability transition pore (mPTP). Structure of the mitochondrial permeability transition pore (mPTP). The structure of the mPTP was classically defined as shown in A. This model proposed a complex of inner and outer mitochondrial membrane proteins including mitochondrial adenine nucleotide translocator (ANT), voltage-dependent anion channel (VDAC), hexokinase (HK), Bcl-2 and translocator protein (TSPO). In response to reperfusion, the redox and Ca^{2+} sensitive pore, is modulated by cyclophillin D (CypD), allowing the passage of solutes into the mitochondrial matrix. The current opinion of the structure of the mPTP is shown in B. This model proposes that the ATP synthase of the electron transport chain (ETC) forms dimers to allow the passage of water/solutes into the mitochondrial matrix in a redox and Ca^{2+}-dependent manner. This model suggests CypD is not an absolute requirement for pore opening but instead acts as a pore sensitiser. The outer membrane component of the mPTP in this model is not yet defined.

1.2.2 PGC-1α

1.2.2.1 PGC-1 family and PGC-1α structure and function

The group of transcriptional coactivators, peroxisome proliferator-activated receptor gamma (PPARγ) coactivator-1 (PGC-1), are inducible factors that can bind to both nuclear receptors (NR) and non NRs to drive gene transcription. PGC-1α was originally identified as a cold-inducible coactivator, following observation of its functional capacity to respond to and interact with peroxisome proliferator-activated receptor gamma (PPARγ) in mitochondrial-rich brown adipose tissue in response to cold exposure[43]. Other family members include PGC-1β[78, 79] and (PRC)[80]. PGC-1β and PGC-1α are highly expressed in muscles and tissues with high oxidative capacities such as heart, skeletal muscle and brown adipose tissue whereas less is known about the expression

of PRC[80]. Interestingly, these coactivators cannot bind DNA directly. However, in response to activation signals such as changes in metabolism, exercise or cold, these transcriptional coactivators bind to receptors to provide a platform for protein interaction resulting in coactivator complexes. In turn, these complexes are capable of triggering the transcription of certain target genes.

PGC-1α's N amino terminal region provides the platform for proteins containing histone acetyltransferase (HAT) activity including p300/ cAMP response element binding protein (CREB)-binding protein and steroid receptor coactivator-1 (SRC-1)[43]. The carboxy terminal region allows for the interaction with a second activating complex, the thyroid hormone receptor-associated protein/vitamin D receptor-interacting protein (TRAP/DRIP) complex[81]. To initiate gene transcription, the transcription factor binds to the DNA response element in the promoter region of the target gene. Recruitment of PGC-1α allows association of the p300/CREB-binding protein and causes chromatin remodelling by histone acetylation. The subsequent and direct interaction with TRAP/DRIP provides a molecular bridge between the coactivator complex and RNA polymerase II. Remodelling of chromatin increases the accessibility of this transcriptional machinery and aids gene transcription. PGC-1α alone does not possess this ability but it acts as a scaffold for recruiting these proteins[81]. Of note, PGC-1α also possesses an RNA processing domain at the Carboxy terminus that may contribute to further transcriptional regulation[82]. A generalised scheme demonstrating the docking of protein regulatory complexes to PGC-1α and subsequent gene transcription is shown in Figure 1.12.

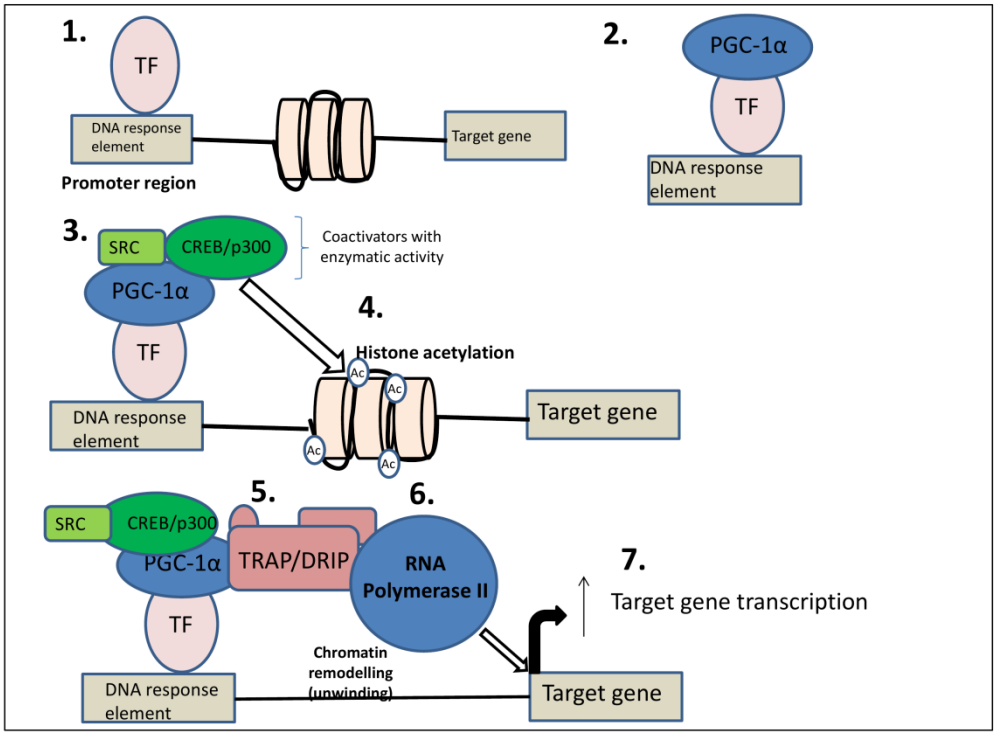

Figure 1.12: PGC-1α coactivation of transcription factors. Transcription factors (TF) bind to the DNA response element of their respective target gene (1), with subsequent recruitment of PGC-1α to the TF/DNA response element complex (2). PGC-1α interacts with p300/cAMP response element binding protein (CREB)-binding protein and steroid receptor coactivator-1 (SRC-1) causing histone acetylation and chromatin remodelling (3 &4). This process allows the direct interaction with a second activating complex, the thyroid hormone receptor-associated protein/vitamin D receptor-interacting protein (TRAP/DRIP) (5). The TRAP/DRIP complex provides a molecular bridge for the association of RNA polymerase II (6) which drives gene transcription (7).

1.2.2.2 Transcriptional control of PGC-1α

The diverse actions of PGC-1α led to the consensus that this coactivator is able to interact with numerous transcription factors. Within the heart, there are numerous NR and non-NR targets of PGC-1α; NRs include PPARα, PPARβ, estrogen-related receptors-α and γ (ERRs). The non NR targets include, forkhead box class-O (FoxO1), myocyte enhancing factor-2 (MEF-2) and nuclear respiratory factor-1 and -2 (NRF-1 and -2)[42]. The key functional domains involved in the interaction of PGC-1α with the aforementioned transcription factors are shown in Figure 1.13. The capacity of PGC-1α to interact with these transcription factors serves to coordinate a plethora of effects on the mitochondria such as the control of mitochondrial biogenesis, energy substrate utilisation and cellular respiration[83].

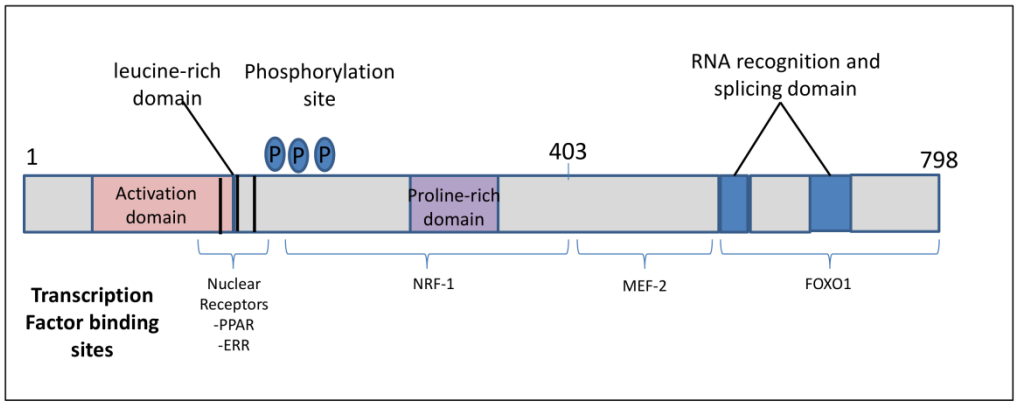

Figure 1.13: The key functional domains involved in the interaction of PGC-1α with transcription factors

The activity of PGC-1α can be modulated by gene transcription. PGC-1α gene transcription and protein expression can be regulated by numerous proteins in response to certain physiological stimuli such as changes in metabolic demand, exercise and nerve innervation. Depending on the upstream activator eliciting an increased requirement for PGC-1α activity, the appropriate transcription factor can be co-activated by PGC-1α to meet the demands of the cell [84-86]. These effects are summarised in Figure 1.14.

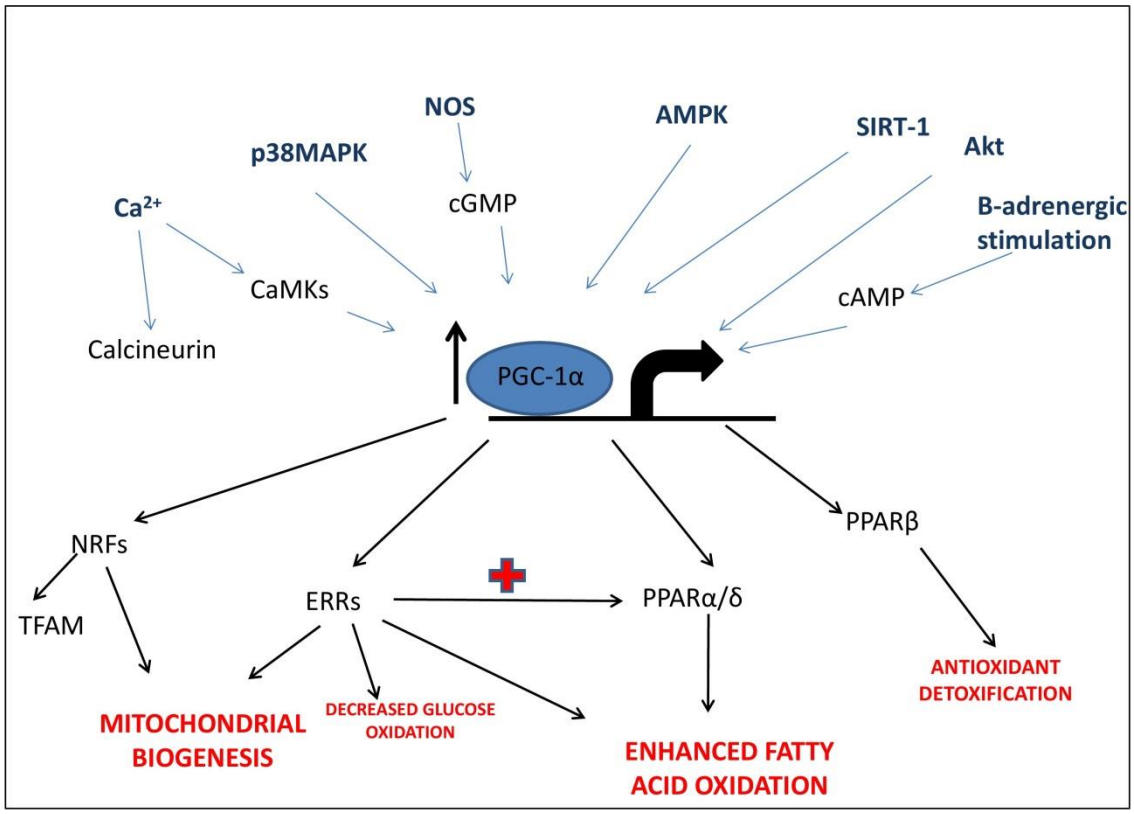

Figure 1.14: Transcriptional targets of PGC-1α. PGC-1α responds to changes in the intracellular environment driving gene transcription depending on the requirement of the cell.

AMPK is a crucial signalling molecule that acts as an energy sensor within the cell. In response to an increased AMP to ATP ratio, a range of catabolic pathways are initiated, including a rise in mitochondrial biogenesis and function which drives ATP production[87]. Treatment of muscle cells with a specific AMPK activator such as 5-aminoimidazole-4-carboxamide-1-b-d-ribofuranoside (AICAR) led to an increase in PGC-1α transcription[88, 89]. Moreover, PGC-1α activity has been shown to be essential for AMPK-mediated mitochondrial activation[90]. The signalling events leading to an AMPK associated increase in PGC-1α expression remain unclear; however data obtained in human skeletal muscle suggest potential transcription targets that need further investigation[91]. The transcription factors FoxO1, CREB and MEF_2 can bind to specific promoter regions of PGC-1α to drive transcription; moreover, inhibition of MEF_2 activity by class II histone deacetylases (HDACs) suppresses this activity[84, 92]. Interestingly, insulin a key signalling molecule which is involved in energy storage and control of catabolic pathways has also been suggested to impact on PGC-1α transcription in muscle. Insulin responsive elements exist within the binding domain of the promoter region of the PGC-1α gene. These elements can be activated by FoxO1 driving the transcription of PGC-1α. Insulin signalling phosphorylates Akt which in turn can phosphorylate and inhibit FoxO1 thereby reducing the transcription of PGC-1α[93]. The defective insulin signalling exhibited in diabetes could impact on the regulatory role of PGC-1α.

1.2.2.3 Post translational modifications of PGC-1α

Post translational modifications of PGC-1α include acetylation, phosphorylation, methylation, GlcNAcylation[94] and most recently SUMOylation [95]. Phosphorylation and acetylation of PGC-1α have been the most extensively studied modifications. Numerous proteins can target and phosphorylate PGC-1α at numerous sites; AMPK alongside its direct transcriptional activity can also activate PGC-1α through phosphorylation at threonine-177 and serine-538 and hence enhance its transcriptional coactivity[90]. Cytokine activation of kinase p38 MAPK phosphorylates PGC-1α, increasing its stability and potentiating its transcriptional activity[96]. This kinase can also indirectly potentiate PGC-1α activity by inhibiting co-repressor p160MBP in myoblasts[97]. Akt phosphorylates PGC-1α directly[98] and indirectly[99] thereby reducing its activity. Phosphorylation of Akt induced by insulin, can directly phosphorylate PGC-1α at serine-570 alternatively this axis has been shown to phosphorylate and stabilize protein kinase Clk2. Clk2 can phosphorylate PGC-1α resulting in specific down regulation of PGC-1α/FoxO1 related activity consequently repressing gluconeogenesis and inhibiting the production of glucose[99]. Interestingly, proteasomal degradation of

PGC-1α in the nucleus can be enhanced by GSK-3β mediated phosphorylation during acute oxidative stress[100], moreover this inhibitory phosphorylation limits silence information regulator 2-type 1 (SIRT1)-activation of PGC-1α, thereby further reducing its activity and transcription. Sustained oxidative stress favours SIRT-1 activity and overcomes the inhibitory nuclear accumulation of PGC-1α and drives the transcription and cytoplasmic translation of PGC-1α[94].

De/acetylation is another key regulatory mechanism of PGC-1α function; SIRT-1 deacetylates and increases the coactivation of PGC-1α to its transcription targets, whereas acetylation by histone acetyltransferase KAT2A (GCN5) has the opposing effect. The activity of SIRT-1 is dependent on the energy status of the cell. In times of energy demand, for example during exercise or oxidative stress, SIRT-1 substrate coenzyme nicotinamide adenine dinucleotide (NAD^+) and subsequently the NAD^+/NADH ratio are increased as energy stores are being depleted. This triggers SIRT-1 mediated deaceytlation of PGC-1α, promoting mitochondrial metabolism and increasing energy within the cell. Interestingly, AMPK plays another vital role in the regulation of PGC-1α activity; AMPK increases the level of NAD^+ by enhancing FAO[101] or the activity of nicotinamide phosphoribosyltransferase (Nampt)[102] thereby promoting the deacetylation action of SIRT1[101]. Moreover, it appears the phosphorylation of PGC-1α by AMPK is required for SIRT-1 to target and deacetylate PGC-1α[101]. Post translational modifications are summarised in Figure 1.15.

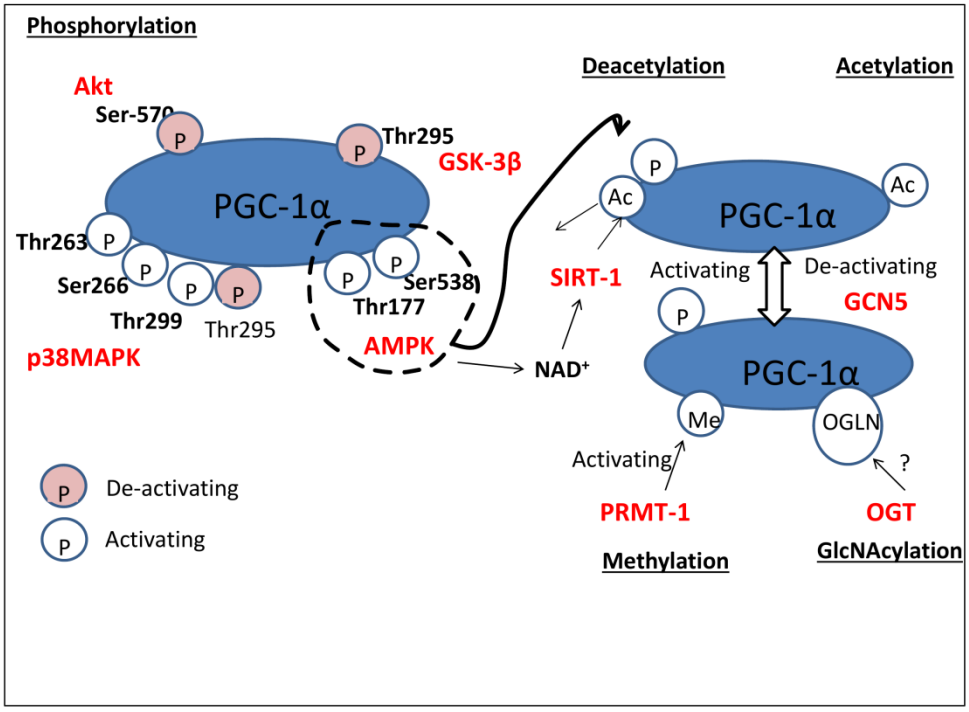

Figure 1.15: Post translational modifications of PGC-1α

1.2.2.4 PGC-1α signalling in the heart

PGC-1α is abundantly expressed in the heart; after birth PGC-1α expression is increased as the heart switches to favour mitochondrial FAO as the main source of energy[42, 103]. In other physiological modifications such as fasting, the heart also increasingly relies on FAO for the production of ATP and therefore an increase in the expression of PGC-1α is observed with a subsequently increased coactivation of PPARα and ERRα[42, 103]. Gain-of-function and knock-down studies using PGC-1α transgenic mice have demonstrated many biological functions of PGC-1α *in vivo* hearts. Enhanced activation of cardiomyocyte mitochondrial biogenesis was seen in mice that constitutively overexpress cardiac PGC-1α by control of the cardiac α-myosin heavy chain promoter (MHC-PGC-1α mice), moreover this enhanced activation led to eventual death by heart failure[103] suggesting that a tight control of mitochondrial biogenesis is extremely important. A subsequent, tetracycline-inducible PGC-1α mouse (cs-tet-on PGC-1α mouse) further demonstrated the exquisite control PGC-1α has on mitochondrial biogenesis and function during development into adulthood[104]. Acute overactivation of PGC-1α during the neonatal period caused mitochondria to become dramatically oversized within the heart whereas ultrastructural changes within mitochondria only developed following chronic up regulation of PGC-1α expression[104]. Interestingly, PGC1α $^{-/-}$ mice produced by the Spiegelman group demonstrate a moderate decline in cardiac function with age associated with diminished expression of genes associated with mitochondrial FAO, oxidative phosphorylation and the Krebs cycle which led to a modest impairment of ATP maintenance[105]. In support of the first knock down model created, mitochondrial proteins and enzymes involved in FAO are down regulated in the failing heart[106, 107]. Whereas, the PGC-1α $^{-/-}$ mouse model created and used by Leone et al, fail to observe the deviations in gene expression recorded in the mouse generated by Spiegelman lab[108].

PGC-1α has also been implicated in the oxidative stress response by regulating the expression of ROS scavengers. In cultured cells, PGC-1α and –β induce the expression of antioxidant scavenger's catalase, glutathione peroxidase and SOD-1/2 in response to hydrogen peroxide induced oxidative stress[109]. Moreover, PGC-1α deficient mice have reduced levels of these scavengers. Interestingly, overexpression of PGC-1α in endothelial cells reduced the accumulation of ROS and reduced cell death as well[110].

The succeeding section focus on the cellular mechanisms implicated in the death of cardiomyocytes and the cell survival pathways which can be up regulated in order to limit the damage caused by ischaemia-reperfusion injury.

1.3 Cell death pathways

Myocardial cell death following ischaemia-reperfusion can occur via numerous pathways namely: apoptosis, necrosis and autophagy, with the mitochondria playing a crucial role in all processes. The fate of cells is dependent on the availability of ATP, with apoptosis initiated in the presence of ATP [111] and necrosis initiated in the absence. Hence, it could be proposed that the majority of cellular damage caused during ischaemia (where ATP levels are low) is due to necrosis, while at reperfusion, when ATP levels are restored, apoptosis will prevail. However, it is suggested that an interplay of necrosis and apoptosis signalling contribute to cellular damage during both ischaemia and reperfusion injury [112]. McNully et al, 2004 showed both necrosis and apoptosis contributed to IRI in isolated rat hearts [113].

1.3.1 Necrosis

Necrotic cell death is initiated as a consequence of ATP depletion. It is characterised by vacuolation of the cytoplasm, breakdown of cellular plasma membranes leading to an infiltration of inflammatory mediators around the dying cell, without fragmentation of DNA [114]. Severe uncoupling of mitochondria during an ischaemic insult leads to rapid ATP depletion and the onset of cellular necrosis. However, if mitochondrial permeabilisation develops heterogeneously and slowly within the mitochondria, ATP will deplete at a slower rate triggering the apoptotic signalling pathways described in the section below [115].

1.3.2 Apoptosis

Apoptosis is also known as ‘programmed cell death’ controlled by distinct cellular signalling pathways leading to blebbing but not complete destruction of the cellular membrane [115]. Apoptotic bodies containing fragmented nuclear and chromosomal DNA of the dying cell are recognised and removed by phagocytic cells without the activation of inflammatory mediators. Apoptotic cell death is achieved via the activation of the caspase cascade. Caspases, which belong to a class of enzymes called proteases, exist in two types: **initiator caspases** (which activate downstream caspases, such as caspase 8 and 9) and effector (executioner) caspases (such as caspase 3 and 6), responsible for the cell damage by cleaving essential functional and structural proteins.

Apoptosis can be initiated via two mechanisms, the extrinsic death receptor pathway or the intrinsic mitochondrial pathway, which require specific signals to be initiated. However, both converge to activate the executioner caspases.

The extrinsic pathway starts with the activation of sarcolemmal death receptors by death-inducing ligands (DIL) such as CD95, Fas, TNF-α and TNF-related apoptosis-inducing ligands (TRAIL) forming a death inducing signalling complex (DISC). Following this, the initiator caspase-8 is triggered and subsequently it activates other downstream executioner caspases such as caspase-3. All DIL's have been linked to the initiation of the extrinsic death pathway of apoptosis following ischaemia and reperfusion [116].

The intrinsic signalling pathway is initiated by non-receptor mediated intracellular stimuli. Intracellular damage such as oxidative stress, DNA modifications or ER stress can trigger this pathway by activating B cell lymphoma 2 (BCL-2) homology 3 (BH3)-only proteins. This activates pro apoptotic BCL-2 associated X protein (BAX) or BCL-2 antagonist protein (BAK) which cause mitochondrial outer membrane permeabilisation (MOMP). Anti-apoptotic BCL-2 (BCL-2/BCL-xL) proteins can prevent MOMP by binding BAX or BAK and inactivating them. Pro-apoptotic BAD forms a heterodimer with anti-apoptotic proteins (BCL-2/BCL-xL), inactivating them and thus allowing BAX/BAK to trigger apoptosis. The MOMP promotes the release of cytochrome c and apoptosis inducing factors. Upon entry into the cytoplasm, cytochrome c forms a complex with apoptotic protease activating factor-1 (Apaf-1). Binding of cytochrome c to Apaf-1 stimulates Apaf-1 dependent dATP hydrolysis, causing a conformational change and oligomerisation of Apaf-1. This leads to the formation of an apoptosome. This structure cleaves and activates caspase-9, initiating activation of the executioner caspases, caspase-3 and -7, resulting in apoptosis[117].

Crosstalk between the two pathways occurs through the activation of caspase-8 in the extrinsic pathway. Caspase-8 activates another member of the BCL-2 family, BID, and subsequently causes MOMP. This initiates the intrinsic mitochondrial pathway of apoptosis[117]. Both pathways are summarised in Figure 1.16.

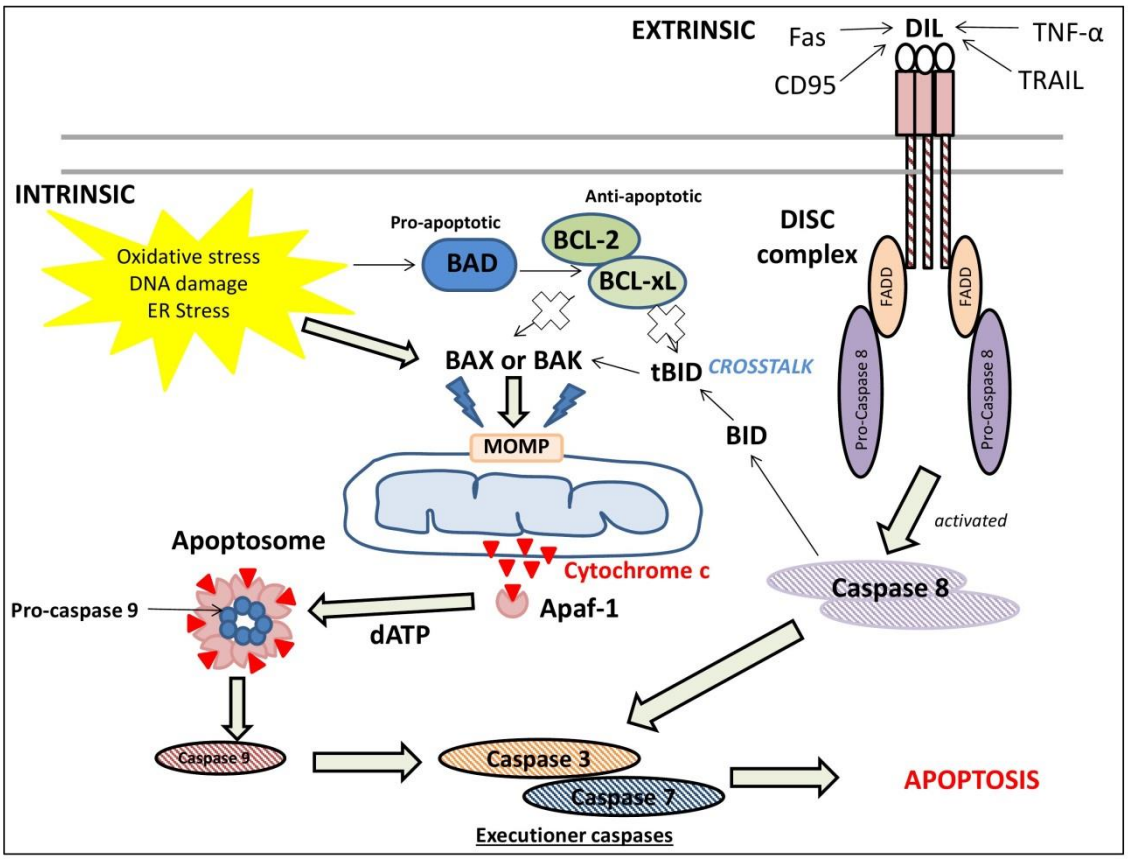

Figure 1.16: Apoptotic cell death pathways. The extrinsic pathway is activated by death-inducing ligands (DIL). Binding of DIL to sarcolemmal death receptors activate a death inducing signalling complex (DISC) subsequently activating caspase 8. Caspase 8 activates the executioner caspases initiating apoptosis. The intrinsic pathway is triggered by intracellular stresses and converges onto the mitochondria. Activation of pro-apoptotic signalling complexes cause mitochondrial outer membrane permeabilisaton (MOMP), releasing cytochrome c and activating executioner caspases. The extrinsic and intrinsic pathways also cross talk through caspase-8/BID.

1.3.3 Other forms of cell death

A third process considered to contribute to cell death is autophagy, a process of self-degradation of damaged or unwanted cellular components or organelles [118]. In response to cellular stress and certain signals, some cell components are engulfed and sequestered by autophagosomes into the cytosol where they are degraded and removed from the cell [118]. Autophagy alongside necrosis and apoptosis occur in cardiac myocytes during myocardial infarction, however, the role of autophagy in ischaemia-reperfusion injury is not fully defined. Hariharan et al, 2011 suggest that oxidative stress generated during ischaemia and reperfusion leads to an increase in autophagosomes and autolysosomes resulting in increased autophagic flux which contributes to IRI damage[119]. In addition, Zhou et al, 2012 showed that cardiac-specific Mfn2 knockout mice had impaired autophagosome-lysosome fusion leading to an increased accumulation of autophagosomes and hence cardiac dysfunction [120], suggesting a role for mitochondrial dynamics in autophagy. Conversely, emerging

evidence suggest a pivotal role of autophagy in cardioprotective strategies against IRI [121]. In the view of these authors, autophagy may increase cell survival by acutely removing damaged cells preventing the initiation of other cell death pathways. Death processes may also share common signals. This has been termed necrapoptosis [122].

1.4 Protecting the heart against ischaemia-reperfusion injury

The heart, as any living tissue, has endogenous protective mechanisms which, when activated, render it resistant to cell death, in other words the heart can be "conditioned" [123] against ischaemia-reperfusion injury. Initial studies by Murry et al, 1986 [124], showed that a protocol of short bursts of ischaemia interspersed with short reperfusion periods prior to a prolonged insult of ischaemia and reperfusion, was associated with a reduction in MI size by 75%. This was termed 'ischaemic preconditioning' (IPC) [124]. The phenomenon of IPC is highly reproducible in all species [123]. IPC elicits a biphasic pattern of protection, an acute phase of protection (transient effect lasting for 2-3 hours) and a second, delayed phase of protection (sustained effect lasting 24-72 hours). This second phase is known as the second window of protection (SWOP)[125, 126].

Over the years, this protective manoeuvre was followed by the discovery of other protective mechanisms such as pharmacological conditioning [127] (protection against myocardial infarction by the administration of specific drugs), ischaemic post conditioning (IPost) [128] (by using a similar procedure as IPC but applied at the moment of reperfusion) and also remote ischaemic conditioning [129] (whereby, an organ or tissue remote from the heart is ischaemically conditioned with a subsequent increase in resistance versus IRI in the heart).

1.4.1 Ischaemic Preconditioning

Since its original discovery, IPC has been extensively studied and the mechanisms by which this phenomenon occurs have been well defined. It is known now that IPC involves complex cellular prosurvival pathways. For IPC to be successful, reperfusion must follow the lethal ischaemic insult [130] to allow the triggering components to activate the protective mediators. These triggering mechanisms include the release of adenosine, opioids, ROS, bradykinin and Ca^{2+} that activate various receptor signalling pathways that converge onto the mitochondria. Initial work by Liu et al, 1991 demonstrated that protection afforded by IPC was blocked by an adenosine receptor antagonist (G_i protein coupled receptor blocker) and the protective effects of IPC could be mimicked by exogenous adenosine [131]. G-protein coupled receptor (GPCR) signalling appeared to play a central role in the IPC induced protection, other

substances such as bradykinin [132] and opioids [133] worked in parallel with adenosine to elicit protection via GPCRs with the end effector being activation of protein kinase C (PKC), albeit via different signalling pathways [130].

One of the most recognised signalling motifs resulting in cardioprotection is the reperfusion injury salvage kinase (RISK) pathway [134]. This pathway involves the activation and signalling of kinase proteins, namely phosphatidylinositol-3-kinase (PI3K) and **Akt,** and also Ras/Raf/MEK1/2 and ERK1/2 following an IPC stimulus. Prior to the establishment of the RISK pathway, PI3K was shown to be instrumental, with attenuation of IPC's cardioprotective effect in the presence of PI3K inhibitors [135, 136].

The serine/threonine kinase Akt is an important cellular signalling molecule that can be activated by the binding of ligands to cell surface receptors in the myocardium. Ligands including growth factors, cytokines or hormones interact with and activate receptors either by initiating the phosphorylation of intracellular domains of receptor tyrosine kinases (RTKs) or causing a conformational change of G-protein coupled receptors (GPCRs). Activation of Akt can result in a plethora of effects depending on the substrate and the receptor that is activated. Upon stimulation, the activated RTK or GPCR binds to the SH2 domain of the p85 subunit of PI3K, ensuing in the movement of the PI3K complex closer to the cell membrane. The PI3K catalytic subunit p110, catalyses the conversion of membrane bound phosphatidylinositol-3,4-biphosphate (PIP_2) to phosphatidylinositol-3,4,5-triphosphate (PIP_3). Akt and phosphoinositide-dependent protein kinase-1 (PDK-1) bind to the PIP_3, resulting in a complex of Akt/PDK-1/PIP_3 at the plasma membrane [137.] Here, Akt is phosphorylated and activated by PDK-1 at threonine-308 and serine-473. Phosphorylated Akt is released from the membrane complex and migrates throughout the cell activating downstream target molecules (summarised in Figure 1.17). Activation of Akt can be hindered by the inhibitory action of phosphoinositide phosphatases on PI3K induced production of PIP_3. Protein phosphatase and tensin homolog deleted on chromosome 10 (PTEN), a protein-lipid phosphatase, specifically catalyses the dephosphorylation of PIP_3 resulting in PIP_2[138].

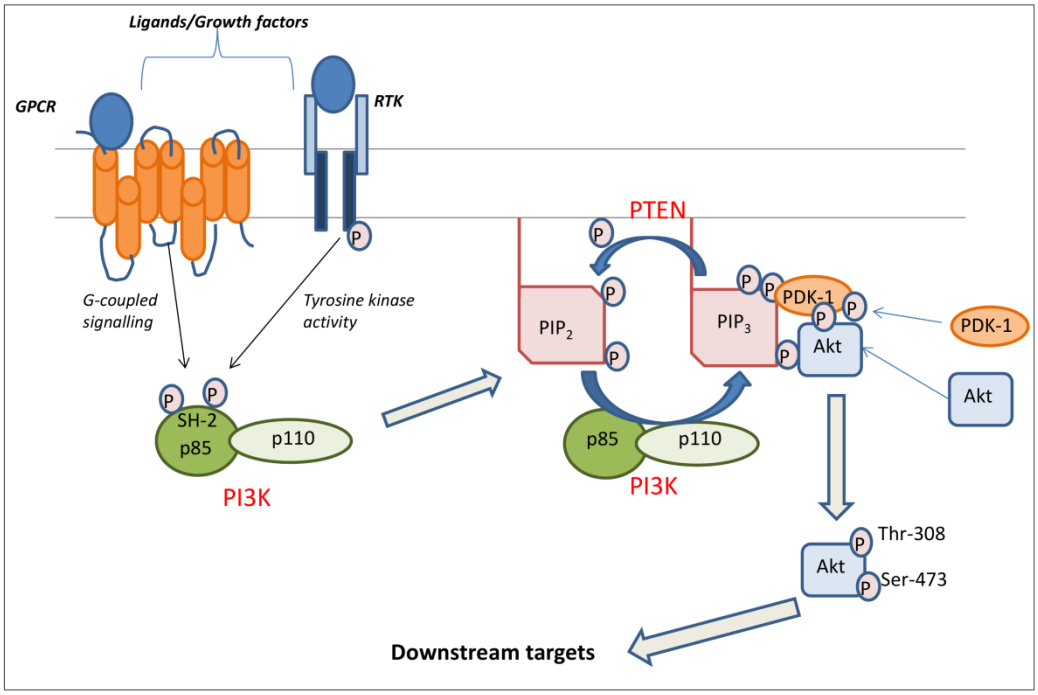

Figure 1.17: Activation of the PI3K/Akt pathway. Activation of Akt. Ligands/growth factors activate receptor tyrosine kinases (RTK) or G-protein coupled receptors (GPCR) on the plasma membrane. Activation promotes phosphorylation of SH2 domain of the p85 subunit of PI3K and sub sequential movement of the PI3K complex closer to the cell membrane. The PI3K catalytic subunit p110, catalyses the conversion of membrane bound phosphatidylinositol-3,4-biphosphate (PIP_2) to phosphatidylinositol-3,4,5-triphosphate (PIP_3). Akt and phosphoinositide-dependent protein kinase-1 (PDK-1) bind to the PIP_3, resulting in a complex of Akt/PDK-1/PIP_3 at the plasma membrane. Akt-P is liberated into the cytoplasm to target downstream signalling molecules.

Akt signalling is central to numerous cellular processes including growth, survival, proliferation, metabolism, glucose uptake and also gene expression[139] (summarised in Figure 1.18). Akt promotes cell survival by blocking anti-apoptotic signals and initiating pro-survival signals, these effects are vital in times of cellular stress such as ischaemia-reperfusion. Pro-survival signals include the activation of endothelial nitric oxide synthase (eNOS), which results in an increase of nitric oxide (NO). NO serves important roles within the heart including ventricular relaxation and regulation of vascular smooth muscle proliferation. In the context of ischaemia-reperfusion injury, Akt activation can increase PKG via eNOS/NO and activate mitochondrial PKCε in response to IPC. This mediates the opening of the mitochondrial K_{ATP} channel[140] and subsequently keeps the mPTP closed, resulting in protection from IRI [141].

Other pro-survival targets include phosphorylation and inactivation of glycogen synthase kinase-3β (GSK-3β) and inhibition of pro-apoptotic mediators. Insulin

stimulated Akt-phosphorylation was shown to phosphorylate BAD at serine-136 releasing anti-apoptotic BCL-xL from the BAD/BCL-xL complex. The dissociation of BCL-xL protected cardiomyocytes from stress induced apoptosis[142]. Phosphorylation of BAX, at serine-184, by Akt causes a conformational change within BAX preventing its translocation to the mitochondria where it usually performs pro-apoptotic actions[143]. In the heart, deletion of the BAX gene has also been shown to decrease IRI[144]. Akt can also reduce the transcription of death receptor ligands by phosphorylating and inactivating the transcription factor FOXO3a. Phosphorylation of FOXO3a in the nucleus by Akt results in the shuttling of FOXO3a into the cytoplasm, where it remains inactive. Therefore the initiation of apoptotic signalling pathways are reduced [145].

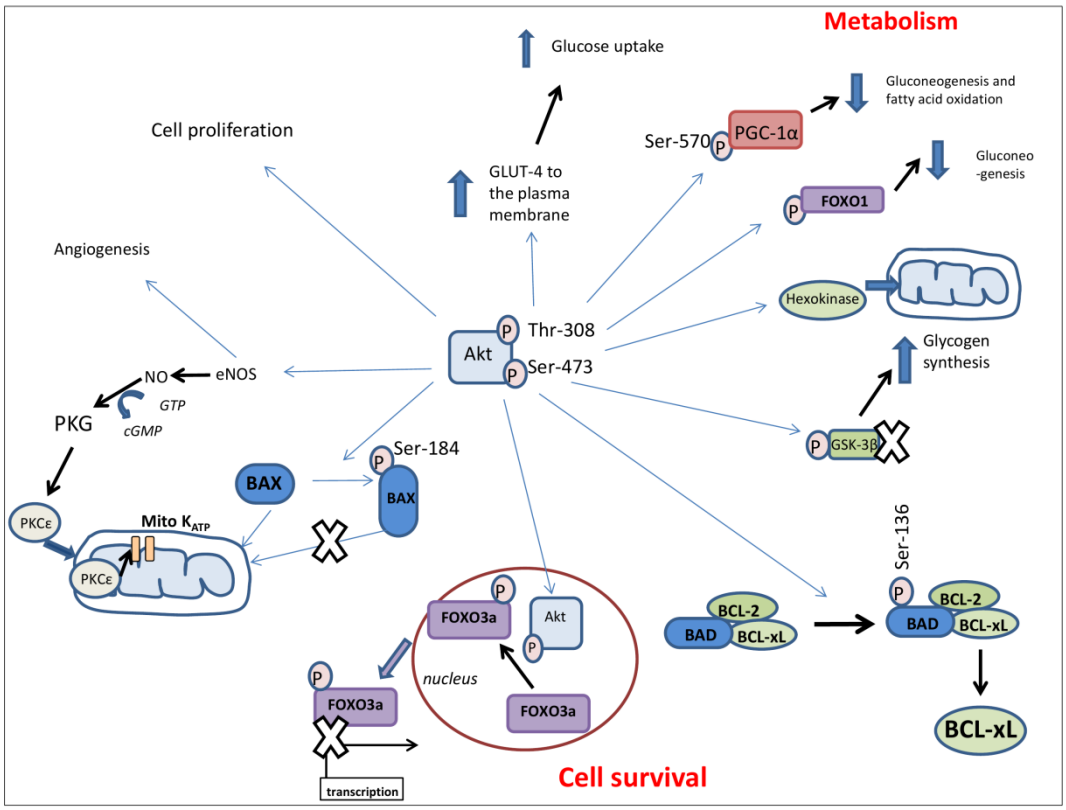

Figure 1.18: Downstream targets of Akt-P Akt is central to numerous cellular processes, it can activate and de-activate signalling molecules and transcription factors by phosphorylation leading to a plethora of effects including cellular survival and metabolism.

Recent advances have suggested post translational modifications other than phosphorylation could be involved in the protection elicited by IPC, in particular lysine acetylation of important signalling molecules during IRI [146]. Silent information regulator of transcription (SIRT-1), a class II histone deacetylase has emerged as an important player in IR and cardioprotection. Cardiac-specific overexpression protected the mouse heart from IRI; moreover this protection was linked to a reduction in oxidative stress through SIRT-1 mediated transcription of FoxO1 driving up regulation of pro-survival

manganese superoxide dismutase and down regulation of proapoptotic molecules[147]. Nadtochiy et al, 2011 demonstrated that lysine acetylation by SIRT-1 also occurs during acute IPC leading to reduction in infarct size; inhibition of SIRT-1 activity directly or indirectly limited this reduction[148]. Moreover, this group also showed that this acute protection was mediated by SIRT-1, however not by transcriptional targets but by lysine deacetylation of signalling molecules. p53, NFκB and eNOS emerged as possible targets[146, 148]. Interestingly, SIRT-1 also modulates the autophagic machinery[146], a critical event in IRI which has recently been linked to IPC related cardioprotection[121, 149]. These pathways are summarised in Figure 1.19.

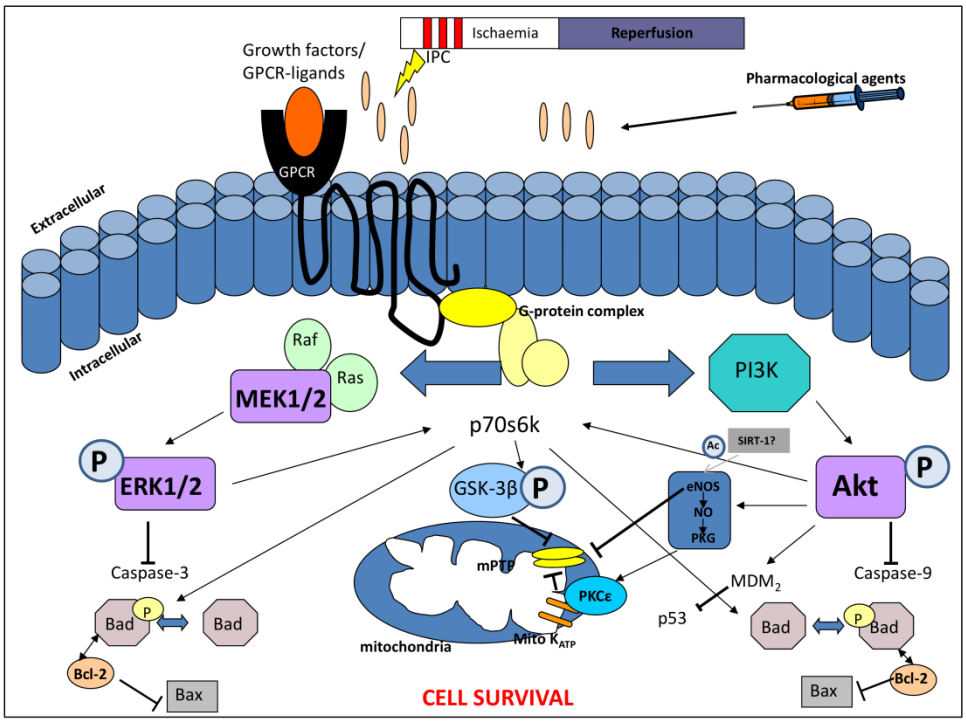

Figure 1.19: The cellular mechanisms involved in ischaemic preconditioning IPC or pharmacological agents initiate the release of G-protein coupled receptor (GPCR) agonists which bind to the receptor and activate numerous signalling pathways. Phosphatidylinositol-3-kinase (PI3K) and Ras activation, can lead to activation of a number of downstream molecules such as Akt, extracellular regulated kinase (ERK), nitric oxide synthase (NOS) and inactivation of glycogen synthase kinase-3β (GSK-3β). These converge to activate the mitochondrial ATP-dependent potassium channel (K_{ATP}), closing the mitochondrial permeable transition pore (mPTP) resulting in protection from IRI

1.4.2 Protective effect of IPC at reperfusion

It was originally proposed by Jenning's group that the protection caused by IPC was targeting detrimental effects caused during ischaemia [150], however Hausenloy et al, 2005 showed that IPC exerts its protection early in reperfusion as well [151]. This led to the development of post conditioning strategies, the ability to apply pharmacological or ischaemic conditioning after a prolonged ischaemic event, at the onset of reperfusion, a scenario that has a more clinically relevant application. The involvement of the RISK

pathway kinases have been extensively studied as a successful cardioprotective strategy at reperfusion [152], but the failure of some groups to demonstrate the involvement of RISK kinases in the cardioprotective effect of IPost led to speculation that an alternative cardioprotective pathway may exist. In this respect, Darling et al, 2005 failed to demonstrate a role for PI3K/Akt signalling following IPost [153] in ex vivo rabbit hearts. Furthermore, in 2009 Lecerda et al demonstrated that application of tumor necrosis factor (TNF) at time of reperfusion could mimic IPost in the absence of Akt activation or in the presence of the PI3K inhibitor Wortmannin [154]. The administration of TNF at reperfusion activated the transcription factor, signal transducer and activator of transcription 3 (STAT3) which leads to the initiation of pro survival JAK/STAT pathway. Thereby, an alternative IPost signalling pathway was proposed: the Survival Activating Factor Enhancement (SAFE) pathway [155].

1.4.3 Clinically relevant conditioning strategies

For obvious reasons, direct ischaemic conditioning of the myocardium is not applicable in human subjects (apart from surgical settings such as CABG). An intriguing concept has emerged that exploits similar endogenous cardioprotective signalling pathways to that seen elicited by direct ischaemic pre and post conditioning of the myocardium itself. This phenomenon is called remote ischaemic conditioning (RIC). An organ or tissue remote from the heart is subjected to short, repeated episodes of ischaemia-reperfusion initiating cardioprotective signalling pathways that can converge onto and protect the heart from the consequences of lethal ischaemia-reperfusion injury. Short bursts of hind limb ischaemia-reperfusion cycles have been shown to successfully elicit cardioprotective effects in animal models when applied before[156], during[157] or after[158] the major ischaemic event. However, the translation of this procedure into clinical settings has been controversial, yielding both negative and positive results[159].

Activation of pro-survival signalling cascades by ischaemic conditioning has been proven to attenuate reperfusion induced cell death. Therefore, it was suggested that application of appropriate exogenous factors or agents may augment endogenous intracellular prosurvival pathways and elicit cardioprotection. Numerous cardio-related drugs that are currently prescribed have been shown to have cardioprotective benefits. These include statins (HMG-CoA reductase inhibitors)[160] and angiotensin-converting enzyme inhibitors (ACE-I)[161]. Atorvastatin, administered during early reperfusion, reduced infarct size via the activation of the PI3K-Akt pathway[162]. The protective effect of ACE-I are attributed to bradykinin (BK) associated activation of GPCRs[163]. Moreover, direct administration of BK at reperfusion also activated the PI3K-Akt pathway[164].

However, BK administration also stimulated other RISK pathway components ERK1/2 kinase and subsequent eNOS activation leading to protection[165].

Interestingly, oral hypoglycaemic agents have also been shown to reduce cardiovascular morbidity/mortality. These include metformin, thiazolidineodiones and most recently incretin therapies (dipeptidyl peptidase-4 inhibitors/ GLP-1 analogues)[166]. These agents have also been investigated in animal models and will be discussed later in more detail.

1.5 Diabetic heart and Ischaemia-reperfusion Injury

1.5.1 Diabetes Mellitus

The incidence of diabetes is increasing at an alarming rate throughout the world. Globally, the estimated prevalence of diabetes for 2010 was 285 million and is expected to affect 438 million people by 2030 [167]. In the UK, there are 2.6 million people who have been diagnosed with diabetes (2009) which equates to a 4.1 % average prevalence and it is estimated that 4 million people will be diabetic by 2025 [168]. Diabetes mellitus is a major risk factor for IHD- patients with diabetes are 2-3 times more likely to develop IHD [169].

Diabetes mellitus is a metabolic disease that is characterised by a high level of glucose in the blood. In normal physiological settings the control of blood glucose is tightly regulated. In response to an increase in circulating glucose levels, GLUT2, a membrane bound glucose transporter initiates the uptake of glucose passively into the pancreatic β cells in the islets of Langerhans. Here, glucose is metabolized by glycolysis, resulting in an increased production of ATP and subsequent closure of the ATP-sensitive potassium channels in the cell membrane. This causes membrane depolarization, opening of voltage gated Ca^{2+} channels and an influx of Ca^{2+} into the β-cell. This accumulation of Ca^{2+} triggers the fusion of insulin vesicles and the release of insulin into the bloodstream. Insulin binds to insulin specific tyrosine kinase receptors (IRS) on the plasma membrane of a variety of tissues, including fat, muscle and liver. In fat and muscle, insulin binds to the α-subunit of the IRS receptor triggering the tyrosine kinase activity of the β-subunit. Phosphorylation of PI3K at the p85 subunit activates Akt leading to the translocation of the glucose transporter GLUT4 to the plasma membrane and entry of glucose into the cell to be used for energy production (Figure 1.20).

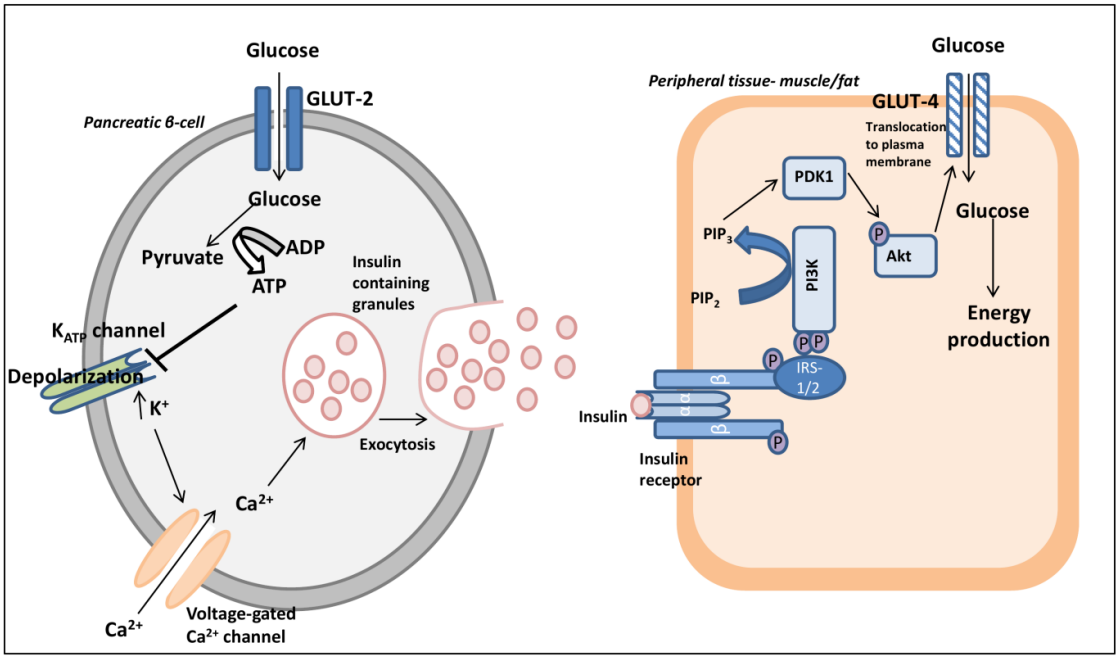

Figure 1.20: Blood glucose regulation. Circulating blood glucose enters pancreatic β cells via the Glut-2 transporter located on the plasma membrane. The generation of ATP from glucose closes the ATP-gated K channels causing the accumulation of K+ inside the cell, depolarisation of the membrane potential and subsequent entry of Ca2+ into the cell. Ca2+ induced exocytosis of granule releases insulin into the circulation where it can act on peripheral tissues and promote glucose uptake.

Glucose levels are tightly regulated by the liver. As described, high glucose levels lead to an increase in insulin secretion. At the level of the liver, insulin binds to its receptors causing cessation of glucose production accompanied to an escalation in glycogen production and storage. When glucose levels fall below a threshold, glucagon a hormone released from the pancreatic α-cells, acts at the liver to increase the production of glucose from the glycogen stores. Insulin and glucagon are two vital hormones required for the liver to ensure glucose levels remain in a narrow range in the circulation (Figure 1.21). An impaired secretion or action of either of these hormones can lead to high or low blood glucose, which if left can manifest into metabolic conditions. Diabetes mellitus is a metabolic disease that is characterised by hyperglycaemia.

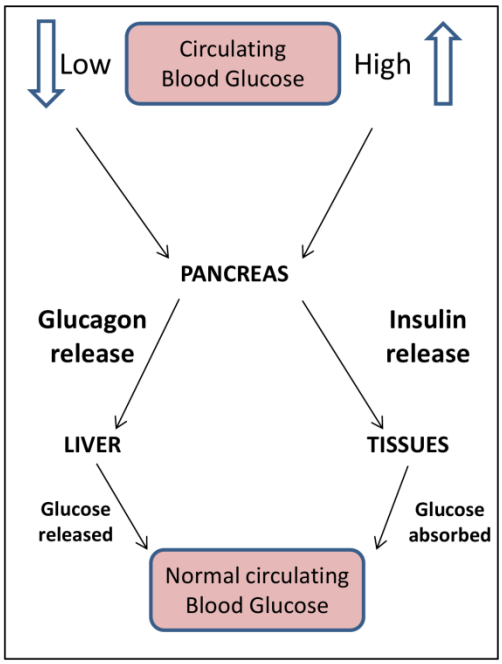

Figure 1.21: Regulation of circulating blood glucose. In response to low glucose, glucagon is released from the pancreatic α cells and acts at the liver stimulating glucose release. In response to high glucose insulin is released from the pancreatic β cells and acts at peripheral tissues stimulating glucose uptake from the circulation.

There are two types of diabetes mellitus, type 1 diabetes and type 2 diabetes. Type 1 diabetes is characterized by the inability of the body to produce insulin; this is caused by cellular-mediated programming of the autoimmune system and subsequent destruction of pancreatic beta-cells, the cells responsible for insulin production. The prevalence of this form of diabetes is relatively low and usually starts early in life [170]. Whereas type 2 diabetes is known as the insulin resistant form; insulin is produced, however, the target tissues gradually become insensitive or resistant to the action of insulin and as a consequence there is an increase in circulating blood glucose levels [171]. Moreover, it has been reported in type 2 diabetic patients, plasma glucagon concentrations are inappropriately high, which consequently increases the hyperglycaemic state driving more production of glucose from the liver[172]. This form accounts for a high percentage of all diabetes and is historically more common in older age groups; however the prevalence of type 2 diabetes in children and young adults is also increasing especially in Westernized societies [173].

Alongside the increased risk that diabetic patients have in developing IHD, vascular complications in chronic diabetic patients are also possible[174] and can be classified into two types: microangiopathy and macroangiopathy [175]. Diabetic microangiopathy is the term coined to describe the damage caused to small blood vessels and capillaries within the body as a consequence of chronic hyperglycaemia.

The vascular endothelial cells demonstrate no significant modifications in glucose transport in response to high glucose therefore the vasculature is particularly vulnerable to intracellular hyperglycaemia and the subsequent associated damage[176]. Damage to these vessels can lead to a decreased supply of oxygen and vital substrates to the tissues, which can result in adverse clinical outcomes such as retinopathy, nephropathy, neuropathy and diabetic foot [177].

Diabetic retinopathy is the most common cause of blindness in the UK, with an increased prevalence in old age and uncontrolled diabetes[178]. Clinical features of diabetic retinopathy include increased vascular permeability resulting in macular oedema, vascular microaneurysms, lipoprotein drusen deposits and eventual vascular proliferation[179]. Hyperglycaemia, oxidative stress and advanced glycation end products leading to increased apoptosis in the eye contribute to these features[180]. Diabetic patients have an impaired ability to generate new blood vessels in response to ischaemia, thereby resulting in reduced collateral vessel formation in ischaemic hearts and foot ulcers[181]. The healing process of foot ulcers and other chronic wounds have been shown both clinically and experimentally to be impaired in diabetes. This impairment is caused by several other intrinsic factors associated with diabetes such as neuropathy and vascular complication, but extrinsic factors such as wound infection and callus formation also contribute to this deficiency[182].

Diabetic nephropathy was classically associated with type 1 diabetes, however its prevalence in type 2 diabetes is rising and is considered a principal cause of renal end-stage disease[183]. This diabetic complication is associated with hyperglycaemia-induced formation of advanced glycation end products [184] or by increased metabolism. This results in elevated levels of oxidative stress and activation of PKC driving the increased production of cytokines[183, 184]. As a result, morphological changes of the glomerular basement membrane and mesangial matrix occur which correlate with impaired glomerular filtration[183].

Macroangiopathy as a consequence of diabetes mainly involves an accelerated form of atherosclerosis [185], another risk factor for cardiovascular disease. It affects the larger blood vessels within the body, where an accumulation of fatty materials such as cholesterol can stick to the vessel walls and impair blood flow [186]. Diabetic complications, atherosclerosis, hypertension and many other CV risk factors such as old age can all interact and render the heart more susceptible to IHD [187].

1.5.2 The diabetic heart

The diabetic heart is prone to developing pathological conditions that can contribute to an increased susceptibility to IHD, such as diabetic cardiomyopathy and angiopathy [188]. Diabetic cardiomyopathy causes structural changes which lead to abnormal functionality of the heart; these include increased fibrosis, myocyte atrophy and apoptosis in the extracellular space of the diabetic myocardium [189]. These changes can eventually result in left ventricular hypertrophy (LVH) and diastolic/systolic dysfunction [190]. Changes also occur at the molecular level including endothelial dysfunction, metabolic perturbations and differences in cellular signalling [190], described in further detail later.

Treatments lowering high blood glucose have proved effective in reducing the clinical complications of diabetes however they have not completely prevented cardiovascular events from occurring. Alternative strategies have been employed to target the cellular changes that may occur during hyperglycaemia.

1.5.2.1 Oxidative stress in diabetes

Oxidative stress caused by excessive blood glucose has been suggested to be a vital link in the progression from diabetes to cardiovascular disease. Oxidative stress is defined by a surplus accumulation of reactive molecules, such as reactive oxygen species (ROS) and reactive nitrogen species (RNS). ROS exist in numerous forms within the cardiovascular system; free radical molecules include superoxide ($^{\bullet}O_2^-$) and hydroxyl ($^{\bullet}OH$), and in non-radical forms like hydrogen peroxide (H_2O_2). RNS molecules also exist including the free radical nitric oxide (NO) and non-radicals such as peroxynitrite ($ONOO^-$) [191]. These molecules have numerous beneficial roles within normal physiology, however become detrimental if they are overproduced or not sufficiently removed. Moreover, ROS or RNS can lead to subsequent production of other free radicals contributing to more pronounced oxidative stress.

$^{\bullet}O_2^-$ can be generated from numerous sources; from the vasculature via the action of oxidase enzymes including NADPH oxidase and xanthine oxidase which reduce O_2 by one electron leading to its formation and also from the electron transport chain (ETC) within the mitochondria. Under normal conditions, $^{\bullet}O_2^-$ produced is subsequently converted to the less cytotoxic radical H_2O_2 via enzymes of the superoxide dismutase (SOD) family, manganese (MnSOD) within the mitochondria and copper/zinc (Cu/Zn-SOD) within the cytosol and H_2O_2 is converted to H_2O by catalase or gluthathione peroxidase (GPx). NO is produced and released in the vasculature,

endothelial nitric oxide synthase (eNOS) a cytochrome p450 reductase-like enzyme uses tetrahydrobiopterin (BH_4) to transfer electrons to the amino acid L-arginine to produce NO. NO has numerous beneficial actions, however NO easily reacts with $^{\bullet}O_2^-$ to generate $ONOO^-$ to cause deleterious downstream effects. In the absence of L-arginine or BH_4, eNOS becomes uncoupled and transfers electrons to molecular O_2 and produces $^{\bullet}O_2^-$ and H_2O_2. The potential sources of ROS production are summarised in Figure 1.22.

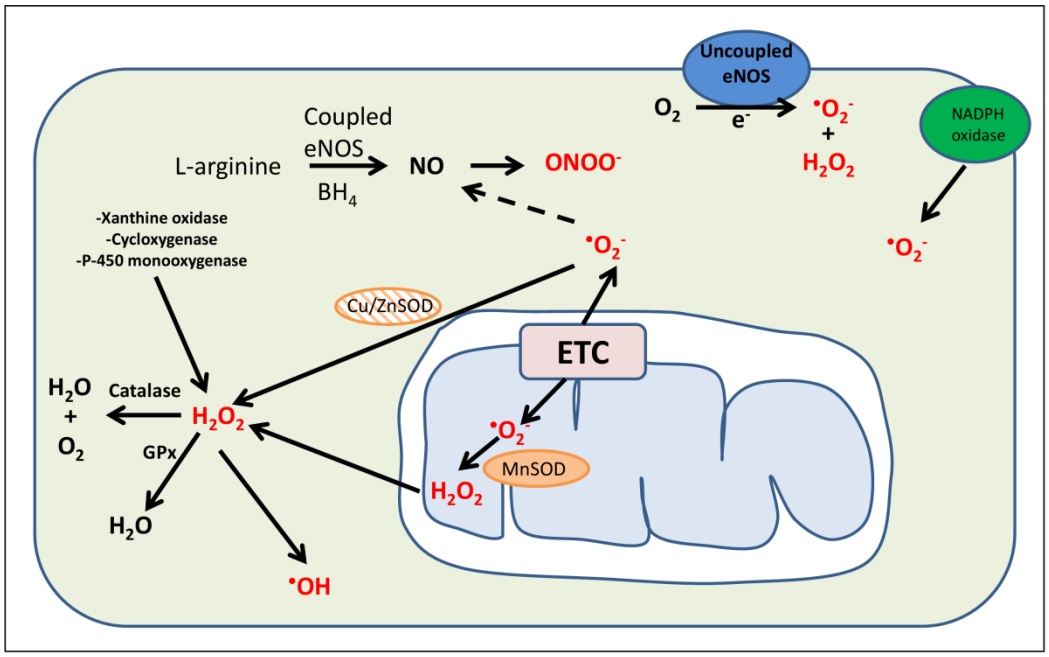

Figure 1.22: The generation of superoxide and reactive oxygen species. There are numerous sources of reactive oxygen species and free radical species in the cell including the electron transport chain (ETC) in the mitochondria and vascular oxidase enzymes. Under normal conditions, superoxide (•O2-) is converted to the less toxic radical hydrogen peroxide (H2O2) via enzymes of the superoxide dismutase (SOD). Furthermore, this radical is changed by catalase or gluthathione peroxidase (GPx) into water and oxygen.

Mitochondrial overproduction of ROS is thought to be the link between hyperglycaemia and diabetic complications. As described earlier, intracellular glucose metabolism begins with glycolysis in the cytoplasm generating pyruvate and NADH, in the presence of O_2 pyruvate is transported into the mitochondria and enters the ETC to produce ATP. An increase in intracellular glucose up regulates this process, driving increased generation of electron donors NADH and $FADH_2$ which lead to an increased movement of protons across the inner membrane and a subsequently high mitochondrial membrane potential. This process inhibits electron transport at complex III, thereby increasing the lifetime of superoxide producing intermediates of ubiquinone such as ubisemiquinone [192]. This increase in oxidative stress has been suggested to be the unifying hypothesis linking the proposed mechanisms of hyperglycaemia induced diabetic complications [192]. The proposed mechanisms are increased polyol pathway

flux, increased activation of PKC, increased advanced glycation end-product (AGE) formation and increased hexosamine pathway flux, which are reviewed in [193].

1.5.2.2 Mitochondria in diabetes

As already described, mitochondria can contribute to the increased oxidative stress seen in diabetes. Mitochondrial function is reflected by their structure, number and morphology. The distortion of mitochondrial organisation, swelling of mitochondria or accumulation of small mitochondria has been frequently reported as a characteristic of the diabetic tissue [194, 195].

Alterations in mitochondrial morphology are linked to mitochondrial dysfunction. Interestingly, dynamic changes in mitochondrial morphology have been associated with glucose-induced overproduction of ROS. Yu et al, 2006 demonstrated that either inhibiting mitochondrial fission or promoting mitochondrial fusion prevented ROS increase under hyperglycaemic conditions in cardiac cells [196]. Their data suggests that mitochondrial fragmentation in response to high glucose leads to ROS overproduction via enhanced respiration and mitochondrial hyperpolarization [196]. In accordance with this study, Makino et al 2011 showed an increased mitochondrial fragmentation in response to high glucose in neonatal cardiomyocytes, with an associated reduced expression of fusion protein OPA-1 and moreover an increased O-linked N-acetyl-glucosamine glycosylation (O-GlcNAcylation) of this protein [197]. Increased O-GlcNAcylation of proteins has been related to an increased activation of the hexosamine pathway, a pathway that is linked to increased oxidative stress production in diabetes. In type 2 diabetic mice, high glucose induced an increased O-GlcNAcylation of mitochondrial proteins [198] and an increased O-GlcNAcylation of cardiac DRP-1 (fission protein) resulting in impaired mitochondrial function [199].

Mitochondria have their own genome and the capability to autoreplicate; their proteins can be encoded either by the mitochondrial or by the nuclear genomes. The double stranded mitochondrial DNA (mtDNA) contains genes encoding ETC complexes and RNAs necessary for translation. Due to their close proximity to the ROS generating ETC complex, mtDNA are considered to be at greater risk of mutation[200]. Diabetes associated increased oxidative stress augments the occurrence of mtDNA mutations leading to a decline in mitochondrial function[200]. Rate of mutation is higher in diabetic patients compared to non-diabetic patients[201]. Left ventricle samples of diabetic GK rat hearts and isolated cardiomyocytes exposed to high glucose had significantly more mtDNA damage, this resulted in an associated decline in mitochondrial function[200]. Oxidative stress can also indirectly damage mtDNA, Medikayala et al, 2011

demonstrated that ROS augmented topoisomerase DNA cleavage activity that resulted in greater mtDNA damage[202].

1.5.2.3 PGC-1α and diabetes?

Compromised mitochondrial biogenesis and hence function can be influenced by environmental stresses and has been linked to numerous diseases[40], especially between metabolic and cardiovascular diseases. Inactivation or down regulation of PGC-1α has been implicated in diabetes[42].

PGC-1α is essential to maintain an efficient control on energy metabolism and mitochondrial functionality. If the expression or modulation of this coactivator is hindered, functional defects can occur such as decreased cardiac contractility. A diabetes-associated down regulation of PGC-1α expression and its associated genes has been demonstrated in skeletal muscle[203, 204] and also in the heart of STZ diabetic rats[205]. Interestingly, Duncan et al showed in their murine model of the metabolic syndrome that in the early phases of insulin-resistance and diabetes, mitochondrial biogenesis is driven by an up regulation of the PPARα/PGC-1α gene regulatory pathway[206]. This overexpression of PGC-1α is likely to be a compensatory mechanism to facilitate the use of the increased fatty acid load in the heart. In the later stages of diabetes or as the diabetic heart ages, the PGC-1α expression and pathway are down regulated and therefore the risk of heart failure may increase [207, 208]. Interestingly, Zhang et al, 2013 showed that chronic administration of a novel small molecule ZLN005, in myotubes and skeletal muscle of diabetic mice, led to activation of AMPK and subsequent up regulation of PGC-1α. This led to increased fat oxidation and improved glucose tolerance, pyruvate tolerance and insulin sensitivity[209].

1.5.2.4 Energy metabolism in diabetes

Myocardial energy is provided in a dynamic manner. Numerous substrates are utilized to produce ATP in order to meet the energy demands of the heart. As previously mentioned, mitochondrial fatty acid oxidation (FAO) is the main source of energy, however the utilization of glucose as an energy substrate is still pivotal in maintaining ATP production under a variety of physiological conditions. In the diabetic heart, the utilization of glucose as an energy substrate is greatly decreased, with an increased reliance on fatty acid oxidation to provide energy (Figure 1.23). Fatty acids are a less efficient substrate than glucose, even though FAO generates a greater amount of ATP, more oxygen molecules are required per ATP molecule produced[210]. This shift in metabolism and reliance on FAO imposes stress on the cardiomyocyte contributing to

eventual diabetic cardiomyopathy. Myocardial glucose utilization can be compromised at numerous points; in type 2 diabetic animals reduced GLUT-4 protein expression and depressed insulin signalling hinders the control of myocardial glucose and uptake, and also increases circulating free fatty acids[210, 211]. Moreover, fatty acids also inhibit insulin signalling pathways reducing insulin action, which further hampers the use of glucose as an energy substrate. Folmes et al 2006 showed that fatty acids also attenuate the insulin regulation of AMPK, the metabolic switch in the heart in the control of glucose and FAO[212]. Enhanced fatty acid uptake is facilitated by increased expression of fatty acid transporters, CD36 and $FABP_{pm}$, in STZ-induced diabetes[213]. Furthermore, in Zucker fatty rats, these transporters translocate to the cardiomyocyte plasmalemmal membrane to enhance fatty acid uptake[214].

The nuclear receptor, PPAR-α, is a main regulator of cardiac fatty acid metabolism. It's target genes include those encoding proteins involved in fatty acid uptake and utilization. In diabetic animal models during early phases of insulin resistance increases in circulating lipids activate PPAR-α and subsequent genes involved in FAO[215]. Alongside this action, PPAR-α activation reduces the expression of genes that regulate the uptake and utilization of glucose[215]. Removal of cardiac PPAR-α restored the expression of such genes including GLUT-4, promoting glucose uptake and improved myocardial recovery following ischaemia[216]. Interestingly, transgenic PPAR-α mice exhibit a metabolic phenotype similar to diabetic hearts. It appears that these diabetes-associated alterations in cardiac metabolism precede the development of cardiomyopathy and cardiac dysfunction.

Changes in cardiac metabolism in the diabetic heart can influence Ca^{2+} homeostasis, cardiac efficiency, glucotoxicity and eventual mitochondrial dysfunction[217], all of which will influence the ability of the heart to withstand injury such as IRI. Hyperglycaemia-induced-diabetic-complications have been linked to diabetic cardiomyopathy. However as described, the decreased uptake of glucose in the diabetic heart may suggest that β-oxidation of fatty acids may drive oxidative stress in diabetes leading to such complications.

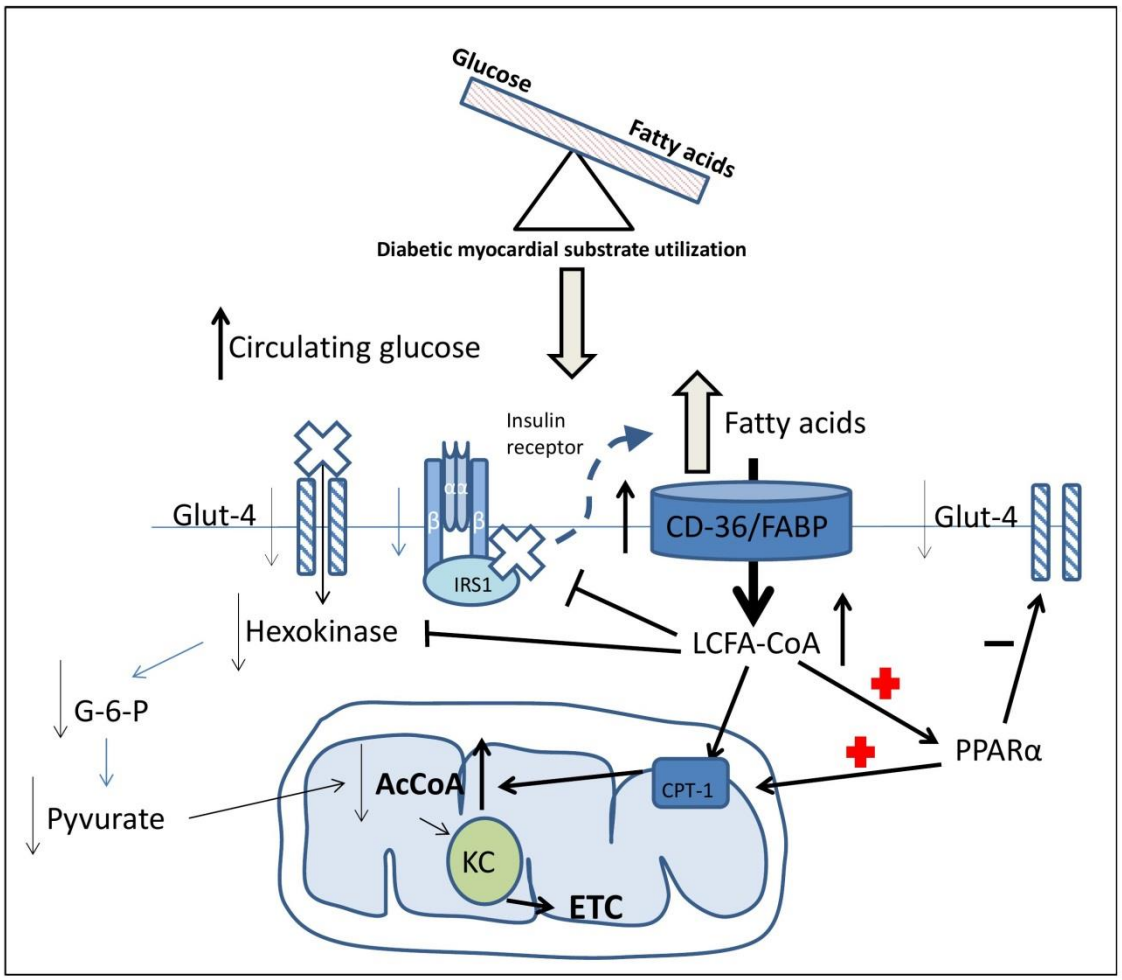

Figure 1.23: Energy metabolism in the diabetic heart. Insulin resistance alongside a decrease in the glucose transporter Glut-4 at the plasma membrane in type 2 diabetes result in a decreased entry of glucose into the cell for the production of ATP. As a compensatory mechanism, the diabetic heart becomes reliant on fatty acids as a substrate for ATP production. Free fatty acids enter the cell via the fatty acid transporters (CD-36/FABP) resulting in an accumulation of long chain fatty acyl CoA (LCFA-CoA). LCFA-CoA is transported into the mitochondria via carnitine palmitoyl transferase 1 (CPT-1) (as described in Figure 1.5), converted to acetyl CoA (AcCoA) and enters the Krebs cycle (KC). An increase in cytoplasmic LCFA-CoA also contributes to decreased glycolysis by inhibitory actions on hexokinase, insulin receptor substrate 1 (IRS1) and increasing the activity of peroxisome proliferator-activated receptor alpha (PPARα). PPARα decreases the transcription of the glucose transporter Glut4 therefore additionally decreasing the possible entry of glucose into the cell.

1.5.3 Susceptibility of the diabetic heart to ischaemia-reperfusion injury

Numerous studies suggest that the diabetic heart is more susceptible to IRI[217, 218]. This has been demonstrated in both type 1 and type 2 diabetic models. Utilizing acute hyperglycaemia and type 1 diabetic models; Marfella et al, 2002 showed that isolated non-diabetic rat hearts retrogradely perfused with a hyperglycaemic (33mmol/L glucose) buffer had a greater infarct size following ischaemia and reperfusion *ex vivo* than rat hearts that were perfused with normoglycaemic buffer [219]. Moreover, diabetic rats induced by a high dose of STZ (70mg/kg for 9 days) exhibiting blood glucose levels of 22mmol/L were more susceptible to ischaemia/reperfusion injury *in vivo* than

normoglycaemic rats [219]. Hyperglycaemic conditions in both models caused a decreased transactivation of the hypoxic inducible factor HIF-1α, which controls the up regulation of vascular endothelial growth factor (VEGF) in response to hypoxia, an essential mediator of neovascularization following ischaemia [219]. An impairment of this axis, as seems the case in these diabetic models and other diabetic tissue[220], will lead to inadequate revascularization of coronary vessels following ischaemia and hence could produce worse outcomes for the diabetic patient[220].

A lower dose of STZ (50mg/kg) administered to rats for a longer time period of 6 weeks caused an increased sensitivity to IRI *in vivo* in rats, accompanied by decreased phosphorylation of Akt, VEGF and NO and increased levels of caspase-3 [221]. Interestingly, in this investigation when STZ was administered for only 2 weeks prior to experimentation, the opposite outcome was recorded with a decreased susceptibility to IRI and subsequent signalling changes were reversed[221]. Other rodent studies also showed infusing high glucose during ischaemia caused an increase in apoptosis and infarct size. They attributed this effect to decreased phosphorylation of 'pro-survival' Akt resulting in de-phosphorylation and increased 'pro death' activity of GSK-3β [222]. With regard to the possible mechanism, hyperglycaemia in rat cardiomyocytes was shown to promote p53-dependent activation of apoptosis[223]. Acute hyperglycaemia has also been shown to increase the susceptibility to infarction in non-rodent models; 15% dextrose infused prior to IRI *in vivo* or chemically induced diabetes (3 weeks STZ) in dogs' increased MI size[224]. Furthermore, rabbits infused with 50% dextrose to elicit a hyperglycaemic state of 600mg/dl prior to ischaemia, also recorded a greater susceptibility to infarction *in vivo*[225].

Models of type 2 diabetes have also demonstrated an increased susceptibility to IRI; interestingly these studies were performed *in vivo* or *ex vivo* with the addition of fatty acid substrates in the perfusate, similar to those likely to be found in the *in vivo* scenario. The GK rat heart subjected to IRI *ex vivo* with extra substrates additional to glucose demonstrated larger infarct sizes compared to control hearts[226]. Studies of IRI in diabetic db/db mice *in vivo* also support a diabetes-associated increase in MI size[227, 228]. The sensitivity of the type 2 diabetic heart in *in vivo* settings has had limited study compared to type 1 diabetes.

On the other hand, there has been a plethora of evidence suggesting the diabetic heart is paradoxically less susceptible to IRI. Investigations using a STZ-rat model both *in vivo* [221, 229] and *ex vivo* [230] demonstrated that acute diabetes (1-4 weeks of STZ treatment) resulted in a decreased susceptibility to IRI. Furthermore, Nawata et

al, 2002 also found that 4 weeks of STZ-induced diabetes reduced sensitivity to low flow global ischaemia followed by reperfusion in the Langendorff-perfused isolated heart model [231]. Interestingly, these isolated heart experiments were conducted in the absence of any additional substrates other than glucose. This phenomenon of protection in the acute diabetic setting was also present in other animal models such as alloxan-induced diabetes in Yucatan pigs[232]. Following regional coronary artery occlusion and reperfusion *in vivo,* myocardial infarct size was smaller compared to control however global left ventricular function was worse in diabetes but function within the area at risk was better. This reduction was accompanied by an increased expression of cell survival proteins[232]. Neonatal rat cardiomyocyte cells were protected against simulated IRI when incubated for 3 days with 25mM glucose compared to 5mM glucose in the medium. The high glucose treatment caused a reduction in necrosis, apoptosis and calcium content during hypoxia, alongside an increase in anti-apoptotic protein Bcl-2 expression. In addition, pro-apoptotic BAD shifted to its inactive state in the presence of 25mM glucose[233].

In contrast to the data described thus far which suggests short term induction of diabetes renders the heart more resistant to IRI, long term induction of diabetes has also been shown to elicit a cardioprotective effect. An 8 week induction of diabetes in rabbits using the chemical alloxan prior to IR resulted in a decreased MI size following 30 minutes myocardial ischaemia and 3 hours reperfusion *in vivo* compared to non-diabetic rabbits[234]. Furthermore, no difference in infarct size was seen in non-diabetic rabbits infused with high glucose throughout myocardial ischaemia and reperfusion compared to controls. They suggested that the presence of type 1 diabetes in the rabbit induced a chronic and metabolic cardioprotective state in the heart [234]. Interestingly, a shorter (6 weeks) alloxan induction protocol in rabbits had no effect on the vulnerability to IRI compared to controls [225]. Intriguingly, chronic administration of STZ for 12 weeks in rats also showed a decreased susceptibility to MI; however experiments were performed *ex vivo* with no additional perfusion substrates[235]. Other investigators have also shown that acute initiation of type 1 diabetes does not influence the susceptibility to MI. Both alloxan and STZ-treated dogs, although at a lower dose to previously mentioned investigations, reported no difference in MI size following IRI *in vivo* [236].

In 2004, Kristiansen et al [237] used two distinct models; the GK rat and ZDF rat to investigate the susceptibility to IRI in type 2 diabetes. They showed in Langendorff-perfused isolated hearts (with no added substrates), that MI size was smaller than their respective non-diabetic controls [237]. Tsang et al, 2005 also utilized

the isolated heart model, however with a shorter ischaemic time, and it appears that the hearts isolated from the GK rat is less susceptible to infarction than the Wistar rat control [238], however no statistics are shown. Of interest the perfusion buffer also contained no extra substrates other than glucose. Supporting these findings, isolated GK rat heart cardiomyocytes were less susceptible to mPTP opening in response to calcium, achieved by adding soluble Ca^{2+} to a phosphate-containing medium. This was accompanied by a larger calcium accumulation, leading to decreased opening of the mitochondrial pore and reduced cardiomyocyte death [239]. Controversially, two recent investigations that have been performed *in vivo* in the GK rat showed no difference in the susceptibility to infarct compared to control rats following 30 or 35 minutes ischaemia and 2 hours reperfusion [240, 241].

Interestingly, Yan et al, 2013 suggest the diabetic ob/ob mouse heart *in vivo* and isolated cardiomyocytes are more vulnerable to IRI. The diabetic mice exhibited hypoadiponectinemia which impaired AMPK-PGC-1α signalling resulting in dysfunctional mitochondrial biogenesis and hence more susceptible to MI injury. Moreover, treating hypoadiponectinemia prevented mitochondrial dysfunction and promoted cardioprotection against IRI[242].

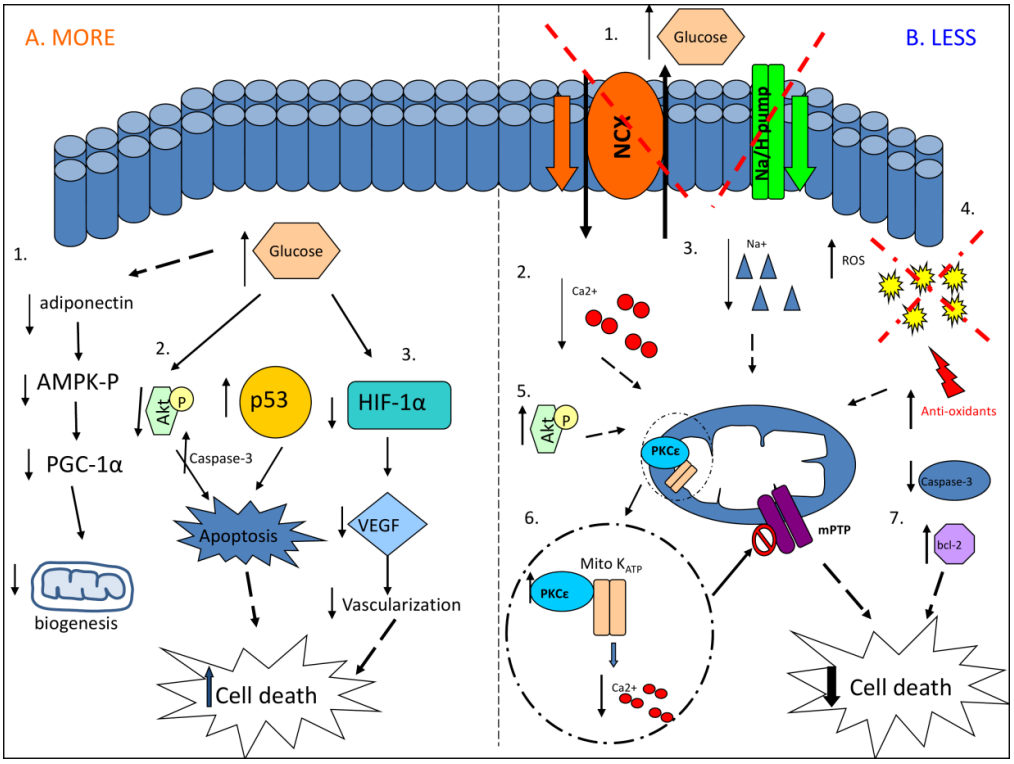

Figure 1.24: Possible intracellular changes within the diabetic heart. Possible intracellular changes that may render the diabetic heart A. more or B. less susceptible to ischaemia-reperfusion injury (see text for more details).

From the experimental data collected thus far it seems a common pattern has developed in the studies that have shown the diabetic heart be less sensitive to acute IRI they used glucose as the only substrate (*ex vivo*); used a short duration of diabetes (<6 weeks); and used a no flow IRI protocol, whereby global ischaemia is initiated by total interruption of the perfusate to the heart. When experimental protocols better reflected the clinical scenario i.e. fatty acids were present in the perfusate *ex vivo*, diabetes was more prolonged and severe and a low-flow IRI protocol was used, the diabetic heart was found to be more sensitive to IRI [218].The aforementioned data is summarised in tables 1.1-1.3.

Study	Model	Ischaemic Protocol	Duration/ onset of diabetes	Substrates	Model of diabetes	Parameters
Jones et al, 1999[228]	db/db mouse	In vivo non recovery, 30min regional ischaemia / 2h reperfusion	In bred strain	In vivo substrates	Type 2 diabetes	Infarction
Kersten et al, 2000 [224]	Dog, Alloxan (40 mg/kg) and STZ (25 mg/kg)	In vivo non recovery, 60min regional ischaemia / 3h reperfusion	3 weeks	In vivo substrates	Type 1 diabetes	Infarction
Kersten et al, 2000 [224]	Dog, Dextrose 15% to cause acute hyperglycaemia	In vivo non recovery, 60min regional ischaemia / 3h reperfusion	70mins	In vivo substrates	Type 1 diabetes	Infarction
Lefer et al, 2001 [227]	db/db mouse	In vivo non recovery, 30min regional ischaemia / 2h reperfusion	In bred strain	In vivo substrates	Type 2 diabetes	Infarction
Fiordaliso et al, 2001[223]	Rat cardiomyocytes	-	1,2 and 4 days of 25mmol/L incubation in medium	-	Type 1 diabetes	Cell death
Marfella et al., 2002 [219]	Sprague-Dawley Rat, STZ (70 mg/kg i.v)	In vivo non recovery, 25min regional ischaemia / 2h reperfusion	9 days	In vivo substrates	Type 1 diabetes	Infarction and protein expression
Marfella et al., 2002 [219]	Sprague-Dawley Rat, isolated heart	Langendorff isolated heart, 25min regional ischaemia / 2hr reperfusion	-	33.3 mmol/L glucose	Type 1 diabetes	Infarction and protein expression
Ebel et al, 2003 [225]	Rabbit- 50% Dextrose infused 30min prior to ischaemia until reperfusion	In vivo non recovery, 30min regional ischaemia / 2h reperfusion	hyperglycemia of 600 mgd1-1 throughout ischaemia	In vivo substrates	Type 1 diabetes	Infarction
Su et al, 2007 [222]	normoglycaemic rat- under intravenous infusion at a rate of 4 ml·kg–1·h–1: of glucose 500 g/l during ischaemia, saline during reperfusion	In vivo non recovery, 30min regional ischaemia / 6h reperfusion	-	In vivo substrates	Type 1 diabetes	Infarction, apoptosis and kinase expression
Desrois et al, 2010 [226]	Ageing Goto kakizaki Rat, male	Langendorff isolated heart, 32min low flow global ischaemia / 32min reperfusion	In bred strain	1.2 mM palmitate, 3% albumin, 11 mM glucose, 3 U/l insulin, 0.8 mM lactate, and 0.2 mM pyruvate.	Type 2 diabetes	Myocardial function

Table 1.1: Studies indicating the diabetic heart is more sensitive to ischaemic injury compared to normoglycaemic controls(tables from [217])

Study	Model	Ischaemic Protocol	Duration/ onset of diabetes	Substrates	Model of diabetes	Parameters
Hadour et al, 1998 [234]	Rabbit, alloxan(100 mg/kg)	In vivo non recovery, 30min regional ischaemia / 3hr reperfusion	2 months	In vivo substrates	Type 1 diabetes	Infarction
Schaffer et al, 2000 [233]	Rat, neonatal cardiomyocytes	10 mM deoxyglucose and and 3 mM amobarbital medium for 1 hr, OR hypoxic chamber: 2.3% O2-5% CO2- balance N2 for 1 hr	3 days incubation with 25mM glucose in medium	-	Type 1 diabetes	Infarction
Oliveria et al, 2001 [239]	Goto Kakizaki Rat, male, isolated cardiomyocyte mitochondria	-	In bred strain	-	Type 2 diabetes	Cell death and mPTP
Nawata et al, 2002 [231]	Rat, STZ (65mg/kg)	Langendorff isolated heart, 30min low flow global ischaemia / 30min reperfusion	4 weeks	11 mmol/L glucose	Type 1 diabetes	Myocardial function
Ooie et al, 2003 [235]	Rat, STZ (65mg/kg)	Langendorff isolated heart: Low-flow global ischaemia for 5min, followed by no-flow ischaemia for 25 min. 30min reperfusion	12 weeks	11 mmol/L glucose	Type 1 diabetes	Myocardial function, creatine kinase release
Ravingerová et al, 2003 [229]	Rat, STZ (45 mg/kg)	In vivo non recovery, 30min regional ischaemia / 4hr reperfusion	1 week	In vivo substrates	Type 1 diabetes	Infarction

Study	Model	Ischaemic Protocol	Duration/ onset of diabetes	Substrates	Model of diabetes	Parameters
Kristiansen et al, 2004 [237]	Goto kakizaki Rat, male	Langendorff isolated heart, 50min regional ischaemia / 2hr reperfusion	In bred strain	11 mmol/L glucose	Type 2 diabetes	Infarction
Kristiansen et al, 2004 [237]	Obese Zucker Diabetic Fatty Rat, male	Langendorff isolated heart, 50min regional ischaemia / 2hr reperfusion	In bred strain	11 mmol/L glucose	Type 2 diabetes	Infarction
Tsang et al, 2005 [238]	Goto kakizaki Rat, male	Langendorff isolated heart, 30min regional ischaemia / 2hr reperfusion	In bred strain	11mmol/L glucose	Type 2 diabetes	Infarction, kinase expression
Ma et al, 2006 [221]	Rat, STZ (50 mg/kg)	In vivo non recovery, 30min regional ischaemia / 2hr reperfusion	2 weeks	In vivo substrates	Type 1 diabetes	Infarction
Chu etal, 2010 [232]	Yucatan pigs, alloxan (200mg/kg)	In vivo non recovery, 1hr regional ischaemia / 2hr reperfusion	5 weeks	In vivo substrates	Type 1 diabetes	Infarction and protein expression
Shi-Ting et al, 2011 [230]	Rat, STZ (60mg/kg)	Langendorff isolated heart, 30min regional ischaemia / 40min reperfusion	4 weeks	11mmol/L glucose	Type 1 diabetes	Infarction and creatine kinase release

Table 1.2: Studies indicating the diabetic heart is less sensitive to ischaemic injury compared to normoglycaemic controls(table from [217])

Study	Model	Ischaemic Protocol	Duration/ onset of diabetes	Substrates	Model of diabetes	Parameters
Hadour et al, 1998 [234]	Rabbit, 10% glucose infusion to 300mg/dl blood glucose	In vivo non recovery, 30min regional ischaemia / 3hr reperfusion	blood glucose maintained at 300mg/dl throughout procedure	In vivo substrates	Type 1 diabetes	Infarction
Tanaka et al, 2002 [236]	Dog, alloxan (40 mg/kg) and STZ (25 mg/kg)	In vivo non recovery, 60min regional ischaemia / 3hr reperfusion	3 weeks	In vivo substrates	Type 1 diabetes	Infarction
Ravingerova et al, 2003 [229]	Rat, STZ (45mg/kg)	In vivo non recovery, 30min regional ischaemia / 4hr reperfusion	8 weeks	In vivo substrates	Type 1 diabetes	Infarction
Ebel et al, 2003 [225]	Rabbit-alloxan(100mg/kg)	In vivo non recovery, 30min regional ischaemia / 2hr reperfusion	6 weeks	In vivo substrates	Type 1 diabetes	Infarction
Desrois et al, 2004 [243]	Aged Goto kakisaki Rat, male	Langendorff isolated heart, 32min low flow global ischaemia / 32min reperfusion	In bred strain	11 mmol/L glucose	Type 2 diabetes	Myocardial function
Ma et al, 2006 [221]	Rat, STZ (50mg/kg)	In vivo non recovery, 30min regional ischaemia / 2hr reperfusion	6 weeks	In vivo substrates	Type 1 diabetes	Infarction
Bulhak et al, 2009 [240]	Goto Kakizaki Rat, male	In vivo non recovery, 35min regional ischaemia / 2hr reperfusion	In bred strain	In vivo substrates	Type 2 diabetes	Infarction
Matsumoto et al, 2009 [241]	Goto kakizaki Rat, male	In vivo non recovery, 30min regional ischaemia / 2hr reperfusion	In bred strain	In vivo substrates	Type 2 diabetes	Infarction

Study	Model	Ischaemic Protocol	Duration/ onset of diabetes	Substrates	Model of diabetes	Parameters
Shi-Ting et al, 2011 [230]	Rat, STZ (60mg/kg)	Langendorff isolated heart, 30min regional ischaemia / 40min reperfusion	8 weeks	11mmol/L glucose	Type 1 diabetes	Infarction and creatine kinase release

Table 1.3: Studies indicating no difference in the sensitivity of the diabetic heart to ischaemic injury compared to normoglycaemic controls(table from [217])

1.5.4 Protecting the diabetic heart against ischaemia-reperfusion injury

1.5.4.1 Ischaemic "conditioning"

Numerous studies have suggested that the diabetic heart is resistant to ischaemic pre conditioning (IPC) protocols that have been successfully shown to reduce infarct size caused by IR in non-diabetic hearts. For example, Kristiansen et al in 2004 showed in both the ZDF and GK rat, that 1 cycle of IPC could not protect hearts from either diabetic model from damage caused by IR[237]. Further to this, Tsang et al, 2005 demonstrated that 1 or 2 cycles of IPC (5 min ischaemia/10 min reperfusion) did not protect the GK diabetic heart from subsequent damage however when subjected to 3 cycles of IPC, infarct size was reduced [238]. Subsequently, they found that in the diabetic heart the basal level of Akt phosphorylation was lower compared to the non-diabetic heart and therefore an increased IPC stimulus is required to achieve an essential level of Akt phosphorylation necessary to mediate cardioprotection [238]. Interestingly, Sivaraman et al also showed that an enhanced IPC stimulus was required to achieve an essential level of Akt phosphorylation to protect atrial trabeculae isolated from diabetic patients[244].

Increasing the stimulus of IPC by increasing cycle number appears important in diabetes; for example Bouchard et al in 1998 also demonstrated that an IPC stimulus consisting of 1 cycle of 5 minutes ischaemia followed by 10 minutes reperfusion (IPC-1) was not sufficient to preserve the vasodilatory response to 5-HT; however when the IPC stimulus was increased to 3 cycles this response was recovered [245]. An impaired vasodilatory response to 5-HT suggested an impairment of endothelial cells in the diabetic heart and consequently the inability to generate and release enough NO. In the same investigation, 30 minutes pre-treatment with adenosine, an important mediator of IPC [246], mimicked the cardioprotective effect of IPC. However, 15 minutes

pre-treatment, showed to be efficient in a non-diabetic heart, was ineffective[245]. These findings suggested that signalling pathways activated by adenosine either endogenously or exogenously may be hindered in diabetic coronary vessels, but have the potential to be recovered by an increased stimuli.

The duration of IPC cycling may also play an important role in producing a protective effect in the diabetic heart; four cycles of 2 minutes ischaemia followed by 3 minutes reperfusion was insufficient to produce protection in two separate models of diabetes [237], whereas 3 cycles of 5 minutes ischaemia and 10 minutes reperfusion in the same animal and experimental setting was[238].

Investigations in diabetic animals have reported a reduced sensitivity to K_{ATP} channel activators [247]; a channel involved in the mechanism of protection by adenosine[58] and IPC[58]. The diabetic heart may need an increased IPC stimulus to achieve sufficient K_{ATP} channel activation to subsequently inhibit the mPTP, reduce apoptosis and limit myocardial cell death [248]. The suggestion of a dysfunctional K_{ATP} channel in diabetes was further supported by a study in alloxan/STZ induced diabetes in dogs [249].

Hotta et al, 2010 [250] failed to elicit cardioprotection with pre-treatment with an opioid agonist[251] or erythropoietin (EPO) [252] in an Otsuka Long Evans Tokushima Fatty (OLETF) type 2 diabetic rat *in vivo* model. These agents known to mediate IPC signalling through Janus kinase (Jak-2), caused insufficient phosphorylation of Jak-2 and Akt[250]. They also found an elevated level of calcineurin activity in diabetic hearts in accordance with other studies[253]. Interestingly, following 2 weeks treatment with Angiotensin II receptor type 1 (AT1) receptor blockers, valsartan or losartan, EPO elicited a cardioprotective effect alongside restoration of Jak-PI3K-Akt signalling [250]. Huisamen et al, 2011 supported the finding that AT1 antagonism can lead to cardioprotection in their *ex vivo* rat model of insulin resistance, diet-induced obesity (DIO) rat [254].

As described, diabetes has an impact on cardioprotective signalling in the heart. A potential role for direct targeting of GSK-3β, a molecule downstream of many of the aforementioned signalling pathways, has been postulated by many groups. Ghaboura et al, 2011, found EPO administration as an IPost mimetric did not increase the phosphorylation of Akt, ERK or GSK-3β and hence protect isolated hearts from STZ rats. Whereas high-fat diet (HFD)-induced insulin resistance syndrome (HFD) rats were protected following EPO. They found that direct administration of a GSK-3β antagonist prior to ischaemia and continued throughout reperfusion had an infarct limiting

effect [255]. Furthermore, Gross et al, 2007 [256] also showed that STZ-induced diabetes caused alterations in pathways upstream of GSK-3β, such as PI3K, Jak/STAT and MAPK pathways, therefore limiting the cardioprotective effects of morphine administered at reperfusion. Similarly, downstream antagonism of GSK-3β was cardioprotective [256]. The direct inhibition of GSK-3β was also proved cardioprotective in a rat model of type 2 diabetes[257].

1.5.4.2 Pharmacological "conditioning" with some anti-diabetic drugs

Numerous risk factors coexist in the insulin resistant state including an adverse lipid profile and a prothrombotic milieu, alongside hyperglycaemia which contributes to endothelial dysfunction and oxidative stress[258]. All of which can enhance the risk of CVD by increasing the development of atherosclerosis[258]. Simply lowering blood glucose provides some beneficial effects on cardiovascular risk reduction, however anti-diabetic agents have proven to have a plethora of effects, including innate cardioprotective properties[259].

Metformin, an oral anti-diabetic drug from the biguanide, insulin sensitizing class, has been suggested to elicit cardioprotective effects [259]. The UKPDS (United Kingdom Prospective Diabetes Study) indicated that patients receiving this drug developed a significantly lower incidence of cardiovascular events [260]. There are various mechanisms that have been suggested to play a role in metformin's glucose-lowering effect, including inhibition of complex I of the mitochondrial respiratory chain [261], decreasing hepatic glucose production [262], increasing glucose uptake [263] and stimulation of adenosine monophosphate-activated protein kinase (AMPK) [264]. However, the cardioprotective effect exerted by metformin could be independent of its hypoglycemic actions. This statement is supported by studies performed in normoglycaemic animals exhibiting smaller infarct volumes following acute metformin administration [265].

1.5.4.2.1 Metformin

1.5.4.2.1.1 Mechanism of action as a diabetic drug

Metformin belongs to the biguanide class of drugs that augments or mimics insulin action and lowers plasma glucose levels in patients with type 2 diabetes[266]. It exerts its glucose lowering effects through inhibition of hepatic gluconeogenesis and increases insulin-stimulated glucose uptake in skeletal muscle and adipocytes[266]. Metformin inhibits complex I of the respiratory chain within mitochondria responsible for oxidative phosphorylation[267]. Due to complex I being the entry point for NADH, inhibition leads to

a change in the mitochondrial proton gradient and ATP production is reduced producing an increase in the AMP to ATP ratio[267]. AMPK is also activated by metformin, subsequently reducing cellular glucose by promoting glucose uptake in skeletal muscle[268], increasing oxidation of fatty acids and inhibiting glucose production in the liver[264]. Alternatively, metformin has been demonstrated to suppress hepatic gluconeogenesis through the induction of SIRT1 and GCN5[269]. In diabetic mice, metformin increased the levels of these proteins with subsequent reduction in plasma glucose and insulin. Moreover, SIRT-1 was increased through an AMPK mediated pathway. Interestingly, levels of GCN5 were dramatically reduced in diabetic mice[269]. Recent evidence disputes the absolute requirement of AMPK for the glucose lowering effect of metformin. AMPK-independent effects of metformin, include an increase in AMP levels through inhibition of AMPdeaminase (AMPD)[270]. Administration of metformin in mice was found to directly decrease energy charge within the cell, independent of AMPK, supressing gluconeogenesis and hence glucose levels[270, 271].

Metformin was also found to decrease the plasma levels of free fatty acids and very low-density lipoprotein, LDL-cholesterol and to increase HDL-cholesterol, hence improving the lipoprotein profile of insulin resistant patients[266]. Studies in animal models and patients have also demonstrated that metformin treatment increases the availability of NO thereby improving endothelium dependent vasodilation[272, 273]. Somewhat unsurprisingly, the beneficial effects of metformin on cardiovascular risk factors was reflected by the United Kingdom Prospective Diabetes Study Group (UKPDS) demonstrating a reduced risk of all-cause mortality in type 2 diabetic patients treated with metformin[274]. Moreover a 39% risk reduction of myocardial infarction compared with conventional treatment[274]. In addition, a more recent study reported metformin was successful in reducing mortality in diabetic patients also with heart failure[275]. Metformin has been shown to be cardioprotective against IRI[266], and AMPK is thought to play an essential role in this.

1.5.4.2.1.2 AMPK

AMPK has evolved as a principal regulator of energy metabolism by phosphorylating key enzymes or transcription factors/coactivators in response to cellular stresses. In 1973, a physiological role for AMPK was described whereby acetyl-coenzyme A carboxylase (ACC) was phosphorylated and dephosphorylated specifically by AMPK in response to changes in intracellular ATP/AMP ratio during energetic stress[276]. AMPK is a heterotrimeric protein, consisting of a catalytic α-subunit and regulatory β- and γ-subunit. In response to cellular stressors such as hypoxia or ATP deficiency, levels of

AMP increase promoting the interaction and binding of AMP to the γ-subunit. AMP can activate AMPK by three mechanisms; allosteric activation, phosphorylation and inhibition of dephosphorylation[277]. AMP promotes activation of AMPK by stimulating phosphorylation of threonine-172 in the activation loop of the α-subunit by upstream AMPK kinases LKB-1 and calmodulin dependent protein kinase kinase (CaMKK); this activation is facilitated by a conformational change within the α and γ subunits [278]. The combined allosteric and phosphorylation effects causes a >1000-fold increase in kinase activity, providing AMPK with the ability to respond to small changes in energy status[279]. The activation and consequences of AMPK are summarised in Figure 1.25.

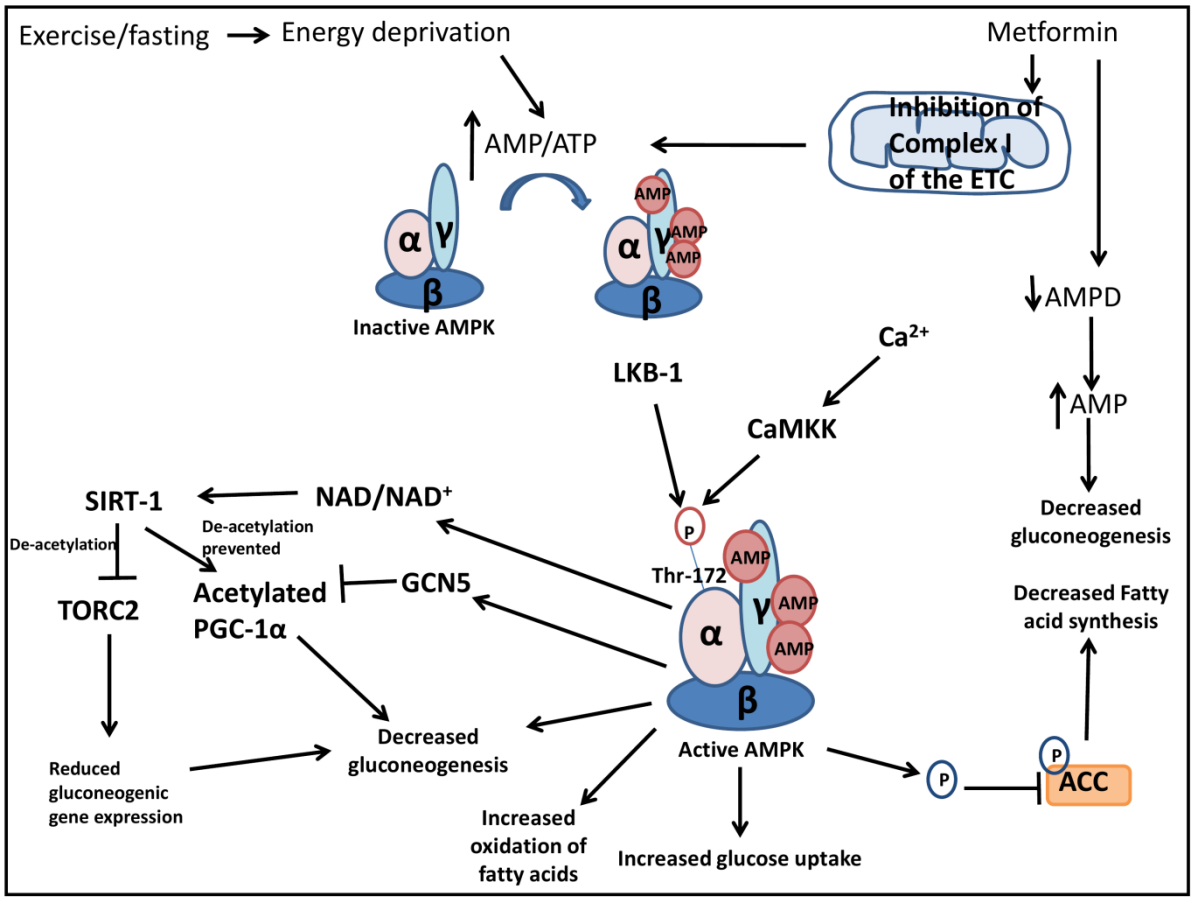

Figure 1.25: Structure, function and activation of AMPK. An increase in the AMP/ATP ratio promotes the interaction and binding of AMP to the γ-subunit, this promotes a conformational change within AMPK allowing phosphorylation and activation by AMPK modulators. Activated AMPK influences metabolic processes and subsequently restores the ATP/AMP ratio.

1.5.4.2.1.3 Metformin and cardioprotection against IRI

An initial study by Charlon et al in 1988 demonstrated the cardioprotective potential of metformin [280]. Oral administration of metformin to rats prior to permanent coronary artery ligation reduced infarct size [280]. Since then, metformin has been demonstrated to elicit protection against myocardial infarction in numerous models of IRI when administered at different time points including before ischaemia and also at the onset of reperfusion. In non-diabetic animals, metformin has consistently demonstrated to reduce infarct size. Solskov et al, 2008 showed that pre-treatment with metformin 24 hours before being subjected an IR protocol in non-diabetic Wistar rats reduced infarct size *ex vivo* compared to control rats and that metformin treatment acutely increased AMPK activity[265]. In further studies using non-diabetic animal models, metformin administered during reperfusion *ex vivo*[281-283] and *in vivo*[282, 284] significantly reduced infarct size. Metformin given before ischaemia also elicited a cardioprotective effect[284]. Interestingly, following the conclusion that metformin can successfully reduce myocardial injury and preserve cardiac function in non-diabetic rats, a clinical trial (GIPS)-III, investigating the efficacy of metformin in non-diabetic patients presenting in the clinic with ST elevation myocardial infarction is now underway [285].

Studies using diabetic animals have been less consistent. Calvert et al, 2008 [284] and Bhamra et al, 2008 [281] report positive effects of metformin in diabetic mice and rats respectively, whereas Kravchuck et al, 2011 [286] fail to see a cardioprotective effect with metformin in diabetic rats. This discrepancy could result from the choice of diabetic model and experimental protocol. Kravchuck et al used a neonatal STZ model of type 2 diabetes and subjected hearts to global ischaemia [286], whereas, the previous studies used genetic or sporadic models of type 2 diabetes and ligated the coronary artery to induce regional ischaemia[281, 284]. Moreover, their injury was not severe enough, with an infarct size of only approximately 25% in diabetic hearts. It is plausible to suggest that this why they could not achieve a significant reduction in infarct size with metformin in their experimental set up.

The cardioprotective effect of metformin has been attributed to numerous signalling pathways, including AMPK activation, adenosine receptor activation and activating the RISK signalling pathway. Bhamra et al, 2008 demonstrated that metformin treatment at the onset of reperfusion induced a significant increase in RISK kinase signalling, specifically an increase in phosphorylation of Akt in both Wistar and diabetic GK rats. Administration of a PI3K inhibitor, LY294002, abolished not only the Akt activation but also the infarct limiting effects of metformin. Furthermore, they

concluded that mPTP opening in isolated cardiomyocytes was delayed with metformin treatment due to the activation of PI3K/Akt signalling [281]. In a murine model of IRI, Calvert et al showed that metformin's protection was dependent on the activation of AMPK[284]. They also showed that the phosphorylation of AMPK occurs and remains active for more than 24 hours following reperfusion. Interestingly, without an ischaemia-reperfusion protocol, AMPK was still activated following low dose metformin administration. Furthermore, metformin failed to reduce infarct size in cardiac specific AMPK-α2 dominant negative transgenic mice[287]. Additional experiments showed that metformin-activation of AMPK is subsequently followed by eNOS phosphorylation; without this activation protection was lost[284, 287]. The importance of AMPK in metformin induced cardioprotection was further elucidated by Yellon and colleagues, metformin-associated reduction in infarct size was abolished by the co-administration of Compound C, an AMPK inhibitor. This inhibitory effect of Compound C was only produced when added during the first 5 minutes of reperfusion, suggesting that AMPK activation may occur early in reperfusion[283].

Adenosine release and the subsequent activation of its receptors is known to trigger the RISK pathway and lead to infarct size limitation[288]. Intracellular AMP, a modulator of AMPK activity[289], also contributes to the intracellular release of adenosine. Blocking the intracellular transport of adenosine outside the cell with nitrobenzylthioinosine or using 8-p-sulfophenyltheophylline (an adenosine receptor blocker) during reperfusion prevented the infarct reducing effects of metformin in non-diabetic rat hearts suggesting an importance of adenosine in metformin associated protection[282]. Whether adenosine plays a role in the diabetic heart has not been investigated. Recent studies have implicated PPAR-α and it's associated coactivator PGC-1α in the cardioprotective action of metformin. Barreto-Torres et al, 2012 showed that metformin increased phosphorylation of AMPK leading to improved recovery of cardiac function during acute IR, a reduction in cell death and an increased respiration at complexes I and II with a subsequent reduction in mPTP opening in isolated mitochondria. These protective effects of metformin were abolished in the presence of a PPAR-α inhibitor, however, intriguingly no changes in PPAR-α or PGC-1α expression were seen following the acute metformin treatment used in this model [290].

Data resulting from the use of acute metformin treatment as a cardioprotective agent have produced mostly positive outcomes; however type 2 diabetic patients usually take metformin on a long term or chronic basis. Not only has metformin been shown to decrease damage caused by IRI but animal models receiving metformin for longer periods of time have shown that this drug can limit cardiac remodelling and the

development of heart failure[287, 291]. Gundewar et al, 2009 showed that a single dose of metformin at reperfusion reduced infarct size but did not prevent cardiomyopathy whereas chronic administration of metformin for 4 weeks was successful in limiting cardiac hypertrophy and associated deteriorations in heart function. Chronic metformin treatment is thought to improve mitochondrial biogenesis, by activating AMPK, eNOS and PGC-1α[287]. Studies investigating the chronic effects of metformin treatment on the heart are more limited, with no studies being conducted in aged, diabetic animals.

1.5.4.2.2 GLP-1 associated therapies

Incretins are a group of gastrointestinal hormones that cause an increase in the amount of insulin released by the pancreas after eating, even before blood glucose become elevated [292]. Enteral nutrition stimulates the secretion of the incretin hormones, glucagon-like peptide-1 (GLP-1) and glucose-dependent insulinotropic polypeptide (GIP). GIP is synthesised in the enteroendocrine K cells in the proximal intestine whereas GLP-1 is derived from proglucagon and synthesised in the enterendocrine L cells in the distal ileum [293]. Circulating GLP-1 has two isotypes: GLP-1 (7-36) and GLP-1(7-37), GLP-1(7-36) is accountable for 80% of active GLP-1[293, 294]. Physiologically, GLP-1(7-36) is rapidly degraded by the enzyme dipeptidyl peptidase-4 (DPP-4) resulting in its metabolite GLP-1 (9-36)[295]. In adults, normal plasma concentrations of GLP-1 are ~5-10 pmol/L in a fasting state and ~15-50pmol/L in a fed state[296]. These hormones exert their effects by binding to G-protein coupled receptors expressed on the pancreatic α and β cells. In a glucose-dependent manner, GLP-1 binds to GLP-1 receptor triggering G-protein receptor activation, increasing cAMP levels and subsequently enhancing insulin secretion from β-cells[297]. Alongside these insulin stimulating effects, GLP-1 also suppresses glucagon release from α-cells in a PKA-dependent manner[298] and slows gastric emptying, resulting in an overall decrease in circulating blood glucose.

Classical studies by Nauck and colleagues, demonstrated that the incretin effect was diminished in subjects with type 2 diabetes[299]. They attributed this effect to defective GIP action and reduced GLP-1 secretion. This is summarised in Figure 1.26. Incretin-based therapies have been developed in an attempt to recover GLP-1 stimulated glucose control in type 2 diabetes. GLP-1 receptor agonists/analogues (exenatide and liraglutide), which are resistant to degradation by DPP-4, can be given to increase activity at GLP-1 receptors and promote insulin secretion. However, these analogues are unsuitable for oral delivery and require at least once daily subcutaneous

injections[300]. Interestingly, numerous experimental investigations showed that GLP-1 or GLP-1 analogues also elicit cardioprotective effects against myocardial IRI[301-309].

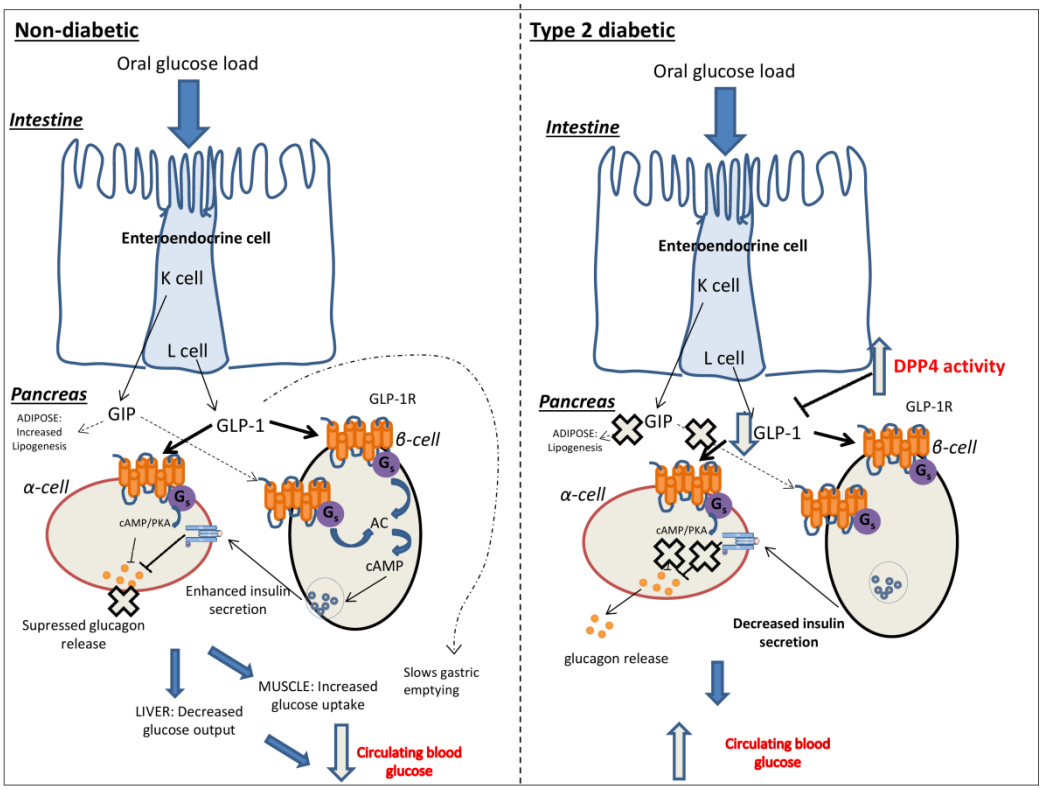

Figure 1.26: The incretin effect. Blood glucose is controlled following an oral glucose load by the incretins, glucose-dependent insulinotropic polypeptide (GIP) and glucagon-like peptide-1 (GLP-1). In type 2 diabetes the incretin effect is reduced by a decreased release of these peptides. GLP-1 is rapidly degraded by an increased level of the enzyme dipeptidyl peptidase-4 (DPP-4) further reducing the signalling of available GLP-1 to its receptor. As a consequence, diminished insulin secretion does not prevent the release of glucagon, increasing circulating blood glucose.

1.5.4.2.3 DPP-4 inhibitors

Incretins have a very short life time due to a circulating protease DPP-4 therefore DPP-4 inhibitors, also known as the gliptins, have emerged as a promising class of glucose lowering agents. This class of drugs have also attracted particular interest from cardiologists, due to their positive effect on the cardiovascular system[310]. DPP-4 exists in two forms, as a membrane-spanning and a soluble serine aminopeptidase enzyme, that can cleave and degrade peptides and proteins[311]. Inactivation of DPP-4 by pharmacological or genetic inhibition led to an increase in levels of bioactive GLP-1 and GIP, confirming its effect on these hormones[294]. DPP-4 rapidly degrades GLP-1(7-36) resulting in its metabolite GLP-1 (9-36)[311]. Prevention of GLP-1 breakdown by DPP-4 inhibitors enhances the level of intact GLP-1, thereby promoting insulin secretion and inhibiting glucagon secretion. Interestingly, DPP-4 activity has been reported to be up regulated in type 2 diabetes [312, 313]. DPP-4 levels and activity

are suggested to be modulated at the transcriptional level. Increased DPP-4 levels were demonstrated as a marker for hypoxia/HIF-1 induction in several cancer cell lines[314]. Interestingly, reduced serum levels of DPP-4 were also observed following metformin treatment[315].

Substrates for DPP-4 degradation are proline- or alanine-containing peptides, therefore DPP-4 is not specific for GLP-1 and targets a wide range of substrates. These include chemokines, growth factors and neuropeptides[310] including B-type natriuretic peptide (BNP)[316], neuropeptide Y (NPY)[317], stromal cell-derived factor 1α (SDF-1α)[318] and substance P[319]. Treatment with a DPP-4 inhibitor, sitagliptin was also associated with a significant reduction in the pro-inflammatory chemokine MCP-1. MCP-1 is involved in regulating the homing of monocytes to atherosclerotic plaques and visceral fat, two processes that are frequently seen in diabetic patients[320]. Hence, the inhibition of this enzyme leads to modifications in the activity of several cardioactive and vasoactive peptides that can produce a plethora of effects including vascular and myocardial protection. Inhibition of DPP-4 can also result in some disadvantageous downstream effects. The possible effects of DPP-4 inhibition are summarised in Figure 1.27.

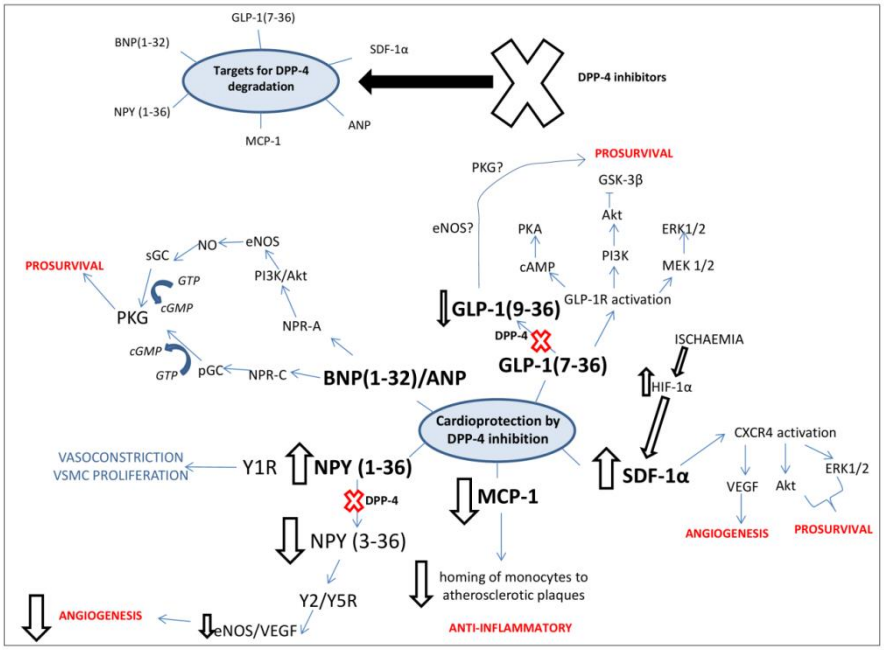

Figure 1.27: Targets for dipeptidyl peptidase-4 (DPP-4) degradation. DPP-4 can degrade numerous substrates, inhibition of this enzyme can result in many advantageous cellular changes but can also cause some unwanted effects. Advantageous effects include the up regulation of stromal-derived factor 1α (SDF-1α), glucagon like peptide-1 (GLP-1) and B-type natriuretic peptide (BNP) which results in the activation of pro survival pathways. Inhibition of DPP-4 activity also causes down regulation of the pro-inflammatory chemokine MCP-1. However, prevention of degradation of neuropeptide Y (NPY)1-36 enhances the unwanted vasoconstriction of blood vessels and inhibits the generation of pro angiogenic NPY(3-36).

1.5.4.2.4 Cardioprotection elicited by DPP4 inhibition

Numerous DPP-4 inhibitors are commercially available including vildagliptin and sitagliptin amongst others. Gliptins have been shown to elicit cardioprotective effects; in insulin resistant DIO rats, pre-treatment with a vildagliptin-analogue attenuated infarct size and improved metabolic control, moreover this cardioprotective effect was attributed to increased phosphorylation of Akt and ERK[321]. Interestingly, no protection was seen in the non-diabetic control rats[321]. However, sitagliptin was protective against IRI *in vivo* in normoglycaemic mice, with the infarct limiting effect positively correlating with the duration of treatment. Gliptins are proposed to limit myocardial injury during IR in animal models at least partly by increasing intracellular cAMP levels and promoting cAMP-dependent activation of PKA[322].

Vildagliptin given intravenously in a swine model of IRI *in vivo* prior to ischaemia stabilized electrophysiological properties of the heart leading to decreased infarct size[323]. Isolated mitochondria from rat cardiomyocytes produced less ROS and subsequently mitochondrial were less depolarized in response to DPP-4 inhibition[323]. The majority of pre-clinical studies have shown protection by reducing DPP-4 activity[310]; the survival rate of DPP-$4^{-/-}$ mice following permanent ligation of the left anterior descending coronary artery (LAD) was improved compared in DPP-$4^{+/+}$ mice, however infarct size was not significantly reduced. Hearts from DPP-$4^{-/-}$ mice contained higher levels of phosphorylated Akt, phosphorylated GSK-3β and atrial natriuretic peptide (ANP). Interestingly, these mice also had increased mRNA levels of PPAR-α[324]. DPP-$4^{-/-}$ mice are resistant to the development of STZ-induced diabetes[325]. Sauve et al, 2010 used diabetic mice to assess the cardioprotective potential of sitagliptin. Interestingly, post MI survival was improved by pharmacological inhibition of DPP-4 with an accompanying increase in phosphorylated Akt but no difference in infarct size was seen. Acute administration of sitagliptin *in vivo* to non-diabetic DPP-$4^{-/-}$ mice improved recovery from subsequent IRI compared to their littermate controls. Furthermore, sitagliptin administered *ex vivo* immediately prior to IR protocol exerted no direct cardioprotective effect[324]. These results suggest the inhibition of DPP-4 could modify cardiovascular outcomes independent of glucose regulation. The preclinical evidence strongly suggest a cardioprotective role for DPP-4 inhibitors, however the majority of these studies were conducted in young healthy animals, or acutely diabetic animals with no other co-morbidites. Therefore studies are required to investigate DPP-4 inhibitors in more clinically relevant models.

1.6 Ageing heart and ischaemia-reperfusion injury

1.6.1 Ageing and the cardiovascular system

1.6.1.1 Age related changes in the vasculature

There are many age related alterations that occur in the CV system in general and in the heart in particular. Increasing age correlates with thickening and reduced compliance of the arterial wall; this is caused by vascular smooth muscle hypertrophy, enhanced intimal thickness, fragmentation of the internal elastic membrane and increased collagen leading to more collagen cross-linking in arterial walls[326]. Alongside arterial thickening, a dilatation of major arteries and arterial stiffness occur presenting as increased systolic blood pressure and widening of pulse pressure[327]. Venous changes can also occur with ageing, however these changes predominantly effect peripheral vessels rather that those within the heart per se. One of the most prevalence venous changes is the reduced compliance of veins in the lower limbs, with a reduction observed in venous compliance in the calf of old versus young humans[328]. The most common manifestations of chronic venous disease are varicose veins, which contain incompetent valves and increased venous pressure, and dilated cutaneous veins[329]. The overall reduced compliance of lower limb veins are thought to affect the total venous return of blood to the heart.

1.6.1.2 Age related changes in the heart

1.6.1.2.1 Structural alterations of the heart

Structurally, aged hearts undergo left ventricular hypertrophy, have enlarged but fewer cardiomyocytes and an overall increase in collagen content [330]. Alongside, these heart specific changes, alterations in the vasculature and response to baroreceptor reflexes also occur. These structural changes impact the functional properties of the heart, causing changes in diastolic function and responses to pharmacological stimulation [330]. There are numerous factors that contribute to these modifications including cumulative damage caused by increased oxidative stress [331], changes in genetic programming [331], increased cell death and systemic ageing [330]. These changes make ageing a recognized risk factor for the occurrence cardiovascular events associated with an increased prevalence of infarction and poor clinical recovery following MI [332].

Within the ageing myocardium, an increased ventricular wall thickness to chamber size ratio leads to an increased ventricular mass[333]; however some studies report that this may be caused by other co-existing diseases rather than the intrinsic

myocardial ageing process[326, 334]. This increased thickness of the ventricular wall alongside more collagen and less ventricular cardiomyocytes combine to augment significant ventricular dysfunction[326, 335].

1.6.1.2.2 The impact of ageing within the cardiomyocyte

Cardiomyocytes are the major constituent of the ventricular and atrial walls of the heart; recent evidence proposes the existence of cardiac stem cells driving the regeneration of cardiomyocytes, however, decrease in cell number with age suggests this regeneration capacity is an insufficient compensatory mechanism. Correct control of ion homeostasis is critical to maintain cardiac function; old age has been linked to a defective and reduced expression of the sarcoplasmic reticulum (SR) Ca^{2+} ATPase pump leading to reduced re uptake of Ca^{2+} into the SR[336, 337] resulting in a significant prolongation of isovolumetric relaxation of the ventricles, moreover adenoviral gene transfer of this Ca^{2+} pump restores diastolic function in the aged rat heart[338]. Expression and function of ATP sensitive K^+ channels are also reduced with old age affecting the electrical activity of the cardiomyocyte[339]. Interestingly, at rest, left ventricular systolic function remains unchanged with no age-related deteriorations in ejection fraction, cardiac output or stroke volume; however these parameters are decreased in response to exercise[326]. In comparison, left ventricular diastolic function is affected by increasing age[340].

Cardiomyocytes in the ageing myocardium undergo changes at both the molecular and cellular level that lead to an increased susceptibility to cellular stress. This can result in an increased number of enlarged and dysfunctional cardiomyocytes and subsequently a reduced number of functional cardiomyocytes. Damage to DNA during the ageing process has attracted much attention and has been the subject of intense research. Telomeres are repetitive sequences at the ends of chromosomes that protect chromosomes from degradation. They maintain their length via the addition of DNA repeat sequences (TTAGGG) by the reverse transcriptase enzyme, telomerase. However ageing results in the loss of telomere reserves leading to eventual shortened DNA sequences[341]. A decrease in telomere length has been observed in the ageing rat myocardium[342]. Interestingly, patients diagnosed with dyskeratosis congenita, a congenital disorder that resembles premature ageing had decreased telomere length which was associated with increased mortality[343].

Telomere shortening leads to activation of DNA damage signalling pathways subsequently activating p53 and hence triggering induction of apoptosis and senescence[341]. Intriguingly, studies have demonstrated that telomere shortening in the

heart inducing p53 activation, specifically leads to mitochondrial and metabolic alterations through repression of PGC-1α and β[344]. Therefore telomere shortening may contribute to 1) increased death of cardiomyocytes, therefore reducing their number and 2) decreased mitochondrial biogenesis and function in the ageing heart. As well as telomere shortening, mutations and alterations in nuclear and mitochondrial gene expression result in an altered cardiomyocyte phenotype in the aged heart [345, 346]. Age related changes in the nucleus therefore have been suggested to trigger mitochondrial dysfunction and impact on the production of mitochondrial free radicals[347].

Interestingly, a shift from fatty acid towards carbohydrate metabolism was observed in mice hearts at 5 versus 30 months[348]. Based on the observations made by Luptak et al, 2007[349], this transition acts perhaps as an adaptive response. These authors found that glucose uptake was enhanced in GLUT-1 transgenic (GLUT-1 TG) mice, and that young and old transgenic mice had similar recovery following IR, which, in addition, exceeded the recovery that was seen in wild type mice of similar ages. In the old GLUT-1 TG mice during the reperfusion phase, glucose oxidation was substantially higher than fatty acid oxidation compared to old wild type mice. They speculate that the reduction in fatty acid oxidation limits the deleterious effects of excessive oxidation such as production of ROS[349, 350].

1.6.1.2.3 Ageing and mitochondria

Mitochondrial dysfunction has been reported in ageing tissues including the heart. Fannin et al, 1999 showed a decreased rate of oxidative phosphorylation and activity of cytochrome oxidase enzyme in in mitochondria from aged compared to the adult rat heart. These changes were specific to the interfibrillar and not subsarcolemma mitochondria[351]. Moreover a decrease in electron transport at complex III due to variations at the cytochrome c binding site led to altered oxidative phosphorylation contributing to increased ROS production in the ageing heart[352].

The formation, stability and function of complexes of the ETC rely on the presence of the phospholipid cardiolipin (CL) in the inner membrane[353]. CL is vital for the correct functioning of cytochrome c oxidase (complex IV of ETC) during mitochondrial energy metabolism. Two CL binding sites on cytochrome c oxidase have been suggested to be involved in the proton transport activity of this complex[354]. The apoptotic mediator cytochrome c preferentially binds to this monolayer of CL, in this bound state cytochrome c is not released limiting the initiation of cell death pathways[355]. A decrease in CL expression has been reported in the ageing heart[356]

with this loss of CL associated with an increased production of ROS. This was caused by dysregulation of the cytochrome c oxidase complex and an increase in unbound and hence released pro-apoptotic cytochrome c in the aged heart[356, 357]. Interestingly, cytochrome c bound to CL was released following peroxidation with a radical initiator[355]. Alongside a decline in oxidative phosphorylation function, numerous studies reveal a wide variety of changes within the mitochondria during ageing; these include disorganisation of mitochondrial structure, accumulation of mtDNA mutations and increased production of ROS leading to oxidative damage to DNA, proteins and lipids[358].

The initial proposal of the free radical theory of ageing by Harman in the 1950s suggested that intracellular ROS are causal for the process of ageing and a determinant of lifespan[359]. This led to an intensive area of research and the development of the mitochondrial free radical theory of ageing[360-362]. This theory suggests that, during oxidative phosphorylation, ROS are produced from the inner mitochondrial membrane and lead to oxidative induced mtDNA damage. The location, lack of protective histones and relatively little DNA repair activity of mtDNA, increase the susceptibility to oxidative induced damage resulting in mutated mtDNA [358]. Since mtDNA encodes for proteins within the respiratory chain, mutations lead to an increased production of ROS triggering a cycle of mitochondrial dysfunction and oxidative damage. Furthermore, autophagocytosis cannot efficiently remove these damaged, enlarged mitochondria mainly due to their size, causing further accumulation of oxidized products within lysosomes[363].

The role of ROS as the underlying stressor that leads to mtDNA mutations is central to this theory; however inconsistent results with ROS-limiting interventions in extending lifespan have proved to be controversial[358]. Mice overexpressing ROS-limiting catalase led to an increase in lifespan[364] and mice lacking Sod2 exhibited neonatal lethality[365, 366] supporting the fundamental role of ROS in ageing. However, in contrast Perez and others showed that the interference with antioxidant enzymes lead to decreased oxidative damage but had no influence on lifespan[367]. Interestingly, some mice that accumulate mtDNA mutations during adult life exhibit no substantial increase in oxidative stress[368]. These controversies led to the hypothesis of the gradual ROS response [369]. This theory postulates that ROS act as signalling molecules in normal physiology that lead to adaptive changes in response to stress[369, 370]. Toxicity caused by ROS is well controlled by the antioxidant system however as ROS-independent damage accumulates with age this system is overwhelmed leading to ROS induced

damaged[358]. This is supported by the critical role of low levels of ROS required for the initiation of cardioprotective signalling cascades[371].

Several other mechanisms contribute to increased mitochondrial ROS formation in the aged heart amongst which there is an increased production or accumulation of H_2O_2. Production of H_2O_2 from the reduction of $O_2^{\bullet-}$ was increased in 14 and 18 months old rat hearts compared to 3 month old rat hearts[372], moreover the age-related increase in H_2O_2 was abolished by the inhibition of monoamine oxidase (MAO)-A in the OMM, an enzyme that leads to enhanced formation of $O_2^{\bullet-}$ [373]**.** The protein $p66^{Shc}$ has also been implicated in enhanced production of H_2O_2 and ROS within the ageing mitochondria[374]. This protein upon translocation into the mitochondria oxidises cytochrome c leading to production of H_2O_2; mice lacking this protein exhibit an increased lifespan consequential of a reduced production of ROS[375], and ROS-mediated endothelial dysfunction[376]. Inhibition of $p66^{Shc}$ also results in protection from IRI[377] and expression of both MAO and $p66^{shc}$ increase with age. Interestingly, translocation of this protein was shown to be mediated by phosphorylation at serine36 residue by PKC-β in response to oxidative stress and led to initiation of apoptosis and increased mPTP opening[378, 379]. Moreover, phosphorylated $p66^{Shc}$ level was demonstrated to be increased with age[380]. Enhanced ROS formation can also be attributed to mechanisms other than the direct release from the mitochondria; increased ROS production resulted from an increased expression of NADPH oxidase subunit $p47^{phox}$ in aged mice myocardium[381] alongside a decreased anti oxidative capacity in aged rat hearts[382, 383]. Ageing associated changes within the cardiomyocyte are summarised in Figure 1.28.

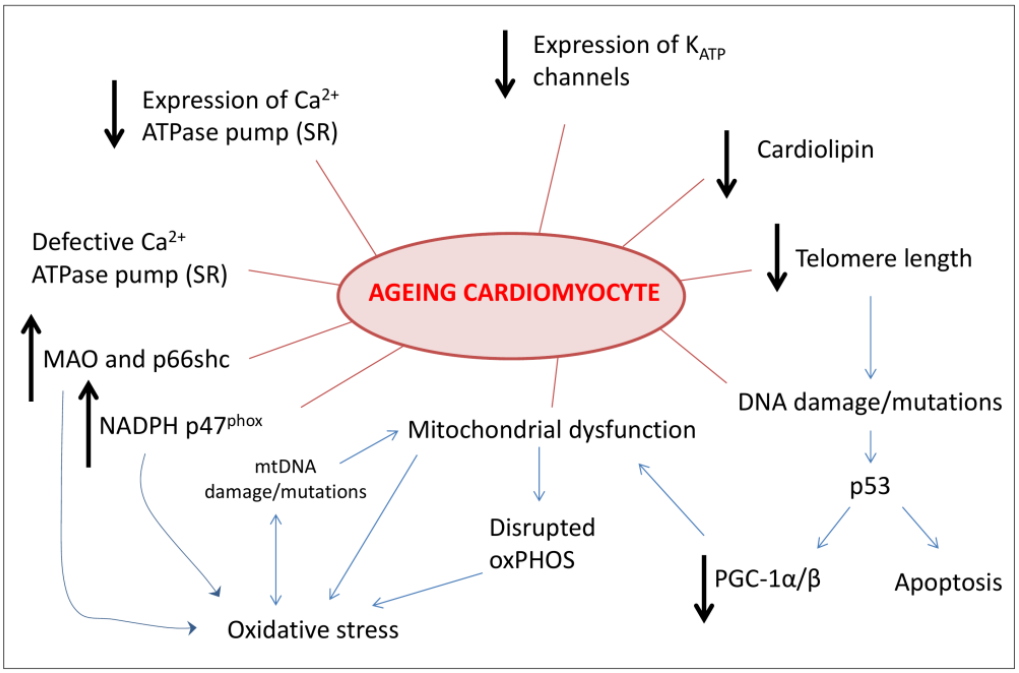

Figure 1.28: Molecular and cellular changes in ageing cardiomyocytes:

1.6.2 Ischaemia-reperfusion injury in the aged heart

The impact of mitochondrial dysfunction, increased oxidative stress and abnormal Ca^{2+} handling in the aged myocardium results in basal disturbances in cardiac function. The myocardium is in a compromised state, and therefore when subjected to a stress such as ischaemia-reperfusion injury, the ability for the heart to recover is hindered [384]. In the clinical setting, elderly patients experienced increased mortality during MI, with those surviving exhibiting greater cardiac damage compared to younger patients even with efficient and successful reperfusion[385]. This has also been well-documented in animal investigations[384]. Isolated heart preparations conducted using hearts from aged (24 months) Fischer 344 rats exhibited decreased hemodynamic recovery and increased creatine kinase release compared to younger counterparts (6-8 months) following ischaemia and reperfusion[386, 387].

Numerous signalling defects have been linked with ageing associated increases in vulnerability to IRI (Figure 1.29). Myocardial ionic imbalance has been demonstrated in the ageing heart; Jahangir et al, 2001 suggest mitochondria from the aged heart have a decreased tolerance to increased Ca^{2+} levels that occur during cardiac injury[388]. In line with this, O'Brien et al, 2008 showed an increased accumulation of Ca^{2+} during ischaemia and early reperfusion in cardiomyocytes isolated from 24 month old rats compared to 3 month old rats[389], which in turn leads to mitochondrial Ca^{2+} overload and

cell death[65]. Tani et al, 1997 also demonstrated decreased ischaemic tolerance in aged rats in relation to increases in intracellular Na^+ after ischaemia[390]. Interestingly, this investigation suggests an age-related increase in the susceptibility to myocardial injury starts to manifest at middle age in rats (approximately 12 months of age)[390]. Loss of intrinsic tolerance to IR was also manifested at 12 months in mice and exaggerated with age increasing up to 22-24 months[391]. Other studies in mice also demonstrated increased infarct size in aged mice[392, 393], however one study suggested mice at 13 months of age had no increased susceptibility to injury. Of note, the ischaemia-reperfusion protocol used in this study was shorter[394].

Enhanced ROS formation in response to IRI has been documented in the aged rat heart. Strategies that limit oxidative damage have proved successful in improving cardiac function and decreasing oxidative stress within the myocardium[395, 396]. Systemic administration of the antioxidant acetylcarnitine before ischaemia increased the transcription of mtDNA, leading to augmented mitochondrial protein synthesis of ETC subunits. This resulted in enhanced cytochrome c oxidase activity, restoring oxidative phosphorylation in aged, rat hearts [397]. Increased generation of mitochondrial ROS during ageing and subsequently in ischaemia-reperfusion has been demonstrated to impact the mPTP, firstly by increasing on its formation and secondly on its open probability, both leading to increased cell death[65, 398].

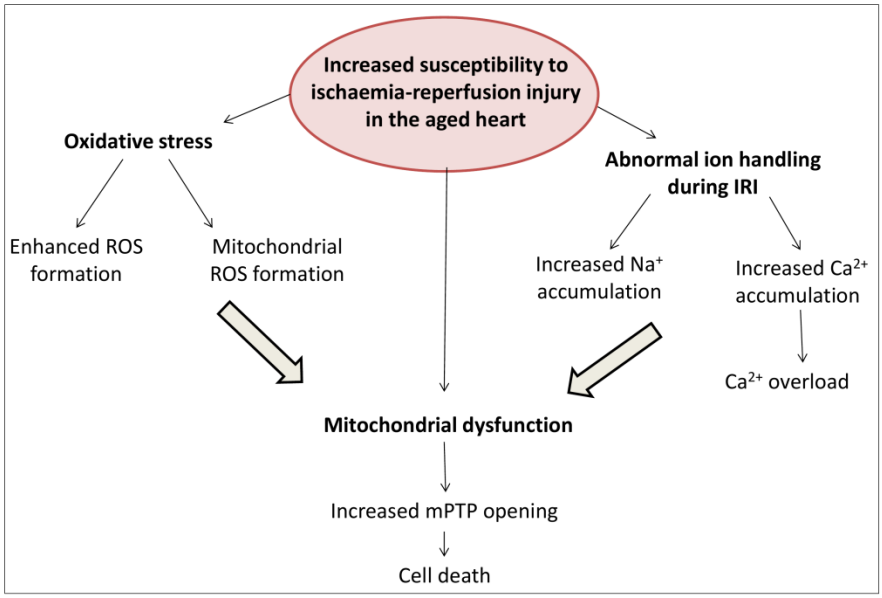

Figure 1.29: The main processes that are suggested to contribute to enhanced damage caused by ischaemia-reperfusion injury in the ageing heart.

1.6.3 Protection against infarction in the aged heart

1.6.3.1 Loss of conditioning against IRI in the aged heart

Considering that the defective changes that exist in the aged heart lead to increased susceptibility to ischaemia-reperfusion injury, converge or involve the mitochondria, it is somewhat unsurprising that the protective effects of IPC that also involves modulation of the mitochondria are more difficult to achieve [399]. The majority of studies show that cardioprotection by IPC is ineffective in the ageing heart[384]. One cycle of IPC in aged hearts[399] or isolated cardiomyocytes[389] from 24 month old rats did not enhance the recovery[399] or cell viability[389] following IR compared to hearts from 6 or 3 month old rats, respectively. Furthermore, infarct size could not be limited using one or two cycles of IPC prior to IR in 12[400], 18-20 [401] and 22[402] month rats. Interestingly, Schulman et al, 2001 showed that increasing the IPC stimulus to 3 cycles protected the aged heart from IRI compared to control hearts [401]. However, Abete et al did not see a cardioprotective effect when cycle number was increased to four in their model[399]. Of note, in this study prolonged ischaemia was only applied for 20 min with 40 min reperfusion in comparison to 35 min ischaemia and 120 min reperfusion used in Schulman's investigation, which may account for the inconsistent finding. IPC was also ineffective in an *in vivo* mouse model of IR in mice greater than 13 months of age[394]. Interestingly, *in vivo* investigations in larger animal models oppose these findings and suggest IPC is still protective against IRI in aged rabbits[403] and sheep[404]. However, this outcome was questioned in respect to their suitability as 'ageing' animal models; protection was still afforded in 2-4 year old rabbits where lifespan is usually approximately 13 years and in 6-8 year sheep where lifespan is approximately 20 years[384, 405]. Maximal lifespans of experimental animals are shown in Table 1.4.

Laboratory animal	Life expectancy
Mice	2 years
Rats	3-4 years
Rabbits	8-10 years
Sheep	~ 20 years

Table 1.4: The life expectancy of laboratory animals:

Pharmacological preconditioning has also been suggested to be ineffective in the aged heart[384]. While middle-aged rabbit hearts were amenable to protection by

1mM adenosine[406], this protection was not possible in old rodents. Acute preconditioning with either adenosine[407] or an opioid agonist [408] was unable to protect isolated hearts of 18 and 24-26 month old mice. Adenosine receptor activation mimics IPC by leading to the activation of similar intracellular pro-survival kinase cascades as IPC[409]. Downstream to adenosine, the direct activation of PKC or mitoK_{ATP} channels also failed to limit infarct size in isolated old rat hearts (18-20 months)[401].

1.6.3.2 Why is it difficult to condition the aged heart?

The effectiveness of myocardial IPC or pharmacological conditioning in young and healthy animals and the mechanisms behind this protection have been intensively investigated [410]. Both trigger a diverse array of signalling cascades, most of which seem to converge towards the preservation of mitochondria's structure and function.

There is less data regarding the state of these signalling cascades during the ageing process, as a result, mechanisms are unclear regarding the increased myocardial susceptibility to IRI in ageing. We think that the impairments that occur in the ageing process may lead to increased susceptibility to IRI. Some authors discuss the possible signalling motifs and interactions that could be affected in the aged heart that lead to lack of protection by IPC, summarised in Figure 1.30 [384]. For example, impaired mitochondrial function including regulation of redox signalling and energy production, defective IPC signalling including defective ligand/receptors signalling and alterations of signalling molecules in the RISK pathway and SAFE pathway [384] and an altered threshold for IPC to trigger protective signalling are underlying mechanisms that may render the aged heart ineffective to IPC. However, more experimental evidence has started to emerge.

Levels of endogenous ligands can limit the cardioprotective response to IPC, reduced IL-6, a component of the SAFE pathway was found in aged mice hearts[411]. Levels of Insulin-like growth factor 1 (IGF-1), a ligand that can initiate the RISK pathway, and it's receptor IGF-1 were decreased in aged hearts[412]. Bradykinin (BK), another well-known cardioprotective signalling molecule can activate both the RISK pathway and the PKC dependent pathway, decreased expression of BK receptors, specifically BK receptor-2, were found in 24month rat heart myocardium[413]. Central for protection mediated by IPC is PKC; PKCε translocates between intracellular compartments to modulate its cardioprotective effect. This translocation was impaired in middle aged mouse hearts[394] and aged rat hearts[414], moreover expression of PKCε in the soluble fraction of isolated rat hearts was decreased in the 24months age group

compared to 5months age group [415]. However, age does not impact on the total level of this protein[384, 414].

The mitochondrial K_{ATP} channel is implemented in the protective effect elicited by IPC; interestingly an aged related decrease is seen in its activity in the rat heart[416]. Boe et al, 2013 demonstrated that the inhibitory effect of cytosolic ATP on channel activity was enhanced in the aged rat heart as a possible consequence of metabolic impairment seen during ageing[417]. Upon application of an IPC stimulus a small amount of ROS is required to initiate protection via the K_{ATP} channel[371, 418]; the redox sensitive nature of this protection was demonstrated by the inhibition of IPC in the presence of a free radical scavenger, N-2-mercaptopropionyl glycine (MPG)[419]. Interestingly, MPG applied at reperfusion prevented protection by IPC [419]. Connexin 43 (Cx43), a gap junction protein that is also found in the mitochondria, is required for the activation of mitochondrial K_{ATP} channels and subsequent cardioprotection by IPC[420, 421]. Morever, reduced levels of Cx43 prevented the release of protective ROS in response to diazoxide stimulation[422]. Interestingly, Cx43 is decreased in the aged myocardium[394], however cardiac Cx43 has been shown to be localised in subsarcolemmal (SSM) not interfibrillar (IFM) mitochondria[423]. The majority of other mitochondrial defects appear to be localised in IFM in the ageing heart; the inability to pre-condition $Cx43^{-/-}$ mice may suggest SSM play an important role in the loss of IPC in aged heart[420].

An important role for SIRT-1 activity has been suggested during IR and also IPC[146, 148], interestingly SIRT-1 activity decreases with age[424], therefore a deficiency in SIRT-1 activity has been suggested as a potential reason for the loss of IPC in the aged heart. However, Adam et al, 2013 show that even though SIRT-1 deacetylase activity is decreased during IR; IPC and resveratrol, a SIRT-1 agonist, failed to protect the aged heart. Moreover, inhibition of SIRT-1 did not limit infarct size in their aged, *ex vivo* rat model but did decrease functional recovery following IR. Controversially, they conclude based on their results that there is no direct role for SIRT-1 in IPC and moreover loss of SIRT-1 activity does not account for ineffective IPC in aged heart [425].

Blunted activation or expression of RISK kinase signalling molecules has been suggested to exist in the ageing heart. Impairment of expression of activation/deactivation of Akt, GSK-3β, ERK or p38, important mediators of cardioprotection in IPC[134] would lead to decreased effectiveness of IPC[384]. Interestingly, by increasing the stimulus of IPC in the aged heart, protection can be restored in some models of ageing, suggesting that the impaired signalling can be recovered. Acute phoshophorylation of Akt during IPC is a component of the RISK

pathway leading to protection, however, intriguingly the aged failing heart has been linked with increased basal levels of Akt-phosphorylation[426]. Whether high levels of signalling molecules prior to stress prevent their acute activation and the initiation of cardioprotective signalling is yet to be fully investigated but may provide an interesting area of research.

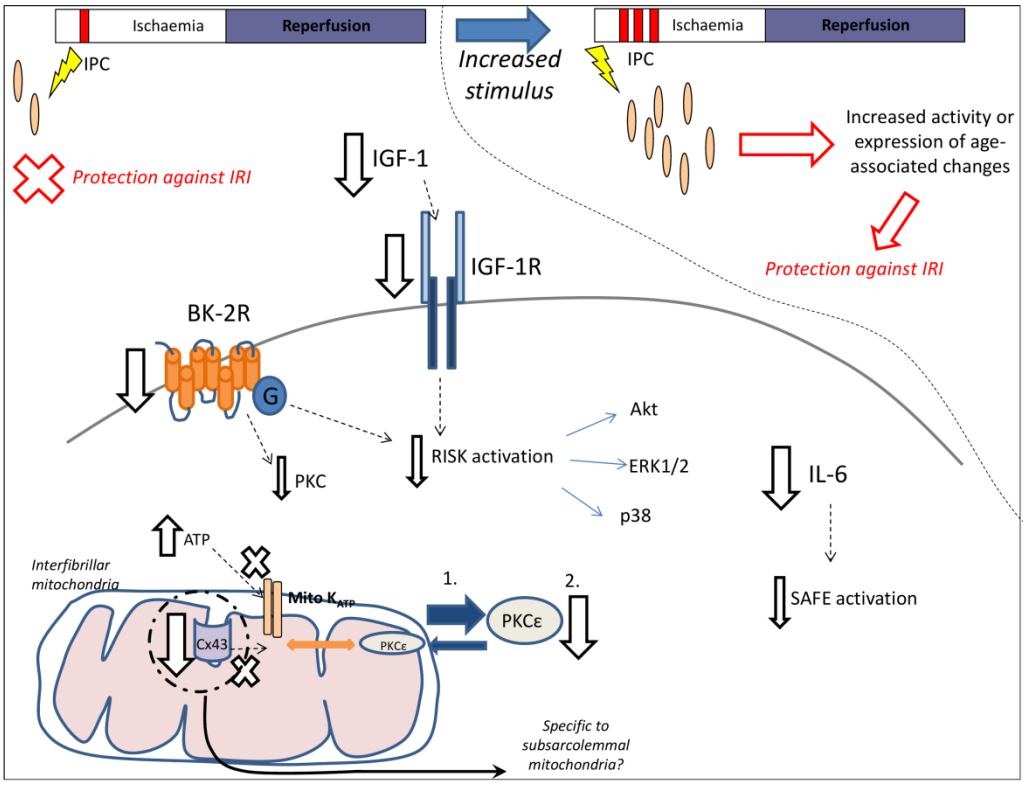

Figure 1.30: Cardioprotection in the ageing heart. One cycle of ischaemic preconditioning is insufficient to protect the aged heart against damage following ischaemia-reperfusion injury. The mechanisms proposed to explain the loss of protection include decreased expression of bradykinin-2-receptor (BK-2R), decreased release of insulin-like growth factor-1 (IGF-1) and expression of its receptor IGF-1R, decreased levels and activation of reperfusion injury salvage kinases (RISK) and survival activating factor enhancement (SAFE) signalling, and mitochondrial changes. Three cycles of ischaemic preconditioning recovers the diminished signalling and protects the ageing heart.

1.7 Ageing and diabetes in myocardial ischaemia-reperfusion injury

1.7.1 Hypotheses and aims

As far as we know there are not yet experimental studies which have investigated the effect of these two aggravating factors, or co-morbidities, on myocardial infarction. The reasons for this are likely to be associated with the experimental costs and the time constraints involved in maintaining ageing, diabetic colonies. Nevertheless, considering the emergent ageing human population and increasing incidence of diabetes, such studies may prove crucial for developing successful cardioprotective strategies specific for this sector of the population.

The main aim of the studies presented in this thesis was to investigate the influence of two comorbidities (diabetes and age) on the susceptibility to myocardial infarction in an experimental model. For this purpose we used a diabetic rat strain, the Goto-Kakizaki rat (a commonly used model of type 2 diabetes) at different ages (3, 8, 12 and 18 months). As a normoglycaemic control, we used the Wistar rat (which is the parent strain for the GK rat).

We hypothesise that:

A. The diabetic heart will age quicker than the normoglycaemic heart and therefore will be more susceptible to infarction and less amenable to cardioprotection in comparison to the non-diabetic heart of the same age.

Aims:

1. To assess ischaemia-reperfusion injury as a function of age and duration of injury (chapter 3.1)

2. To assess the effectiveness of IPC at different ages (chapter 3.2)

3. To assess the cardioprotective effect of anti-diabetic drugs known to protect in young animals under acute administration, when given as chronic treatment in middle aged and older animals (chapter 4).

B. Modifications in the pro survival signalling pathways within the diabetic cardiomyocytes may contribute to the susceptibility to infarction and decreased effectiveness of IPC in the aged heart.

Aims:

1. To assess to the state of mitochondria in aged and/or diabetic animals (Chapter 3).

2. To assess the state of the crucial intracellular systems implicated in cardioprotection in aged, diabetic hearts (such as Akt, PGC-1α, catalase), (Chapter 3).

Main conclusion:

Diabetes seems to accelerate the ageing process in the heart in relation to the susceptibility to infarction and the decreased cardioprotective potential of the ageing heart. The alteration in the endogenous cardioprotective signalling within the cardiomyocyte seems to be at least partially responsible of these changes.

2. GENERAL METHODS

For the investigations which will be described in the following chapters, I learned and employed 2 models of ischaemia-reperfusion and a number of biological techniques:

- *Ex vivo* myocardial ischaemia-reperfusion injury using a Langendorff system (constant pressure, retro-perfused heart)

- *In vivo* myocardial ischaemia-reperfusion injury

-A series of molecular biology techniques applied to whole cardiac tissue or to isolated cardiomyocytes or cell lines.

These techniques will be described in detail in the present chapter, with particular details related to specific subjects added in the respective results chapters.

2.1 Animals

Rat models were used in the studies described throughout this thesis. Initial characterisation of models used the standard Sprague Dawley lab rat (300-350g); all investigative work used both the non-diabetic Wistar rat and the type 2 diabetic Goto Kakizaki rat.

2.1.1 Animal models of Diabetes

Animal models used to investigate diabetes, have been created by different methods such as feeding modified diets, administration of drugs toxic to the pancreas, and inbreeding spontaneous mutations and genetic engineering [427]. This has resulted in the availability of many different diabetic animal models [428]. However, translating results gained from these animal models of diabetes into clinical settings must be interpreted with caution as none of the models completely reflect the human pathology of diabetes.

2.1.1.1 Type 1 Diabetes

Type 1 diabetes is characterized by the insufficient production of insulin as a consequence of autoimmune destruction of pancreatic β cells in the islets of Langerhans [429]. The main experimental models used to investigate this disease are created by the administration of toxic compounds that prevent the production of insulin. These compounds include streptozotocin (STZ) and alloxan. STZ is an alkylating agent based nitrosurea derivative [430], which interferes with numerous cellular processes such as glucokinase function and glucose transport, and can

also cause DNA strand breaks [431]. To induce diabetes in rodents with this agent, the administration of a series of low doses is preferable to avoid the high mortality associated with using a single high dose [432]. Alloxan is a toxic glucose analogue, which preferentially accumulates in the beta cells of the pancreas, causing excessive production of hydroxyl free radicals and destruction of the beta cells hence mimicking type 1 diabetes [433]. In essence, the primary etiopathology caused by administration of these toxins has little autoimmune component and does not truly reflect the pathology of type 1 diabetes in the human [432]. Therefore, it could be argued that the translation of findings from these particular animal models of type 1 diabetes to the clinical setting may be problematic.

Alternatively, genetic or spontaneous models can be employed in investigating type 1 diabetes, with a vast amount of data collected using non-obese diabetic (NOD) and congenic NOD mice [434]. Rat models include the diabetes-prone BB rat, the LETL rat, the KDP rat and the congenic LEW rat. The BB rat derived from an outbred Wistar rat colony that exhibited spontaneous hyperglycaemia and ketoacidosis, are the most extensively studied rat model of type 1 diabetes [435].

2.1.1.2 Type 2 diabetes

Type 2 diabetes in humans is a metabolic disorder which is usually detected during adult-hood [436]. There are a few rodent models of this form of diabetes, for an extensive review of animal models in diabetes please refer to [427]. Both the db/db mice [437] and the Zucker diabetic fatty (ZDF) rat [438] are models that express other co-morbidities such as obesity and dyslipidemia as well as glucose intolerance [439]. The Otsuka Long Evans Tokushima Fatty (OLETF) rat originates from the inbreeding of Long-Evans rats which exhibit glucose intolerance [440], these rats are mildly obese and the diabetic phenotype is more dramatic in males. Another model of type 2 diabetes is the Goto-Kakizaki (GK) rat, described in greater detail below.

2.1.1.2.1 The Goto-Kakizaki rat

The GK rat is an established model of type 2 diabetes, developed by the selective inbreeding over numerous generations of Wistar rats that exhibited hyperglycaemia and glucose intolerance [441, 442]. The polygenic GK rat spontaneously becomes diabetic early in life, showing glucose insensitivity in their pancreatic beta cells with the diabetic status increasing with age. They exhibit mild basal hyperglycaemia, impaired glucose-induced insulin secretion, decreased β-cell mass, hepatic and peripheral insulin

resistance with vascular complications often seen in diabetic patients [443]. A reduced expression of the glucose transporters GLUT-2 and GLUT-4, and insulin receptors have been also observed in the GK rat, contributing to the insulin resistant state in these animals[444]. As the GK rat ages, severe hyperglycaemia develops, however insulin levels remain constant[445]. The plateauing effect of weight gain with age in this model is likely to be related to the absence of an age-related impairment of peripheral insulin[445]. However, the lean nature of this model of type 2 diabetes allows investigation of diabetes without other complications such as obesity [446].

Male and female Goto-Kakizaki (GK) rats (a mild, non-obese diabetic model [427, 447]) were initially obtained from Taconic (Denmark). They were used to establish a colony in the Central Biological Services Unit (BSU), which I supervised throughout my studies. The animals were kept in house until they reached 3, 8, 12 and 18 months of age. These ages are thought to represent the ages shown in Table 2.1, in humans[448]. Male Wistar rats (normoglycaemic) were obtained from Charles River UK Limited (Margate, UK) and kept in house until they also reached 3, 8, 12 and 18 months of age. All animals received humane care and studies were performed in accordance with the United Kingdom Animal (Scientific Procedures) Act of 1986. To perform these experiments I was trained in Modules 1-4 in the UCL BSU and granted a Home Office Personal License for working with animals. In addition, I obtained a grant from Servier to visit their laboratories in Paris, France to learn the surgical model of injury and recovery in myocardial ischaemia-reperfusion in rat.

Rat's age (months)	Human's age (years)
6	18
12	30
18	45
24	60
30	75
36	90

Table 2.1: The rat's age in months and its relationship with human age in years (data taken from [448])

2.1.2 Biological parameters

Blood glucose, glycated haemoglobin A (HbA1c), body mass and heart mass were recorded as needed and the time points of these measurements were included in the respective chapters.

HbA1c is a measure of glycated haemoglobin. Glycation is a form of non-enzymatic or non-controlled glycosylation [449]. The diabetic subjects who have higher or uncontrolled blood glucose also have more glycated haemoglobin. Therefore the level of HbA1c can be used as a marker for diabetes. HbA1c was measured using an A1C now+ test kit (Bayer, UK). Blood glucose was measured using Accu-chek system (Roche) in the overnight fasted animals.

For both tests the animals were placed in a heating chamber to increase the visibility and accessibility of the tail vein, and a small pin-prick of blood was collected for each test. Subsequently, the animals were left to recover for at least 48 hours before any experimental investigations. This is because heat stress has been shown to be protective against myocardial ischaemia-reperfusion injury for a period up to 24-36 h following the procedure.

2.2 Assessment of Infarction using ex vivo and in vivo models

2.2.1 Langendorff model of retroperfused isolated heart

2.2.1.1 Introduction

The mammalian isolated heart model was first described by Oscar Langendorff in the late 19th century and is still a very important and widely used technique in the laboratory setting today [450]. Oscar Langendorff developed the method based on work completed earlier that century by Elias Cyon from the Carl Ludwig Institute of Physiology in Leipzig, Germany, on the isolated perfused frog heart [451]. Both methods were instrumental in aiding the understanding of heart physiology throughout the late 19th and into the early 20th century. Incredibly, only few modifications have been made to the original method described by Langendorff and the technique still remains instrumental in modern cardiovascular and pharmacology-based research today. Throughout the last couple of decades and into the millennium, the technique has not only furthered our understanding of heart physiology but has also been essential in investigating and manipulating cell signalling pathways implicated in cell survival or affected by pathologies such as diabetes, hypertension or heart failure [452].

The principle of the method has remained true to the original description coined by Langendorff himself; the heart is perfused in a retrograde fashion via a cannula inserted into the aorta. The perfusate (normally physiological crystalloid solution) moves into the heart via the aorta, in the opposite direction to normal physiological flow. This retrograde movement of perfusate causes the aortic valve to close under pressure and prevents fluid from entering the left ventricle. Closure of the valve therefore initiates movement of the perfusate through the right and the left coronary ostia located at the aortic root, through the coronary arterial vasculature and into the right atrium via the coronary sinus. This essentially allows the preparation to run without any fluid filling or emptying in either ventricle (Figure 2.1).

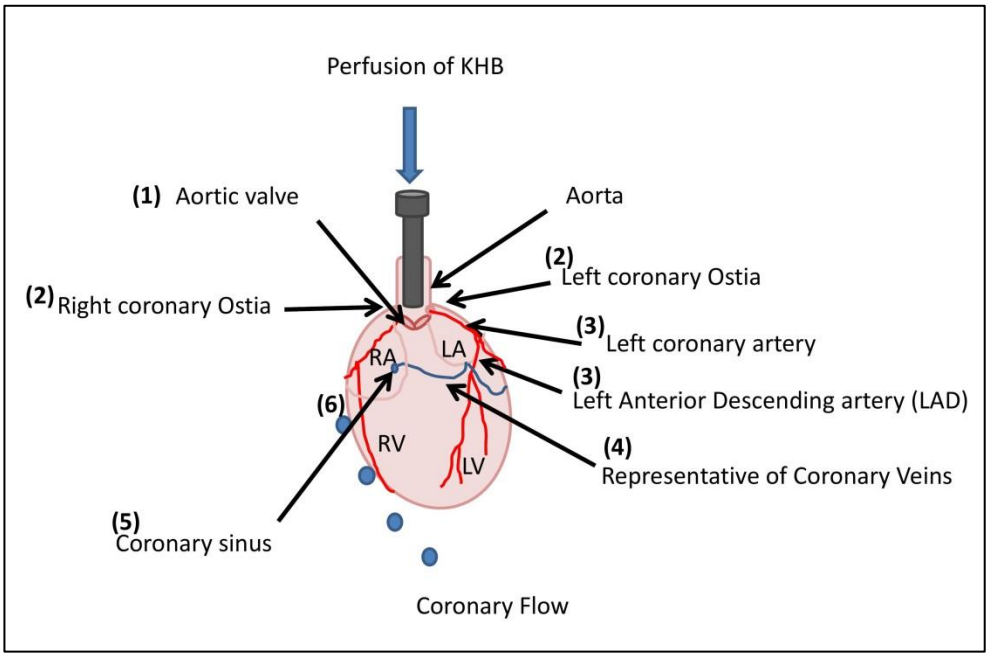

Figure 2.1: Schematic representation of retrograde perfusion of the heart. Krebs Henseleit Buffer (KHB) enters the heart via the aorta: (1) The aortic valve closes under pressure and prevents fluid from entering the left ventricle (2) Movement of the perfusate through the right and the left coronary ostia (3+4) Movement of perfusate through the coronary arterial vasculature (5) Entry into the right atrium via the coronary sinus and (6) coronary flow.

For complete presentation of the isolated heart model I need to mention an alternative model of the isolated, perfused heart: the working heart model. The working heart model was developed by Neely and colleagues[453-455]. Briefly, the perfusate enters the heart by a cannula placed in the left atria, passes through the left ventricle and exits via the aorta. This mode allows the heart to pump fluid and utilize the normal circulatory pathway through the ventricles and is used primarily to assess cardiac function [456].

In my studies, I used only the Langedorff preparation which is considered a better model for investigating infarction following ischaemia-reperfusion injury, which was the main end point of my experiments.

2.2.1.2 Constant flow or constant pressure perfusion?

In the original Langendorff preparation, the heart was perfused at a constant pressure by placing the reservoirs to an adequate height. However, in 1939 a modification was made by Katz, in which he changed the mode of perfusion. Instead of the heart being perfused at a constant pressure, he perfused hearts at a constant flow and measured the coronary perfusion pressure, using this as a tool to assess the coronary vascular resistance. Hence, Langendorff experiments can be conducted in two different modes: constant pressure or constant flow. Each mode has its advantages and disadvantages and the choice is usually dependent on the aim of the experimental investigation. Modern constant flow systems use a peristaltic pump to deliver desired set volumes of perfusate into the heart. This is very easily controlled and monitored by a computer program called Lab Chart. Constant flow mode may be preferred for investigating coronary vascular tone or smooth muscle and endothelial function. Using a known flow rate and perfusion pressure (measured by a pressure transducer placed in before the perfusion cannula) a derivation of Ohm's law can be used to calculate coronary vascular resistance [452]. Hence, in whole heart preparations, the drugs that have potential vasoactivity can be easily and directly investigated.

The original constant pressure system set up by Langendorff is still most commonly used today. Constant pressure systems can easily be achieved as a low cost option for laboratories, by positioning a glass chamber containing a set volume of perfusion buffer at a specific height above the tip of the perfusion cannula which is inserted into the aorta. However, constant pressure can also be achieved in other ways. Langendorff used a sealed pressurised chamber with a connected manometer to measure and maintain a constant pressure of perfusate through the heart. Working on the same principle, pressure control circuits using peristaltic roller pumps creating a negative feedback pressure control loop combined with modern plastic chamber apparatus are now very popular. The main advantages of this regulated system are: smaller perfusate volumes are needed, continuous measurement of coronary flow based on calibration of pump speeds, ease of switching between constant flow and constant pressure and also that two chambers can be simultaneously or alternatively used for the investigation of compounds or agents throughout the experiment. This mode is certainly advantageous and more physiological when investigating ischaemia

and reperfusion. For example, during constant flow mode, when the isolated heart enters ischaemia, autoregulatory changes such as adjustment to heart rate and muscle contraction cannot occur. The constant pressure set up is shown in Figure 2.2.

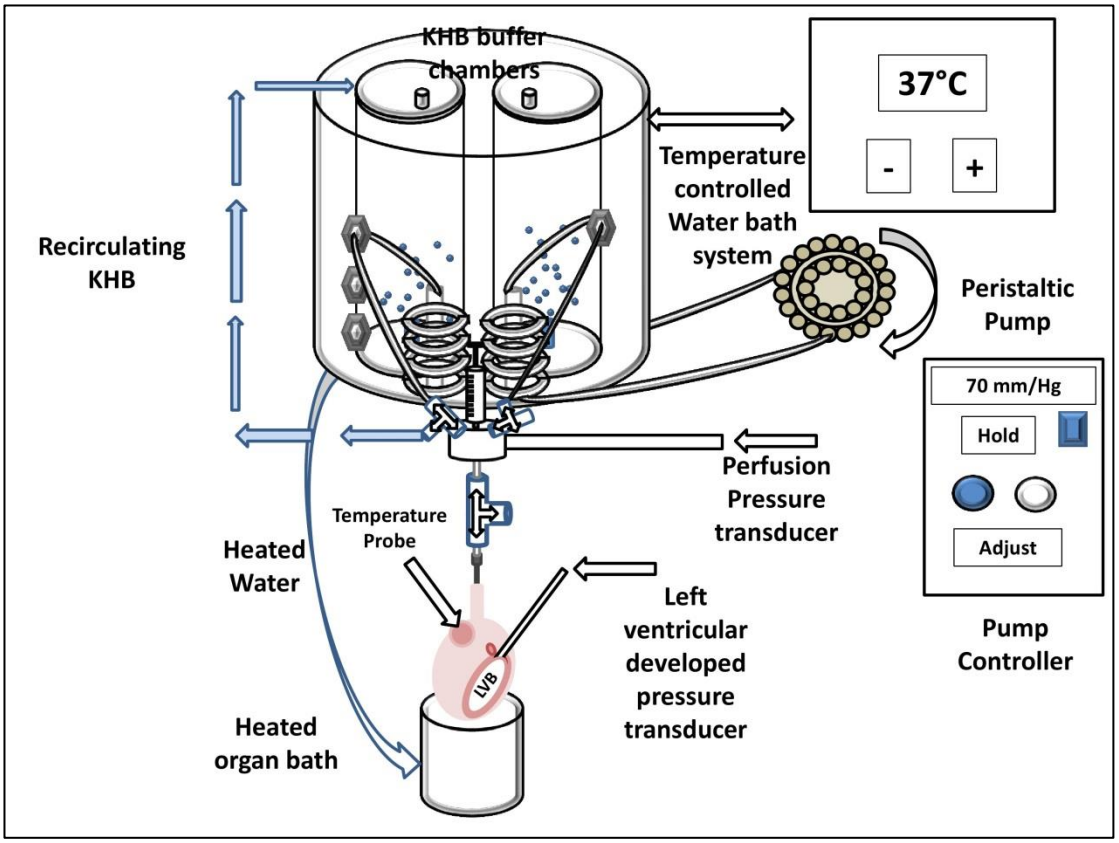

Figure 2.2: Constant pressure Langendorff system controlled by Peristaltic pump

2.2.1.3 Langendorff isolated rat heart-experimental steps

2.2.1.3.1 Preparation of the Langendorff rig and perfusion buffer

My investigations used the Langendorff constant pressure perfusion system (ADInstruments, Chalgrove, UK) demonstrated in figure 2. The rig was regularly thoroughly cleaned with warm water to ensure all perfusion tubes are clean and free of any precipitated salts and the surrounding water bath systems were heated. The perfusion buffer I used was modified Krebs and Henseleit (KHB) physiological salt solution containing mM: NaCl 118.5, $NaHCO_3$ 25.0, KCl 4.8, $MgSO_4$ 1.2, KH_2PO_4 1.2, $CaCl_2$ 1.7 and glucose 11.0 **(**Table 2.2). To maintain a pH of 7.4, the buffer was gassed with 95% O_2/5% CO_2.

Compound	Molecular Weight	mM	g/L
NaCl	58.44	118	6.896
$NaHCO_3$	84.01	25	2.1
d-Glucose	180.2	11	1.98
KCl	74.55	4.7	0.35
$MgSO_4.7H_2O$	246.5	1.22	0.3
KH_2PO_4	136.1	1.21	0.165
Mix thoroughly then add			
$CaCl_2.2H_2O$	147	1.84	0.27

Table 2.2: Krebs and Henseleit (KHB) physiological salt solution composition

2.2.1.3.2 Anaesthesia and excision of the heart

Prior to any surgical procedure including excision of the heart, the animals need to be under general anaesthesia. There are numerous anaesthetics and delivery methods none of which are completely ideal, most commonly used is an intraperitoneal (I.P.) injection of barbiturates (thiopental/sodium pentobarbital) or an inhalation of volatile anaesthetics (Halothane, Isoflurane). The latter is rarely used for an excision of the heart procedure as complicated equipment is required for administration and induction. Also, inhaled volatile anaesthetics can be cardioprotective; this is an important consideration in studies like those conducted in this thesis assessing cardioprotective regimens. Sodium pentobarbital is usually the preferred method of induction in non-recovery experiments; it is a barbiturate that has depressant activity on the central nervous system (CNS) by enhancing the action of GABA at the $GABA_A$-receptor/chloride channel [457]. It provides deep anaesthesia in animals;

however, care must be taken as these compounds can have a very narrow therapeutic window where deep anaesthesia quickly develops into cardiorespiratory suppression. When used as a single injection of 50-60 mg/kg I.P. the rate of anaesthesia can be very safe and effective.

Rats were injected with 55 mg/kg sodium pentobarbital with 300 units heparin I.P. Heparin was added to reduce any potential risk of coronary thrombus formation. The rats were placed in a clean box in a stress-free environment and monitored for loss of consciousness. Eventual loss of the pedal withdrawal reflex demonstrated that the animal was under surgical anaesthesia. Now it could be removed from the box and positioned supine for easy access to the chest. Briefly, an incision was made through the skin to expose the sternum and then the diaphragm. To expose the thoracic cavity the diaphragm was cut and two diagonal incisions made from the base of the ribs towards the upper part of the forelimbs, to create a clamshell thoracotomy. The heart was slightly raised by cradled fingertips and the aorta, vena cava and pulmonary artery were excised in one movement. The heart was placed in ice cold KHB to clear the blood and to stop beating to preserve the organ from any possible ischaemic damage.

2.2.1.3.3 Cannulation of the aorta and perfusion of the coronary system

If necessary, the heart was gently cleaned of any connective tissue to expose the aorta whilst in the ice cold KHB solution. If the aorta was too long, a cut below the branching was made and then it was held by the forceps on either side of the opening and gently slipped over the cannula whilst supplying low flow of warm, oxygenated KHB. The aorta was carefully positioned so that the cannula sat above the ostia of the coronary arteries and was then held in place by a crocodile clip. The aorta was secured to the cannula by a suture and the clip removed. The heart immediately started to contract as the KHB flowed in a retrograde fashion through the coronary system. Any remaining blood was washed out and the heart turned pink as regular heart beat returned. Any remaining connective tissue or fat was removed to clean the preparation.

2.2.1.3.4 Measuring physiological parameters

Next, an opening was made by removing the left atrial appendage and a deflated, latex balloon inserted via the open atria through the mitral valve and into the left ventricle, this allowed measurement of cardiac function throughout the experiment. The balloon is attached to a catheter which connects to a pressure transducer and bridge amplifier. The balloon, the catheter and the transducer communicate with each other and are filled with distilled water, with no air bubbles to disrupt the fluid continuity. The size and

material of the balloon is very important; the balloon must not be too large to obstruct the natural rhythm of the heart but must be large and sensitive enough to be able to recognise any changes that occur throughout the experiment. Using tips of unlubricated latex condoms are now very popular due to their thin, flexible and biological compatible nature. Commercially available latex balloons did not always fulfil these criteria and therefore homemade cling film balloons were also often used. However, the cling film balloons need to be replaced regularly due to their properties changing over time and usage, especially in ischaemia/reperfusion investigations, where the balloon will undergo more stress.

The balloon was then precisely inflated within the left ventricle using a syringe to give a preload (resting) left ventricular end diastolic pressure (LVEDP) of 8-10mmHg to optimise left ventricular pressure without over-loading the heart according to the Frank–Starling curve [452]. The rhythmic pressure of contraction which the heart exerted onto the balloon, transferred via the attached transducer and was visualised on a computer screen. From this recording, left ventricular systolic pressure and heart rate (HR) were monitored and used to calculate rate pressure product (RPP) or workload efficiency of the heart and also the left ventricular developed pressure (LVDP) was measured. Another incision was made at the base of the pulmonary trunk not only to facilitate coronary venous drainage but also to give access to the temperature probe which was inserted into the heart via this aperture. Lastly, the flow rate was adjusted to give a perfusion pressure of 70 mm/Hg and set at this value for the entire experiment i.e. in constant pressure mode. The heart was then left to stabilise.

2.2.1.3.5 Ischaemia

Following stabilisation, Langendorff heart preparations can be used to investigate ischaemia-reperfusion injury. Two degrees of ischaemia can be applied: Global or regional ischaemia. Global ischaemia is achieved simply by preventing flow to the entire heart for a set period of time by turning off the flow to the entire heart. Temperature is maintained externally by bathing the heart in a KHB filled, water insulated jacket at 37°C. Alternatively, regional ischaemia can be applied. This is considered to represent an acute myocardial infarction whereby a blockade in the coronary system occurs. Regional ischaemia is achieved by passing a suture through the surface of the heart to surround the left anterior descending coronary artery (LAD), the vessel that supplies the left ventricular coronary system with perfusate. The consistency of the rat coronary system [458] allows reference points to be used to place the suture around the LAD (Figure 2.3). Ideally, the suture placement will allow for

approximately 50% of the left ventricle to be 'risk zone'. When required, the suture can be temporarily tightened using a snare system created from pipette tips and occlude the LAD hence causing ischaemia. In constant pressure mode, at least a 30% reduction in coronary flow and developed pressure is expected to confirm correct positioning of the suture. When using regional ischaemia, it is important to place the suture before inserting the intraventricular balloon to prevent any possible puncturing.

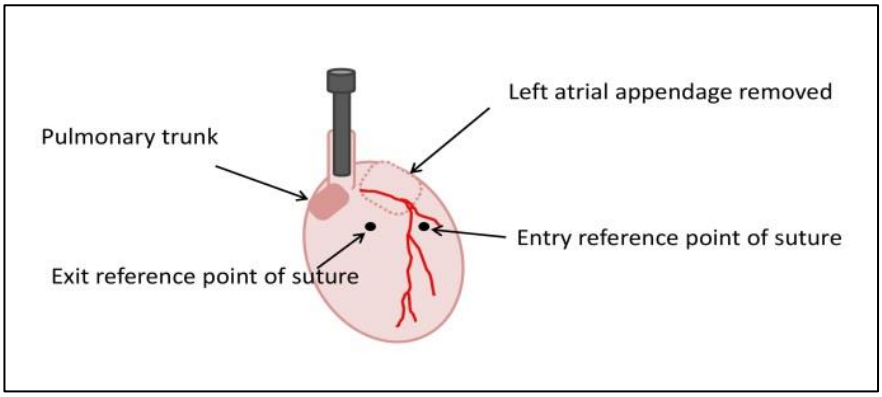

Figure 2.3: Reference points used to ensure suture is placed surrounding the left anterior descending coronary artery (LAD):

2.2.1.3.6 Reperfusion

Reperfusion is an essential part of a Langendorff experiment; in either ischaemic models it involves the return of the flow to the ischaemic area. In the case of global ischaemia, it is simply by switching the pump controller back on or a three-way tap to open. In regional ischaemia, flow is re-established by loosening the snare system; as a sign of sufficient reperfusion, one would expect at least an initial partial recovery of coronary flow and developed pressure. It is important that the suture remains intact for area at risk determination. Traditionally 120 minutes of reperfusion was used for isolated rat heart preparations however recent studies have shown a clear infarct demarcation after 60 minutes [459, 460], this is explained further in characterisation of the model section.

2.2.1.4 Essential criteria for a successful Langendorff experiment

To achieve consistent and reproducible data using the Langendorff isolated heart model there are key stages throughout the experiment that need special attention. Firstly, accurate preparation of the buffer and sufficient heating and oxygenation are required to reach an appropriate pH prior to perfusing the heart[461]. This should be monitored using a blood gas analyser to ensure that the pH is consistent throughout the experiment. Perfusion tubing should be carefully checked to ensure no air bubbles

are in the system, which could block coronary arteries and result in a deleterious or a complete loss of function in the perfused heart.

Excision of the heart and cannulation of the aorta are the most important and sometimes most difficult steps of the experiment. Care must be taken in the handling and excision of the heart, any damage caused to the organ can lead to inconsistent results [462, 463] and a sufficient length of aorta is required to allow for successful cannulation. Speed of cannulation and hence return of coronary perfusion to the heart is vital, prolonged cannulation time can either lead to myocardial damage or activation of stress signalling pathways causing the heart to enter a preconditioned state [464, 465].

The depth at which the cannula is inserted into the aorta can cause numerous problems and is normally signalled by an unexpectedly high or low flow rate through the heart. High flow rates often indicate a tear in the aortic wall, which can occur during instrumentation of the heart or a damaged aortic valve possibly caused by the cannula being inserted too deep and then being removed during cannulation. It is therefore difficult to tell whether the increased flow rate is indicative of perfusion through the coronary branches. Low flow rates often coincide with poor heart function and arrhythmias; this can often be caused by a deeply-positioned cannula partially occluding the coronary ostia and therefore restricting coronary flow. Embolisation of the coronary vessels by air bubbles or buffer particulate can also cause low flow rates.

Maintaining temperature throughout the entire procedure is an essential component of an isolated heart perfusion. Temperature should be tightly controlled; a small fluctuation in temperature by as little as 2°C can lead to distinct changes in myocardial contractility and heart rate [463, 466]. Temperature change can lead to substantial differences in end point assessment of cell death following ischaemia-reperfusion[467]. Triggering of signalling pathways that lead to preconditioning-like cardioprotection can occur in response to either hypothermia [468] or hyperthermia [469] and will interfere with studies investigating cardioprotective manoeuvres. Therefore it is vital that temperature is continuously monitored and adjusted throughout the experiment.

To ensure consistency of data analysis and interpretation of results, exclusion criteria are set for heart preparations that undergo technical errors and display some of the aforementioned problems. These exclusion criteria should be strictly adhered to and are summarised in Table 2.3**.**

Parameter	Rat heart
Time to perfusion (min)	>3
Coronary flow (ml/min)	<10 or >28
Sustained Arrhythmias (min)	>3
Heart rate (beats per min)	<150 or >400
Left ventricular developed pressure (mm Hg)	<70
Rate Pressure Product (mm Hg/sec)	<17000

Table 2.3: Exclusion criteria for rat Langendorff experiments. The numbers displayed for each criterion are the minimum value accepted to deem a heart appropriate for experimental investigation.

2.2.1.5 Advantages and disadvantages of the Langendorff isolated heart

There are numerous advantages and disadvantages of the Langendorff isolated heart, these are outlined in Table 2.4**.**

Advantages	Disadvantages
❖ Provides highly reproducible results	❖ Heart is vulnerable to damage caused by excision and oedema caused by crystalloid solutions
❖ Cost effective	❖ Heart can be inadvertently preconditioned
❖ Not as time consuming or technically demanding as other techniques	❖ Retrograde perfusion can cause aortic valve incompetence if perfusion pressure is high
❖ High data output from a single experiment	❖ Non physiological coronary flow rate
❖ Physiological preparation (whole myogenically beating heart)	❖ Lacks normal humoral and neuronal regulation

Advantages	Disadvantages
❖ Direct assessment of cardioprotective myocardial drugs	
❖ Pathological parameters easily controlled and assessed (hypoxia, arrhythmias,infarction)	
❖ Cardiotoxicity assessment of potential drug compounds	

Table 2.4: Advantages and disadvantages of the Langendorff isolated heart preparation

2.2.2 In vivo coronary artery occlusion/2 hour reperfusion (non-recovery model)

2.2.2.1 Introduction

In vivo myocardial ischaemia-reperfusion injury is however a more physiologically relevant model. The heart is being supplied with blood not a crystalloid buffer solution, allowing for inflammatory factors to contribute to cell death and to investigate whole body influence on infarct size.

2.2.2.2 Surgical Procedure

The Surgical procedure is summarised in Figure 2.4. Rats were anesthetised with sodium pentobarbital (20mg/kg intraperitoneally). Surgical depth of anaesthesia was confirmed by the loss of the pedal withdraw reflex, the area of fur surrounding the incision point was shaved and the rats secured onto a self-regulated temperature control mat (CMA450, Harvard apparatus) on a flat board (A). The flat board was tilted to a 45° angle (B), the rats were intubated and ventilated with a Harvard ventilator (room air, 70 strokes/min, tidal volume: 8-9ml/kg). Body temperature was maintained at 37.4±1°C by means of a rectal probe thermometer attached to the temperature control system and electrical activity of the heart monitored by placement of ECG probes (C). A lateral thoracotomy was performed between 4th and 5th intercostal space (D) and a chest clamp inserted to expose the heart (E). The pericardium was gently removed and location of LAD was confirmed by sight. A 6-0 suture passed around the LAD by a sweeping semi-circular motion from left to right to ensure the suture did not puncture the exposed lung (F). The loop system was carefully placed onto the sutures and left on the surface of the heart (G). Following stabilisation, the suture was tightened using

the loop system to create LAD ligation and clamped to maintain pressure throughout the experiment (H). Regional ischaemia was confirmed by ST segment elevation, blanching and colour change of the myocardium (I). After 30 minutes of ischaemia, the loops were pulled free to loosen the suture and reperfuse the vessel for 120 minutes. Successful reperfusion was classified by colour return to the occluded area and a decrease in ST elevation seen during ischaemia. Typical ECG changes are shown in Figure 2.5. Depth of anaesthesia was checked every 5 min throughout the experiment and animals were topped up as needed.

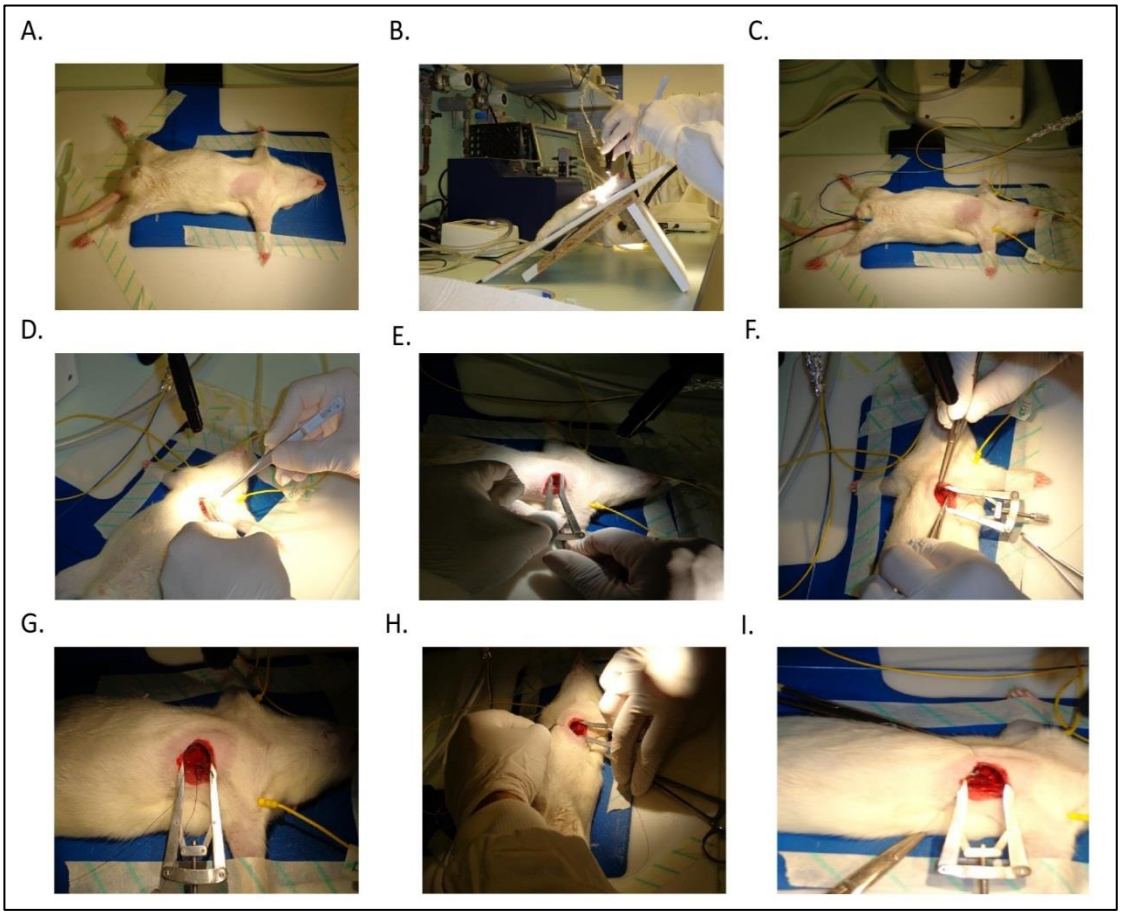

Figure 2.4: Surgical steps for In vivo coronary artery occlusion/ reperfusion model. (A). Fur was removed around the incision point and the rats secured onto a self-regulated temperature control mat on a flat board (B) The flat board was tilted to a 45° angle and the rats were intubated (C). Insertion of rectal probe thermometer and placement of ECG probes. (D) A lateral thoracotomy 4th and 5th intercostal space (E) Chest clamp inserted to expose the heart (F) Removal of the pericardium, LAD located and a 6-0 suture passed around the LAD by a sweeping semi-circular motion from left to right to (G). The loop system placed onto the sutures and left on the surface of the heart (H). Tightening of the suture caused LAD ligation (I) Suture clamped to maintain pressure throughout the experiment.

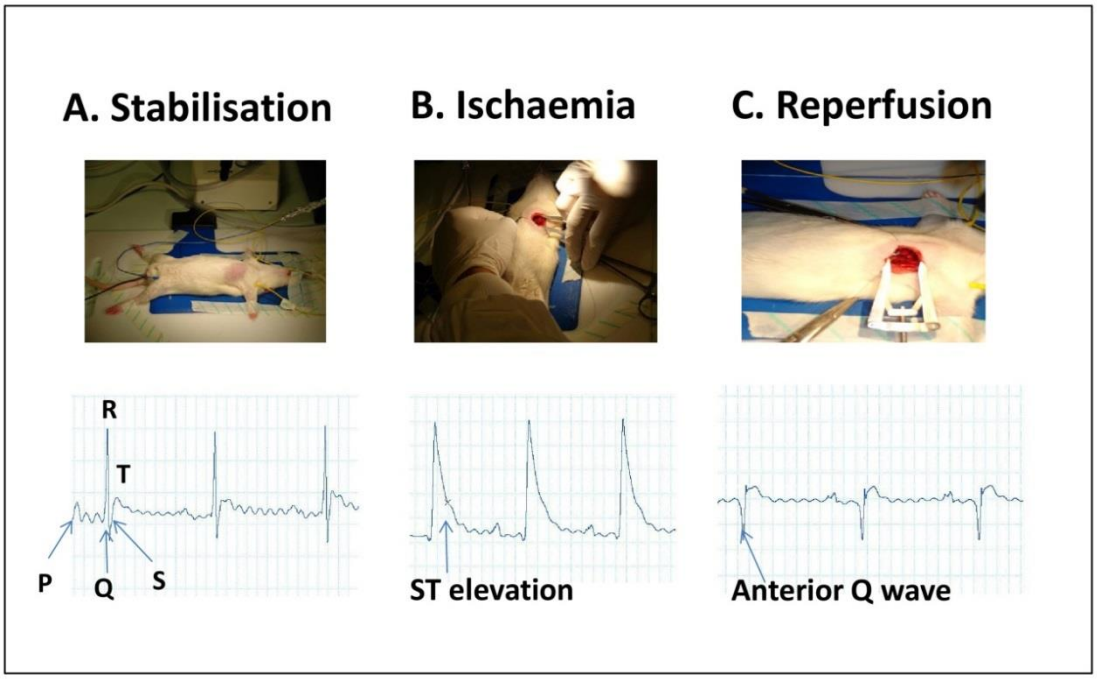

Figure 2.5: Typical ECG changes during ischaemia-reperfusion model. A. During stabilisation normal ECG profile seen. B. Upon occlusion of the LAD, elevation and widening of the ST segment. C. During reperfusion, ST segment elevation is decreased, often accompanied by an anterior Q wave.

2.2.3 In vivo coronary artery occlusion/reperfusion (recovery model)

2.2.3.1 Surgical Procedure

Rats were anesthetised with a cocktail containing ketamine (65 mg/kg), xylazine (13 mg/kg), and acepromazine (1.5 mg/kg) (I.P) and the surgical procedure performed as described above, however during ischaemia Buprinorphine was administered I.P. At the end of ischaemia, the suture was left surrounding the LAD and the ends cut short to tuck into the chest cavity. The intercostal space was closed with a 4-0 suture and the skin incision closed with wound clips. Care was taken to remove the air from the chest cavity by creating an end positive pressure and the skin simultaneously clamped together before stapling. The ventilator was removed and the rat immediately received a loose supply of carbogen (95% O_2/5% CO_2) to aid recovery. The rat was kept warm and was monitored until it regained its 'righting reflex'. Depending on the aim of the study, the animal can be allowed to recover upwards of 2 hours. Although successfully performed whilst learning the technique, this method was not used to generate results in this thesis.

2.2.4 Infarct size determination

Infarct size is determined by triphenyltetrazolium chloride (TTC) staining. TTC is a reducing agent which can cross cellular membranes to react with intracellular dehydrogenases such as NADPH, to form a formazan pigment. In viable tissue, TTC reacts with preserved NADPH within cells and forms a red precipitate. However, dead cells have disrupted membranes which allow enzymes' to wash out, less therefore the reaction cannot occur and the tissue appears as a pale white colour. Other surrogate end-points such as enzyme release, cell viability in cultured cells and recovery of post ischaemic function are often used; however these are not accurate measurements of tissue death. Though, TTC method of staining has become very reliable, considerations still must be taken for false negative or false positive staining. For example, tissues could stain positive (red) because sufficient enzyme washing out has not occurred.

2.2.4.1 Preparation of TTC solution

TTC powder was dissolved in a buffer (pH of 7.4) obtained by mixing a 2 part phosphate buffer system. Initially, two phosphate buffer solutions were made: a high pH solution (1) consisting of Na_2HPO_4 [0.1M] and a low pH solution (2) consisting of NaH_2PO_4 [0.1M]. To make 0.1M stock solutions of (1) and (2): the molecular weight of NaH_2PO_4 is 120 therefore 12g was mixed in 1L of distilled water for solution (1) and the molecular weight of Na_2HPO_4 is 142 therefore 14.2g was mixed in 1L of distilled water for solution 2. To give a final pH of 7.4, these solutions were mixed in a ratio of 8 parts of solution 1 to 2 parts of solution 2. An appropriate volume of TTC solution was made fresh for each day of use, for each heart 10 mls is sufficient. TTC solution was used at 1% weight/volume (1g/100ml), i.e. for 10 mls 100 mg of powder was added.

2.2.4.2 Regional Ischaemia infarct assessment

On completion of regional ischaemia/reperfusion protocol either *ex vivo* or *in vivo*, hearts undergo a two-step staining procedure using Evans blue dye and TTC. For Langendorff perfused hearts: at the end of reperfusion, the suture surrounding the LAD was permanently retied and Evans blue (0.5% in distilled water) was infused via the cannula into the coronary system. For *in vivo* hearts: at the end of reperfusion, the heart was removed as described (section 2.2.1.3.2). The heart was attached to a cannula via the aorta and secured with a suture. The heart is perfused with warmed modified KHB and the blood cleared from the coronary system**.** The LAD was then permanently re-occluded and Evans blue (0.5% in distilled water) was infused via the

cannula into the coronary system. The dye defines the area at risk within the myocardium, by perfusing and staining all regions supplied above the LAD suture occlusion. The area at risk remains a pale pink colour as the suture prevents entrance of blue dye in the arteries below it. This process is summarised in Figure 2.6. Hearts are decannulated, weighed, wrapped in cling film (to prevent freeze-drying) and then frozen at -20°C. Freezing of the hearts is not essential; however it allows for easier slicing and puts the heart into a rigor state. If fresh hearts are put into TTC the tissue enters contracture which can distort the infarct making analysis very problematic.

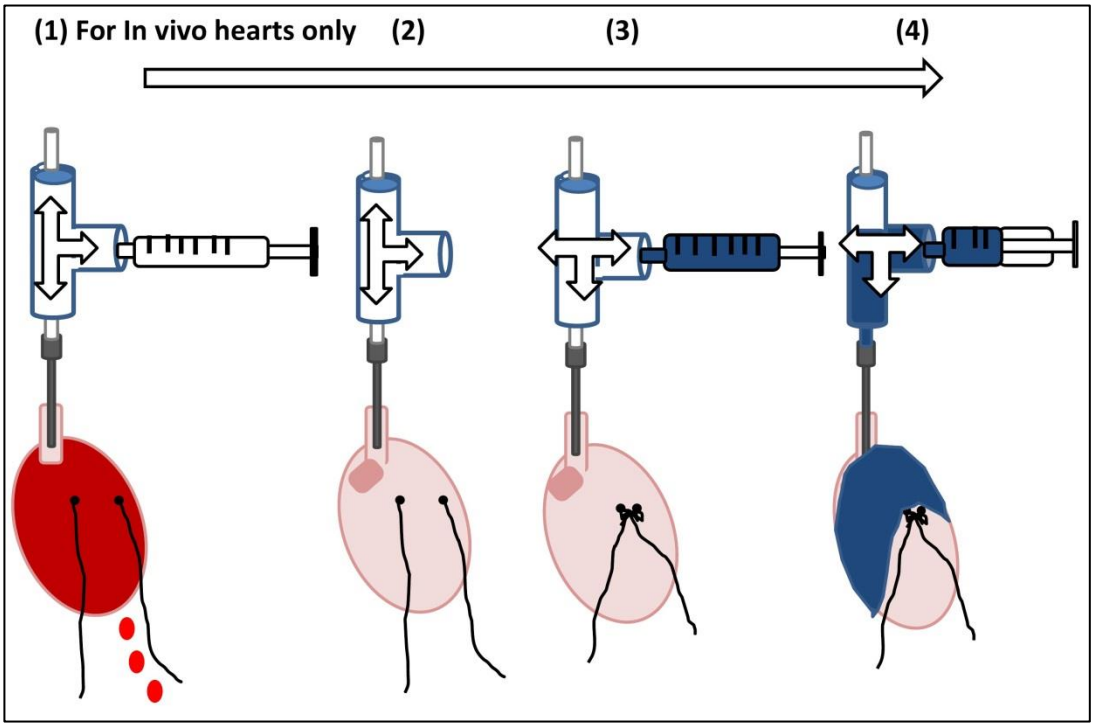

Figure 2.6: Evans blue staining at the end of reperfusion.(1) In vivo hearts were excised from the animal following an ischaemia-reperfusion protocol, cannulated via the aorta and perfused with warm KHB to remove the blood (2). For all hearts: (3) the suture was then permanently retied occluding the LAD. (4) 0.5% Evans Blue dyed was then perfused via the aorta to dilineate the area at risk (AAR) within the left ventricle.

2.2.4.3 Global Ischaemia infarct assessment

In this case, the use of Evans blue dye is not necessary as all the heart was at risk during ischaemia. On completion of global ischaemia/reperfusion, hearts undergo a one-step staining protocol using TTC. Hearts were decannulated, weighed, wrapped in cling film (to prevent freeze-drying) and then frozen at -20°C.

2.2.4.4 General heart slicing and TTC staining protocol

The frozen hearts were sectioned perpendicular to the long axis into a number of slices, for most rat hearts 5, 2-3mm slices are appropriate. Heart slices were arranged and compressed for a few minutes under a heavy block to prevent any curling when entering warm TTC solution. Heart slices were then incubated in 10 ml pre-warmed 1% TTC solution in a 37°C water bath for 20 min, every 5 min the tubes were swirled to ensure equal incubation of all slices. Following TTC incubation, the regionally ischaemic hearts should express 3 colours: red, white and blue and the globally ischaemic hearts just red and white (Figure 2.7). The hearts were then incubated in 10% formalin solution overnight to help increase the contrast between the viable (red) and non-viable (white) tissue.

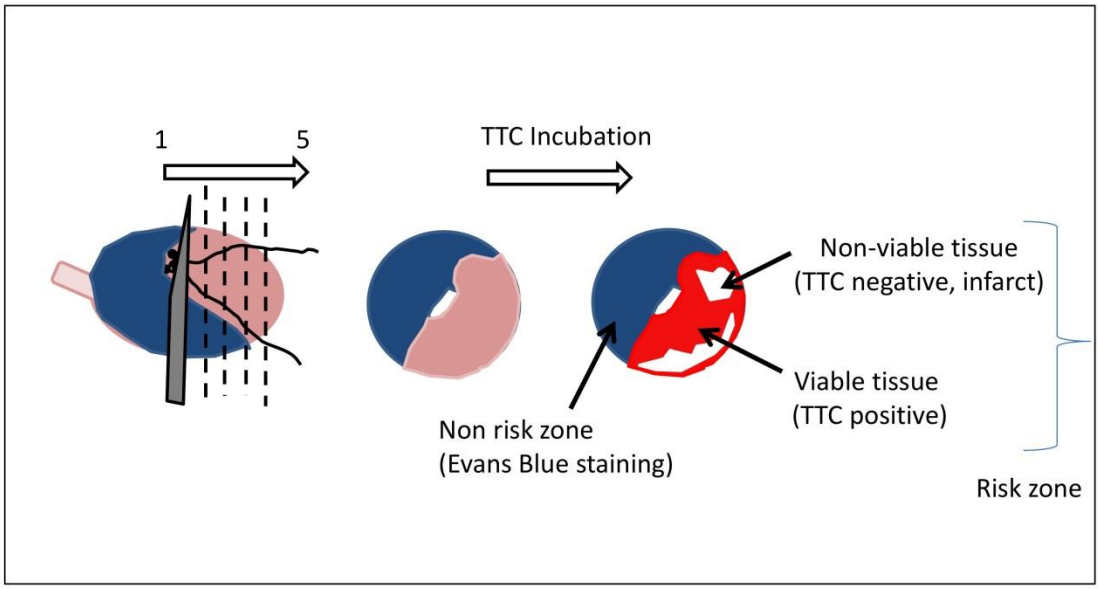

Figure 2.7: Heart slicing and infarct staining. Hearts are removed from the freezer and sliced perpendicular to the long axis into 5 slices. Slices incubated with 1% TTC solution should express 3 colours: red, white and blue.

2.2.4.5 Infarct size measurement

The following day, heart slices were arranged in order from apex to base between two glass plates, compressed to a 2mm thickness and scanned into a digital image using a flatbed scanner. The image was calibrated, enabling the conversion of slice area to slice volume, allowing for computerised analysis of infarct volume within each slice (for global ischaemia) and within the risk zone of each slice (for regional ischaemia) using image J software. Regional ischaemia was used for all infarction studies in this thesis, and the results are expressed as infarct to risk zone ratio (I/R%).

2.3 Characterisation of the Langendorff isolated heart model

2.3.1 Introduction

The Langendorff isolated heart model has been well characterised by many laboratories; the most common experimental protocol used for the isolated rat heart is 35 min of ischaemia followed by 120 min reperfusion [450]. This protocol was deemed successful due to the length of ischaemia and reperfusion causing reproducible levels of cell death to allow for accurate examination of potential cardioprotective strategies. Reperfusion time is extremely important, not only to allow for reperfusion injury to occur, but also when assessing infarct size using TTC staining. As described earlier, accurate TTC staining requires adequate 'wash out' of dehydrogenase enzymes, if this does not occur results can be misleading. In 2009, Ferrera et al, demonstrated that 60 min of reperfusion was enough to assess function and infarct size with TTC in the Langendorff rat model. They found no significant differences in infarct size in control groups or hearts subjected to IPost followed by either 60 min or 120 min reperfusion [459]. Therefore, characterisation of different reperfusion times following hearts subjected to ischaemia was needed to ensure this could be repeated in our Langendorff model. To confirm successful set up of the Langendorff preparation in my hands, as a positive control, I also subjected 2 groups of hearts to IPC protocols followed by either 60 min or 120 min reperfusion.

2.3.2 Experimental protocol

For determination of infarct size, Sprague Dawley rats (300-350g) were anesthetized with sodium pentobarbital (55 mg/kg I.P.) and heparin (300 IU). The hearts were rapidly excised, placed into ice cold Krebs-Henseleit buffer, and quickly mounted onto a Langendorff constant pressure perfusion system (ADInstruments, Chalgrove, UK). The hearts were perfused via the aorta with modified Krebs-Henseleit bicarbonate buffer (KH) (mM: NaCl 118.5, $NaHCO_3$ 25.0, KCl 4.8, $MgSO_4$ 1.2, KH_2PO_4 1.2, $CaCl_2$ 1.7 and glucose 11.0). The buffer was gassed with 95% O_2/5% CO_2 to maintain a pH of 7.4. A suture was placed around the LAD and secured in place by a snare created from two pipette tips. A fluid filled latex balloon was inserted into the left ventricle through an incision in the left atrial appendage and inflated to a left ventricular end developed pressure (LVEDP) of 8-10mmHg. Perfusion pressure was set at 70mmHg, LVDP, heart rate (HR) and coronary flow (CF) were permanently monitored and the rate pressure product (RPP) calculated. An electronic thermo probe inserted into the pulmonary artery continuously monitored temperature which was kept in range of 37°C ± 0.5.

Following stabilization, hearts were randomly assigned to receive one of the protocols summarized in Figure 2.8. Regional ischaemia was initiated by tightening the suture around the LAD and holding it in place with the snare. The snare was then removed and the hearts reperfused for either 60 or 120 min. At the end of this period the suture was permanently tied to occlude the LAD and Evans blue dye (0.25% in saline) was infused through the aorta to delineate the risk zone, with the myocardial tissue not at risk staining blue. Hearts were stored at -20°C for several hours before being transversely sliced into 2mm thick sections and incubated in TTC. The slices were then transferred to 10% formalin overnight for better delineation between zones. The following day the slices were scanned into the computer for analysis. Image J was used to calculate the infarct to risk zone ratio (I/R%).

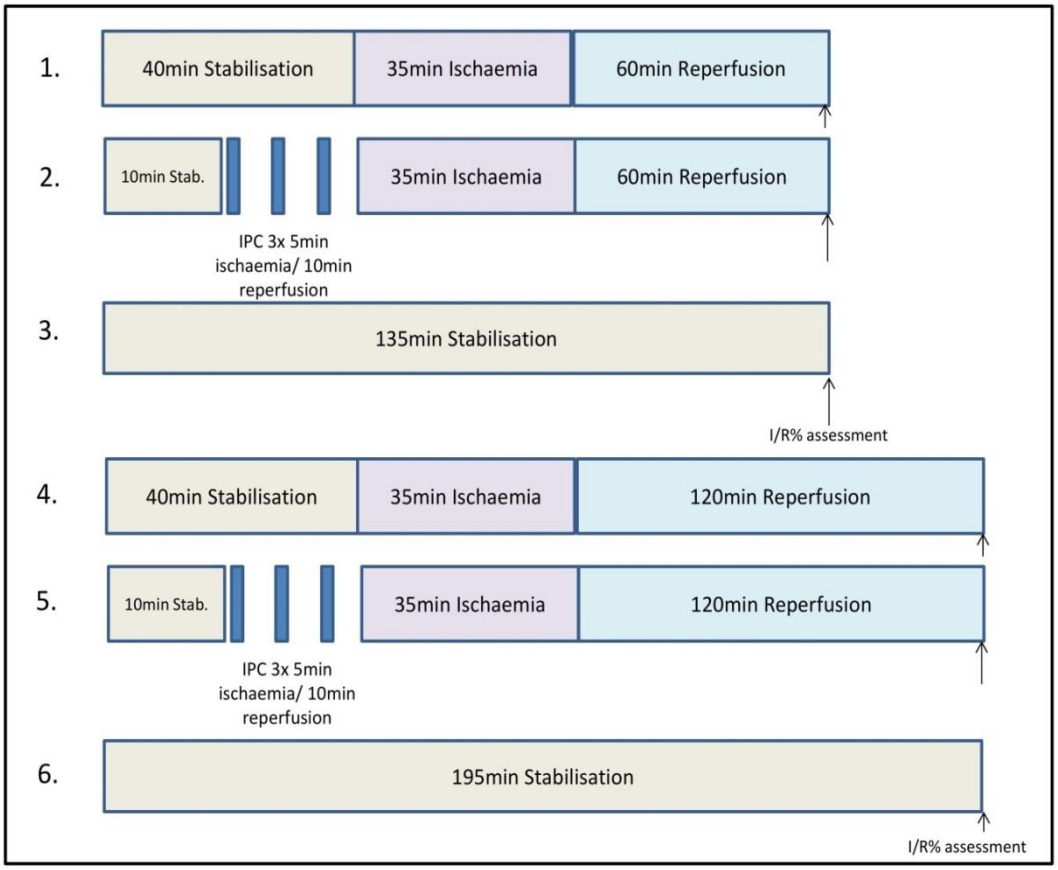

Figure 2.8: Langendorff experimental protocols. Hearts isolated from Sprague-Dawley rats were isolated and subjected to one of the following protocols: (1) Control (60 min reperfusion) (2) IPC (60 min reperfusion) (3) Sham (60 min reperfusion) (4) Control (120 min reperfusion) (5) IPC (120 min reperfusion) or (6) Sham (120 min reperfusion. At the end of each protocol hearts were collected for infarct size assessment (I/R%-Infarct to risk zone ratio).

2.3.3 Infarct size in Sprague Dawley rats: reperfusion time and assessment of ischaemic preconditioning

To confirm successful set up of the model it was important to assess the procedural damage caused to the heart during the experimental procedure itself, these are known as 'sham' experiments. For results to be deemed statistically significant, the difference between groups should be greater than the damage produced by the sham alone. Sham experiments are simply hearts that are perfused with KHB in Langendorff mode for the same duration of an ischaemia/reperfusion experiment but they are not subjected to any injury. There was no difference in the necrotic tissue extent between sham matched experiments for ischaemia/60 min reperfusion and ischaemia/120 min reperfusion (I/R%: 10.1±2.1 *vs* 12.1±1, p=NS), that is 135 min and 195 min *ex vivo*.

Another important step in validating the Langendorff regional ischaemia model was the reproducibility of the suture placement, i.e. the area at risk in the myocardium (AAR). For an experiment to be accepted AAR must be between 45-65% of the left ventricle. If the AAR was outside of these limits, it was likely that either the main coronary artery was ligated and the injury will be extremely severe and the heart may die during the procedure, or lower branches have been occluded by the suture and in this case, the injury will be minimal and will give a false positive result. AAR was consistent between all groups shown in Figure 2.9 .

Infarct size assessment showed that there was no significant difference in I/R% between the hearts reperfused for 60 min compared to 120 min (I/R%: 43.7±2.3 *vs*. 45.1±3.9, p=NS, Figure 2.10). My results confirmed that 60 min of reperfusion following release of the snare is sufficient to give a reproducible and accurate assessment of infarct size assessment using TTC in rat hearts.

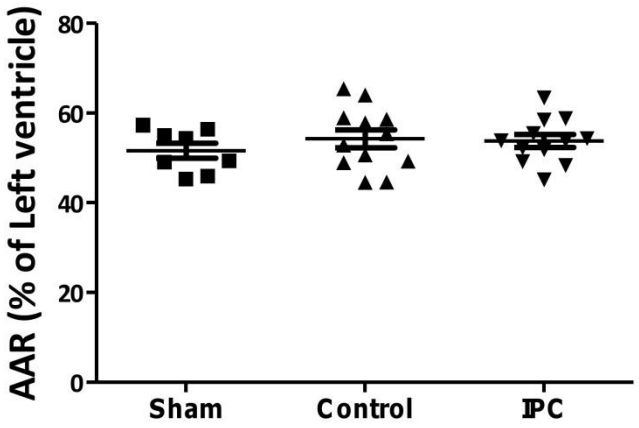

Figure 2.9: Area at risk (AAR) in isolated Sprague-Dawley rat hearts subjected to ischaemia-reperfusion protocols. No difference was recorded in the area at risk (AAR) delineated by Evan's blue staining, between hearts subjected to sham, control or IPC protocols.

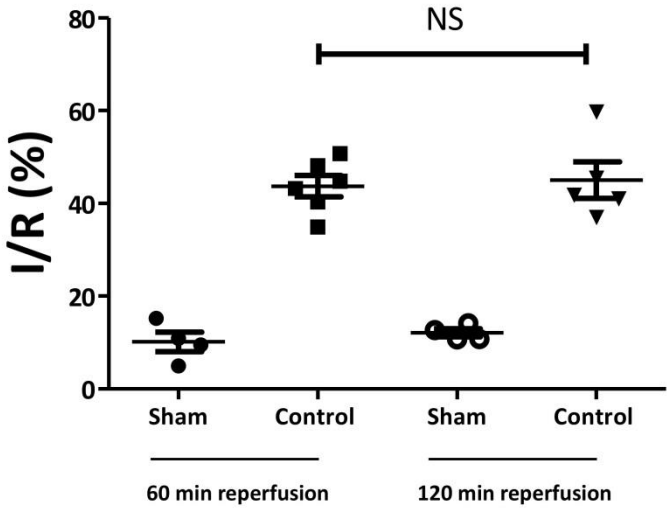

Figure 2.10: Comparison of reperfusion times in isolated hearts isolated from Sprague-Dawley rats subjected to either sham or control protocols. Infarct size assessment showed that there was no significant difference in the infarct to risk zone ratio (I/R%) between the hearts reperfused for 60 min compared .to 120 min in either protocol. Statistical analysis was determined using One-way ANOVA followed by Tukey's post hoc analysis, $p<0.001$, $n>4$.

IPC has proven to be a highly reproducible, protective phenomenon against IRI in numerous species [123].To further validate the model, I assessed whether Sprague Dawley rat hearts could be protected against IRI by 3 cycles of IPC and whether different lengths of reperfusion affected the outcome of this cardioprotective manoeuvre. IPC reduced infarct size in Sprague Dawley hearts by approximately 50% and there was no difference between 60 min or 120 min reperfusion (I/R%: control, 43.7±2.3 *vs.* IPC, 22.8±2.3 for 1 hour reperfusion, and control, 45.0±3.9 *vs.* IPC, 20.7±2.3 for 2 hours reperfusion, Figure 2.11.

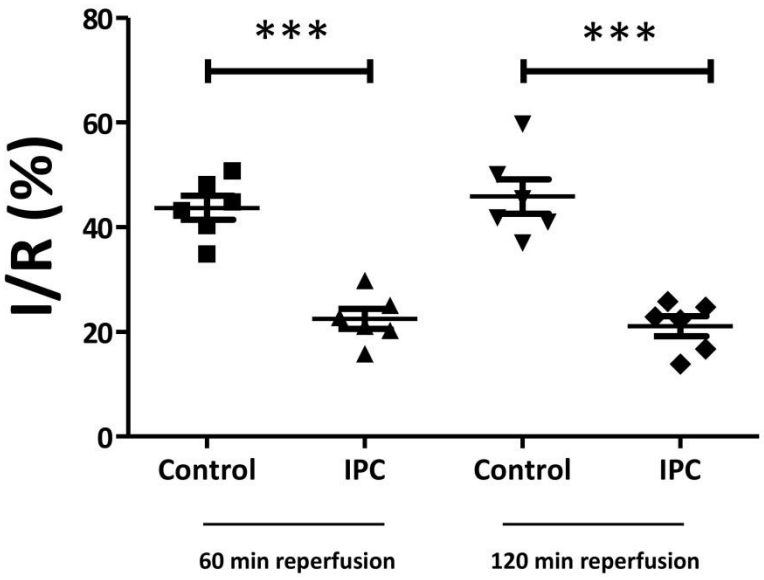

Figure 2.11: Comparison of reperfusion times in isolated hearts from Sprague-Dawley rats subjected to control or ischaemic preconditioning (IPC) protocols. Infarct size assessment showed that there was a significant reduction in infarct to risk zone ratio (I/R%) when IPC was applied prior to ischaemia-reperfusion irrespective of reperfusion time. Statistical analysis was determined using One-way ANOVA followed by Tukey's post hoc analysis, $p<0.001$, $n>6$.

2.4 Isolated adult cardiomyocytes

2.4.1 Introduction

Myocyte isolation has been performed for almost 40 years. Since Powell and Twist described a rapid technique for the isolation and purification of adult cardiac muscle cells [470], it has become a widely used and scientifically important tool. Many investigators simply use enzymatic digestion of the left ventricle using agitation and dicing techniques, however, an alternative reproducible method yielding high quality cardiomyocytes is the use of the Langendorff isolated heart method. This method perfuses the heart with digestion buffer via the coronary system ensuring that minimal damage is caused to the heart cells and that equal exposure of the ventricles to digestion occurs.

2.4.2 Standard Isolation protocol

Hearts were extracted and rapidly hung via the aorta onto a cannula attached to a simplified Langendorff system, and perfused with a constant flow rate of 10ml/min. For collagenase digestion, a stock perfusion solution was prepared (Table 2.5), and then five different perfusion solutions were made by the additions shown in Table 2.6.

Ions	Concentration (mM/L)	g/500ml	g/L	g/2L
NaCl	130	3.79	7.59	15.18
KCl	5.4	0.2	0.4	0.8
$MgCl_2$	1.4	0.066	0.133	0.266
Na_2HPO_4	0.4	0.028	0.057	0.114
HEPES	4.2	0.5	1	2
pH to 7.3 at 37ºC				
Glucose †	10	0.9	1.8	3.6
Taurine †	20	1.25	2.5	5
Creatine †	10	0.655	1.31	2.62

Table 2.5: Composition of the stock perfusion solution required for isolation of cardiomyocytes.

Stock Perfusion Solution	Final concentration	Addition to volume stated in first column
(1) 50 mls **(to clear heart of blood)**	750 µM $CaCl_2$	**37.5 µl of 1M $CaCl_2$**
(2) 50 mls **(to arrest heart)**	100 µM EGTA	**2 mg of EGTA**
(3) 40 mls **(to digest heart)**	100 µM $CaCl_2$ and 0.5mg/ml Collagenase	**40 µl of 100mM $CaCl_2$** **15-20 mg of collagenase**
(4) 50 mls **(to re-introduce $CaCl_2$)**	0.5 mM $CaCl_2$	**25 µl of 1M $CaCl_2$**
(5) 50 mls **(to re-introduce $CaCl_2$)**	1 mM $CaCl_2$	**50 µl of 1M $CaCl_2$**

Table 2.6: Additional components to be added to each specific stock perfusion solution on day of isolation.

Hearts were initially perfused with solution (1), containing a low concentration of calcium which is required to initiate a stable contraction and clear the heart of blood. After 4 minutes of perfusion with solution (1), any remaining solution (1) was carefully removed and replaced with solution (2). Solution (2), containing EGTA, arrests the heart to prevent contracture of the cardiomyocytes. Following 4 minutes perfusion with

solution (2), any remaining solution was carefully removed and replaced with solution (3) to initiate enzymatic digestion. Solution (3) contained type II collagenase and was re circulated to allow for 8minutes of digestion or until the heart appeared swollen and changed colour. The heart was sectioned below the atria, and the ventricular tissue was cut up into smaller pieces and resuspended in 20 mls of solution (3). This solution was kept at 37 °C and agitated gently with pure O_2 for between 15 and 20minutes to continue digestion. Pieces of ventricular tissue were finally teased apart using a cut Pasteur pipette.

Undigested tissue was removed by filtration through a piece of sterile gauze and the remaining suspension was left for 8 minutes to allow viable cardiomyocytes to form a pellet at the bottom of the falcon. The supernatant containing dead cells was removed and the pellet of live cells was resuspended gently in warmed solution (4), and then repeated using solution (5). Myocytes were finally resuspended in M199 medium with added penicillin (100 IU/ml), streptomycin (100 IU/ml), L-carnitine (2 mM), creatine (5 mM), taurine (5 mM) and BSA (2g/L) (Medium 199, Sigma, UK) and plated on pre-laminated 6 well plates for 2-24 hours prior to experimental investigations described in later chapters.

2.4.3 Isolation of cardiomyocytes from old, diabetic rat hearts

Traditional collagense type II digestion worked when characterising the model using young, healthy Sprague Dawley rats, however, problems arose when attempting to isolate old and diabetic cardiomyocytes. Modifications of the method included increasing the concentration of collagenase, increasing digestion time and allowing cells to pellet for longer however the yields were still disappointing. For old, diabetic rat hearts, better results were obtained when the digestion was performed with Liberase TM (Roche applied science), which consists of an equal ratio blend of highly purified Collagenase I and II and also the neutral protease thermolysin, giving a higher protease activity. Liberase-digestion protocol was previously characterised by another lab member. The same stock perfusion buffer was used Table 2.5, however the additions were adjusted as shown in Table 2.7.

Stock Perfusion Solution	Final concentration	Addition to volume stated in first column
(1) 50 mls **(to clear heart of blood)**	750 µM $CaCl_2$	**37.5 µl of 1M $CaCl_2$**
(2) 50 mls **(to arrest heart)**	100 µM EGTA	**2 mg of EGTA**
(3) 30 mls **(to digest heart)** **(Stablise solution in incubator for at least 30 min prior to use)**	0.2 mg/ml Liberase 0.14 mg/ml Trypsin $5x10^{-3}$ U/ml DNAse 12.5 µM $CaCl_2$	**5 mg of Liberase** **167 µl of 2.5% Trypsin** **1.5 µl of 100U/ml DNAse** **3.75 µl of 100 mM $CaCl_2$**
(4) 18 mls **(to stop Liberase and re-introduce $CaCl_2$)**	12.5 µM $CaCl_2$ 10% Fetal Bovine Serum (FBS)	**25 µl of 10 mM $CaCl_2$** **2 ml of 100% FBS**
(5) 19 mls **(to stop Liberase and re-introduce $CaCl_2$)**	12.5 µM $CaCl_2$ 5% FBS	**25 µl of 10 mM $CaCl_2$** **1 ml of 100% FBS**

Table 2.7: Additional components to be added to stock perfusion solution on day of isolation

Hearts were subjected to the same protocol of perfusion as described above solutions (1) to (5). However, a slower reintroduction of calcium was required. 10 ml aliquots of solution (5) were made containing increasing concentrations of $CaCl_2$ (60µM-1mM). Cells were resuspended and left to pellet in each solution until 1 mM $CaCl_2$ was introduced.

2.5 Western Blot Analysis to detect protein expression or activation status

2.5.1 Introduction

Western Blot Analysis is an analytical method by which protein expression, identification and quantification can be assessed. It is a powerful and reproducible method, consisting of three distinct steps: (1) SDS-PAGE gel electrophoresis to separate a complex mixture of proteins based on their size, (2) Western blotting to transfer proteins from a gel to a membrane support and (3) detection of proteins using horse-radish peroxidase (HRP)-linked antibodies.

2.5.2 Extraction and quantification of protein samples

Protein can be extracted from a variety of sources including whole tissue samples (heart), primary cells (cardiomyocytes) or cell lines (HL-1). All 3 can be subjected to different protocols such as drug treatments, hypoxia or ischaemia/reperfusion and samples collected at different time points to assess protein expression, activation or translational modifications using Western Blot analysis.

2.5.2.1 Sample collection (tissues and cells)

Whole heart samples were collected using the Langendorff set up; hearts were prepared as described in **section 2.2.1.3.3**, cannulated via the aorta and retrogradely perfused with oxygenated KHB. Following the desired protocol, hearts were cut below the atria and immediately snap frozen using liquid N_2 and stored at -80°C until used. Heart tissue was homogenised using a PBS based homogenisation buffer containing a phosphatase inhibitor, a protease inhibitor and EDTA to preserve proteins of interest and their activation states. Protease and phosphatase enzymes are usually tightly controlled within cellular compartments and play a vital role in many signalling pathways, however homogenisation and subsequent cell lysis disrupts the regulated cellular environment. Hearts were homogenised at 100mg/ml using an electric tissue homogeniser and kept on ice.

2.5.2.2 Protein content determination

Protein content was determined using bicinchoninic acid (BCA) protein assay (Sigma, UK) and an automated 96-well plate reader (Fluostar Omega, BMG Labtech). The assay consists of two distinct reactions: BCA is an alkali colorimetric assay reagent containing Cu^{2+}, in the presence of protein, peptide bonds reduce Cu^{2+} to Cu^{1+} leading to the completion of reaction 1 and the formation of a light blue complex (the biuret reaction). Reaction 2 involves BCA chelating Cu^{1+} in a temperature sensitive reaction aided by the three amino acid residues cysteine, tyrosine and tryptophan. The intensity of the purple-coloured product is proportional to the level of protein in the sample. Plates were read at an absorbance wavelength of 563nm and contained a series of samples with known protein concentrations (0-2mg/ml protein). All samples were run in duplicate. A protein standard curve was created by plotting absorbance against the protein concentration of the known samples and used to determine the concentration of the unknown samples (Figure 2.12).

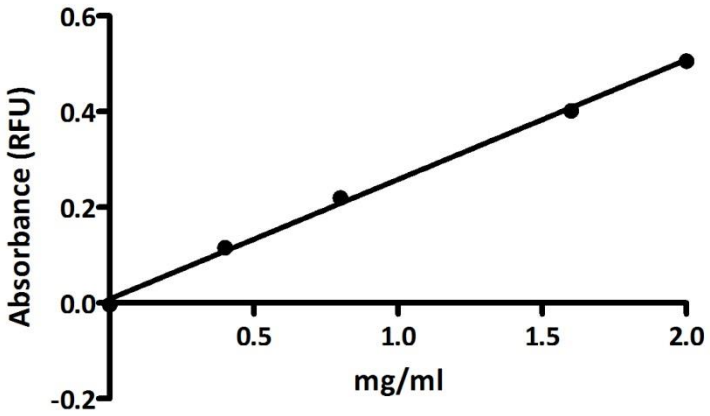

Figure 2.12: Typical protein standard curve using a BCA assay

2.5.2.3 Sample preparation

Based on the result of the protein content determination described above, samples were corrected to equal concentrations. All samples were adjusted to the sample that contained the lowest concentration of protein by adding different volumes of homogenisation buffer (Table 2.8). All heart samples were diluted in Laemelli lysis buffer (Sigma, UK) containing 5% β-mercaptoethanol, at a 1:1 ratio. β-mercaptoethanol denatures the proteins and Laemelli lysis buffer ensures a uniform charge across samples. Plated cardiomyocytes and HL-1 cells were simply collected by washing with warm PBS, followed by addition of 100µl of Lamelli lysis buffer containing 5% β-mercaptoethanol and then the wells scraped and collected into ependorffs. Samples were then heated to 80-90°C for 10 minutes to ensure protein denaturation. Finally, samples were centrifuged at 8000 rpm for 5 minutes, and kept on ice.

Concentration of protein (mg/ml)				Sample volume required (ml)			Homogenisation Buffer volume required (ml)		
GK3-1	**GK3-2**	**GK3-3**		**GK3-1**	**GK3-2**	**GK3-3**	**GK3-1**	**GK3-2**	**GK3-3**
1.113	0.946	1.275		0.850	1.000	0.742	0.150	0.000	0.258
GK8-1	**GK8-2**	**GK8-3**		**GK8-1**	**GK8-2**	**GK8-3**	**GK8-1**	**GK8-2**	**GK8-3**
0.995	1.471	1.767		0.950	0.643	0.535	0.050	0.357	0.465
GK12-1	**GK12-2**	**GK12-3**		**GK12-1**	**GK12-2**	**GK12-3**	**GK12-1**	**GK12-2**	**GK12-3**
1.555	1.438	1.569		0.608	0.658	0.603	0.392	0.342	0.397
GK18-1	**GK18-2**	**GK18-3**		**GK18-1**	**GK18-2**	**GK18-3**	**GK18-1**	**GK18-2**	**GK18-3**
1.605	1.134	1.501		0.589	0.834	0.630	0.411	0.166	0.370
The number highlighted in red represents the sample with the lowest concentration of protein.									

Table 2.8: The adjustment of samples to give equal protein concentrations within in sample.

2.5.3 Gel electrophoresis

Electrophoretic separation of proteins is performed using gels containing Sodium-dodecylsulfate (SDS) and Polyacrylamide (PAGE) gels. SDS is an ionic detergent that denatures multimeric proteins and polypeptide chains so that all proteins have similar charge:mass ratios; this allows size to be the sole determinant of migration rate. When an electrical field is applied, smaller proteins migrate faster through the gel than larger proteins therefore proteins can be separated according to their molecular weight. SDS-PAGE gels contain pores made from a solution of acrylamide monomers being cross linked into a polyacrylamide chain matrix. The percentage of the gel is related to the pore size and this can be adjusted by the amount of acrylamide added. The rates at which proteins migrate are affected by the electrical field applied and the pore size.

SDS-PAGE electrophoresis was conducted using the Mini Protean III system (BioRad, UK). Different gel percentages were made in respect to the protein of interest being analysed, gel compositions are shown in Table 2.9, TEMED and APS were added immediately prior to use. Gels were made by pouring approximately 3.5mls of resolving gel between two glass plates held in a casting frame, 50% isopropanol was gently pipetted onto the unset resolving gel to ensure it set flat. Once the resolving gel was set, the isopropanol was removed and TEMED and APS added to the stacking gel. Quickly, 1ml (or the volume needed to fill the remaining space between the plates) was pipetted between the plates on top of the resolving gel and either 12 or 15 well combs were inserted into the stacking gel to provide wells for sample loading. Plates were removed from the casting frames, placed into running tanks, immersed in running buffer (0.25mM Tris-Base, 0.19M glycine, 0.1% SDS) and the combs removed. Molecular weight marker (BioRad, UK) was loaded into the first well on the left hand side of the gel, and lamelli-diluted protein samples loaded from left to right into the wells. An electric field was applied to the gel (180-200V) until the bromophenol blue dye had run off the gel and in some cases until the blue 50mW marker was near the bottom to allow for a further separation of proteins.

Solution	Volume to add to make two 10 % resolving gels.	Volume to add to make two 8% resolving gels.	Stacking gel composition
1M Tris-HCl (pH 8.8)	3.75 ml	3.75 ml	
1M Tris-HCl (pH 6.8)	-	-	0.625 ml
30% Acrylamide	3.34 ml	2.66 ml	0.75 ml
Water	2.795 ml	3.432 ml	3.456 ml
10% SDS	100 µl	100 µl	50 µl
Add the following when ready to pour gel between plates			
TEMED	7.5 µl	7.5 µl	7.5 µl
10% Ammonium Persulphate	75µl	75µl	75µl

Table 2.9: Composition of SDS-PAGE gels

2.5.4 Transfer of proteins from the gel to a membrane support

Gels were carefully removed from glass plates and transferred onto polyvinylidene fluoride (PVDF) membranes (Amersham, UK) using semi-dry transfer. Briefly, PVDF membranes were activated by pre-soaking in 100% methanol and equilibrated in transfer buffer (25mM Tris-base, 0.19M glycine, 20% v/v methanol). Stacking gels were removed from the plates, leaving resolving gels to be placed on top of pre-wetted PDVF membranes. This created a sandwich of PVDF membrane with gel in between 4 pieces of pre-soaked blotting paper. Air bubbles were removed by rolling a pipette across the upper most blotting paper, and semi-dry transfer cell was closed. The gel was set to transfer at 10V with a current limited at 1A for up to 2 gels and at 15V with a current limited at 1.5A for 4 gels for 45 minutes.

2.5.5 Membrane blocking and antibody incubation

PDVF membranes were blocked overnight to prevent non-specific binding of antibodies, in either 5% skimmed milk or 5% bovine serum albumin (BSA) dissolved in PBS-Tween (PBS Tablets (Sigma, UK) containing: 10mM phosphate buffer, 2.7mM KCl, 137mM NaCl and 0.1% Tween 20 (Sigma, UK)). Milk contains casein; a highly prevalent phosphoprotein, therefore 5% BSA/PBS-T was used for blocking when assessing Akt phosphorylation within samples to prevent any possible non-specific binding. Membranes were probed with rat specific primary antibodies diluted in 5% BSA/milk in PBS-T at 1:1000 (unless stated otherwise) for 3 hours at room temperature or overnight at 4°C on a continuous shaking platform. Prior to washing, membranes were incubated with primary antibody to α-tubulin at 1:10000 for 45 minutes. Membranes were then washed for one hour with PBS-T, changing solution every 10minutes to remove unbound antibody, before incubation with the horseradish peroxidase(HRP)-linked secondary antibody (Cell signalling, UK) for another hour. Washing was repeated as before.

2.5.6 Protein detection using enhanced chemiluminescence (ECL)

The primary antibodies used have a binding region specific to the protein of interest and the secondary antibody binds to a species-specific portion of the primary antibodies. Secondary antibodies were linked to HRP. When incubated with the ECL reagent, HRP catalyses the oxidation of luminol, a reaction which emits light. This light can then be detected with autoradiography film and represents the localisation of primary antibody bound to specific proteins on the membrane.

Membranes were incubated in ECL reagent (GE healthcare, UK) on a shaking platform for 2 minutes before the membrane is carefully placed face down onto flat Saran wrap. The Saran wrap was folded around the membrane before turning the membrane face up and removing any air bubbles. The Saran-wrapped membrane was secured into an X-ray film cassette (Kodak, UK) and exposed to Hyperfilm ECL high performance chemiluminescence film (GE Healthcare, UK). Different exposure time was required to optimise band intensity. The film was developed and fixed using Kodak processing chemicals (Sigma, UK). Films were left to dry and annotations of molecular markers were made using the membranes. Films were transferred to computerised images using a flatbed scanner and the intensity of the bands quantified using Image J.

2.6 Immunoprecipitation

Immunoprecipitation (IP) in combination with Western Blot analysis is routinely used to detect post-translational changes of specific proteins. Briefly, specific antibodies bind to the protein of interest in solution to form antibody-protein complexes. These complexes are precipitated out of solution with the addition of insoluble binding proteins. Protein A (agarose) or Protein G (sepharose) are most commonly used and often referred to as 'beads'. Centrifugation of the solution promotes pelleting of the antibody-protein complex attached to the beads. These complexes can then be diluted in Lamelli sample buffer and treated as described in chapter 2.5.

2.6.1 Preparation of lysates from heart tissue

Hearts were cleared of blood and snap frozen as described in section 2.5.2.1**.** Homogenisation buffer (PBS, phosphatase inhibitor, protease inhibitor, EDTA) (500 µl/300mg tissue) was added to the tissue placed in round bottom microfuge tubes and incubated on ice for 20 minutes on ice. For experiments investigating PGC-1α, 10 µM Nicotinamide (NAM) a deacetylase inhibitor was added to the homogenisation buffer. The tissue was emulsified with an electric homogeniser and then spun for 3 min at 4000 rpm. The supernatant was aspirated and the pellet re-suspended in 300 µl lysis buffer. For experiments investigating cytosolic proteins a non-denaturing lysis buffer was used. For nuclear proteins, RIPA (RadioImmunoPrecipitation Assay) lysis buffer was used for nuclear membrane disruption (Table 2.10). The homogenised sample was vortexed 3 times for 15 sec, centrifuged for 10 min at 16000 rpm and then the supernatant was collected and protein content was quantified (as described in section 2.5.2.2**).**

Non-denaturing lysis buffer	RIPA(RadioImmunoPrecipitation Assay) buffer (in PBS)
20 mM Tris HCl pH 8	1% NP-40
137mM NaCl	0.1% SDS
10% Glycerol	0.5% NaDeoxycholate
1% NP-40	Immediately before use add:
2mM EDTA	Protease inhibitors (Roche)

Immediately before use add:	Phosphatase inhibitors (Roche)
Protease inhibitors (Roche)	
Phosphatase inhibitors (Roche)	

Table 2.10: Lysis buffer compositions:

2.6.2 Immunoprecipitation

Following protein determination, 500 µg of protein was diluted in at least 3 volumes of PBS containing TSA and protease inhibitors (for PGC-1α, NAM was also added). To this solution, the antibody specific to the protein of interest was added and rotated overnight at 4°C. Following this incubation step, a mixture of protein A and protein G beads were added to the mixture and the solution containing protein sample, antibody and beads were rotated for 2-4 hours at 4°C. Tubes were centrifuged at 3000 rpm for 30 sec at 4°C and the supernatant carefully and completely removed (Figure 2.16). The bead/protein/antibody complex was then washed three times with 500 µl of ice-cold lysis buffer. Between each wash, the beads were pelleted by centrifugation. To minimize the background, the supernatant was completely removed between each wash step. The bead/protein/antibody complex was resuspended in 100 µl of 2x lamelli sample buffer and mixed gently. The sample was boiled at 90–100° C for 5–10 min to dissociate the immunocomplexes from the beads and then centrifuged at 13000 rpm to pellet the beads. The supernatant was carefully removed and used to load onto an SDS-PAGE gel to separate proteins prior to Western blot analysis as described in sections 2.5.3-2.5.6**.**

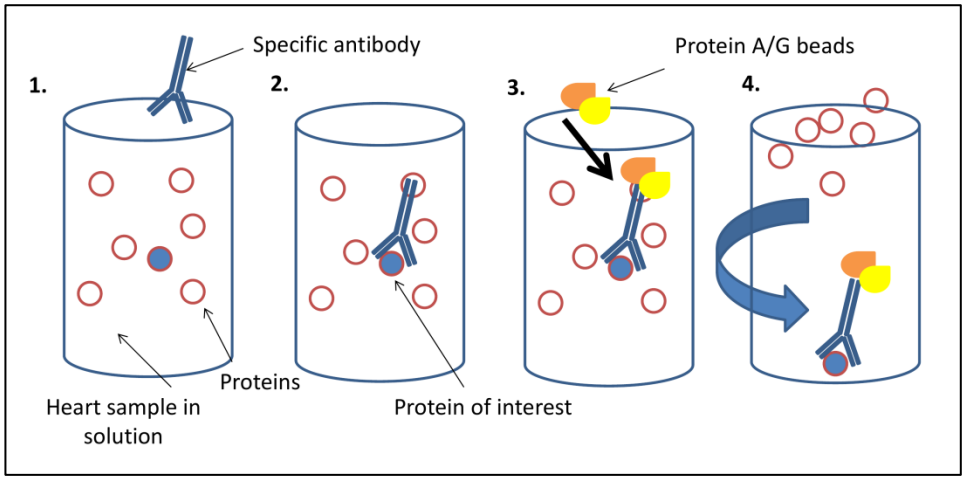

Figure 2.13: Illustration of immunoprecipitation process. (1) Antibody added to heart sample and sample rotated overnight (2) Antibody binds to protein of interest (3) Protein A/G beads added to solution and rotated for a further 2-4 hours (4) Solution centrifuged to leave a pellet consisting of the antibody/protein/bead complex.

2.7 Biochemical assays

2.7.1 Measurements of intracellular ATP in heart tissue

Experiments were conducted to investigate the basal levels of adenosine triphosphate (ATP) in the ageing and diabetic heart and whether drug treatments affected the level of this metabolite. A well characterised ATP-bioluminescent assay kit (FL-AA, Sigma, UK) was used to determine the concentration of ATP in heart samples. In the presence of ATP and luciferin, luciferase an enzyme from fireflies can catalyse a light emitting reaction. This 2 step reaction is summarised in

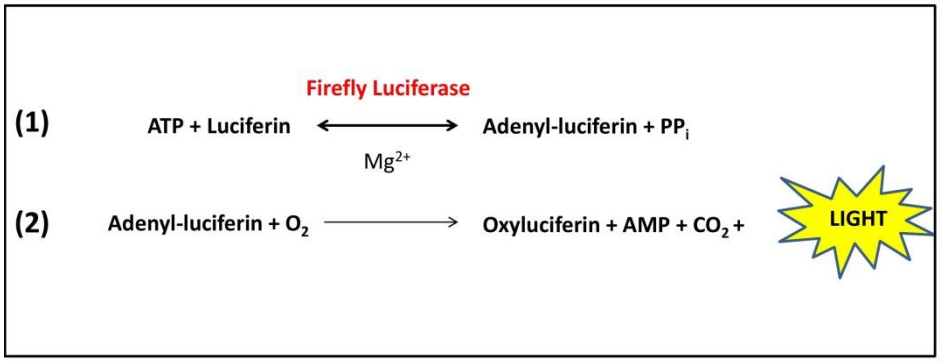

Figure 2.14. The amount of light emitted is proportional to the concentration of ATP. ATP concentration was determined in heart samples using a 96 well plate reader FLUOstar Omega (BMG LabTech).

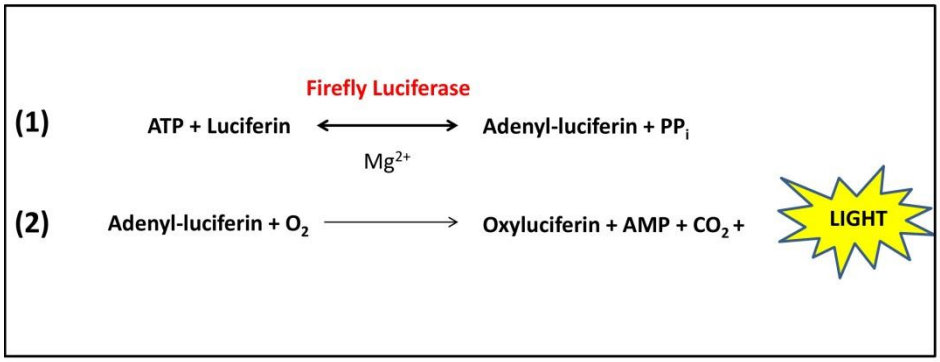

Figure 2.14: Illustration of reaction of luciferase in presence of ATP

Briefly heart homogenates were diluted 1 in 10 in homogenisation buffer and incubated at 95°C on a heating block for 1 min. A clear 96-well plate was prepared with heart samples, standards and blanks. ATP standards were made using the supplied ATP concentrate which was diluted to 1mg/ml. From this stock concentration a serial dilution was performed to give standards in [µM]: 0.4, 0.2, 0.1, 0.05, 0.025, 0.0125 and 0.00625. The ATP bioluminesence assay mix was used at 1:25 fold dilution with supplied ATP assay dilution buffer, and was prepared seperately for each run. Next, the assay plate was prepared. 100 µl of the assay mix was transferred to the required wells of a white-bottomed plate, suitable for the measurement of luminescence. Following the incubation, 100 µl of each sample was transferred from the sample plate to the assay plate and luminescence was immediately read using 96 well plate reader. Luminescence was read every 9 seconds for 6 cycles. The amount of ATP in each sample was calculated with the use of a standard ATP curve (example shown in Figure 2.15).

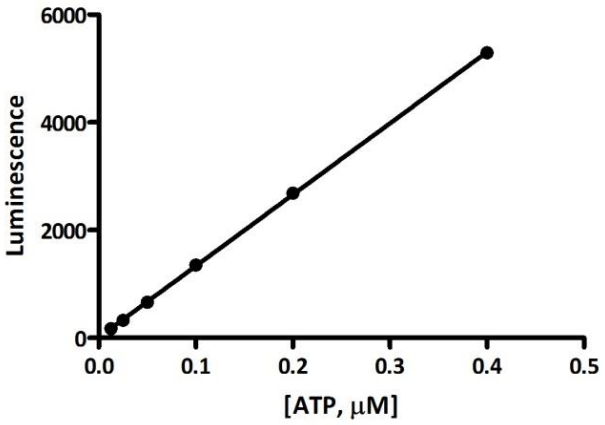

Figure 2.15: Typical ATP standard curve

2.7.2 Measurement of free radicals in heart tissue

Intracellular reactive oxygen species (ROS) and reactive nitrogen species (RNS) are well known molecules that play a vital role in disrupting cellular signalling during oxidative stress. Experiments were performed using the *OxiSelect In vitro ROS/RNS Assay Kit* (Cell Bio Labs) to measure total free radical presence in samples from aging and diabetic rat hearts. The assay used a specific fluorogenic, ROS/RNS probe dichlorodihydrofluorescin DiOxyQ (DCFH-DiOxyQ) which reacted with free radicals within the samples including hydrogen peroxide (H_2O_2), peroxyl radical ($ROO^{\cdot}$), nitric oxide (NO) and peroxynitrite anion ($ONOO^{-}$). Briefly, the DCFH-DiOxyQ probe was primed and then stabilized in its highly reactive DCFH form. On contact with a ROS or RNS species (for example in tissue samples or standards) DCFH was rapidly oxidized to its fluorescent form 2',7'-dichlorodihydrofluorescein (DCF) (Figure 2.16). Fluorescence was proportional to the total level of ROS/RNS within the samples. Relative fluorescence was measured using a 96 well plate reader FLUOstar Omega (BMG LabTech) at 480 nm excitation / 530 nm emission. Unknown samples were compared against a hydrogen peroxide or DCF standard. This method was conducted according to the manufacturer's instructions.

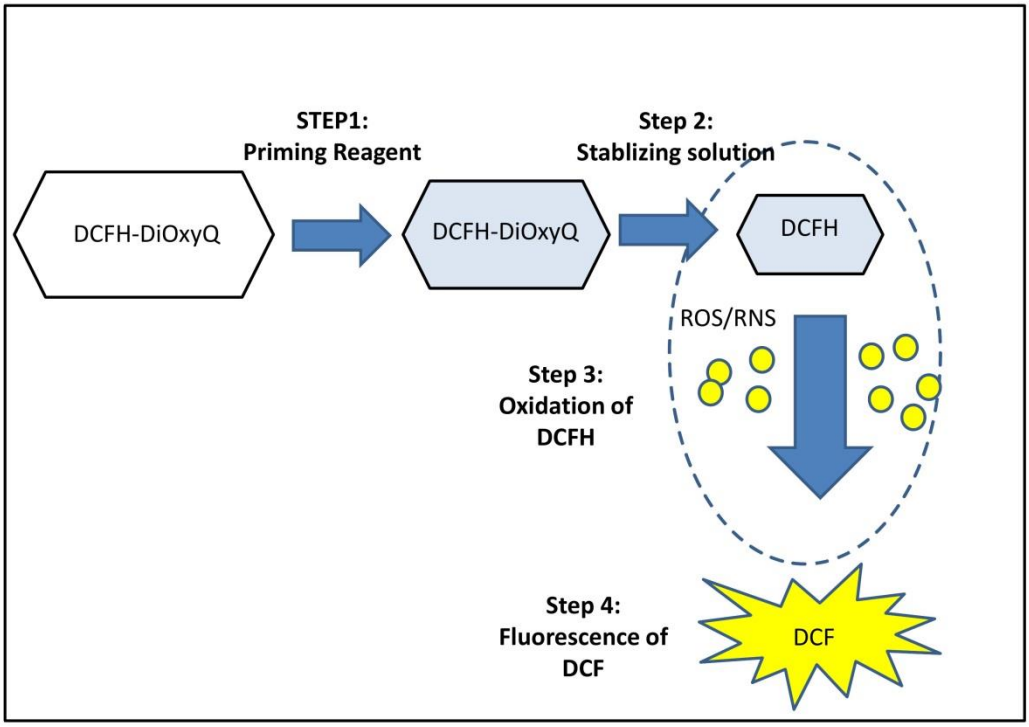

Figure 2.16: Illustration of how fluorescence is produced in response to reactive oxygen/nitrogen species

2.8 Electron Microscopy imaging of mitochondria

The transition electron microscope (EM) was used to assess mitochondrial appearance within the heart samples. This method uses electrons rather than light to visualize fine details of cells at high magnifications. The electromagnetic lens within the microscope focuses the electrons into a thin beam. The electrons scatter in accordance with the density of the material they shine upon. Any un-scattered electrons remain in line with the beam and a shadow image is projected which can then be visualized by the operator.

2.8.1 Sample collection and preparation

Samples used to analyse mitochondrial appearance were taken from the hearts which also supplied material for Western Blot analysis. As described in section 2.2.1.3.3**,** hearts were cleared of blood using the Langendorff apparatus. Prior to freeze clamping a small section of the heart apex were collected and stored in EM fixative. Ultrathin sections were then prepared using an in house service by Mark Turmaine, UCL.

2.8.2 Assessment of structure and organisation of mitochondria

All samples were blindly coded and ultrathin sections were viewed with a Joel 1010 transition electron microscope (Joel Ltd, Warwickshire, UK.). From these ultrathin sections, at least 6 electron micrographs of each section were viewed and photos of the interfibrillar mitochondria taken in each heart. The photos for each heart were assessed for structural and organisational differences examined. Heart samples were grouped according to similarities. Subsequently the codes were revealed.

2.9 Statistical Analysis

All statistical analyses were conducted using GraphPad Prism 5 software. Student's t test was applied to the data when a comparison was made between two groups (treated *vs*. non-treated). In experiments where a comparison was made between multiple groups, an Analysis of Variance (ANOVA) was used followed by appropriate post-hoc analysis (Bonferroni's test). In experiments where parameters were repeatedly measured for example before and after a drug treatment, data was analysed using a repeated measures ANOVA. Comparison between groups at multiple time-points was analysed by two-way repeated measures (mixed model) ANOVA with a Bonferroni correction for multiple comparisons. Statistical significance was assumed at $P<0.05$. All data presented represents the mean ± the standard error of the mean (SEM).

3. ISCHAEMIA-REPERFUSION INJURY IN AGEING AND DIABETIC HEARTS

3.1 Susceptibility to infarction in ageing and diabetes

3.1.1 Introduction: The old diabetic heart and myocardial infarction

Elderly, type 2 diabetic patients have been suggested to have an enhanced probability of developing heart failure, an increased prevalence of AMI and subsequently poor clinical recovery following a lethal event [332, 471]. Experimental research has identified both the aged heart and the diabetic heart as separate entities which could render the heart more susceptible to damage caused by ischaemia and reperfusion. Surprisingly, there are limited investigations that use animal models that represent both risk factors. Understanding the alterations that occur within the aged **and** diabetic myocardium in the experimental setting could assist in the development of cardioprotective interventions that are required to improve clinical outcomes in this group of patients.

There has been great discrepancy between clinical and animal data, regarding the susceptibility of the diabetic heart to IRI. Experimental results from animal models of diabetes have yielded confusing results, suggesting the diabetic heart is either more[219, 223, 224] or less[235, 237, 238] susceptible to IRI. Moreover some investigations see no influence of diabetes on infarct size[229, 240, 241]. The discrepancy in the outcome of animal investigations has been attributed to the choice of animal model, experimental protocol and severity of diabetes[218]. Clinically, Fazel et al, 2005 showed that diabetic patients presenting with AMI had similar or lower release of cardiac markers of injury such as troponin or creatine kinase myocardial band (CK-MB) which suggested a smaller infarction. However, these diabetic patients exhibiting lower levels of infarct markers experienced worse clinical outcomes compared to the non-diabetic patients [472]. In line with this study, Alegria et al, 2007 demonstrated that infarct size was only modestly higher and left ventricular ejection fraction (LVEF) modestly lower in diabetic patients compared to non-diabetic patients with acute ST-segment elevation MI, however mortality rate was 4 to 6 fold higher in the diabetic group[473].

3.1.2 Hypothesis and aim

Based on these apparent contradictory data, we hypothesised that the diabetic heart, may develop smaller infarcts but could be more susceptible to ischaemic damage i.e. the threshold at which infarct size translates into worse outcomes is lower for the diabetic heart and that age may additively effect this threshold for damage. Using an inbred lean model of type 2 diabetes (T2D), Goto Kakizaki (GK) rat and its original source, the normoglycaemic Wistar rat, at different ages (between 3 and 18 months). We aimed to determine the infarct size in isolated ageing, diabetic hearts subjected to

ischaemia times during ischaemia and reperfusion protocols using different lengths of ischaemia.

3.1.3 Experimental Protocols

3.1.3.1 Animals

Male Goto-Kakizaki (GK) rats (a mild, non-obese, insulin resistant diabetic model [427, 447]) and male Wistar rats (normoglycaemic) were obtained from Taconic (Denmark) and Charles River UK Limited (Margate, UK), respectively. They were kept in house until they reached 3, 8, 12 or 18 months of age; all animals received humane care in accordance with the United Kingdom Animal Scientific Procedures Act of 1986. Fasting blood glucose levels (Accu-chek system, Roche) and HbA1c (A1C now+ test kit. Bayer, UK) were measured at least 48hours prior to excision of the heart to avoid the upregulation of cardioprotective stress proteins [474]. Body weight and heart weight were recorded on the experimental day.

3.1.3.2 Langendorff Isolated heart perfusions

For determination of infarct size, GK and Wistar rats of 3, 8, 12 and 18 months of age were anesthetized with sodium pentobarbital (55 mg/kg I.P.) and heparin (300 IU). The hearts were rapidly excised, placed into ice cold Krebs-Henseleit buffer, and quickly mounted onto a Langendorff constant pressure perfusion system (ADInstruments, Chalgrove, UK), described in detail in Chapter 2. Briefly, the hearts were perfused via the aorta with modified Krebs-Henseleit bicarbonate buffer (KH) (mM: NaCl 118.5, $NaHCO_3$ 25.0, KCl 4.8, $MgSO_4$ 1.2, KH_2PO_4 1.2, $CaCl_2$ 1.7 and glucose 11.0). The buffer was gassed with 95% O_2/5% CO_2 to maintain a pH of 7.4. A suture was placed around the LAD and secured in place by a snare created from two pipette tips. A fluid filled latex balloon was inserted into the left ventricle through an incision in the left atrial appendage and inflated to a left ventricular end diastolic pressure (LVEDP) of 8-10mmHg. Perfusion pressure was set at 70mmHg, left ventricular developed pressure LVDP, heart rate (HR) and coronary flow (CF) were permanently monitored and the rate pressure product (RPP) calculated. An electronic thermo probe inserted into the pulmonary artery continuously monitored temperature and was kept in range of 37°C ± 0.5.

For infarct analysis (n=6 per group) hearts were randomly assigned to receive sub-lethal (20 min regional ischaemia) or lethal (35 min regional ischaemia) followed by 60 min reperfusion (summarised in Figure 3.1). Regional ischaemia was initiated by tightening the suture around the LAD and holding it in place with the snare. The snare

was then removed and the hearts reperfused for 60 min. At the end of this period the suture was permanently tied to occlude the LAD and Evans blue dye (0.25% in saline) was infused through the aorta to delineate the risk zone, with the myocardial tissue not at risk staining blue. Hearts were stored at -20°C before being transversely sliced, incubated in triphenyltetrazolium chloride solution (TTC; 1% in phosphate buffer) and TTC transferred to 10% formalin overnight. The following day the slices were scanned and the volume of infarction within the risk zone (I/R %).

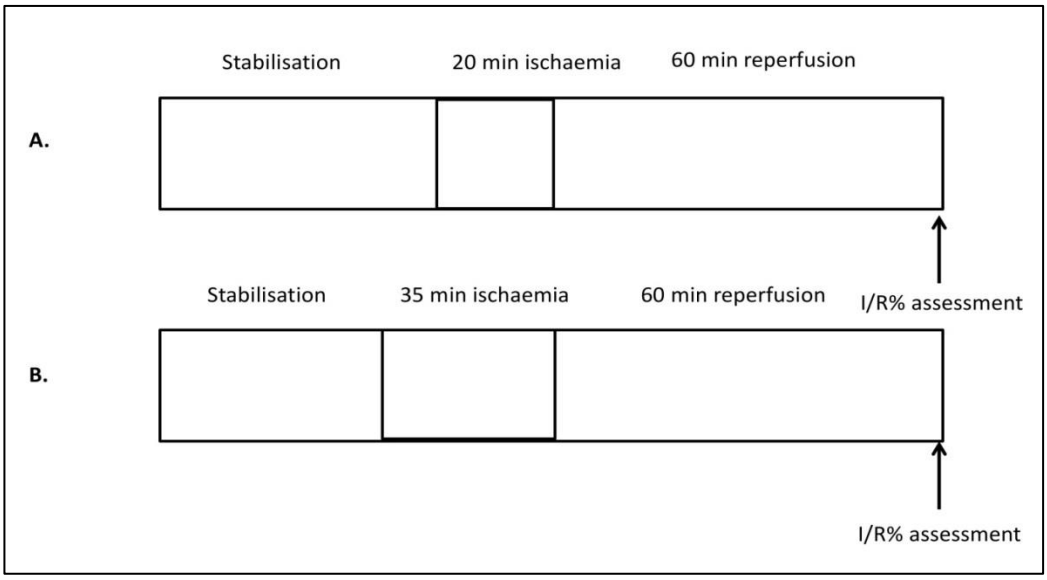

Figure 3.1: Scheme of Langendorff experiments performed. For infarct analysis (n=6 per group) hearts were randomly assigned to receive A. sub-lethal (20 min regional ischemia) or B. lethal (35 min regional ischemia) followed by 60 min reperfusion.

3.1.3.3 Statistical Analysis

As described in Chapter 2, the values are presented as mean ± standard error mean (SEM) and analysed by one-way ANOVA, followed by a Tukey post hoc comparison using GraphPad Prism 5.0 (GraphPad Software Inc, San Diego, California, USA). Differences within the data were considered statistically significant when $P < 0.05$.

3.1.4 Results

3.1.4.1 Blood glucose and HbA1c

Clinically, patients are considered diabetic with HbA1c reading of >48 mmol/mol. However, due to rapidly expanding blood volumes in young growing animals the HbA1C fraction may be kept "artificially" low by the constant expansion of red cell numbers. Therefore in these investigations, the diabetic status was considered at HbA1c values> 40 mmol/mol, a status achieved at approximately 8 months of age in

the GK rat. Blood glucose and HbA1c levels increased with age in the GK rat ($p<0.05$). In the 3 month age group, blood glucose levels were within diabetic range (9.6±0.4 mmol/L), however HbA1c was within the non-diabetic threshold (23.7mmol/mol). GK rats had higher blood glucose and HbA1c levels than their counterpart Wistars, with the exception of the 3 month GK group having similar HbA1c levels to the 3 month Wistar group. Data is summarised in Figure 3.2**.**

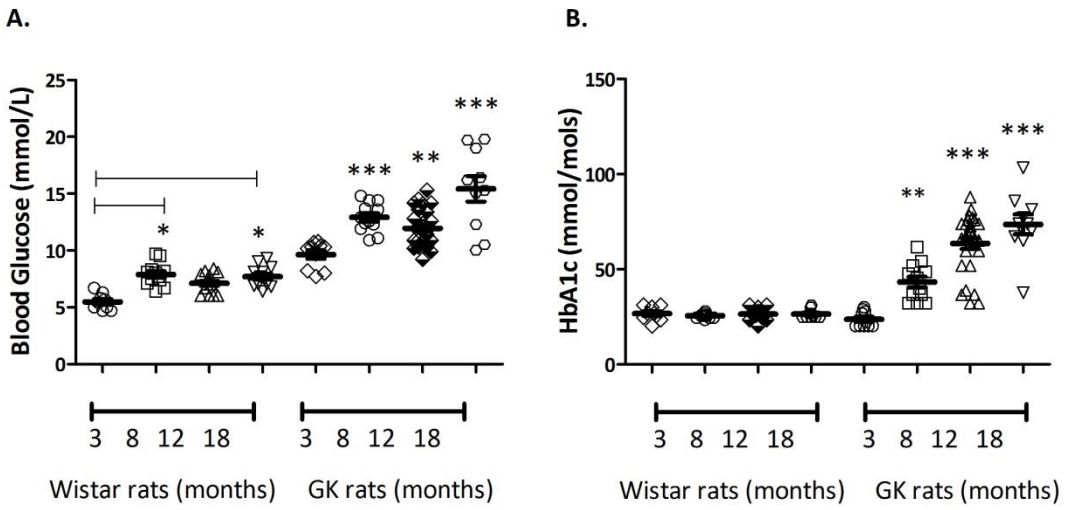

Figure 3.2: Blood Glucose and HbA1c levels in ageing and diabetic rats. A. Fasting blood glucose levels (Accu-chek system, Roche) and B. HbA1c (A1C now+ test kit. Bayer, UK) were taken at least 48 hours prior to excision of the heart. Data is shown as mean ± S.E.M, n≥10.*p<0.05 versus 3 month Wistar measurement. **p<0.005, ***p<0.001 versus 3 month GK measurements. Diabetic status increased with age in the GK rat. One way ANOVA and Tukey's post hoc analysis were used for statistical analysis between all groups.

3.1.4.2 Phenotypic changes associated with age and diabetes

The diabetic Goto-Kakizaki rats were lighter than the non-diabetic Wistar rats in all age groups; however their heart/body weight ratio (HW/BW%) was significantly greater ($p<0.001$). HW/BW% decreased significantly in the Wistar rats over time (Pearson R^2 0.97; $p=0.013$), driven by a large increase in body mass; this trend was absent in the Goto-Kakizaki rats (Pearson R^2 0.03; $p=0.82$), whose body mass stayed relatively constant after the age of 8 months. These parameters are summarized in Table 3.1.

	3 months		8 months		12 months		18 months	
	Wistar	**GK**	**Wistar**	**GK**	**Wistar**	**GK**	**Wistar**	**GK**
Heart weight (g)	2.3±0.5	1.6±0.1	1.9±0.2	2.2±0.2	2.1±0.3	2.4±0.2	2.1±0.3	2.6±0.3
Body mass (g)	478.9± 83	276.8± 16.1	457.6± 33.2	409.5± 32.8	592.8± 82	435.8± 37.4	642.2± 63.6	450.6± 37.4
Heart/body %	0.521	0.586	0.420	0.542*	0.362	0.559*	0.327	0.587*

Table 3.1: Summary of biological parameters. Body mass was recorded prior to excision of the heart. Heart mass was measured following isolated Langendorff heart preparation. Data is represented as mean ± S.E.M, n≥18. *P<0.05 versus counterpart wistar at each age group. One-way ANOVA was used to determine statistical significance.

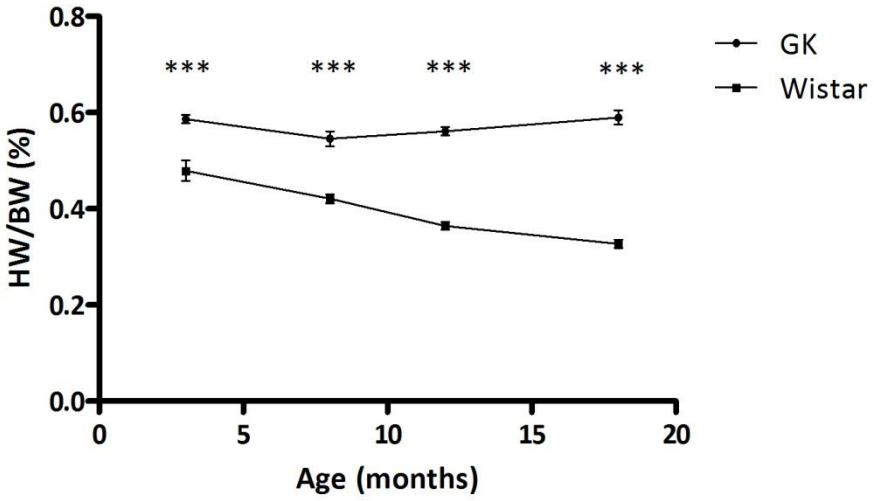

Figure 3.3: Heart to body weight ratio in ageing diabetic and non-diabetic rats. Heart/body weight ratio (HW/BW%) was calculated following the experimental investgations. Data was analysed using Pearson's regression analysis and demonstrated that the hypertrophy that exists in the diabetic heart did not appear to worsen with age.

3.1.4.3 Cardiac function during ischaemia and reperfusion in the ageing and/or diabetic heart

Functional parameters of the isolated hearts were monitored throughout each experimental protocol. In diabetic hearts, data collected during the 20 min ischaemia experiments, suggested baseline function to deteriorate in relation to age; at 3 months the baseline RPP in GK rat hearts was significantly higher than in the 18 months age groups ($p<0.05$), however there was no significant difference between 8, 12 and 18 months (P=NS). HR also followed this pattern, with a significantly faster HR noted in the 3 month versus 12 and 18 months age groups ($P<0.005$). HR was also significantly lower in the 18 month versus the 12 month age group, but no significant difference was noted between hearts from 3 and 8 month GK rats (P=NS). The percentage of LVDP recovery following 20 min ischaemia and 60 min reperfusion was higher in the 3 month group compared to all other age groups, however this trend did not reach statistical significance. Data from these experiments are summarised in Figure 3.4.

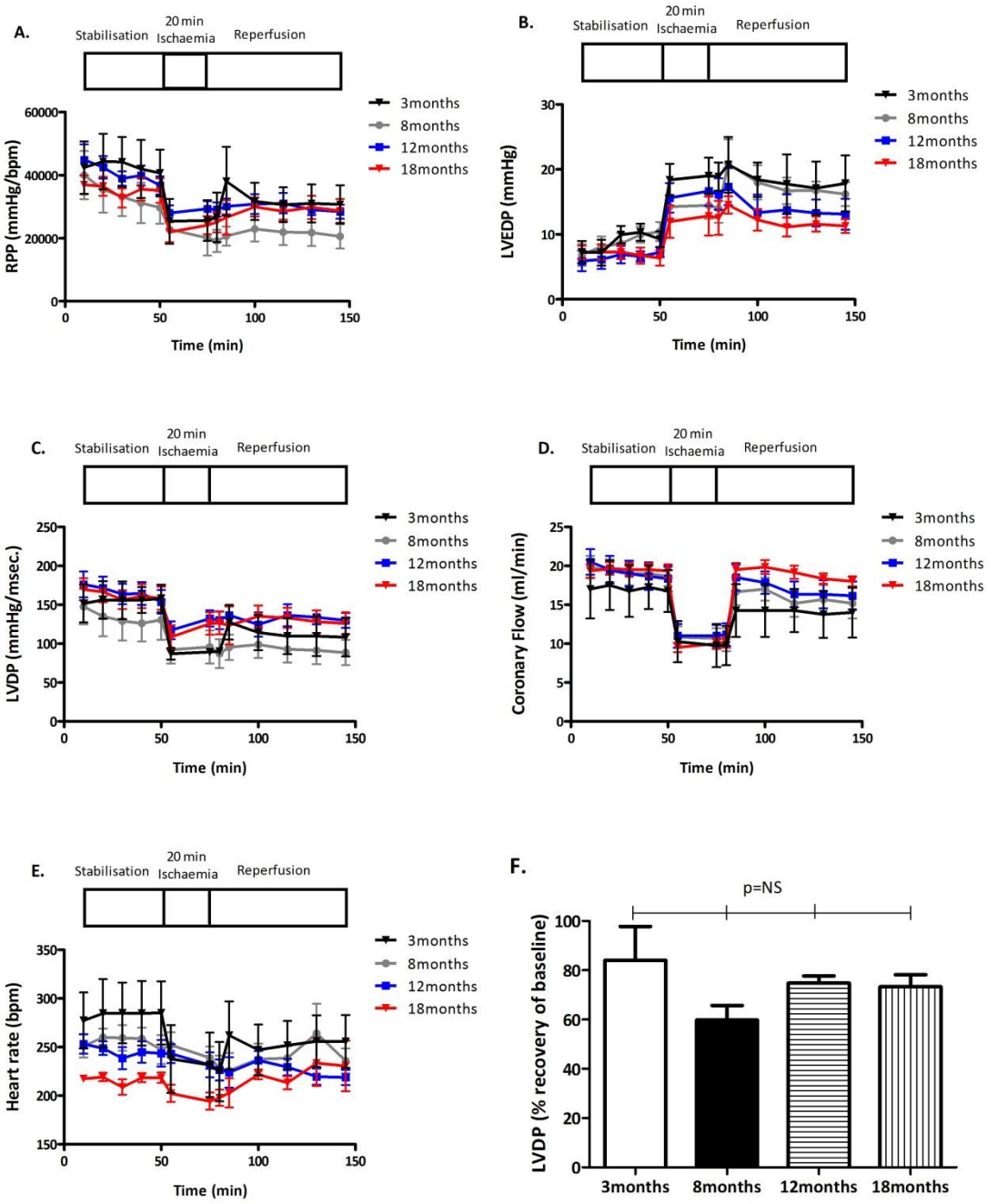

Figure 3.4: Cardiac function assessment in the diabetic heart subjected to 20 min ischaemia/ 60 min reperfusion. A. Rate Pressure Product (RPP) B. Left ventricular end diastolic pressure (LVEDP) C. Left ventricular developed pressure (LVDP) D. Coronary flow E. Heart Rate (HR) and F. % recovery of LVDP following 20 min ischaemia/60 min reperfusion. LVEDP. LVDP and HR were monitored via an inserted ventricular latex balloon, RPP was calculated as HR x LVDP as a measure of cardiac workload. No significant difference was in any of the parameters in the ageing, non-diabetic heart. Data is shown as mean ± S.E.M, n≥6. Comparison between groups at multiple time-points was analysed by two-way repeated measures (mixed model) ANOVA with a Bonferroni correction for multiple comparisons. One way ANOVA followed by a Tukey Post-Hoc analysis were used for statistical analysis between groups.

Cardiac function data monitored throughout 35 min ischaemia/reperfusion experiments in GK hearts showed a similar pattern to the shorter ischaemic duration. Baseline RPP output deteriorated with age; 3 and 8 month GK hearts had a significantly higher cardiac output than their aged counterparts ($p<0.05$), moreover no difference was seen between 12 and 18 months hearts. In the 8 month group, LVEDP following induction of ischaemia was significantly increased compared to the other groups ($p<0.005$) but the recovery was similar. Initial readings of LVDP showed no significant difference between the age groups; however throughout stabilisation LVDP deteriorated in the 12 and 18 months groups compared to the younger groups. Of note, coronary flow was significantly lower in the 3 month age group throughout the entire protocol compared to the other groups ($p<0.05$). At the end of reperfusion, LVDP in the 3 month group recovered to 70% of the baseline compared to only 49% recovery in the 18 month group. Data from these experiments are summarised in Figure 3.5.

In non-diabetic Wistar rats, RPP and LVDP function were significantly reduced in hearts isolated from the 18 month group compared to 3 and 12 month groups ($p<0.005$) when subjected to 20 min ischaemia and subsequent reperfusion. Coronary flow values were similar between all age groups with a reduction in flow noted in the 18 month age group; however this did not reach statistical significance. Hearts isolated from the 18 month non-diabetic group had a significantly slower HR compared to all other groups ($P<0.005$). The percentage of LVDP recovery was only significantly reduced in the 18month group. Data summarised in Figure 3.6.

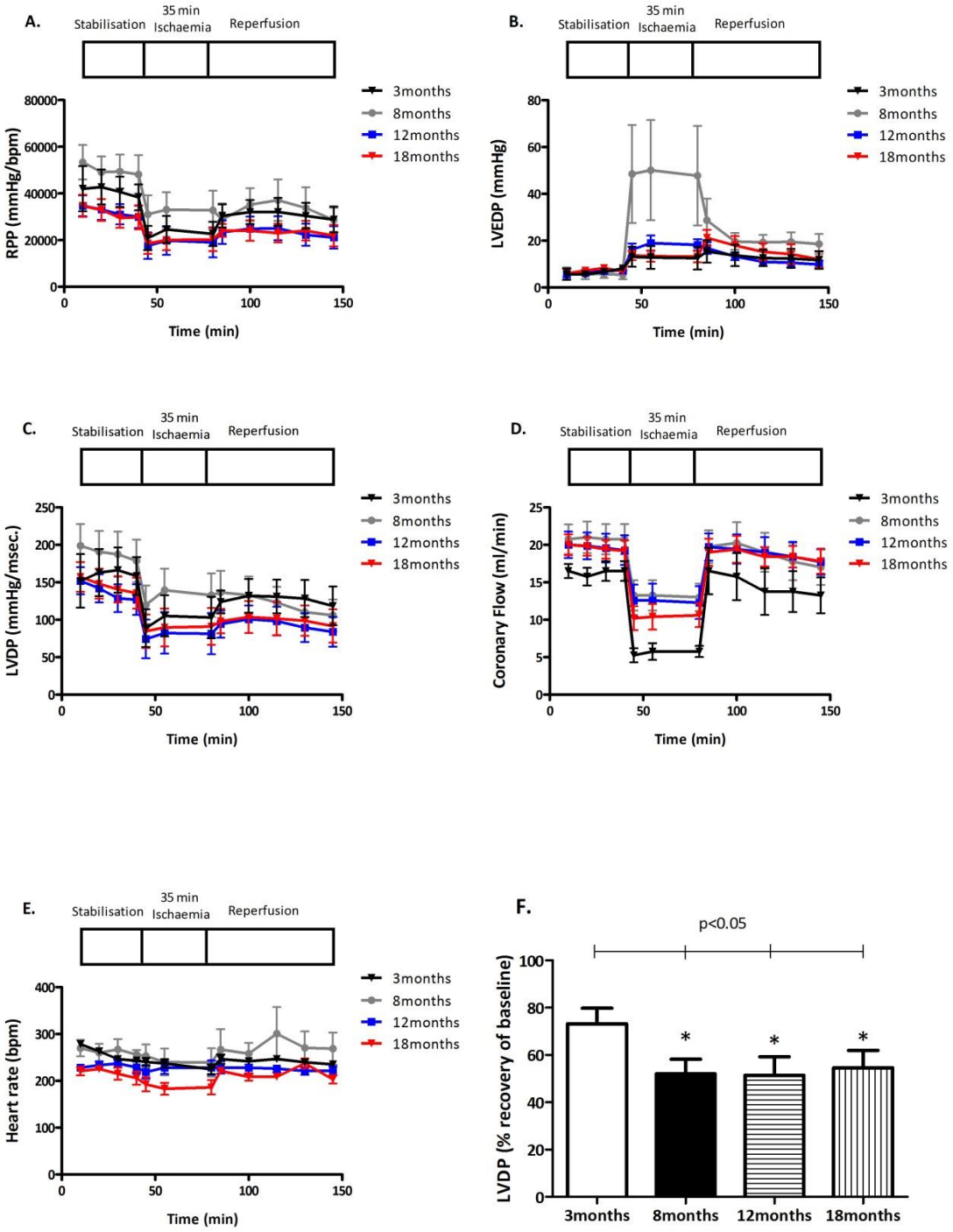

Figure 3.5: Cardiac function assessment in the diabetic heart subjected to 35 min ischaemia/ 60 min reperfusion. A. Rate Pressure Product (RPP) B. Left ventricular end diastolic pressure (LVEDP) C. Left ventricular developed pressure (LVDP) D. Coronary flow E. Heart Rate (HR) and F. % recovery of LVDP following 20 min ischaemia/60 min reperfusion. LVEDP. LVDP and HR were monitored via an inserted ventricular latex balloon, RPP was calculated as HR x LVDP as a measure of cardiac workload. A significant reduction in LVDP recovery was seen the ageing, diabetic heart. Data is shown as mean ± S.E.M, n≥6. Comparison between groups at multiple time-points was analysed by two-way repeated measures (mixed model) ANOVA with a Bonferroni correction for multiple comparisons. One way ANOVA followed by a Tukey Post-Hoc analysis were used for statistical analysis between groups.

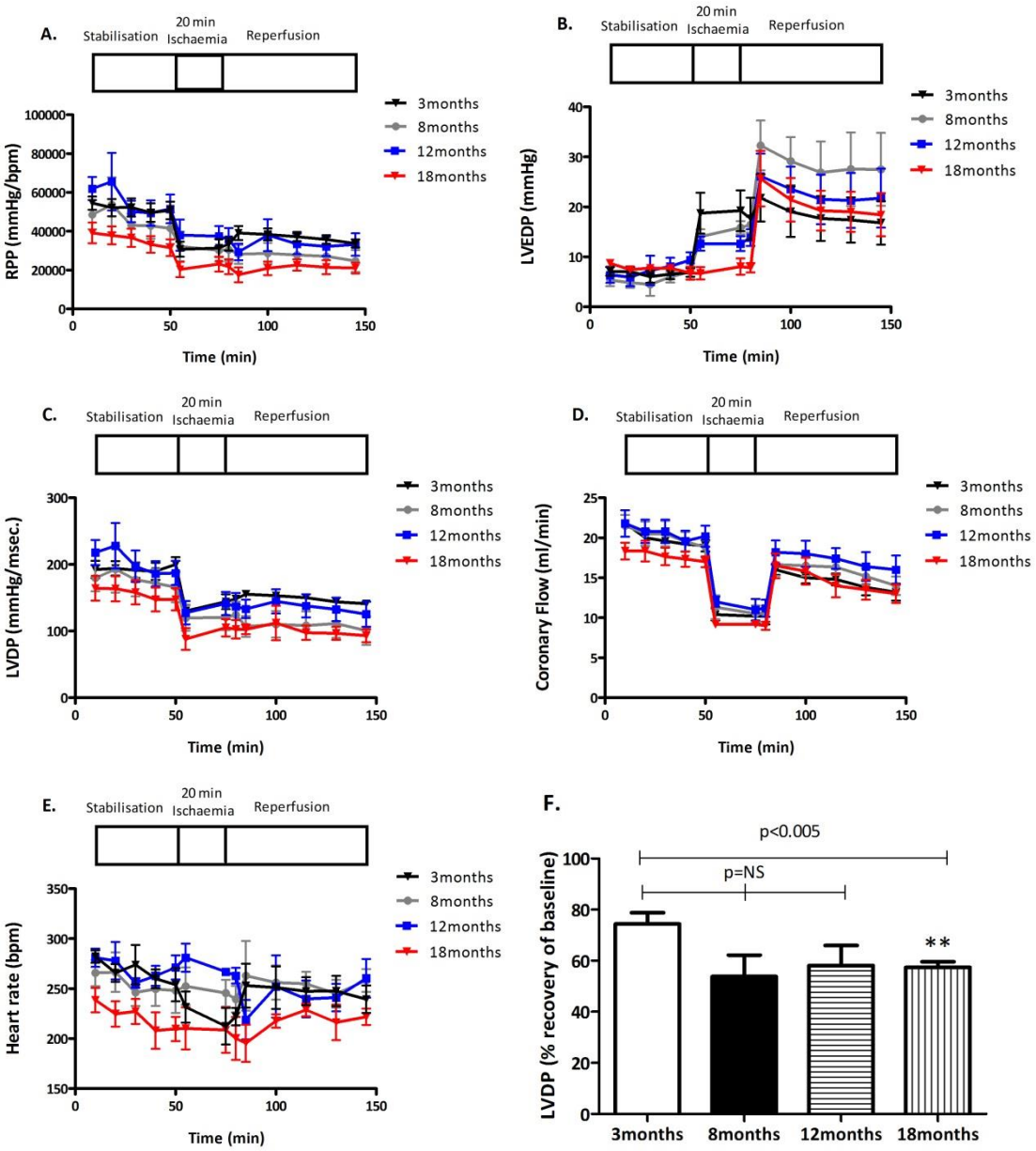

Figure 3.6: Cardiac function assessment in the non-diabetic heart subjected to 20 min ischaemia/ 60 min reperfusion. A. Rate Pressure Product (RPP) B. Left ventricular end diastolic pressure (LVEDP) C. Left ventricular developed pressure (LVDP) D. Coronary flow E. Heart Rate (HR) and F. % recovery of LVDP following 20 min ischaemia/60 min reperfusion. LVEDP. LVDP and HR were monitored via an inserted ventricular latex balloon, RPP was calculated as HR x LVDP as a measure of cardiac workload. A significant reduction in LVDP recovery was seen the aged, diabetic heart. Data is shown as mean ± S.E.M, n≥6. Comparison between groups at multiple time-points was analysed by two-way repeated measures (mixed model) ANOVA with a Bonferroni correction for multiple comparisons. One way ANOVA followed by a Tukey Post-Hoc analysis were used for statistical analysis between groups.

The 18 month Wistar heart had significantly worse RPP function compared to the other age groups ($P<0.05$) when subjected to 35 min ischaemia/reperfusion whereas no significant differences were seen in coronary flow (p=NS). Similar to the function recorded for 20 min ischaemia, HR was significantly slower throughout the experimental protocol in the 18 month age group compared to 3 and 8 month groups ($P<0.005$), HR did not differ between 12 and 18 months hearts (p=NS). LVDP function at baseline was significantly lower in the 18 month age group compared to the other groups. During ischaemia function declined further and less recovery was seen during reperfusion, however this value did not reach significance (p=0.052). Data is summarised in Figure 3.7.

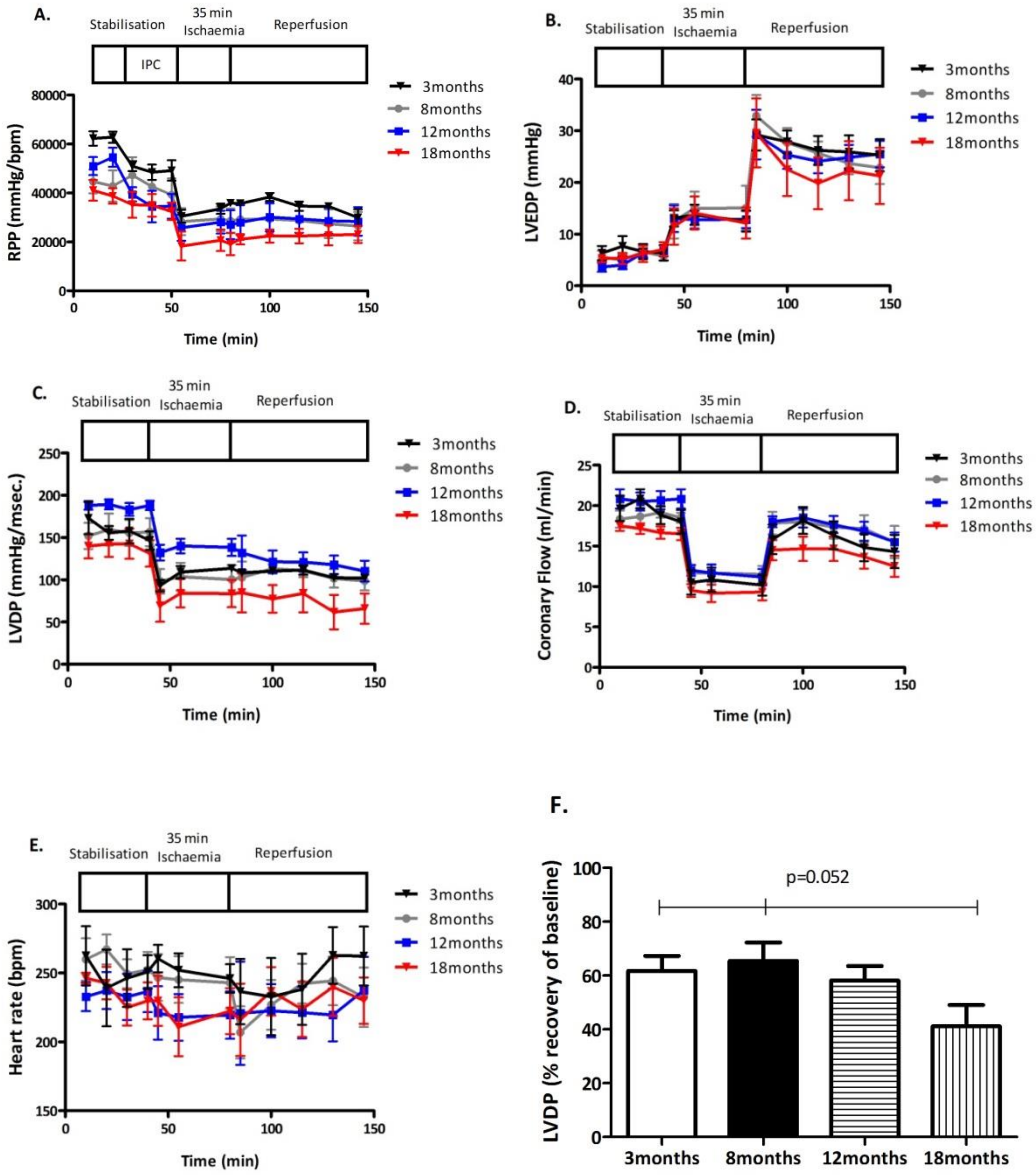

Figure 3.7: Cardiac function assessment in the non-diabetic heart subjected to 35 min ischaemia/ 60 min reperfusion. A. Rate Pressure Product (RPP) B. Left ventricular end diastolic pressure (LVEDP) C. Left ventricular developed pressure (LVDP) D. Coronary flow E. Heart Rate (HR) and F. % recovery of LVDP following 20 min ischaemia/60 min reperfusion. LVEDP. LVDP and HR were monitored via an inserted ventricular latex balloon, RPP was calculated as HR x LVDP as a measure of cardiac workload. No significant differences in functional parameters were seen the ageing, non-diabetic heart. Data is shown as mean ± S.E.M, n≥6. Comparison between groups at multiple time-points was analysed by two-way repeated measures (mixed model) ANOVA with a Bonferroni correction for multiple comparisons. One way ANOVA followed by a Tukey Post-Hoc analysis were used for statistical analysis between groups.

Interestingly, at 3 months of age the non-diabetic and diabetic heart had similar RPP function throughout ischaemia and reperfusion, however at 8 months RPP is superior in the diabetic versus the non-diabetic heart. Function begins to deteriorate at 12months in the diabetic heart, with decreased RPP output compared to aged matched Wistars; at 18 months RPP is similar in both the diabetic and non-diabetic heart (Figure 3.8). Young Wistar hearts subjected to 20 min ischaemia had significantly greater RPP function during ischaemia and reperfusion compared to hearts subjected to 35 min ischaemia. This function was superior than hearts subjected to either 20 min or 35 min ischaemia and reperfusion in the 18 month Wistar group. Interestingly, no difference in function was noted in hearts subjected to 20 min or 35 min ischaemia and reperfusion in either the young or old diabetic group (Figure 3.9).

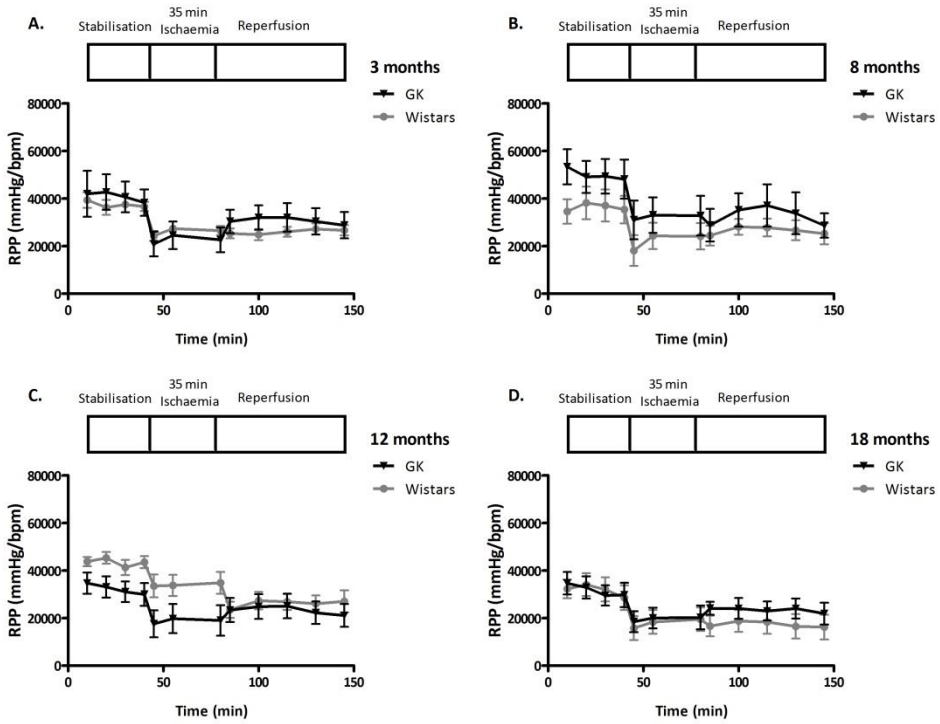

Figure 3.8: Comparison of RPP in the diabetic versus non-diabetic heart. Rate Pressure Product (RPP) was calculated as Heart rate (HR) x Left ventricular developed pressure (LVDP) and compared between diabetic GK rats and non-diabetic Wistar rats at A. 3 months of age B. 8 months of age C. 12 months of age and D. 18months of age. Data is shown as mean ± S.E.M, n≥6. Comparison between groups at multiple time-points was analysed by two-way repeated measures (mixed model) ANOVA.

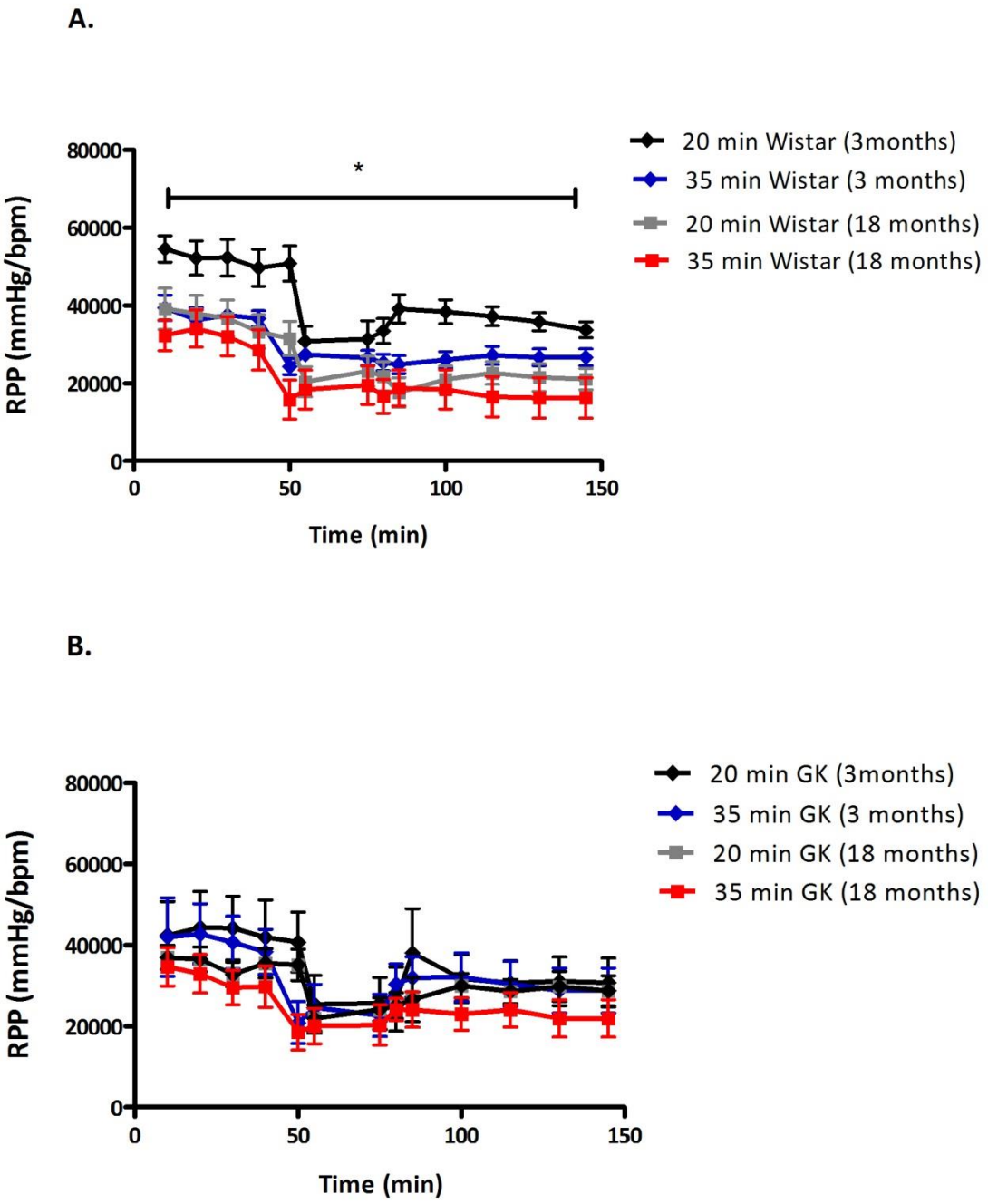

Figure 3.9: Comparison of RPP in the diabetic and non-diabetic heart subjected to either 20 min or 35 min ischaemia followed by reperfusion. Rate Pressure Product (RPP) was calculated as Heart rate (HR) x Left ventricular developed pressure (LVDP) and compared between diabetic GK rats and non-diabetic Wistar rats at A. Non-diabetic Wistar rat hearts B. Diabetic Goto-Kakizaki (GK) rats. 3 month old non-diabetic hearts subjected to 20 min ischaemia and 60 min reperfusion had significantly greater cardiac function compared to hearts of the same age subjected to 35 min ischaemia and 60 min reperfusion. In contrast, no difference was seen between the 3 month diabetic hearts subjected to either 20 or 35 min ischaemia followed by 60 min reperfusion. Data is shown as mean ± S.E.M, n≥6. Comparison between groups at multiple time-points was analysed by two-way repeated measures (mixed model) ANOVA with a Bonferroni correction for multiple comparisons were used for statistical analysis between groups.

3.1.4.4 Age and diabetes contribute to susceptibility to infarction

Infarction that developed after 20 and 35 min of ischaemia followed by reperfusion was compared between non-diabetic Wistar and diabetic GK rats at different ages. In this model, 20 min regional ischaemia is not sufficient to develop a significant infarct in normoglycaemic hearts. In fact, this model is often used to investigate stunning [475] and not cell death.

'Pre-diabetic' 3 month GK rat hearts were less vulnerable to a 20 min ischaemic insult (I/R%: 30 ± 4.3) than to a longer 35 min ischaemic insult (I/R%: 46.6 ± 4.1). However, 8 month old GK rat hearts following either 20 min and 35 min ischaemia developed a similar infarct (I/R%; 35.5 ± 2.5 *vs.* 39.4 ± 2.3, P=NS). Similar data were obtained in the 12 month and 18 month age groups which developed comparable infarct sizes following both 20 and 35 min ischaemia: I/R% was 43.2 ± 3.7 (20 min) *vs.* 42.0 ± 3.9 (35 min) (P=NS); I/R% 55.5 ± 4.7 (20 min) *vs*. 62.1 ± 6.0 (35 min), (P=NS). Interestingly, at the oldest age, the infarct sizes were significantly greater compared to the younger age groups (39.4% ± 2.3, 42.0 ± 3.9, *vs.* 62.1 ± 6.0, $p<0.005$). Data are summarised in Figure 3.10. In contrast, the non-diabetic Wistar rat hearts subjected to 20 min of ischaemia in 3, 8 and 12 months age groups developed significantly less damage compared to 35 min ischaemia. However, in the 18 month group there is no significant difference in the infarction following 20 or 35 min ischaemic insult, similar to that seen in the diabetic hearts from 8-18 months. Data are summarised in (Figure 3.11). Moreover, the comparatively lower infarct size seen in the younger diabetic animals compared to their non-diabetic counterparts when subjected to 35 min ischaemia and reperfusion is lost as the diabetic heart ages; with the 18 month groups exhibiting similar infarct sizes (I/R%: 62.1 ± 6.0 in GKs and 59.6 ± 4.1 in Wistars). These data seem to indicate that the age-induced susceptibility to infarction is manifested earlier in the diabetic rats.

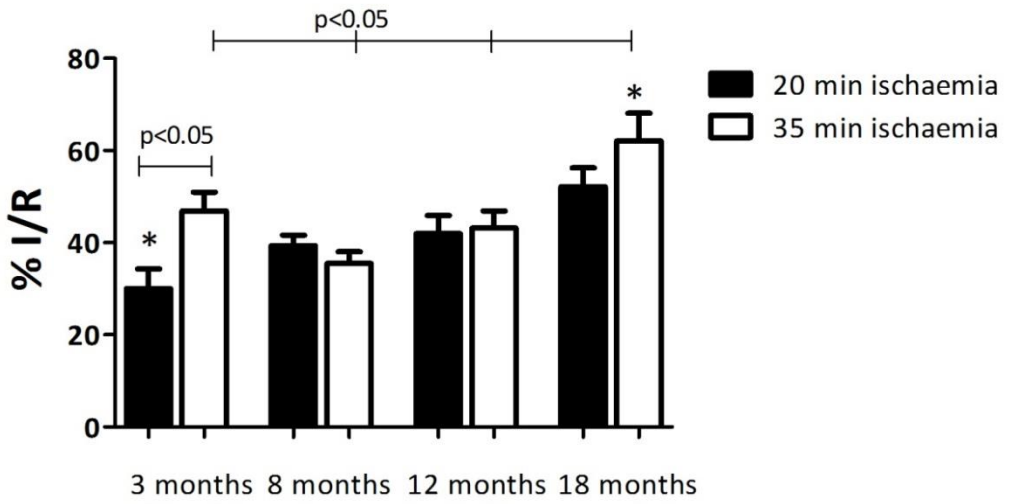

Figure 3.10: The variations in susceptibility to ischaemia with age and diabetes (GK rats). Infarct size is expressed as the ischaemic volume within the area at risk of the left ventricle (% I/R). All hearts were stabilized for 40 min, subjected to either 20 min (black bars) or 35 min (white bars) of coronary artery occlusion followed by 60 min reperfusion. The diabetic GK rat heart exhibits an increased susceptibility to 20 min ischemia between 8-18months, whereas the youngest GK group is less susceptible to shorter ischaemia. Data is shown as mean ± S.E.M, n≥6. One way ANOVA and Tukey's post hoc analysis were used for statistical analysis between all groups

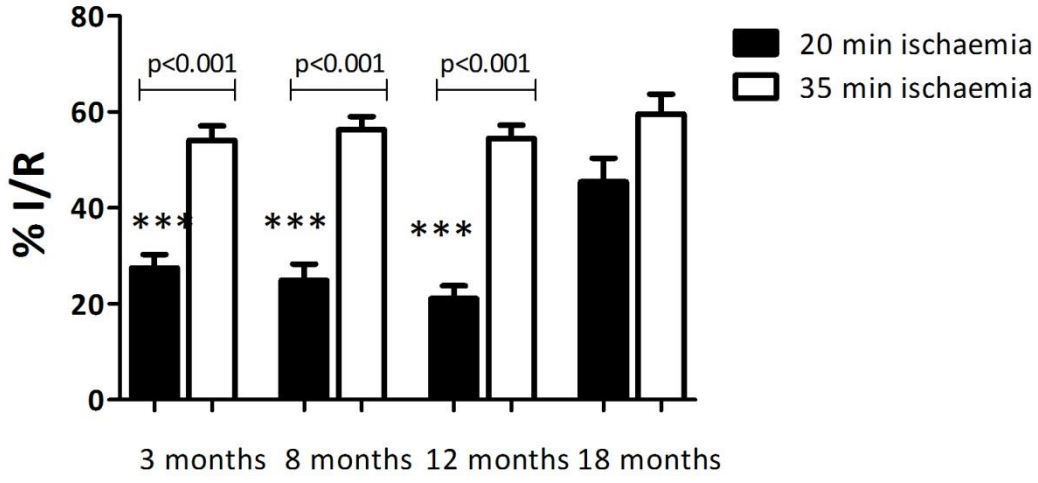

Figure 3.11: The variations in the susceptibility to ischaemia with age (Wistar rats). Infarct size is expressed as the ischaemic volume within the area at risk of the left ventricle (% I/R). All hearts were stabilized for 40 min, subjected to either 20 min (black bars) or 35 min (white bars) of coronary artery occlusion followed by 60 min reperfusion. The non-diabetic Wistar rat hearts develop an increased susceptibility to shorter ischaemia with old age. Data is shown as mean ± S.E.M, n≥6. One way ANOVA and Tukey's post hoc analysis were used for statistical analysis between all groups.

3.1.5 Summary of results

In summary, in the setting of type 2 diabetes, even at a young age, shorter ischaemic time caused equivalent damage to lethal ischaemia. This increased susceptibility was not evident in 'pre-diabetic' 3 month hearts. The 18 month diabetic group demonstrated a greater vulnerability to lethal IRI compared to all other groups. Interestingly, the non-diabetic 3 month, 8 month or 12 month rat hearts were not vulnerable to a shortened ischaemic time whereas this effect manifested at 18 months. Even though our results support previous findings in isolated heart preparations that non diabetic hearts have larger infarcts than diabetic hearts when subjected to lethal ischaemia, this difference was lost in old age. In regard to function, the non-diabetic heart at young and middle age maintains good basal properties and recovery of function following both 20 min or 35 min ischaemia and reperfusion, however hearts isolated from the 18 month group have a decreased ability to recover following ischaemia/reperfusion. In the diabetic heart, basal function and functional recovery following ischaemia/reperfusion deteriorated earlier in life, in both the 12 and 18 month group's compared to the younger diabetic rat hearts.

3.2 Is ischaemic preconditioning possible in the aged, diabetic heart?

3.2.1 Introduction

The observations from the previous section suggest that type 2 diabetes and age in combination render the heart more vulnerable to damage caused by ischaemia-reperfusion (IR). Ischaemic preconditioning (IPC), a cardioprotective strategy involving a short protocol of ischaemia and reperfusion prior to sustained ischaemia has been successful in reducing lethal cell injury in experimental models [124]; how this phenomenon works has been extensively studied. Briefly, IPC causes the release of G-protein coupled receptor (GPCR) agonists such as adenosine/bradykinin, which bind to the receptor and activate numerous signalling pathways. Phosphatidylinositol-3-kinase (PI3K) activation, can lead to stimulation of a number of downstream molecules, directly phosphorylating and activating Akt. Other signalling molecules involved in IPC include extracellular regulated kinase (ERK), nitric oxide synthase (NOS), inactivation of glycogen synthase kinase-3β (GSK-3β) and also protein kinase C (PKC). These converge to activate the mitochondrial ATP-dependent potassium channel (K_{ATP}), closing the mitochondrial permeability transition pore (mPTP) resulting in protection from IRI [141].

The animal data suggests that the diabetic heart is resistant to ischaemic conditioning such that the IPC stimulus needs to be increased to induce cardioprotection [245]. Similar to studies examining cardioprotection in diabetes, conditioning the aged heart has also remained controversial. In animal studies using rodent models, most studies show that the protective effect of IPC is lost with age[384], however in *in vivo* studies using rabbits[403] and sheep models[404], the protective effect of IPC is enhanced. Of course, these investigations use different experimental IPC protocols and a diverse range of animal models, which could, to some extent, explain the discrepancies. As far as we know, assessment of the cardioprotective effects of IPC has not been performed in animal models exhibiting both co-morbidities. Therefore, studies investigating cardioprotection in ageing, diabetic models could provide a vital link in the translational process of basic research into clinical practice.

3.2.2 Hypothesis and aim

We hypothesised that age and diabetes combined may alter the effectiveness of ischaemic preconditioning. Using an inbred lean model of type 2 diabetes (T2D), Goto Kakizaki (GK) rat and its original source, the normoglycaemic Wistar rat, at different

ages (between 3 and 18 months), we aimed to determine if an increased IPC stimulus of 3 cycles is able to achieve cardioprotection in an animal model exhibiting both old age and type 2 diabetes.

3.2.3 Experimental protocols

3.2.3.1 Langendorff Isolated heart perfusions

Langendorff isolated heart experiments were performed as described in the previous section. For infarct analysis (n=6 per group) hearts were randomly assigned to receive control (35 min regional ischaemia) or IPC (3 cycles of 5 min global ischaemia/10 min reperfusion) prior to 35 min regional ischaemia, followed by 60 min reperfusion (summarised in Figure 3.12). The staining and the quantification of the infarct were performed as previously described.

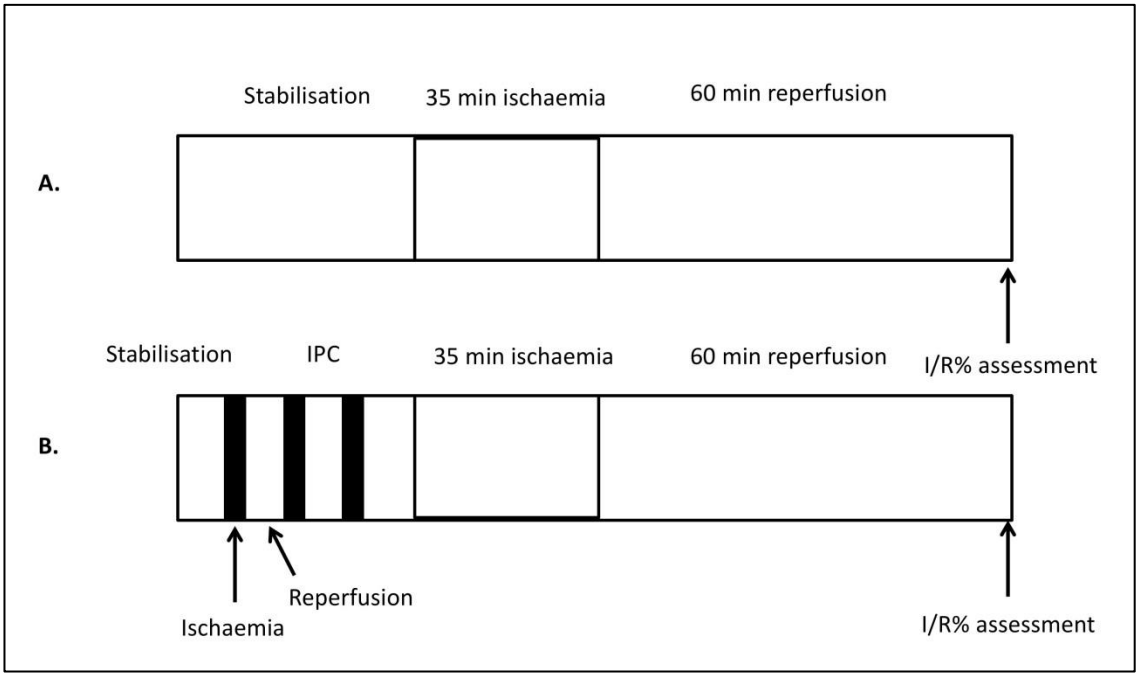

Figure 3.12: Scheme of Langendorff experiments performed. For infarct analysis (n=6 per group) hearts were randomly assigned to receive A. Control (35 min regional ischemia) or B. IPC (3 cycles of 5 min global ischaemia/10 min reperfusion preceding 35 min regional ischemia) followed by 60 min reperfusion.

3.2.4 Results

3.2.4.1 The diabetic heart manifests a decreased recovery of function following IPC at a younger age than non-diabetic hearts

In the non-diabetic heart, IPC caused a similar recovery of LVDP function at 3, 8 and 12 months of age, however recovery in the 18 month group was significantly lower

(p<0.05) (Figure 3.13A.). Interestingly, in the diabetic heart, a decline in recovery of LVDP occurred in both the 12 and 18 month groups (Figure 3.13B.). IPC did not have a significant impact on functional recovery compared to the control group in the non-diabetic hearts in this model (Figure 3.14). In the diabetic heart, IPC trended to improve function compared to control at 3 and 8 months, with a reduction in recovery in the two older age groups, however due to the spread of the data these findings did not reach significance (Figure 3.15). All other parameters are shown in Figure 3.16 for non-diabetic heart and in Figure 3.17 for the diabetic heart.

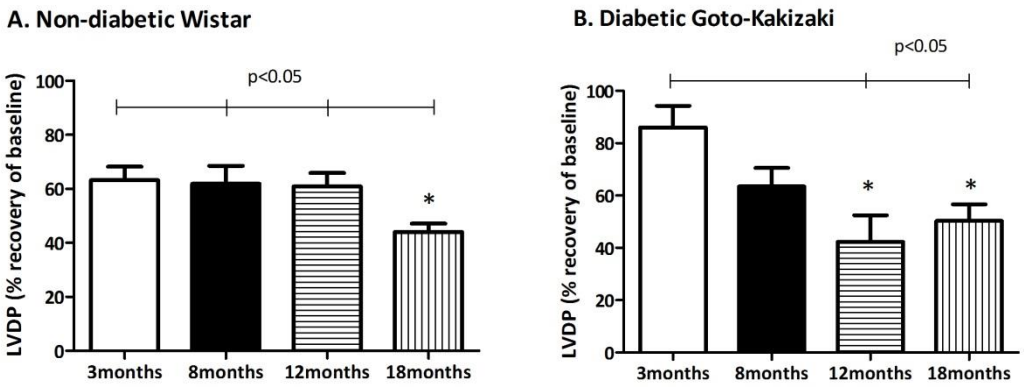

Figure 3.13: Recovery of function following ischaemia-reperfusion : Percentage recovery of Left ventricular developed pressure (LVDP) following 3 cycles of ischaemic preconditioning followed by 35 min ischaemia and 60 min reperfusion A. Non-diabetic Wistar rat hearts and B. Diabetic Goto-Kakizaki (GK) rat hearts at 3, 8, 12 and 18 months of age. The diabetic heart demonstrated a decreased recovery of LVDP function at an earlier age than the non-diabetic heart. Data is shown as mean ± S.E.M, and is calculated by comparing the value recorded at the last time point as a percentage of the value recorded at the first time point. n≥6. One way ANOVA followed by a Tukey Post-Hoc analysis were used for statistical analysis between groups.

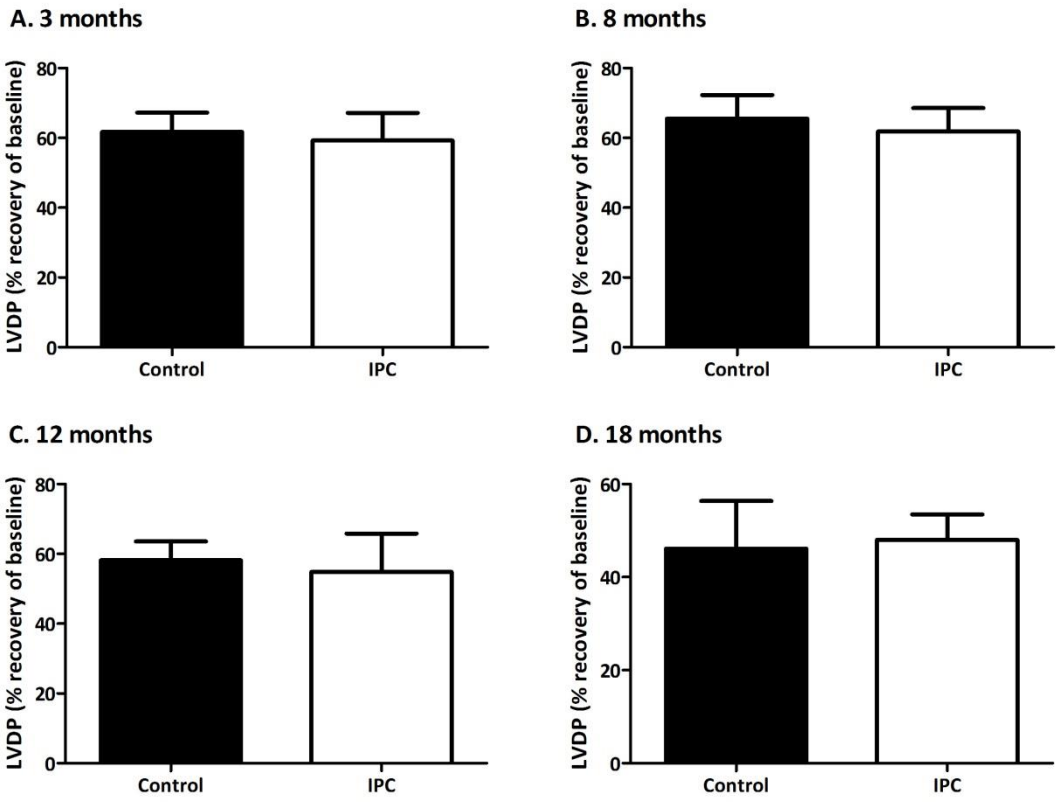

Figure 3.14: Recovery of function following ischaemia-reperfusion in the non-diabetic heart. Percentage recovery of Left ventricular developed pressure (LVDP) following either Control (35 min ischaemia/60 min reperfusion) or IPC (3 cycles of ischaemic preconditioning prior to 35 min ischaemia/60 min reperfusion) in non-diabetic Wistar rat hearts. A. 3 months B. 8 months C. 12 months D 18months. Data is shown as mean ± S.E.M, n≥6. T-test was used for statistical analysis between the two groups.

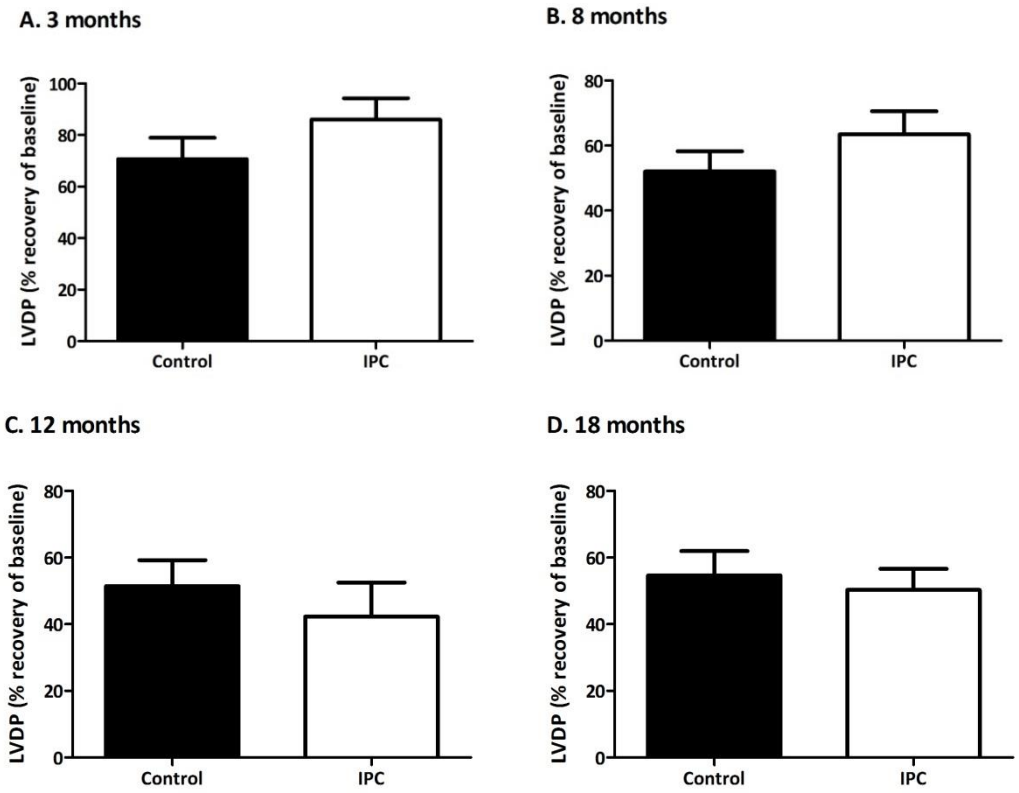

Figure 3.15: Recovery of function following ischaemia-reperfusion in the diabetic heart. Percentage recovery of Left ventricular developed pressure (LVDP) following either Control (35 min ischaemia/60 min reperfusion) or IPC (3 cycles of ischaemic preconditioning prior to 35 min ischaemia/60 min reperfusion) in Diabetic Goto-Kakizaki rat hearts. A. 3 months B. 8 months C. 12 months D 18months. Data is shown as mean ± S.E.M, n≥6. T-test was used for statistical analysis between the two groups.

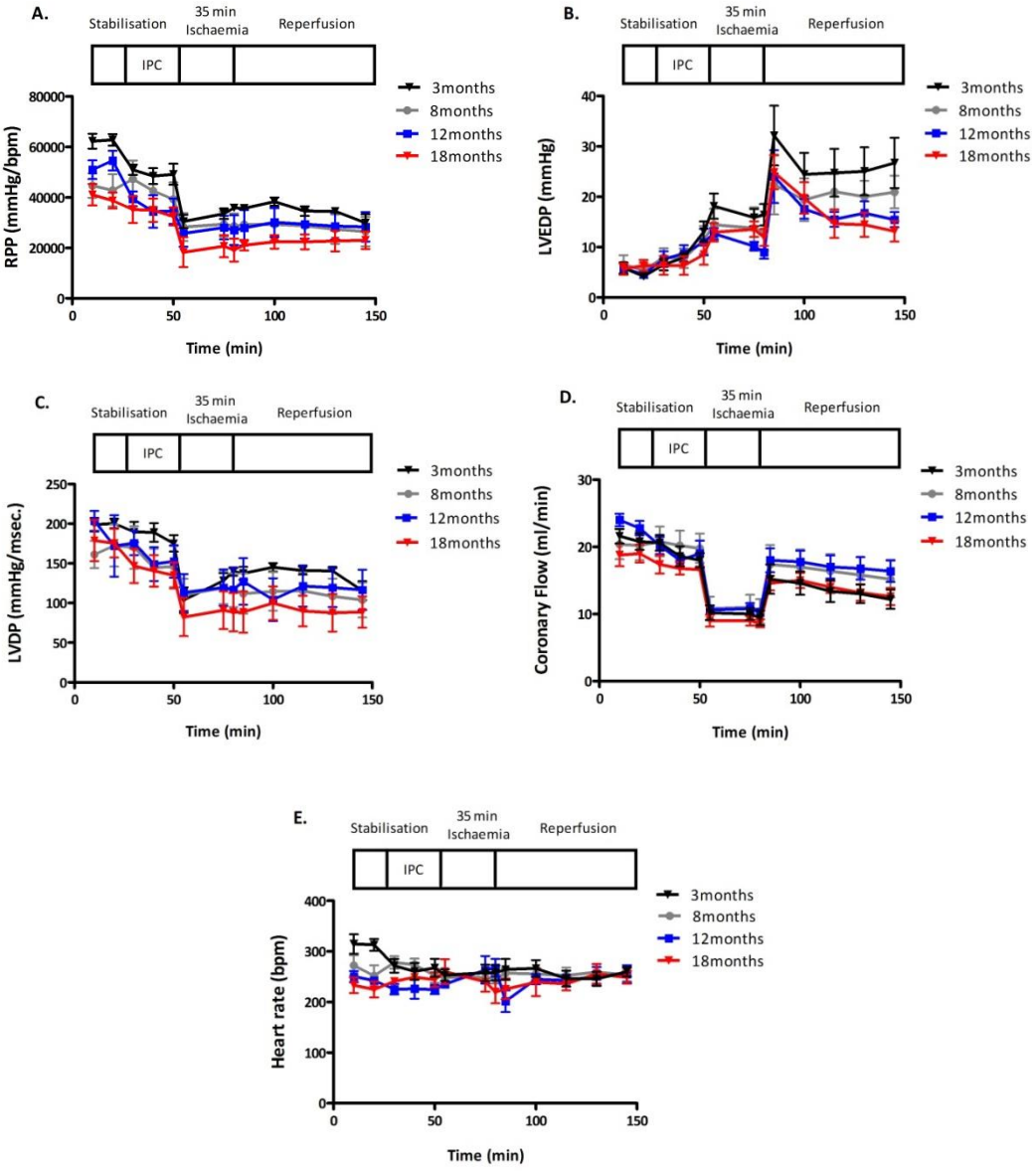

Figure 3.16: Recovery of function following IPC prior to ischaemia-reperfusion in the non-diabetic heart: Cardiac function assessment in the non-diabetic heart subjected to 3 cycles of ischaemic preconditioning followed by 35min ischaemia and 60 min reperfusion. A. Rate Pressure Product (RPP) B. Left ventricular end diastolic pressure (LVEDP) C. Left ventricular developed pressure (LVDP) D. Coronary flow E. Heart Rate (HR) and F. % recovery of LVDP following 20 min ischaemia/60 min reperfusion. LVEDP. LVDP and HR were monitored via an inserted ventricular latex balloon, RPP was calculated as HR x LVDP as a measure of cardiac workload. Data is shown as mean ± S.E.M, n≥6. One way ANOVA followed by a Tukey Post-Hoc analysis were used for statistical analysis between groups.

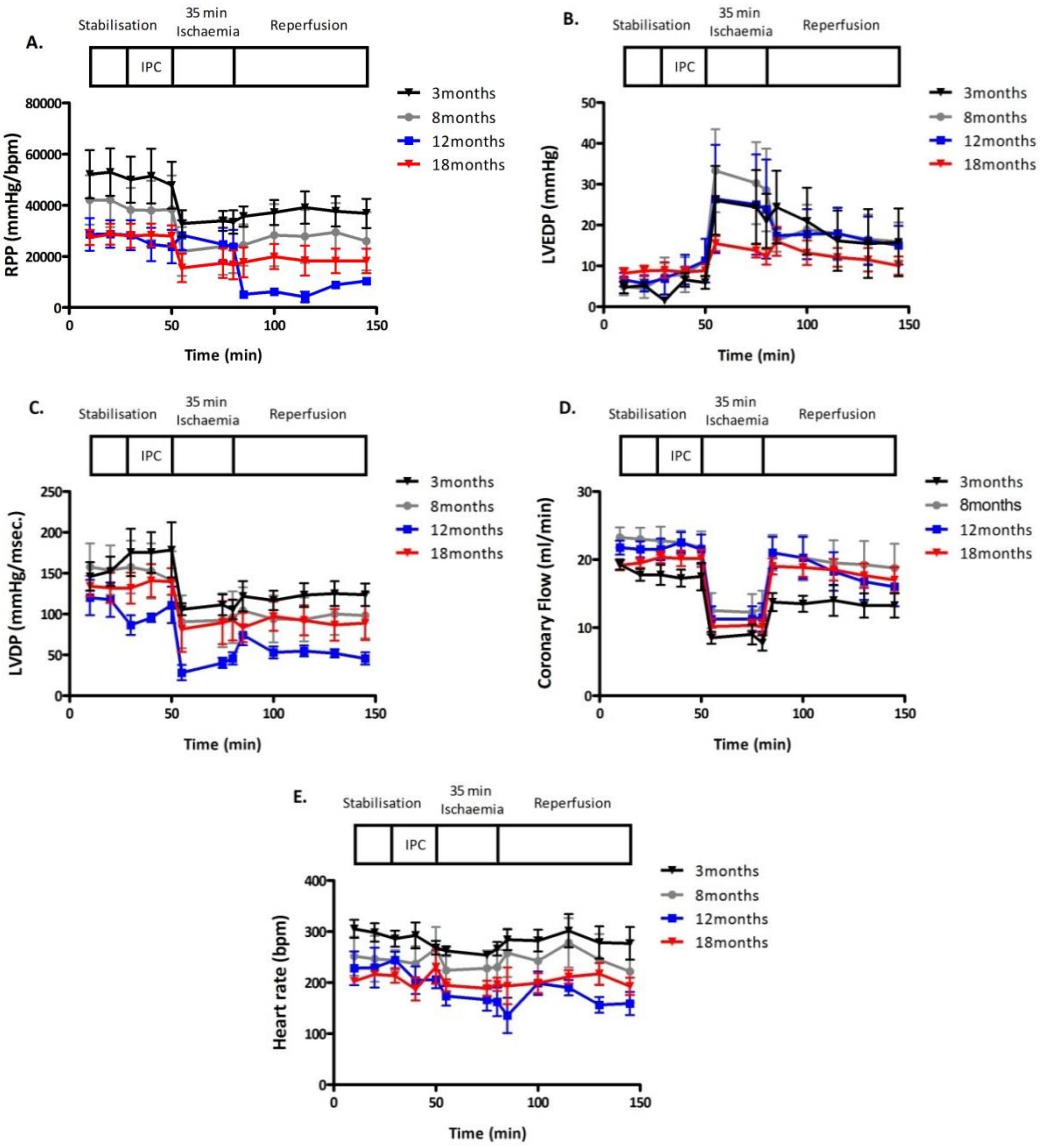

Figure 3.17: Recovery of function following IPC prior to ischaemia-reperfusion in the diabetic heart. Cardiac function assessment in the diabetic heart subjected to 3 cycles of ischaemic preconditioning followed by 35min ischaemia and 60 min reperfusion. A. Rate Pressure Product (RPP) B. Left ventricular end diastolic pressure (LVEDP) C. Left ventricular developed pressure (LVDP) D. Coronary flow E. Heart Rate (HR) and F. % recovery of LVDP following 20 min ischaemia/60 min reperfusion. LVEDP. LVDP and HR were monitored via an inserted ventricular latex balloon, RPP was calculated as HR x LVDP as a measure of cardiac workload. Data is shown as mean ± S.E.M, n≥6. Comparison between groups at multiple time-points was analysed by two-way repeated measures (mixed model) ANOVA with a Bonferroni correction for multiple comparisons were used for statistical analysis between groups.

3.2.4.2 The diabetic heart manifests a decreased protective response to IPC at a younger age than non-diabetic hearts

In hearts that were isolated from non-diabetic Wistar and diabetic GK rat hearts at 3 and 8 months of age, the ischaemic preconditioning protocol used was successful in limiting the damage caused by ischaemia-reperfusion injury. IPC caused a 46% and 38% reduction in infarct size in 3 and 8 month Wistar (non-diabetic) hearts and 55% and 40% reduction in 3 and 8 month GK diabetic hearts when compared with control groups ($p<0.005$ for all groups versus their respective controls). At 12 and 18 months of age the non-diabetic heart was protected by IPC, albeit to a lesser extent in the 18 month group (38.2% *vs*. 25% reduction in infarct size, Figure 3.18). However, the diabetic heart was not amenable to preconditioning protection in either the 12 or 18 month groups (I/R% for 12 month group, 42.0 ± 3.9 vs. 46.9 ± 5.5 and I/R% for 18 month group, 62.1 ± 5.9 vs. 69.1 ±4.3. P=NS, Figure 3.19).

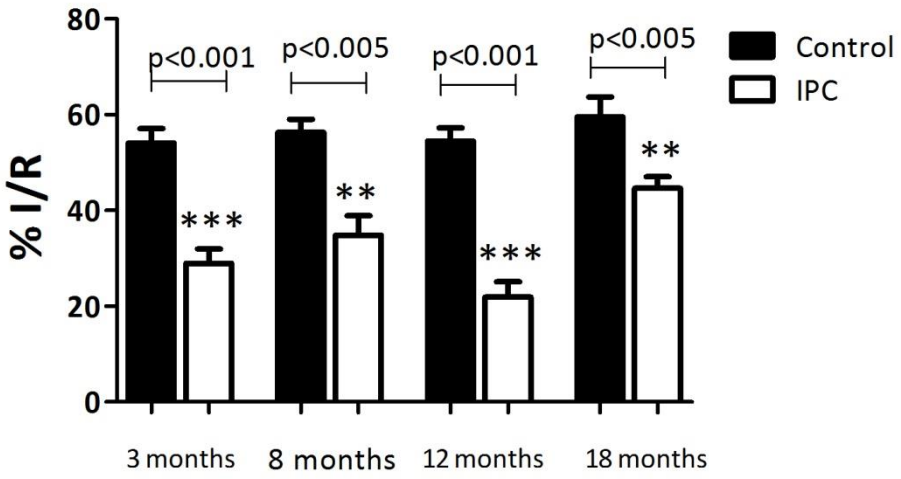

Figure 3.18: The effectiveness of Ischaemic Preconditioning (IPC) on infarct size reduction in the setting of ageing in normoglycaemic Wistar hearts. Infarct size is expressed as the ischaemic volume within the area at risk of the left ventricle (% I/R). Hearts were stabilized for 40 min or subjected to 3 cycles of 5 min ischaemia/reperfusion then subjected to 35 min of coronary artery occlusion followed by 60 min reperfusion. Black bars represent control group (35 min ischemia/reperfusion) and white bars represent IPC group. The non-diabetic Wistar rat heart is amenable to protection by 3 cycles of IPC, though the effectiveness decreases with age. Data is shown as mean ± S.E.M, n≥6. One way ANOVA and Tukey's post hoc analysis were used for statistical analysis between all groups.

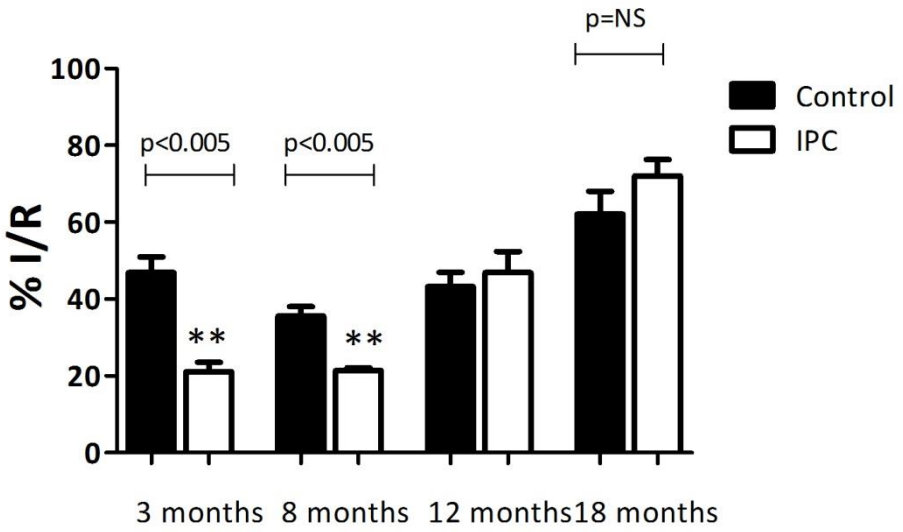

Figure 3.19: The effectiveness of Ischaemic Preconditioning (IPC) on infarct size in the setting of ageing and type 2 diabetes. Infarct size is expressed as the ischaemic volume within the area at risk of the left ventricle (% I/R). Hearts were stabilized for 40 min or subjected to 3 cycles of 5 min ischaemia/reperfusion then subjected to 35 min of coronary artery occlusion followed by 60 min reperfusion. Black bars represent control group (35 min ischemia/reperfusion) and white bars represent IPC group. The diabetic GK rat heart was amenable to protection by 3 cycles of IPC at 3 and 8 months of age, however this effectiveness was lost with age. Data is shown as mean ± S.E.M, n≥6. One way ANOVA and Tukey's post hoc analysis were used for statistical analysis between all groups.

3.2.5 Summary of Results

In summary, the positive effect of IPC on functional recovery following ischaemia-reperfusion injury is lost earlier in diabetic hearts (at 12 months) compared to non-diabetic hearts (18 months). Most importantly, our data confirm that 3 cycles of IPC are sufficient to achieve protection against lethal cell injury in young type 2 diabetic hearts. Furthermore, we endorse that this stimulus of IPC is adequate to protect the ageing, non-diabetic heart as well. However, the combination of diabetes with age renders the heart resistant to protection elicited by 3 cycles of IPC. Interestingly, in the oldest diabetic group, IPC caused more damage than in the control protocol alone.

3.3 Signalling defects in the ageing and diabetic heart

3.3.1 Introduction

The experiments presented in this section were conducted with the aim of characterising potential changes in expression and activation of pro survival signaling pathways. Based on the results presented in the previous sections that showed the diabetic heart was firstly more susceptible to 'sub lethal' ischaemia-reperfusion injury than the non-diabetic heart and that this effect was augmented with age and secondly, that the effectiveness of IPC was lost in the ageing, diabetic heart. We initiated these investigations starting with Akt.

As discussed in the introduction, the role of pro-survival PI3K/Akt signaling in endogenous cardioprotection against IRI has been well documented, firstly, as an anti-apoptotic kinase [476] and secondly, as a key element of the reperfusion injury salvage kinase (RISK) pathway that is initiated following ischaemic or pharmacological conditioning[151]. Defects in the signaling of this kinase can impair normal cell processes and lead to detrimental effects culminating with cell death.

Akt, a serine/threonine kinase (also known as protein kinase B) has emerged as a pivotal kinase involved in molecular signal transduction pathways underlying normal and pathological conditions. The diverse regulatory functions of Akt including the promotion of cellular growth, survival and metabolism have led to opposing concepts in exploiting Akt biology to 1) treat cancer by inhibiting these functions and 2) improve the outcome of cardiovascular diseases by promoting these actions either directly or indirectly to limit or repair myocardial damage[139]. Existing in three distinct isoforms, Akt1-3 can be activated in response to numerous growth factors and hormones[139] and also by stress stimuli like hypoxia[477] and oxidative stress[478, 479]. In the heart, Akt-1 and Akt-2 are most abundantly expressed and have a variety of functions. Akt-1 has been related to cell survival and growth[480, 481] whereas Akt-2 is involved in glucose homeostasis[482]. The importance of Akt isoforms were cemented by loss-of-function experiments. Global knock out of the Akt-1 gene retards growth and increases apoptosis in mice[481, 483]. Whereas, Akt-2 $^{-/-}$ mice develop insulin resistance and a type 2 diabetic phenotype, moreover in response to myocardial ischaemia exhibit increased apoptosis[484, 485].

Activation of Akt in response to certain physiological stimuli inhibits apoptosis and promotes cell survival by phosphorylating proapoptotic BAX at the serine 184 residue preventing BAX-induced permeablisation of the mitochondrial membrane[486];

and also at the serine 136 residue of proapoptotic BAD releasing antiapoptotic BCL-XL[487]. Akt can also interact with metabolic enzymes and transcription factors such as members of the FOXO family[488]; phosphorylation of FOXO3a promotes its cytosolic accumulation therefore preventing transcriptional activity of death receptor ligands and reduces apoptosis[145], Akt can also directly phosphorylate FOXO1 and 4[139]. These transcription factors can interact with numerous downstream targets including PGC-1α[93], a master of mitochondrial biogenesis[39].

Unsurprisingly, an innate cardioprotective role for Akt activation was suggested especially in the setting of IRI[134]. Gene transfer of constitutively active Akt into rats 48 hours prior to IRI, significantly reduced infarct size and limited hypoxia induced cardiomyocyte dysfunction in vitro[489]. Acute activation of Akt via phosphatidyl-inositol-3-kinase (PI3K) occurs in response to IPC, protecting the heart against lethal reperfusion injury. The resulting downstream signalling following Akt activation are thought to converge onto the mitochondria, inhibiting mPTP opening and preventing cell death[134].

A hallmark of type 2 diabetes is defective insulin signalling at insulin receptors leading to impaired glucose uptake and utilization. The PI3K-Akt pathway is a major downstream component following insulin receptor activation. Therefore, it is unsurprising that Akt signalling becomes altered in the setting of diabetes. Krook et al, 1997 were the first to demonstrate a decrease in insulin-stimulated Akt activity in soleus muscle of type 2 diabetic Goto-Kakizaki rats[490]. Muscle biopsies collected from type-2 diabetic patients were also found to have an impaired Akt signalling axis[491]. At the level of the heart, baseline Akt-phosphorylation in both diabetic animals [238] and humans [244] are reduced compared to non-diabetic hearts. This impairment could lead to a plethora of detrimental effects on the balance of anti and pro apoptotic intracellular signaling, potentially rendering the diabetic heart more susceptible to IRI.

Defects in Akt signalling have also been suggested in ageing. An age-associated reduction in Akt activation was seen in both liver and hepatocytes isolated from aged rats[492]. A decrease in baseline Akt phosphorylation adversely affected cellular responses to oxidative stress in these cells.[492] An impairment of pro survival signaling in the ageing heart led to the development of compromised cardiac function; some studies suggest that a reduction in Akt activity and expression levels correlate with this cardiac dysfunction[493]. In contrast, others suggest that chronically activated Akt in the ageing heart leads to pathological hypertrophy[494].

3.3.2 Hypothesis and aim

Following our data highlighting the changes in the endogenous cardioprotective potential with age and diabetes we hypothesised that a possible impairment in Akt signaling occurs in the ageing, diabetic heart. Furthermore, these changes may lead to downstream de-regulations in the levels of PGC-1α (a key transcriptional regulator) and catalase (an indicator of antioxidant defense), which can both be directly or indirectly controlled by Akt. We aimed to investigate whether Akt expression and activation could be affected by these comorbidities.

3.3.3 Experimental Protocols

3.3.3.1 Western Blot Analysis

To assess changes in the expression or activation of proteins, Western blot analysis (WB) was performed in ageing and/or diabetic hearts from 3, 8, 12 and 18 month old Wistar and GK hearts. Hearts were collected at baseline (following 2 min perfusion on the Langendorff apparatus, to clear the blood which may interfere with the results).

To determine whether the lack of protection in the ageing, diabetic heart was related to changes in activation of Akt in response to IPC, GK hearts at 3 and 18 months were collected after stabilisation or following 3 cycles of IPC.

At the end of the procedures, the hearts were immediately freeze-clamped in liquid nitrogen and frozen at -80°C. For analysis, the heart samples were homogenized in PBS based buffer, the protein content was determined using BCA protein assay reagent and protein levels corrected accordingly to ensure equal protein loading. Equal volumes of heart homogenate were added to Laemmli lysis buffer and denatured by heating (the method is described in detail in Chapter 2).

The samples collected at baseline were assessed for phosphorylated-Akt (Ser-473) (Akt-P), total-Akt (Akt-T), PGC-1α and catalase expression and the IPC samples and their respective controls were assessed for phosphorylated-Akt (Ser-473) and total-Akt using WB analysis as described in detail in Chapter 2.5. Akt-P, Akt-T and catalase antibodies were purchased from Cell Signalling, UK, PGC-1α was purchased from Santa Cruz Biotechnology and α-tubulin (used as a loading control) purchased from Abcam, UK.

3.3.3.2 Electron Microscopy

For electron microscopy (EM) visualisation of mitochondria in the ageing and/or diabetic heart, myocardial tissue samples from 3 and 18 month old Wistar and GK rats were collected at baseline (following 2 min on the perfusion apparatus to clear blood) and immersed in EM-fixative (n=4 per group). The method is detailed in Chapter 2.8.

3.3.3.3 Measurement of Free Radicals in heart tissue

Intracellular reactive oxygen species (ROS) and reactive nitrogen species (RNS) are well known molecules that play a vital role in disrupting cellular signaling during oxidative stress [495]. Experiments were performed using the OxiSelect in vitro ROS/RNS Assay Kit (Cell Bio Labs) to measure total free radical presence in samples from 3, 8, 12 and 18 month GK and Wistar rat hearts. The assay used a specific fluorogenic, ROS/RNS probe which reacted with free radicals within the samples including hydrogen peroxide (H_2O_2), peroxyl radical (ROO·), nitric oxide (NO) and peroxynitrite anion (ONOO·). Fluorescence is proportional to the total level of ROS/RNS within the samples. The method is described in detail in Chapter 2.7.

A scheme of collection of all samples is summarised in Figure 3.20.

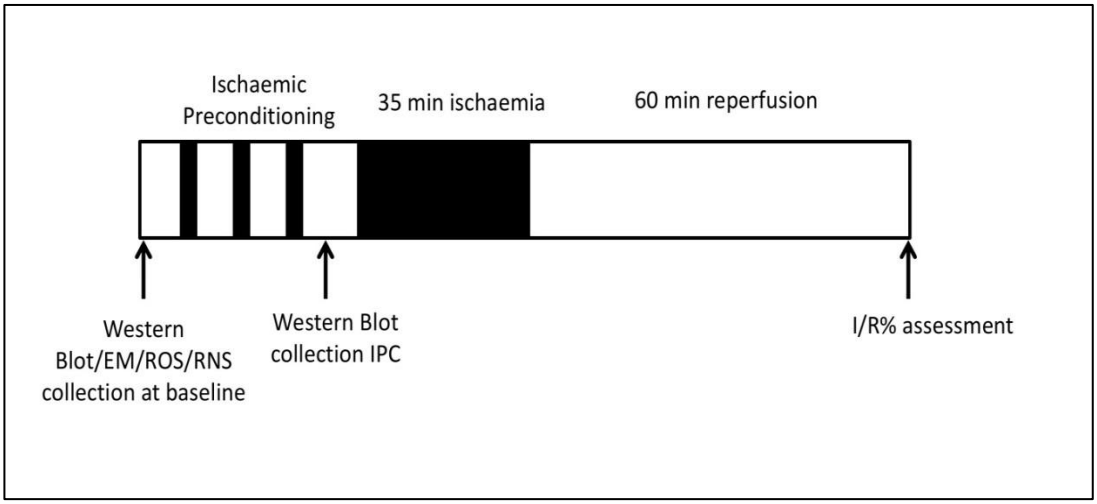

Figure 3.20: Scheme of collection of samples using the Langendorff apparatus. Tissue was collected for examination by Western Blot, electron microscopy (EM), and reactive oxygen species (ROS)/reactive nitrogen species (RNS) content (n=3/4 per group).

3.3.3.4 Statistical Analysis

Values are presented as mean ± standard error mean (SEM) and statistical analysis was performed as described in Chapter 2.9.

3.3.4 Results

3.3.4.1 Age alters the expression and activation of key pro survival signalling proteins in the diabetic heart

Akt is essential for cardioprotection via IPC. IPC induces acute Akt phosphorylation [151], therefore activation, and in this state the enzyme is cardioprotective via its multiple anti-apoptotic [134] and anti-necrotic effects. Surprisingly, a gradual increase in baseline Akt phosphorylation (Akt-P) was seen in the ageing GK rat heart, with a significant surge at 18 months versus either 3 or 12 months (Arbitrary units (A.U.): 0.5±0.2 *vs*. 0.2±0.2 or 0.1±0.05 P<0.05, Figure 3.21). Akt-P in the ageing, non-diabetic heart appeared to follow a similar trend but the changes were not as pronounced or significant (Figure 3.22). Interestingly, in young diabetic animals the phosphorylation of Akt at baseline is very low which supports the requirement of an increased IPC stimulus to induce cardioprotection as demonstrated by Tsang et al, 2005 [238].

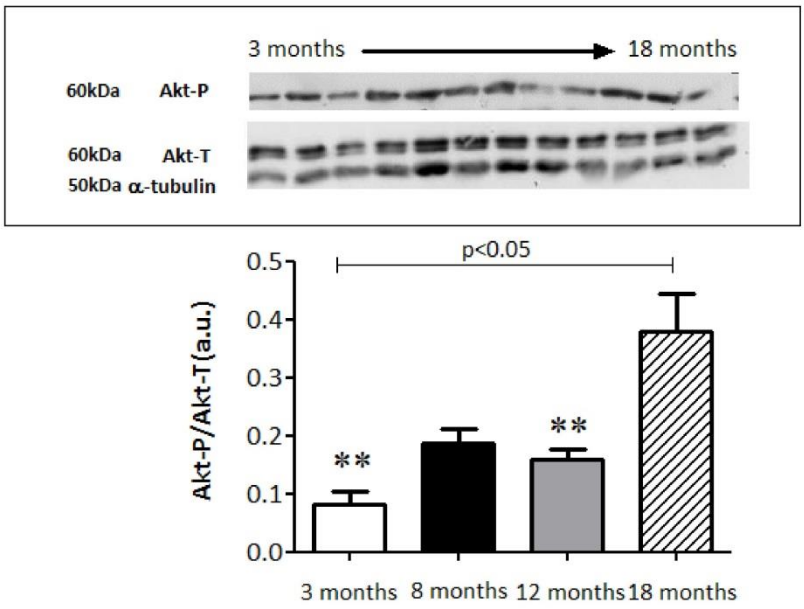

Figure 3.21: Phosphorylation of Akt in the diabetic heart. Phosphorylation of Akt increased with age in the diabetic heart. Values determined by densitometry of Akt-phosphorylation (Akt-P) corrected to respective α-tubulin over the relative expression of Akt-total (Akt-T) corrected to respective α-tubulin. Data is shown as mean ± S.E.M, n=3 per group. One way ANOVA and Tukey's post hoc analysis were used for statistical analysis between all groups

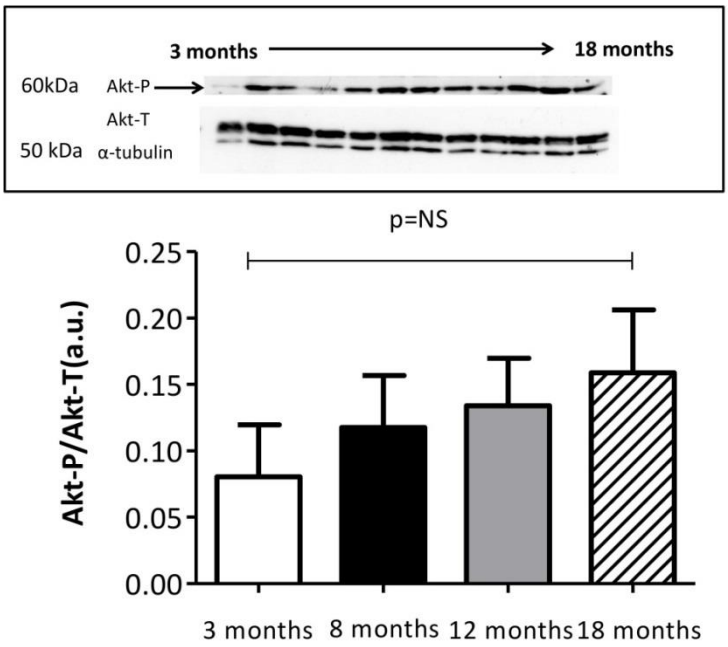

Figure 3.22: Phosphorylation of Akt in the non-diabetic heart. Phosphorylation of Akt trended to increase with age in the non-diabetic heart, however these changes did not reach significance. Values determined by densitometry of Akt-phosphorylation (Akt-P) corrected to respective α-tubulin over the relative expression of Akt-total (Akt-T) corrected to respective α-tubulin. Data is shown as mean ± S.E.M, n=3 per group. One way ANOVA and Tukey's post hoc analysis were used for statistical analysis between all groups

An age-related decrease was also seen in the expression of PGC-1α in the diabetic heart (Figure 3.23), with significant decrease between the 3 and 8 month groups and 12 and 18 month groups: (Arbitrary units (A.U.): 1.2±0.05, 0.8±0.01 *vs.* 2.9±0.3, 2.1±0.5, respectively). Interestingly, PGC-1α expression in the non-diabetic heart decreased with age. However, the only significant differences were noted in the 18 month group (Figure 3.24).

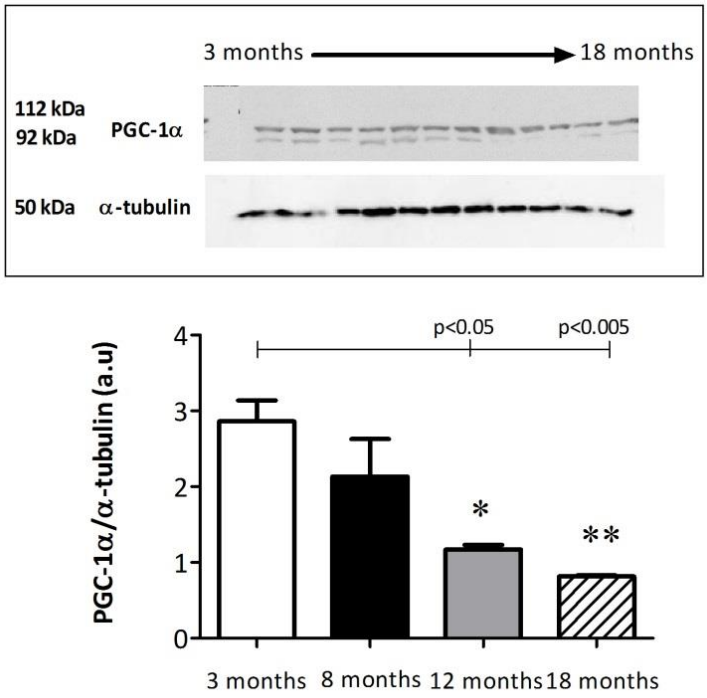

Figure 3.23: PGC-1α expression in the diabetic heart. PGC-1α expression decreases with age in the diabetic heart. Values determined by densitometry of PGC-1α corrected to respective α-tubulin. Data is shown as mean ± S.E.M, n=3 per group. One way ANOVA and Tukey's post hoc analysis were used for statistical analysis between all groups.

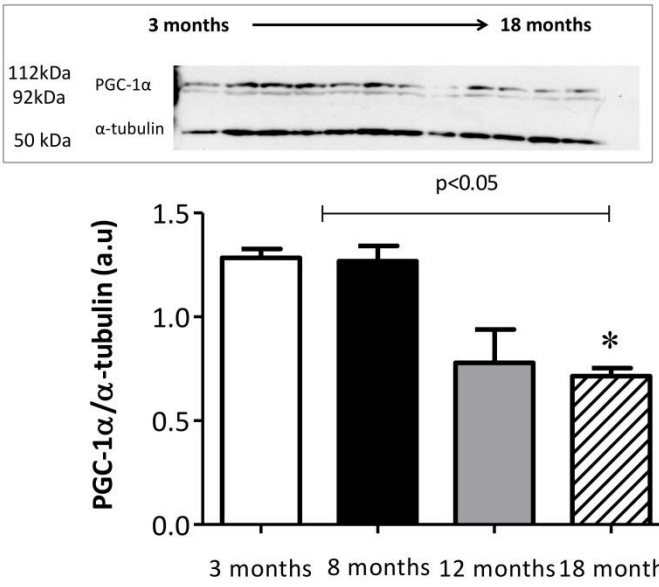

Figure 3.24: PGC-1α expression in the non-diabetic heart. PGC-1α expression decreased with age in the non-diabetic heart. Values determined by densitometry of PGC-1α corrected to respective α-tubulin. Data is shown as mean ± S.E.M, n=3 per group. One way ANOVA and Tukey's post hoc analysis were used for statistical analysis between all groups.

3.3.4.2 Oxidative stress is increased in the aged, diabetic heart

To further elucidate the potential mechanism that renders the aged, diabetic heart more susceptible to ischaemic injury, we used Western Blot analysis to determine the expression level of catalase, an antioxidant enzyme which can be transcriptionally regulated by PGC-1α [110].Catalase expression increased during the progression of diabetes, with the 8 and 12 month hearts expressing a higher level of catalase compared to the 3 month group ($p<0.005$). However, as the diabetic heart progressed into old age (18 months), the expression of catalase dramatically decreased to a significantly lower level than the 3 month group ($p<0.05$, Figure 3.25). Catalase catalyses the breakdown of H_2O_2 leading to less oxidative stress related molecules within the cell. Oxidative stress caused by an excessive accumulation of reactive oxygen or nitrogen species (RNS) are implicated in myocardial injury [495]. We found baseline levels of H_2O_2 and RNS were significantly increased in the 18 month diabetic heart compared to the 3, 8 and 12 month diabetic hearts (Figure 3.26). Interestingly, no significant differences were seen in catalase expression and ROS/RNS production in the ageing, non-diabetic heart (Figure 3.27, Figure 3.28).

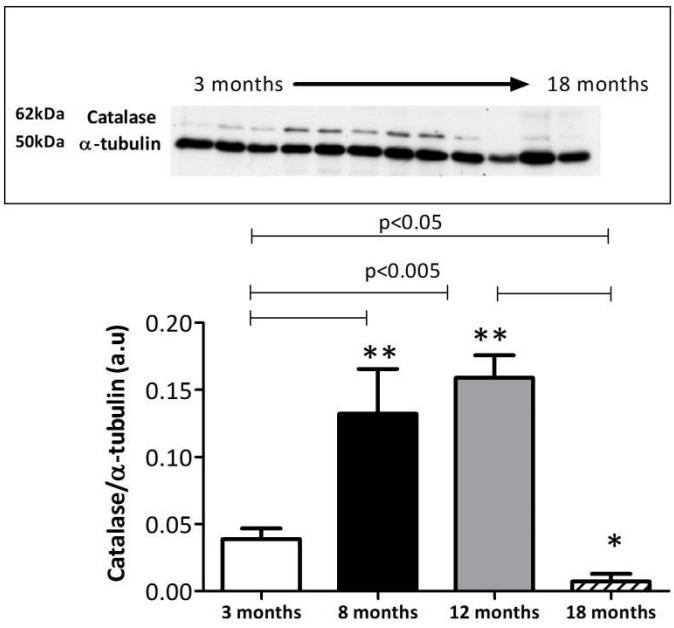

Figure 3.25: Catalase expression in the diabetic GK heart. Catalase expression decreases with age in the diabetic heart. Data is shown as mean ± S.E.M, n=3 per group. One way ANOVA and Tukey's post hoc analysis were used for statistical analysis between all groups

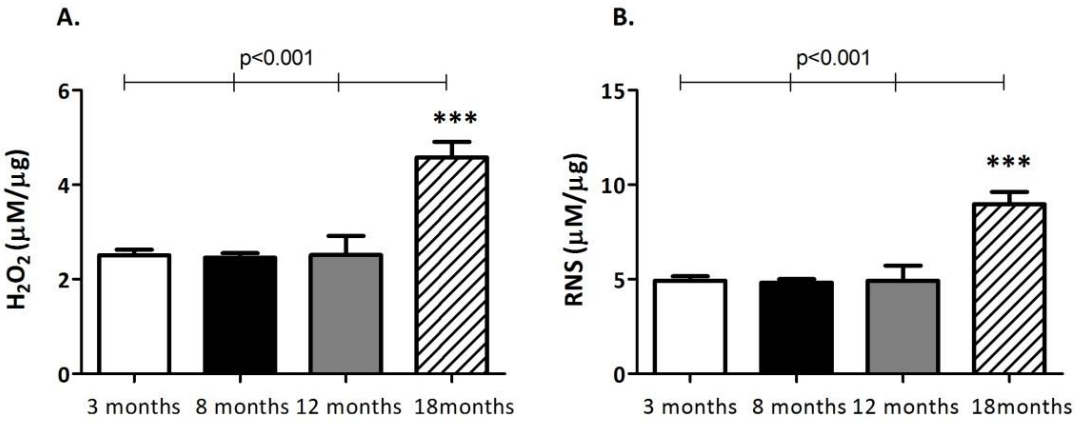

Figure 3.26: Oxidative stress levels in the ageing, diabetic heart. Basal assessment of total free radicals within the diabetic heart using OxiSelect OxiSelect ROS/RNS Assay Kit (Cell Bio Labs). A. Hydrogen peroxide (H2O2) and B. reactive nitrogen species (RNS) increase with age in the diabetic heart. Data is shown as mean ± S.E.M, n=4 per group. One way ANOVA and Tukey's post hoc analysis were used for statistical analysis between all groups.

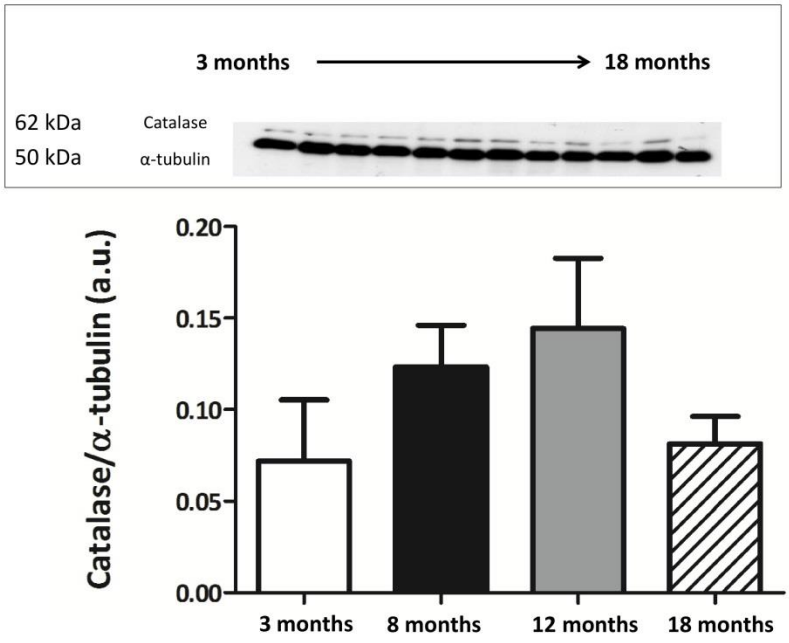

Figure 3.27: Catalase expression in the non-diabetic Wistar heart. There were no significant differences in baseline catalase expression in the ageing, non-diabetic heart. Data is shown as mean ± S.E.M, n=3 per group. One way ANOVA and Tukey's post hoc analysis were used for statistical analysis between all groups

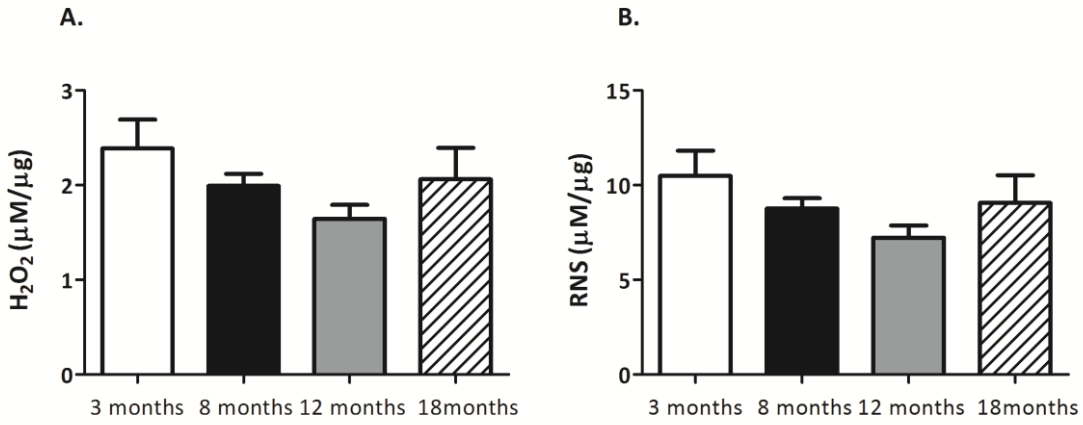

Figure 3.28: Oxidative stress levels in the ageing, non-diabetic heart. Basal assessment of total free radicals within the diabetic heart using OxiSelect OxiSelect ROS/RNS Assay Kit (Cell Bio Labs). There were no significant changes in A. Hydrogen peroxide (H2O2) or B. reactive nitrogen species (RNS) in respect to age in the non-diabetic heart. Data is shown as mean ± S.E.M, n=4 per group. One way ANOVA and Tukey's post hoc analysis were used for statistical analysis between all groups.

3.3.4.3 Mitochondrial changes with age and diabetes

The results thus far suggest impairment in basal Akt signalling in the aged, diabetic heart leading to decreased expression of PGC-1α. PGC-1α is a master regulator of mitochondrial biogenesis[39], therefore we sought to assess if these hearts had phenotypic changes in respect to mitochondrial organisation and appearance. In-depth visualisation using electron microscopy showed that the appearance and the organisation of mitochondria in the aged, diabetic heart are different when compared to the young pre-diabetic rat heart. The interfibrillar mitochondria (IFM) in the 3 month old, pre-diabetic heart and 3 month old, non-diabetic heart appeared organised and more elongated whereas in the aged, diabetic heart (18 months old) the mitochondria were unorganised and more spherical in shape. The IFM in the 18 month old Wistar heart appeared less organised than the younger age groups however, more organised than the old diabetic heart.

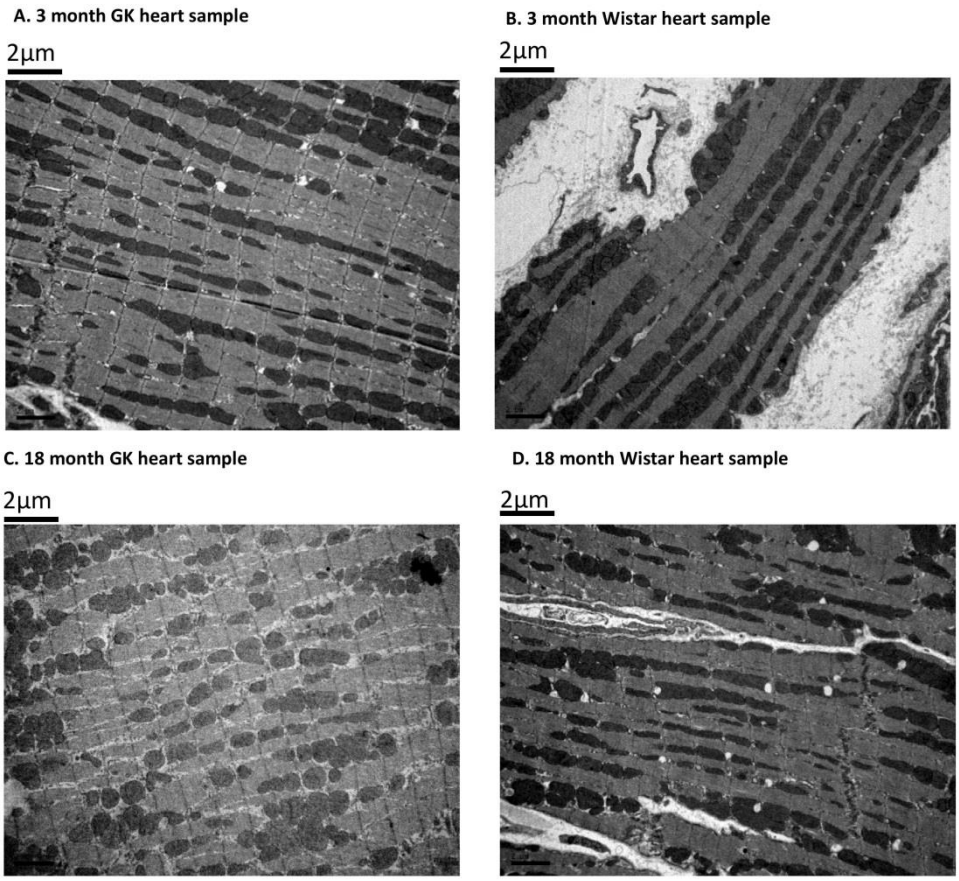

Figure 3.29: Mitochondrial appearance and organisation in the aged and diabetic heart. Mitochondrial organisation is compromised in the aged, diabetic heart. Basal samples demonstrating mitochondrial appearance and organisation within the diabetic heart using electron microscopy (EM). To analyse mitochondrial appearance the heart samples were coded and 2 ultrathin sections were prepared by a blinded operator. The sections were viewed with a Joel 1010 transition electron microscope (Joel Ltd, Warwickshire, UK.). Between 6 and 8 electron micrograph photos were taken of interfibrillar mitochondria (IFM) in each section. Representative pictures from A. 3 month GK heart, mitochondria appear elongated and organised along the interfibrillar bands of the cell B. 3 month Wistar heart C. 18 month GK heart; loss of mitochondrial organisation and more spherical shaped mitochondria D. 18 month Wistar heart.

3.3.4.4 IPC failed to increase the phosphorylation of Akt in the aged, diabetic heart

Lastly, baseline and IPC-induced Akt-P were assessed in young (3 months) and old (18 months) GK and Wistar hearts. Basal phosphorylation of Akt was significantly lower in young GK hearts compared to the old GK hearts ($p<0.05$). 3 cycles of IPC resulted in an increased phosphorylated state of Akt in the young hearts but no further change was observed in the older hearts (Figure 3.30). As expected in the young, non-diabetic hearts IPC elicited an increase in Akt-P. Interestingly, following the IPC stimulus in the aged, non-diabetic heart, a decrease in Akt-P was seen (Figure 3.31).

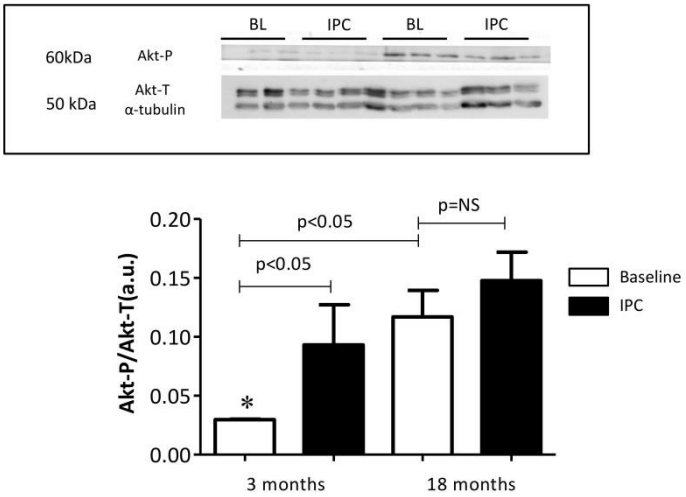

Figure 3.30: Phosphorylation of Akt following IPC in young and old diabetic rat hearts. Phosphorylation of Akt increases with age in the diabetic heart, with no further activation following IPC. Values determined by densitometry of Akt-phosphorylation (Akt-P) corrected to respective α-tubulin over the relative expression of Akt-total (Akt-T) corrected to respective α-tubulin. Data is shown as mean ± S.E.M, n=3 per group. One way ANOVA and Tukey's post hoc analysis were used for statistical analysis between all groups

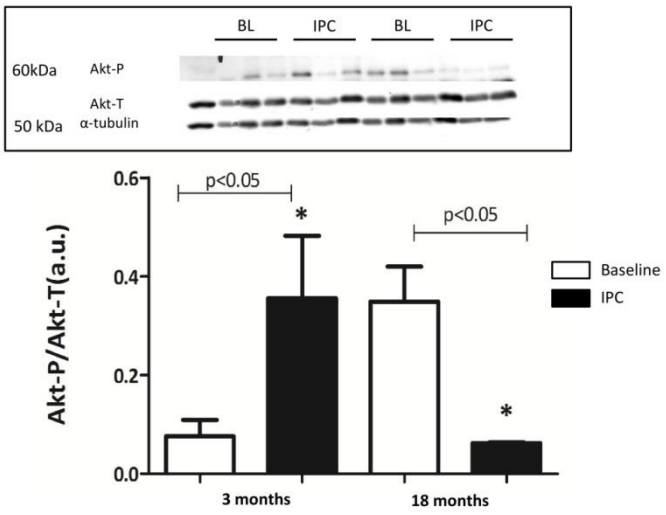

Figure 3.31: Phosphorylation of Akt following IPC in young and old non-diabetic rat hearts. Phosphorylation of Akt increases with age in the non-diabetic heart, however phosphorylation was decreased following IPC.. Values determined by densitometry of Akt-phosphorylation (Akt-P) corrected to respective α-tubulin over the relative expression of Akt-total (Akt-T) corrected to respective α-tubulin. Data is shown as mean ± S.E.M, n=3 per group. One way ANOVA and Tukey's post hoc analysis were used for statistical analysis between all groups.

3.3.5 Summary of Results

The data collected in this section suggests a chronic up regulation of Akt phosphorylation, and reduced expression of the mitochondrial regulator PGC-1α and of antioxidant enzymes such as catalase, potentially due to the Akt up regulation. Consequently the aged, diabetic heart exhibited less organised and more spherical than elongated mitochondria compared to the young, diabetic heart and enhanced level of oxidative stress. Moreover, IPC failed to activate Akt above the already raised baseline levels in the aged, diabetic heart.

3.4 Discussion

The key findings presented in this chapter are:

- The diabetic heart develops an increased susceptibility to shorter ischaemia at an earlier age than the non-diabetic heart.
- The extent of the injury induced by ischaemia-reperfusion increases with age in all hearts but this detrimental age related phenomenon seems to appear earlier in the diabetic heart.
- Three cycles of IPC previously shown to protect both the aged and the diabetic heart are ineffective in protecting the aged, diabetic heart.
- An impairment in Akt signalling, involving the chronic activation of Akt in the ageing, diabetic heart may contribute to these detrimental effects, possibly by affecting downstream targets such as PGC-1α and catalase levels and function. These alterations may induce an increase in oxidative stress and affect mitochondrial structure.

3.4.1 Relevance of study

Clinical data suggest that the diabetic heart is more susceptible to acute ischaemic damage [167], however, the animal data has been conflicting with experimental studies showing more [219, 223-225], equal [229, 230, 240, 241] or less [234, 235, 237-239] sensitivity to this injury [217, 218]. In the GK rat model, as in humans, diabetes develops in time, becoming further established with age [496], however there has been limited investigations of ischaemia reperfusion injury in this setting. In parallel with the clinical setting of diabetes, our data demonstrates that the older diabetic hearts were more susceptible to ischaemia: infarct size was increased in response to a shorter ischaemic insult in diabetic adult and aged hearts, and the older hearts developed larger infarcts compared to the non-diabetic

hearts. Furthermore, to our knowledge, this is the first study that has shown that an increased stimulus of ischaemic-preconditioning previously shown to protect the young diabetic and aged non-diabetic heart is unsuccessful in inducing a cardioprotective effect in a model exhibiting both old age and diabetes.

3.4.2 The activation of Akt in the myocardium – a double edged sword?

It is largely accepted that Akt activation by phosphorylation is strongly implicated in the cardioprotective response to IRI [497] and that this signalling cascade leads to inhibition of mPTP opening [238], reducing the apoptotic and necrotic effects of reperfusion. However, it is clear that the increase in baseline Akt-P we saw within the ageing, diabetic heart did not serve a cardioprotective role in this setting. It is worth considering that despite a crucial role for the acute activation of Akt by phosphorylation being implented in the survival of a stressed cell [134], it has been shown that a chronic increase in basal phosphorylation of Akt may have detrimental effects. One of these effects was described by Hunter et al who suggested that a chronic increase in Akt phosphorylation in aged, non-diabetic rats could induce hypertrophy [494]. In this investigation, the HW/BW % did not increase with age in the GK rat (Table 3.1, Figure 3.3). The GK rat exhibited an increased HW/BW% at all ages compared to the Wistar rat. Hypertrophy has been suggested to increase the susceptibility of the heart to IRI[498], however the ageing diabetic heart exhibits dissimilar responses to IPC and shortened ischaemia compared to the young diabetic heart. All age groups have similar HW/BW% suggesting that hypertrophy alone is not responsible for these differences in this setting.

In accordance with this study, Nagoshi et al, 2005 suggested a detrimental role for chronic activation of Akt[499]. Transgenic mice with cardiac-specific overactivation of Akt had little functional recovery and larger infarcts following IR compared to transgenic mice expressing cardiac specific dominant-negative Akt. Biochemical analysis demonstrated that chronic Akt activation induced feedback inhibition of PI3K through degradation and inhibition of the insulin receptor substrate (IRS)-1 and -2. Moreover, cardiac gene transfer of constitutively active PI3K restored the detrimental effects of chronic Akt activation in response to IR[499]. Shiojima et al also reported deleterious consequences of chronic overexpression of Akt in the heart. Using a tetracycline-regulated Akt-1 transgenic mouse model, they demonstrated that long term Akt activation caused severe cardiac dysfunction[500]. In contrast, modulation by exercise and IGF activation upstream of Akt led to chronic activation of this kinase but cardiac dysfunction did not occur[501, 502]. Taking these studies into consideration and also that type 2 diabetes is related to a decrease in insulin receptor signaling[444, 503], it is possible

to speculate that the chronic activation of Akt could be linked to decreased IRS signalling in the diabetic heart. The upstream cause of chronic Akt phosphorylation seen in this study was not investigated. However, it appears that impairment caused by insulin resistance [504] leads to detrimental outcomes, augmented in combination with old age.

It is worth considering that studies demonstrating chronic activation of Akt leading to detrimental outcomes utilize transgenic models, which may cause non physiological over activation of Akt. Therefore, the finding in this study that the aged, diabetic myocardium exhibits chronically activated Akt could provide a platform for examining the impact of physiological Akt overactivation on the myocardium and heart function.

3.4.3 Is there a link between chronic Akt activation, PGC-1α and antioxidant defence?

Profiling of gene expression in hearts from transgenic mice with cardiac-specific expression of activated Akt demonstrated an array of consequential alterations. Interestingly, in these hearts, amongst other changes, Akt mediated a downregulation of PPARα and PGC-1α expression[505]. PGC-1α is a transcriptional co-activator and a key regulator of energy metabolism and mitochondrial biogenesis [506] and also regulates ROS detoxification systems [110]. Efficient control of these systems plays a vital role in increasing the tolerance of the heart to IRI; regulatory proteins such as PGC-1α allow the mitochondria to maintain its energetics and to reduce oxidative stress when subjected to IRI [507]. Pathological hypertrophy, which appears evident in the ageing diabetic hearts in this study, has also previously been linked to decreased PPARα/PGC-1α expression[508]. As a master regulator of energy metabolism, a reduction in PGC-1α expression directs a shift from FAO to the less oxygen-consuming process, glycolysis to maintain ATP production[508]. Interestingly, physiological hypertrophy is associated with increased PPARα/PGC-1α[508], which could account for the increased heart weight noted in the ageing Wistar heart. Schiekofer et al, 2006 also demonstrated that Akt activation resulted in changes in gene transcription; using an inducible Akt transgenic mouse model they compared changes in gene expression following either acute (2 weeks) or chronic (6 weeks) activation. They found acute activation resulted in maintained cardiac function and reversible hypertrophy classified as ‘physiological’ hypertrophy whereas chronic expression of activated Akt replicated ‘pathological’ hypertrophy. Intriguingly, within this complex study using microarray analysis, SOD was also downregulated in response to chronically activated Akt[509].

Interestingly, fundamental studies by Duncan et al, 2011 suggest that alterations in PGC-1α activity in the setting of diabetes could have detrimental consequences leading to an increased susceptibility to cardiovascular disease [510]. Our results showed an age-related decrease in PGC-1α expression in diabetic hearts, with 18 month old GK rats expressing significantly less PGC-1α compared to their 3 month counterparts. Moreover, we saw a decreased functional capacity of the heart in the 18 month old GK rat, a possible consequence of decreased mitochondrial energetics in the heart driven by decreased PGC-1α expression. Interestingly, in the non-diabetic heart, Akt phosphorylation and PGC-1α expression appeared to decrease with age. However, significant reduction was seen only in the oldest age group corresponding with the infarction data whereby the 18 month Wistar heart had an increased susceptibility to infarction. This may suggest that changes occur at an accelerated rate in the diabetic heart compared to the non-diabetic heart, therefore rendering the heart more vulnerable to damage at an earlier age.

It has been demonstrated by other groups that Akt phosphorylation can reduce the activation of PGC-1α, directly by phosphorylating PGC-1α at Ser570[98] and indirectly by inactivation of FoxO1, a stimulator of the PGC-1α promoter[93]. Interestingly, Tonks et al demonstrated that Akt phosphorylation was impaired in insulin-resistant human muscle, and that hyperinsulinaemia inactivated FoxO1 preventing its transcriptional activity [504]. In addition, Akt has close regulatory links with other members of the FoxO family such as FoxO3, which phosphorylates and inactivates its transcriptional activity via promoting nuclear extrusion and accumulation in its inactive state in the cytosol in cardiomyocytes[145]. Olmos et al, 2009 showed that the transcriptional regulator Foxo3b and the co-activator PGC-1α interact directly to drive the expression of antioxidant genes such as catalase [511]. Therefore, chronic Akt activation could result in decreased FOXO3 mediated transcription of PGC-1α, supporting the subsequent down regulation of catalase we observed in the aged, diabetic heart. It is possible that the less organised, almost spherical interfibrillar mitochondria we saw in these hearts, is a consequence of decreased PGC-1α and catalase expression. This thesis provides no direct linking evidence for the transcriptional regulation of Akt on PGC-1α; attempts were made to immunoprecipitate out the PGC-1α protein from the aged diabetic heart to assess post translational modifications such as phosphorylation status; however this proved problematic and may have been caused by the use of frozen not fresh heart tissue.

A main process that contributes to the damage caused by IRI is the rapid production of reactive oxygen species (ROS) upon reperfusion of the myocardium [512].

The availability of endogenous antioxidants, such as catalase, to counterbalance this release of ROS, is crucial to reduce the myocardial damage [513]. Diabetes is accompanied by an increased production of intracellular ROS [193], and a compensatory increase in catalase [514]. However, it is suggested that the increase in the level of the antioxidant enzymes is likely to be insufficient to completely counteract ROS overproduction [514]. Interestingly, our results support this and suggest that in young diabetic hearts, where diabetes is not fully established the level of H_2O_2 and RNS are low, therefore low levels of catalase are required to counteract oxidative stress. However, it appears that as the diabetic ages into 8 and 12 months, oxidative stress remains low possibly by a concurrent increase in catalase expression. Interestingly, this antioxidant defence is lost with age, with a reduction in catalase expression and a subsequent increase in oxidative stress within the heart. These changes in regulation of oxidative stress production may possibly due to the down regulation of catalase via high Akt-P and low PGC-1α levels in the diabetic heart.

Interestingly, catalase expression and H_2O_2 and RNS levels did not significantly change in the ageing, non-diabetic heart. Therefore, the increased phosphorylation of Akt in the aged, non-diabetic heart may not be associated with changes in these downstream pathways in the non-diabetic heart. This suggests the aforementioned alterations in signalling may be a diabetes-associated phenomenon.

3.4.4 Is IPC possible in the aged, diabetic heart?

Having found that the diabetic heart is more susceptible to infarction we moved on to investigate if the endogenous cardioprotective potential is also affected by age in the diabetic heart. Previously it was demonstrated that the young, diabetic heart is still amenable to ischaemic preconditioning protection but the threshold is raised, therefore an increased stimulus is required[245]. Yellon and colleagues, 2005 found that this increased IPC stimulus was required to achieve an essential level of Akt phosphorylation necessary to mediate cardioprotection [238]. Similar to the studies examining cardioprotection in diabetes, conditioning the aged heart has also remained a controversial issue. Yellon and colleagues showed in 2001 that the Sprague-Dawley ageing heart required an increased IPC stimulus to elicit cardioprotection [401]. However, to our knowledge no investigations have combined the two comorbidities, age and diabetes. Therefore we investigated whether the aged, diabetic heart could be protected against lethal IRI by 3 cycles of IPC. Our data shows that IPC protection cannot be achieved in older diabetic animals. One could argue that an even higher IPC stimulus is required for protection to be elicited in these aged diabetic hearts. However, our data showed that the 18 month diabetic hearts undergoing 3 cycles of IPC

exhibited more damage following ischaemia than their respective control; therefore it is unlikely that an increased stimulus would be effective. In aged, non-diabetic hearts this protocol was successful in limiting IR damage, however to a lesser extent than the younger non-diabetic hearts. It seems that the initial increased threshold for cardioprotection observed in young diabetic hearts evolves with age towards the complete loss of this ability. We found that the basal level of phosphorylated – therefore activated, Akt was increased with age and no further increment was observed following a preconditioning protocol in aged diabetic hearts. Interestingly, a similar increase in phosphorylated-Akt, had been linked to the aged heart [515]. Kunuthur et al, 2012 demonstrated that young Akt2$^{-/-}$ mice exhibiting a diabetic phenotype were not amenable to protection by 1 cycle of IPC, however increasing the stimulus to 3 cycles restored protection. Interestingly, diabetic status determined by HbA1c levels in aged Akt2$^{-/-}$ mice was enhanced; however whether an increased stimulus of IPC would have an infarct limiting effect in these mice was not investigated. Furthermore, Akt1$^{-/-}$ mice were not amenable to protection by either stimulus suggesting a vital role for this isoform in IPC[516].

3.5 Conclusion

There are many possible mechanisms responsible for the loss of cardioprotection in the ageing [384], as well as in the diabetic myocardium [517]. From the network of intracellular signalling pathways which could affect the myocardial susceptibility to infarction this investigation was focussed on Akt which is a key regulator of survival in general and of myocardial preservation following ischaemia-reperfusion injury, in particular. In conclusion, this section of my thesis suggests increased susceptibility of the aged, diabetic rat heart to ischaemia-reperfusion injury and the inability of these hearts to be preconditioned against this insult. One of the major causes of these negative outcomes could be the chronically augmented phosphorylation of Akt in the aged, diabetic myocardium which may lead to detrimental downstream effects such as the down regulation of PGC-1α and catalase, leading to compromised defense against oxidative stress. Moreover, there is no biochemical reserve for sufficient additional Akt phosphorylation to be activated by preconditioning and hence this form of cardioprotection is lost. It is noticeable, based on this study, that old age and diabetes associate to impact on signalling pathways that mediate IPC (summarised in Figure 3.32). Further exploration of signalling deficits in the aged, diabetic heart using suitable animal models could prove crucial in successful translation of conditioning strategies into the clinical setting.

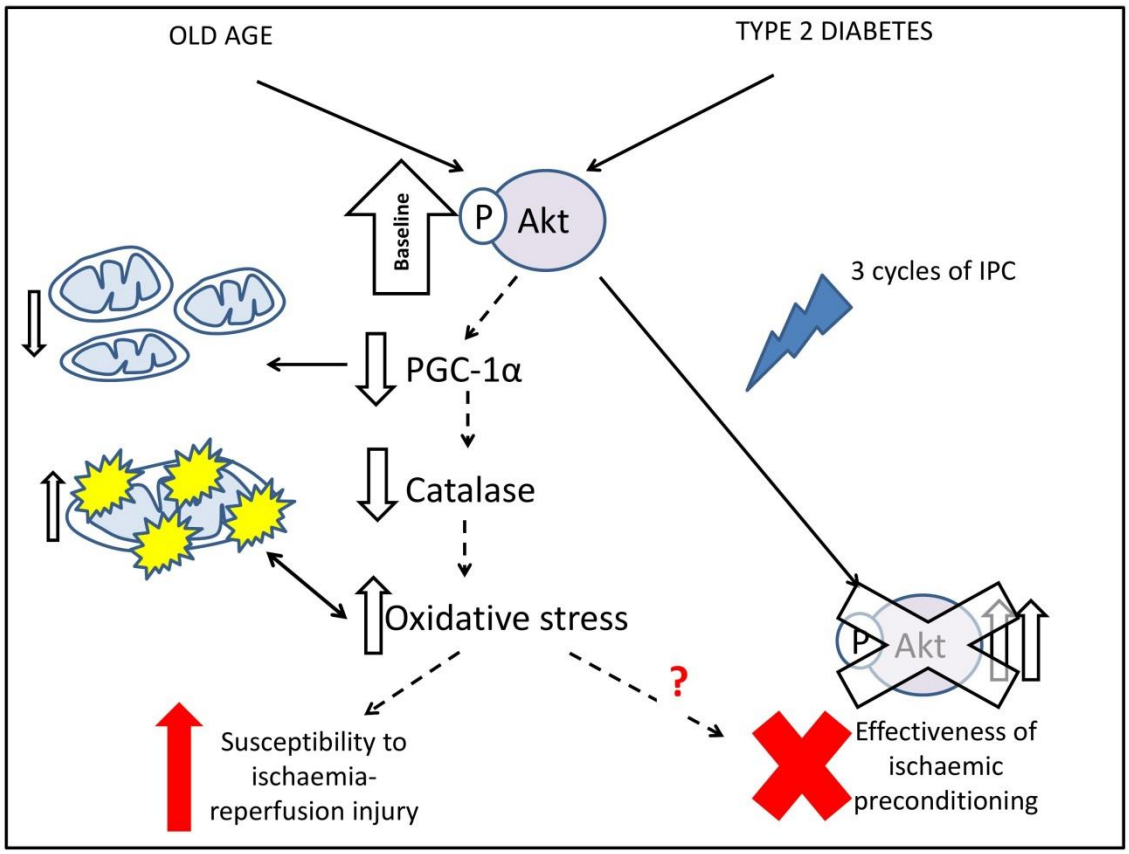

Figure 3.32: Possible consequences of the chronically activated RISK kinase Akt, in the aged, diabetic heart.

4. PHARMACOLOGICAL CARDIOPROTECTION AGAINST ISCHAEMIA-REPERFUSION INJURY IN AGEING AND DIABETES

Novel cardioprotective strategies are required in order to reduce the increased cardiovascular risk in diabetic patients. The hyperglycaemic profile and associated microvascular consequences of diabetes have been suggested to play an important role in increasing patient's susceptibility to infarction [518]. As mentioned, the heart can be conditioned by pharmacological agents; interestingly anti-diabetic drugs have been linked to improved cardiovascular outcomes and protection against ischaemia-reperfusion injury. Some may argue that sufficient glycaemic control by oral anti-diabetic agents have proved vital in reducing cardiovascular risk, however whether these agents have independent protective mechanisms distinct from their glucose-lowering properties is still unclear. From these anti-diabetic drugs with cardioprotective properties we were interested in the biguanide drug, metformin and the dipeptidylpeptidase-4 (DPP-4) inhibitor, sitagliptin.

This chapter is structured into 3 main sections and a final discussion:

1. The effect of chronic metformin treatment in 12 month old diabetic and non-diabetic rats on myocardial infarction in response to acute ischaemia-reperfusion injury and whether this treatment modulates prosurvival kinases.
2. The investigations regarding metformin's cardioprotective mechanisms when given chronically using a cardiac cell line and isolated cardiomyocytes.
3. The effect of chronic sitagliptin treatment in diabetic and non-diabetic rats on myocardial infarction in response to acute ischaemia-reperfusion injury.

4.1 The effect of chronic metformin treatment in aged, diabetic rats.

4.1.1 Background

Metformin, an oral anti-diabetic drug from the biguanide, insulin sensitizing class, has been suggested as potential cardioprotective agent [259] following the UKPDS (United Kingdom Prospective Diabetes Study) observation that there is a significantly lower incidence of cardiovascular events in patients receiving this drug[260]. Numerous mechanisms have been attributed to the successful glucose lowering effects of metformin including inhibition of complex I of the mitochondrial respiratory chain [261], decreasing hepatic glucose production [262], increasing glucose uptake [263] and stimulation of adenosine monophosphate-activated protein kinase (AMPK) [264]. However, experimental myocardial ischaemia-reperfusion injury performed in normoglycaemic animals following acute metformin administration resulted in smaller

infarct volumes without any change in blood glucose levels [265]. This suggested that the cardioprotective effect exerted by metformin could be independent of its hypoglycaemic actions.

Alongside its insulin-sensitizing effects [519], metformin has been shown to have direct beneficial control on cellular mechanisms by up regulating kinases such as Akt[281] and AMPK [264], implicated in cell survival and metabolism, respectively.

Akt is an important pro survival kinase and its role in cardioprotection has been discussed in detail in Chapter 1.4). In experimental models of ischaemia-reperfusion injury, acute administration of metformin phosphorylated and activated Akt leading to closure of the mitochondrial permeability transition pore (mPTP) and subsequent protection against myocardial infarction[281].

AMPK, a serine-threonine kinase that can sense and restore energy homeostasis when a cell becomes deprived of energy, is an important component in the pathway by which metformin produces its glucose lowering affects [264]. Alongside this action, recent investigations have also implicated this kinase cardioprotection [284]. For instance the AMPK activator, A-2769662, was shown to successfully reduce infarct size in both diabetic and non-diabetic isolated rat hearts [520].

Metformin pre-treatment reduced infarct size in both diabetic and non-diabetic animal models. This protection was associated with the activation of pro survival kinases including AMPK via phosphorylation [284] and components of the reperfusion injury salvage kinase (RISK) pathway such as the PI3K-Akt axis [281]. Metformin given during reperfusion following an ischaemic insult in a rat model of ischaemia reperfusion injury (IRI) can also reduce infarct size [284] indicating a potential use for this agent in setting of acute myocardial infarction.

In comparison, there has been little experimental work investigating ***chronic*** effects of metformin, a scenario that may be a better reflection of patients on metformin treatment in the clinic.

It is important to note that the mechanisms underlying cardioprotection following an acute treatment with an agent can be very different when the same agent is administered chronically. For example, it has been shown that acute treatment with atorvastatin for 1-3 days in rats decreased infarct size via Akt-PI3K activation, however when given chronically for a 2 week period the cardioprotective effect was lost [521]. This was attributed to a compensatory increase in PTEN levels, a negative regulatory of the

PI3K pathway [522]. These observations were confirmed with a different statin, lovastatin in a cell-based model [523]. This does not come as a surprise as chronic Akt activation can promote unwanted cellular and tissue growth, therefore negative feedback mechanisms will be up regulated. Therefore, we investigated possible downstream mechanisms of chronic metformin treatment, which may play a role in cardioprotection.

Metformin is a pleotropic drug that can control numerous factors involved in cellular survival; amongst them is Peroxisome Proliferator-Activated Receptor Gamma Coactivator-1α (PGC-1α) [524], a tissue-specific transcriptional co-activator which plays a key role in regulating energy metabolism [525]. PGC-1α is predominantly expressed in mitochondrial-rich tissues such as brown adipose tissue, skeletal muscle and the heart[525]. As PGC-1α plays a vital role in energy metabolism [525], it is suggested that this coactivator can interact with mitochondrial regulatory pathways [526] and possible with factors involved in mitochondrial dynamics such as mitofusin-2 (Mfn-2) [526].

Interestingly, the diabetic status has been associated with a reduced level of PGC-1α [203, 204], while metformin has been shown to increase the expression of PGC-1α in skeletal muscle possibly via AMPK activation [524]. Gundewar et al, 2009 showed that chronic low dose (125µg/kg) metformin administered after irreversible LAD ligation in mice, exerts beneficial effects on cardiac function and survival in this heart failure model via an increase in AMPK activation and an increase in PGC-1α expression [287]. However, there is limited information regarding these effects in the diabetic heart and their role in the protection against IRI. In addition to diabetes, age can also contribute to the IRI damage [527]. Interestingly, Reznick et al, 2007 compared AMPK activity in young (3 months) and old (28 months) rats and demonstrated an age-associated decrease in AMPK activation and mitochondrial biogenesis following AICAR treatment [528]. Age related changes in metabolism and mitochondrial biogenesis, suggest PGC-1α as a potential target for anti-ageing strategies [529, 530].

4.1.2 Hypothesis

We hypothesized that chronic metformin treatment could possibly activate AMPK and restore PGC-1α expression in diabetic hearts. Furthermore, this restoration of PGC-1α could lead to improved mitochondrial biogenesis in these hearts and hence could provide an enhanced capacity for the heart to be protected against an ischaemic insult. The aim of this chapter was to investigate in aged, rat hearts, whether chronic metformin treatment reduces myocardial infarct size through a mechanism independent of lowering blood glucose.

4.1.3 Experimental Protocols

4.1.3.1 Animals

Male Goto-Kakizaki (GK) rats (a mild, non-obese diabetic model [427] obtained from Taconic (Denmark), were bred in UCL facilities and kept in house until they reached 12 months of age; they received humane care in accordance with the United Kingdom Animal (Scientific Procedures) Act of 1986. Male Wistar rats (normoglycaemic) were obtained from Charles River UK Limited (Margate, UK) and kept in house until they also reached 12 months of age.

4.1.3.2 Treatments

Rats were singly housed and randomly assigned to receive either 300mg/kg/day metformin (Sigma, UK) sweetened with a non-caloric sweetener in drinking water, or sweetener alone in drinking water for 4 weeks. The metformin was sweetened to mask its metallic taste [531] otherwise animals tended to have a reduced water intake. A pilot study was performed on 6 animals, whereby the drinking rate was monitored for 7 days in order to estimate the water consumption. Throughout the treatment the drinking rate was monitored every 2 days and then the amount of powdered metformin was adjusted to ensure each rat received a dose of 300mg/kg/day. Biological parameters including body weight, HbA1c (A1C now+ test kit, Bayer, UK) and overnight fasting blood glucose (Accu-chek system, Roche) were collected prior, at 2 weeks and at 4 weeks after treatment

The animals were randomly selected for IRI followed by infarct measurements or for Western blot analysis and electron microscopy studies. There were 4 experimental groups: Wistar and Goto Kakizaki control groups which received only the sweetener in the drinking water and Wistar and Goto Kakizaki treated groups which received metformin added with the sweetener in the drinking water.

4.1.3.3 Ex vivo Langendorff isolated heart experiments

For determination of infarct size, GK and Wistar rats were anesthetized with sodium pentobarbital (55 mg/kg I.P.) and heparin (300 IU). The hearts were rapidly excised and quickly mounted onto a Langendorff constant pressure perfusion system (ADInstruments, Chalgrove, UK), hearts were subjected to the ischaemia-reperfusion protocol as presented in (Figure 4.1). Experiments were performed as described in the previous chapter, including the monitoring of cardiac function and assessment of infarct size using two-step staining comprising of Evan's blue and TTC.

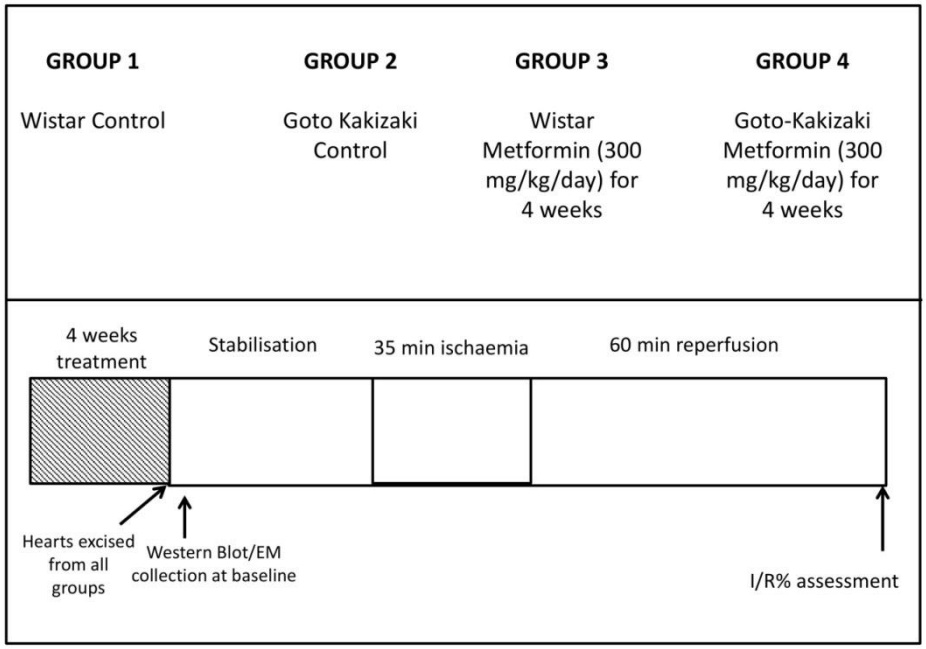

Figure 4.1: Experimental groups and Langendorff experimental protocol. Rats were randomly assigned into 4 treatment groups; Group 1 Wistar (non-diabetic) control and Group 2 Goto-Kakizaki (diabetic) control which received 4 weeks of water control artificially sweetened. Group 3 Wistar (non-diabetic) treated and Group 4 Goto-Kakizaki (diabetic) treated received 300mg/kg/day metformin in sweetened drinking water for 4 weeks.

4.1.3.4 Western Blot and electron microscopy sampling

For these investigations, three groups of animals, all 12 months of age, were used: group 1 (non-treated Wistar rats), group 2 (control GK rats receiving only the sweetener) and group 3 (treated GK rats which received metformin) (n=4 in each group). The animals were anesthetized with sodium pentobarbital (55 mg/kg I.P.) and heparin (300 IU). Hearts were harvested and perfused with Krebs buffer for 2 min to ensure the heart was cleared of blood. A small section of tissue from the left ventricle was collected in the electron microscopy fixative buffer and the remaining tissue was snap frozen in liquid nitrogen for Western blot analysis.

4.1.3.5 Electron microscopy

Electron microscopy (EM) visualisation of mitochondria was performed in diabetic metformin treated, diabetic non-treated hearts and non-diabetic non-treated hearts. The method is detailed in Chapter 2.8.

4.1.3.6 Western Blot Analysis of heart samples

Western Blot analysis was performed as described in the previous chapter; membranes were probed for phospho-α-AMPK (Thr 172), total α-AMPK, phospho-Akt (Ser 473), total Akt, PGC-1α and mitofusin-2 (Mfn-2). For detection of PGC-1α in different sub cellular compartments, nuclear and cytoplasmic extracts from GK and metformin treated GK rat hearts were prepared using a nuclear/cytosol fractionation kit (Qiagen-Qproteome nuclear protein kit) according to the manufacturer's instructions. Equal amounts of nuclear or cytoplasmic protein were subjected to western blotting of PGC-1α, and the fractions verified using nuclear TATA binding protein and cytosolic α-tubulin.

4.1.3.7 ATP assay

Heart samples collected for Western Blot analysis of protein expression were also used to investigate the basal levels of adenosine triphosphate (ATP) in hearts from groups 1-3. We sought to assess whether levels of ATP were affected in the diabetic versus non-diabetic heart and whether metformin had any effect on these levels. ATP is a fundamental player in many cellular processes including energetics, signalling and metabolism and its production can be regulated by AMPK. ATP concentration was determined using ATP-bioluminescent assay kit (FL-AA, Sigma, UK) and the protocol is described in details in general methods chapter 2.7.1.

4.1.3.8 Metformin treatment in HL-1 cell line

Next, we utilized a cardiac cell line HL-1 to further explore the relationship between chronic metformin treatment, AMPK and PGC-1α. We hypothesised that the metformin-dependent phosphorylation of AMPK was required for the metformin dependent effects on PGC-1α.

The HL-1 cardiac cell line (derived from murine atrial cardiomyocytes) which contracts and maintains the characteristics of the adult cardiomyocyte[532], were grown in Claycomb media supplemented with Noradrenaline, FBS, Penstrep and L-Glutamine. Cells were grown in T-25 flasks coated with Fibronectin and gelatin until confluent when they were split using 0.25% trypsin. For experiments, cells were plated at 200,000 per well.

Firstly, we wished to characterise the concentration of AMPK inhibitor, Compound C (Sigma, UK) required to abolish metformin induced phosphorylation of AMPK. Following 2 hours of plating, cells were incubated with fresh plating medium

containing: (1) Compound C only (0-40μM) (2) AICAR (AMPK activator, Millipore) + Compound C (0-40μM) and (3) Metformin + Compound C (0-40μM) for 16 hours, summarised in Figure 4.2 or Figure 4.3. Following treatment, HL-1 cells were collected by gently washing with warm PBS and removed from the plates by suspension in 100μl of Lamelli lysis buffer containing 5% β-mercaptoethanol by a cell scraping technique. Samples were then heated to 80-90°C for 10 minutes to ensure protein denaturation. Finally, samples were centrifuged at 8000 rpm for 5 minutes, and kept on ice. Samples were assessed for protein activation and expression using Western Blot analysis already described in this chapter.

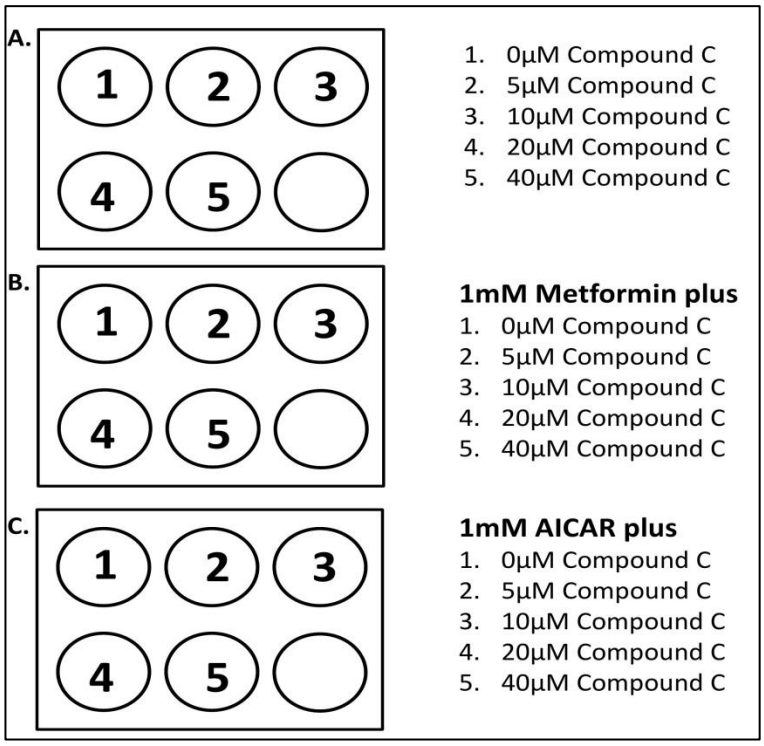

Figure 4.2: Treatment scheme for HL-1 cells. The HL-1 cells were plated at 200,000 per well. For experiments cells were incubated for 16 hours with A. Increasing concentrations of AMPK inhibitor Compound C. B. Metformin (1mM) in additions to increasing concentrations of Compound C. and C. AICAR (a known AMPK activator) in addition to increasing concentrations of Compound C.

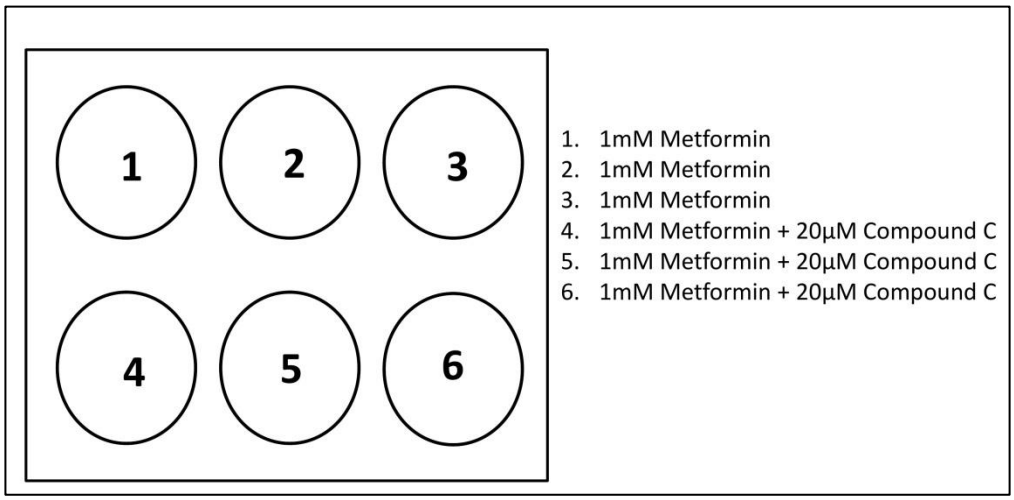

Figure 4.3: Treatment scheme for HL-1 cells. The HL-1 cells were incubated for 16 hours with (1-3) 1mM Metformin or (4-6) 1mM Metformin and 20µM AMPK inhibitor Compound C. Metformin treatment in aged, diabetic isolated cardiomyocytes

4.1.3.9 Metformin treatment in isolated cardiomyocytes

Adult ventricular cardiomyocytes were isolated from 12 month rat diabetic GK rat hearts as described in chapter 2.4.3. Isolated cardiomyocytes were resuspended in M199 medium with added penicillin (100 IU/ml), streptomycin (100 IU/ml), L-carnitine (2 mM), creatine (5 mM), taurine (5 mM) and BSA (2g/L) (Medium 199, Sigma, UK) and transferred onto laminin-coated 6 wells plates. Following 2 hours of plating, the media was gently removed leaving only attached, viable cardiomyocytes in the wells. For experiments 1ml of fresh media was added to each well containing: (1) No treatment (2) Compound C (20µM) (3) Compound C (40µM) (4) Metformin (1mM) (5) Metformin + Compound C (20µM) (6) Metformin (1mM) + Compound C (40µM) for 16 hours, summarised in Figure 4.4. Subsequently, cardiomyocytes were collected by gently washing with warm PBS and removed from the plates by suspension in 100µl of Lamelli lysis buffer containing 5% β-mercaptoethanol by a cell scraping technique. Samples were then heated to 80-90°C for 10 minutes to ensure protein denaturation. Finally, samples were centrifuged at 8000 rpm for 5 minutes, and kept on ice. Samples were assessed for protein activation and expression using Western Blot analysis already described.

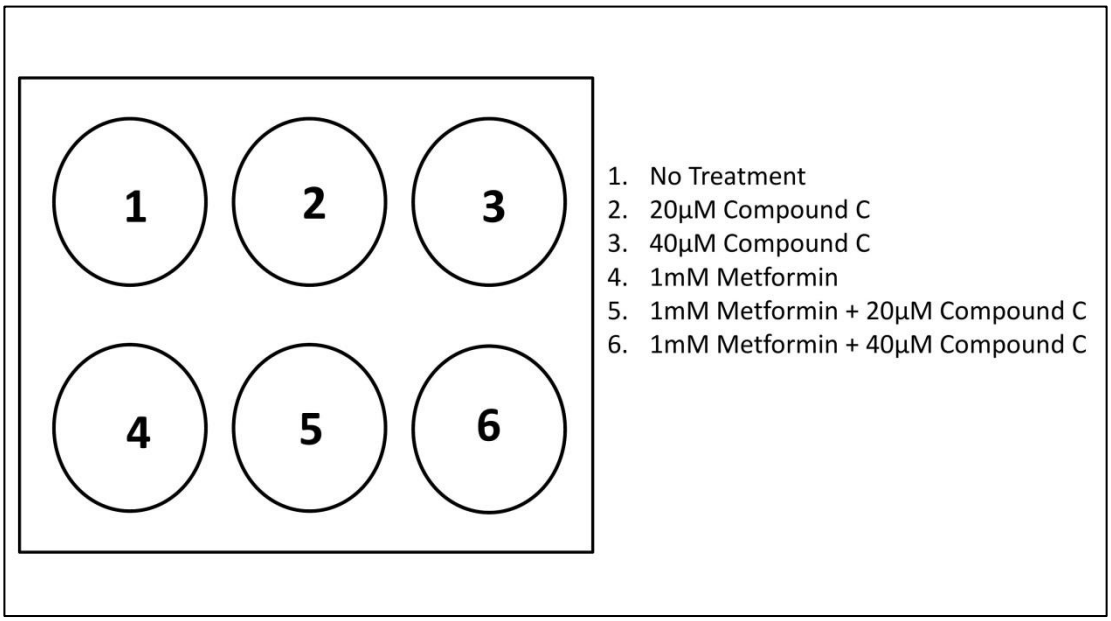

Figure 4.4: Treatment organisation for isolated cardiomyocytes. For experiments cardiomyocytes were incubated for 16 hours with 1) Media alone (no treatment) 2) 20µM AMPK inhibitor Compound C 3) 40µM AMPK inhibitor Compound C 4) 1mM Metformin 5) 1mM Metformin and 20µM AMPK inhibitor Compound C and 6) 1mM Metformin and 40µM AMPK inhibitor.

4.1.3.10 Statistical Analysis

Data were analysed by either one-way ANOVA followed by Bonferroni's multiple comparison test, students t-test or repeated measures ANOVA using GraphPad Prism 5.0 (GraphPad Software Inc, San Diego, California, USA). The choice of test is noted in the figure legend. A p-value <0.05 was considered to be statistically significant. Values are presented as means ± standard error mean (SEM).

4.1.4 Results

4.1.4.1 The effect of chronic metformin treatment on physiological parameters

Due to the insulin-sensitizing effects and hence blood glucose lowering potential of metformin, diabetic status was monitored throughout the 4 week study. Blood glucose and body mass were measured prior to the study, then at 2 weeks and at 4 weeks, whereas glycated haemoglobin (HbA1c) was measured prior to and at 4 weeks. Metformin reduced blood glucose and HbA1c by 33.4% and 23.8% ($p<0.005$), respectively following 4 weeks of treatment in GK rats, however, no change was seen in normoglycaemic Wistar rats (p=ns). As expected, as a side effect of metformin treatment, GK rats receiving the drug showed a 7.4% ($P<0.005$) decrease in body weight. No significant changes were recorded for any parameters in groups that

received sweetened water control. Data is summarised in Table 4.1 and Table 4.2. Mean plasma insulin levels were not assessed in this study, however in accordance with Portha et al, 1991, the glycaemic status we report is consistent with impaired insulin secretion and resistance previously reported in the GK model of type 2 diabetes [443].

	Goto Kakizaki - Control			Goto Kakizaki -Metformin		
Measurement	**Initial**	**2weeks**	**4weeks**	**Initial**	**2weeks**	**4weeks**
Body mass (g)	439.7 ± 8.2	436.4 ± 8.5	432.4 ± 7.9	461.4 ± 8.4	431.9 ± 6.7*	427.1 ± 7.1**
Heart mass (g)	-	-	2.77 ± 0.07	-	-	2.66 ± 0.08
Blood Glucose (mmol/L)	12.4 ± 0.8	10.5 ± 0.6	11.8 ± 0.9	15.5 ± 1.6	9.7 ± 0.4	10.3 ± 0.5**
HbA1c (mmol/mol)	67.6 ± 3.3	-	61.4 ± 3.7	58.2 ± 5.2	-	44.3 ± 3.4*

Table 4.1: Summary of metformin treatment in Goto-Kakizaki rats. Summary of parameters measured before, during and at the end of the treatment with either water +non-caloric sweetener or 300mg/kg/day metformin in water + non-caloric sweetener in 12 month diabetic GK rats. Body mass, blood glucose and HbA1c were measured initially, at 2 weeks and at 4 weeks prior to excision of the heart for experimentation. Heart mass was measured following isolated Langendorff heart preparation. Data is represented as mean ± S.E.M, n≥6. *P<0.05 versus initial reading within group. **P<0.005 versus initial reading within group. Repeated measures ANOVA was used to determine statistical significance.

	Wistar - Control			Wistar -Metformin		
Measurement	**Initial**	**2weeks**	**4weeks**	**Initial**	**2weeks**	**4weeks**
Body mass (g)	573.1 ± 14.1	550.3 ± 14.3	544.5 ± 13.9	553.6 ± 26.1	543.3 ± 23.7	549.1 ± 29.1
Heart mass (g)	-	-	1.85 ± 0.06	-	-	1.90 ± 0.08
Blood Glucose (mmol/L)	7.5 ± 0.2	7.0 ± 0.4	6.8 ± 0.9	7.6 ± 0.4	7.1 ± 0.3	7.5 ± 0.5
HbA1c (mmol/mol)	26.6 ± 0.6	-	25.7 ± 1.6	27.9 ± 1.2	-	24.3 ± 0.7

Table 4.2: Summary of metformin treatment in Goto-Kakizaki rats. Summary of parameters measured before, during and at the end of the treatment with either water +non-caloric sweetener or 300mg/kg/day metformin in water + non-caloric sweetener in 12 month non-diabetic Wistar rats. Body mass, blood glucose and HbA1c were measured initially, at 2 weeks and at 4 weeks prior to excision of the heart for experimentation. Heart mass was measured following isolated Langendorff heart preparation. Data is represented as mean ± S.E.M, n≥6.. Repeated measures ANOVA was used to determine statistical significance.

4.1.4.2 Chronic metformin treatment reduces infarct size in a glucose-independent manner

Oral metformin treatment given chronically for 4 weeks at 300mg/kg/day significantly reduced infarct size in both non-diabetic and diabetic rat hearts. In the diabetic group, infarct size was reduced by 65.4% compared to non-treated GK rats (I/R %; 16.6%± 2.0 *vs*. 47.8 ± 2.0, p<0.001,Figure 4.5). This reduction in infarct size was greater than the protection afforded by metformin in the non-diabetic group. In the normoglycaemic Wistar rat hearts, metformin reduced infarct size by 31.1% with no effect on blood glucose (I/R %; 40.8 ± 4.5 *vs*. 58.9 ± 3.5, P<0.005, Figure 4.5). However, one of the most interesting observations is the correlation between metformin's protection, blood glucose level and diabetic status. While metformin protects both diabetic and non-diabetic hearts, the degree of protection is higher in the diabetic heart in which metformin induces a significant decrease in blood glucose.

In this model metformin had no significant effect on any of the functional parameters monitored by the intra-ventricular balloon in either the non-diabetic or diabetic heart (Figure 4.6).

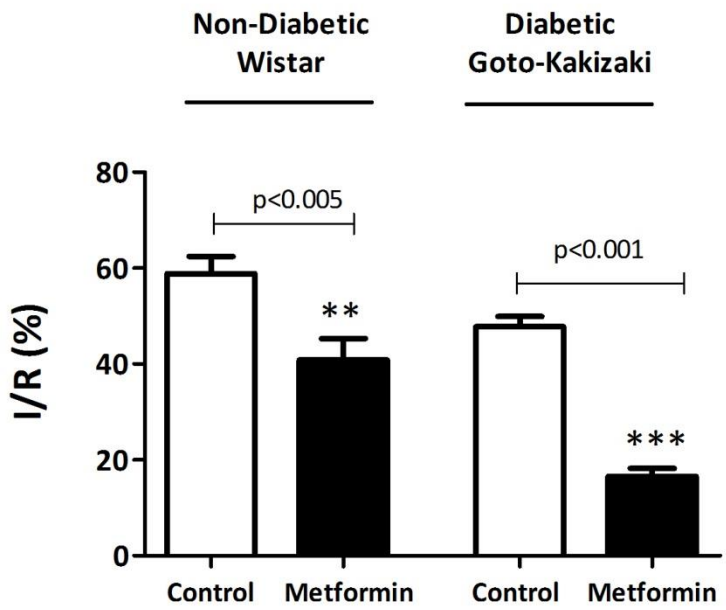

Figure 4.5: The effect of chronic metformin treatment on infarct size in the Wistar and GK rat. Infarct size is expressed as the infarcted volume within the area at risk of the left ventricle (% I/R) in hearts either treated with metformin for 4 weeks or control hearts. Chronic metformin significantly reduced the infarct size compared to the control group in both the non-diabetic and diabetic heart. Data is shown as mean ± S.E.M, n≥6. ** p<0.005, ***p<0.001 versus respective control. One way ANOVA followed by a Tukey Post-Hoc analysis were used for statistical analysis between groups.

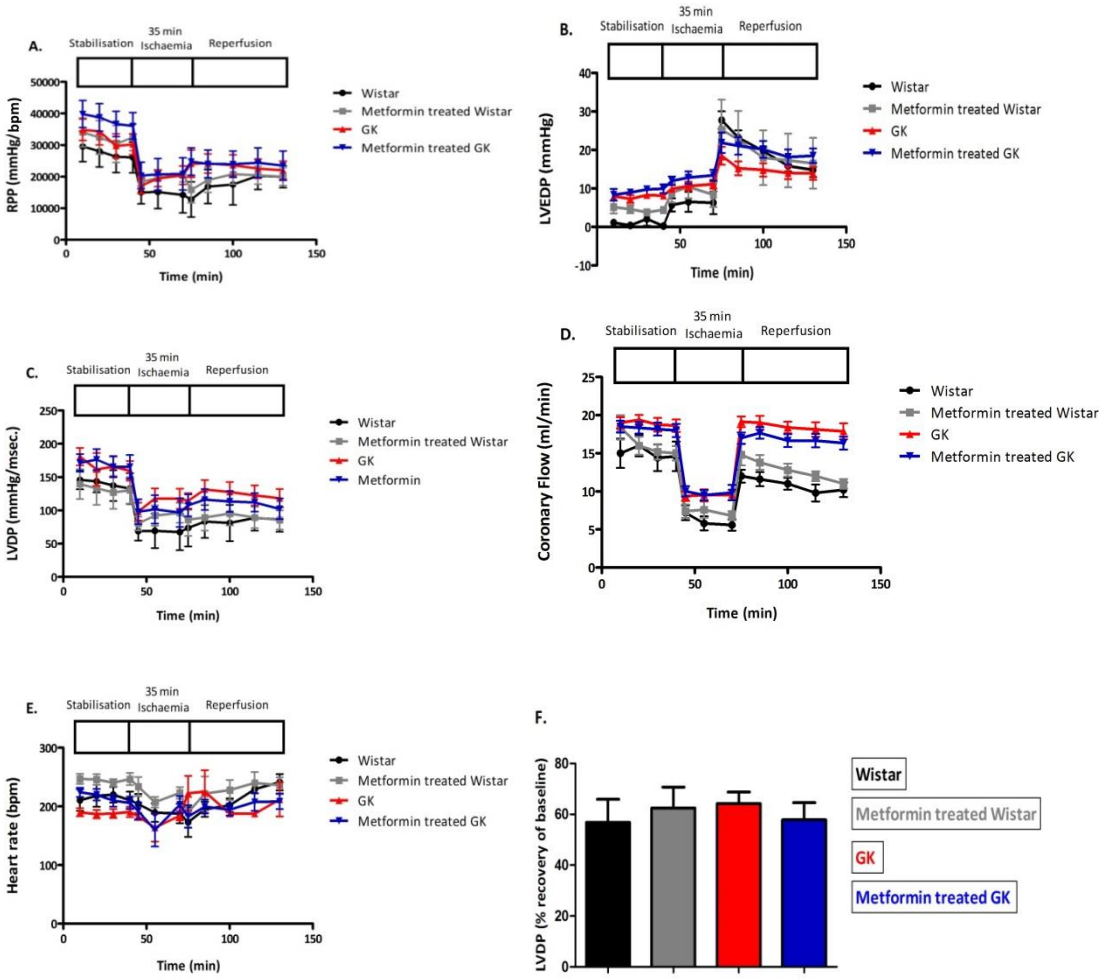

Figure 4.6: Cardiac function assessment following chronic metformin treatment in the Wistar (non-diabetic) and Goto-Kakizaki (GK, diabetic) heart. Function was monitored throughout the entire protocol. A. Rate Pressure Product (RPP) B. Left ventricular end diastolic pressure (LVEDP) C. Left ventricular developed pressure (LVDP) D. Coronary flow E. Heart Rate (HR) and F. % recovery of LVDP following 35 min ischaemia/60 min reperfusion. LVEDP. LVDP and HR were monitored via an inserted ventricular latex balloon, RPP was calculated as HR x LVDP as a measure of cardiac workload. Data is shown as mean ± S.E.M, n≥6. Comparison between groups at multiple time-points was analysed by two-way repeated measures (mixed model) ANOVA with a Bonferroni correction for multiple comparisons were used for statistical analysis between groups.

4.1.4.3 The effect of chronic metformin treatment on pro-survival kinases in the diabetic heart

To examine the potential mechanism that could be responsible for the cardioprotective effect of chronic metformin treatment in the diabetic heart, we assessed the expression and activation of pro-survival kinases Akt and AMPK. The reduction in infarct size was mirrored by a significant increase in the phosphorylation of AMPK at baseline (1.4±0.1 *vs* 0.9±0.1 *a.u.,* P<0.05, Figure 4.7) with no change noted in total AMPK protein levels. In contrast, phosphorylated Akt was unchanged following 4 weeks of metformin treatment (3.9 ± 0.4 *vs* 4.0 ± 0.2 *a.u. p= ns,* Figure 4.8).

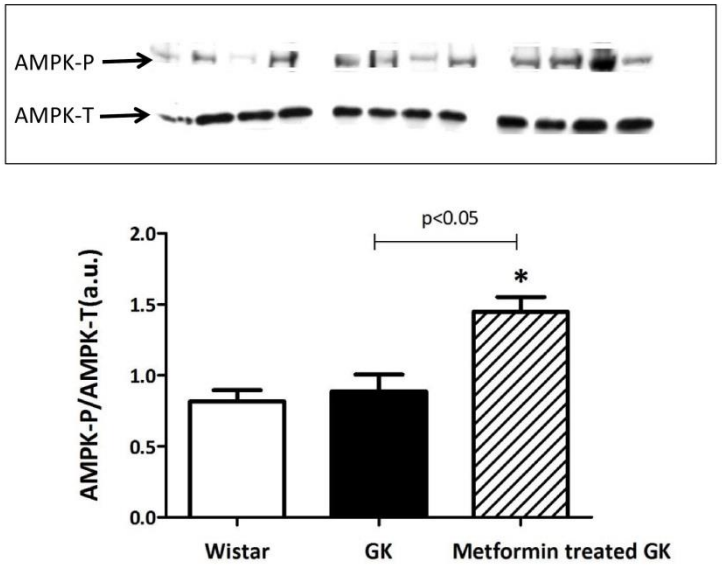

Figure 4.7: The effect of chronic metformin treatment on AMPK expression and phosphorylation. Metformin increases AMPK phosphorylation but has no effect on AMPK's total levels in Goto Kakizaki (GK) rat hearts. AMPK-P/T molecular weight 62 kDa. Data is shown as mean ± S.E.M, n=4 per group. *P<0.05 versus non-treated GK. One-way ANOVA followed by Bonferroni's multiple comparison test were used to determine statistical significance.

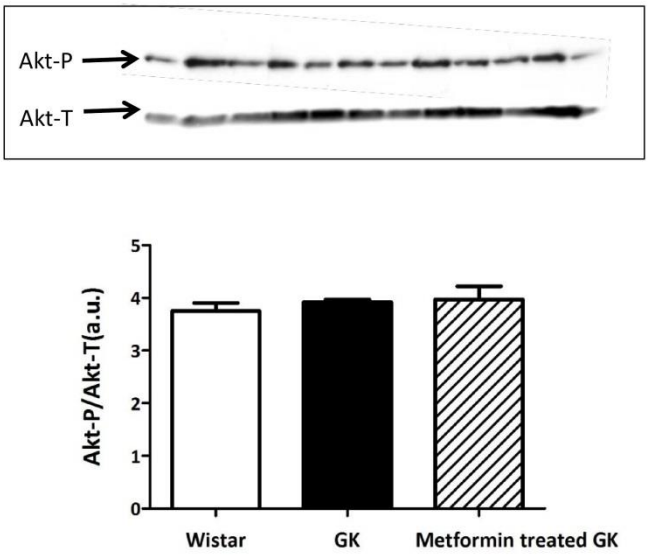

Figure 4.8: The effect of chronic metformin treatment on Akt expression and phosphorylation. Metformin has no effect on Akt expression or baseline activation in Goto Kakizaki (GK) rat hearts. Akt-P/T molecular weight is approximately 60 kDa. Data is shown as mean ± S.E.M, n=4 per group. One-way ANOVA followed by Bonferroni's multiple comparison test were used to determine statistical significance.

4.1.4.4 Mitochondrial regulators are enhanced following chronic metformin treatment in the diabetic heart

Recent advances in the literature suggest that AMPK can interact and modulate mitochondrial regulators such as PGC-1α. Following the confirmation that AMPK phosphorylation was enhanced subsequent to chronic metformin treatment in the diabetic heart, we assessed whether the expression of PGC-1α is also effected. Interestingly, previous studies showed that PGC-1α's expression was down regulated in type 2 diabetes [203, 204] and that metformin can increase the expression of PGC-1α in skeletal muscle [524]. In accordance with these previous findings, we observed a diabetes-associated down regulation of PGC-1α expression in the diabetic heart (0.38 ± 0.1 *vs* 0.54 ± 0.1, $p<0.001$, Figure 4.9) and a significant restoration of PGC-1α expression following metformin treatment (0.38 ± 0.1 *vs* 0.47 ±0.1, $p<0.05$, Figure 4.9).

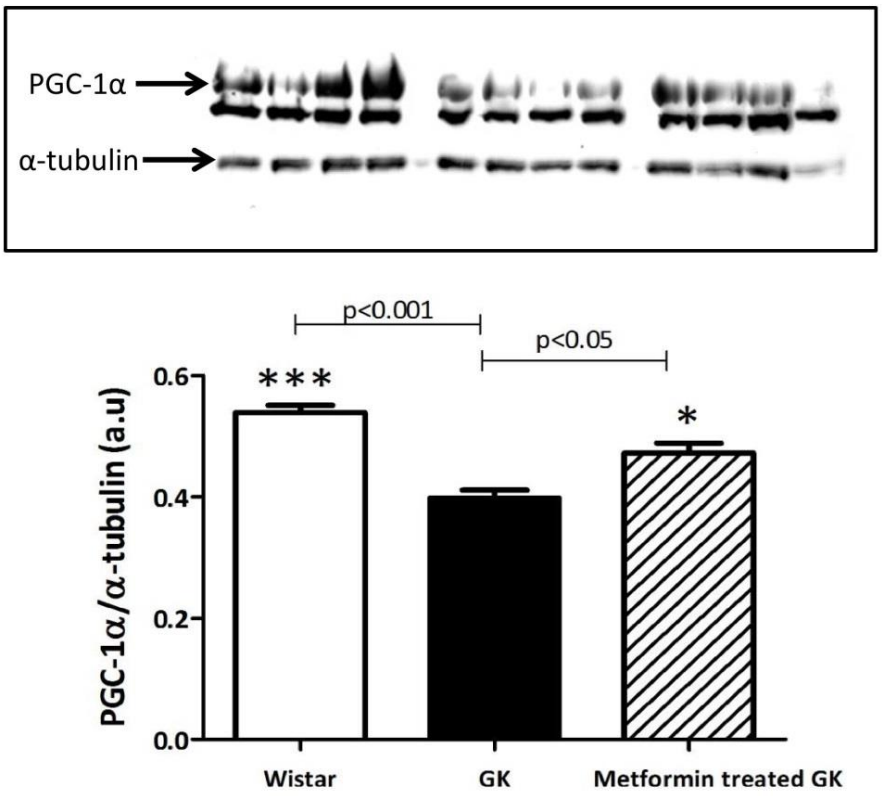

Figure 4.9: The effect of chronic metformin treatment on PGC-1α expression in the diabetic heart. A diabetes-related decrease in PGC-1α expression was observed in the GK rat heart. Chronic metformin treatments (4 weeks) enhanced PGC-1α expression in Goto Kakizaki (GK) rat hearts. PGC-1α molecular weight is approximately 92/112 kDa. Data is shown as mean ± S.E.M, n=4 per group. One-way ANOVA followed by Bonferroni's multiple comparison test were used to determine statistical significance.

As a regulator of mitochondrial biogenesis, changes in PGC-1α expression will impact on the structure, organisation and function of the mitochondria. Alongside its predominant role in mitochondrial energy metabolism, PGC-1α has also been shown to influence the morphology of mitochondria[39]; a subject that has attracted much interest in the setting of ischaemia reperfusion injury. We therefore assessed whether chronic metformin treatment effected the expression of the mitofusin protein Mfn-2 and used electron microscopy images to highlight any structural and organisational changes within the mitochondria. Diabetic status had no significant effect on the levels of Mfn-2 at baseline (2.6 ± 0.2, Wistar *vs* 2.3 ± 0.2, GK *a.u. p=ns*); however, metformin treatment significantly increased the expression of Mfn-2 in diabetic hearts to a level greater than that seen in the normoglycaemic Wistar hearts (2.6 ± 0.2 vs 3.3±0.1 *a.u.,* p<0.005, Figure 4.10). Mfn-2 promotes fusion of mitochondria, thereby creating an inter connecting network of highly functional organelles. Electron microscopy images demonstrate that mitochondria in the untreated hyperglycaemic GK hearts appeared unorganised and more spherical in shape. Interestingly, following metformin treatment,

the mitochondria seem more organised and elongated, resembling those in the Wistar normoglycaemic heart (Figure 4.11).

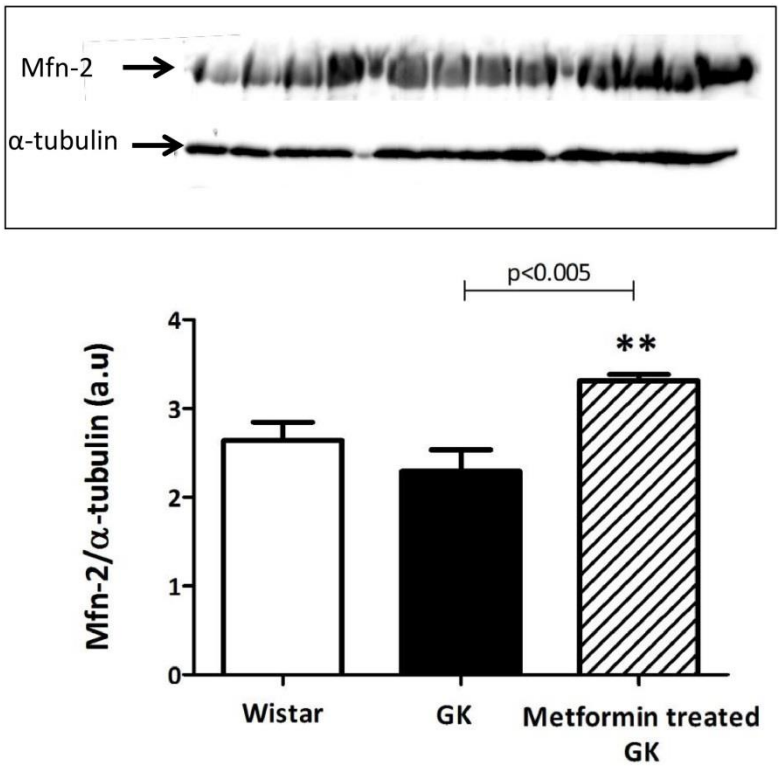

Figure 4.10: The effect of chronic metformin treatment on Mfn-2 expression in the diabetic heart. Chronic metformin treatments (4 weeks) enhanced Mfn-2 expression in Goto Kakizaki (GK) rat hearts. No significant difference was seen in Mfn-2 expression between the non-diabetic and diabetic heart. Mfn-2 molecular weight 82 kDa. Data is shown as mean ± S.E.M, n=4 per group. One-way ANOVA followed by Bonferroni's multiple comparison test were used to determine statistical significance.

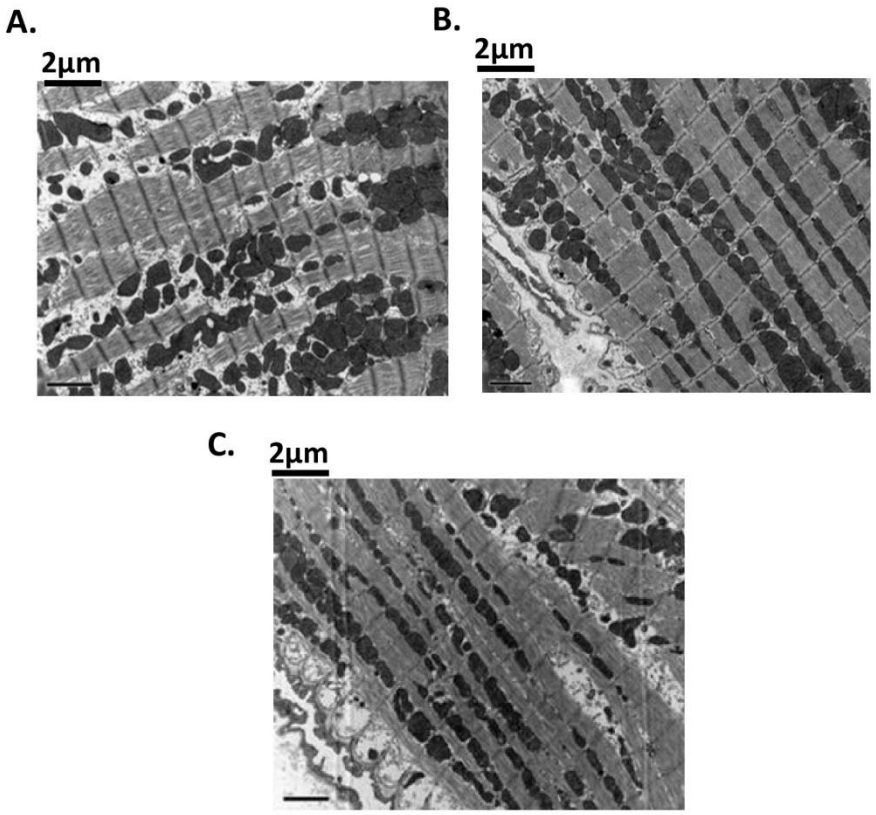

Figure 4.11: The effect of metformin treatment on mitochondrial appearance in the diabetic heart. Chronic metformin treatment correlates with changes in mitochondrial appearance in the diabetic heart. A. Non treated 12 month old Goto-Kakizaki diabetic heart. B. Metformin treated (4 weeks 300mg/kg/day) Goto-Kakizaki diabetic heart. C.. 12 month old Wistar normoglycaemic heart. (Representative electron micrograph photos).

PGC-1α is a dynamic molecule that is known to migrate between different subcellular compartments of the cell to exert different effects [100]; therefore we sought to investigate if metformin treatment had an impact on this process. Following subcellular fractionation we found that the nuclear PGC-1α expression decreased following metformin treatment compared to untreated GK hearts. Surprisingly, the cytosolic fraction showed no difference in PGC-1α expression. Moreover, the cytosolic fractions appear as a single band compared to the double band seen in the total cell extract and in the nuclear fraction (Figure 4.12).

ATP is produced via numerous mechanisms including glycolysis and mitochondrial fatty acid oxidation in the heart, depending on the availability of substrates and the oxygen supply. As the energy powerhouses of the cell, functional mitochondria are essential for efficient energy production. PGC-1α can influence the shift between metabolic pathways that provide ATP; therefore we sought to assess the level of ATP in the diabetic and non-diabetic heart, and whether chronic metformin

treatment had any influence on ATP levels in diabetic hearts. Intriguingly, we found that basal ATP levels in the 12 month GK heart were significantly higher than levels found in the 12 month Wistar heart. Moreover, chronic metformin treatment diminished the elevated levels of ATP in the diabetic heart (Figure 4.13).

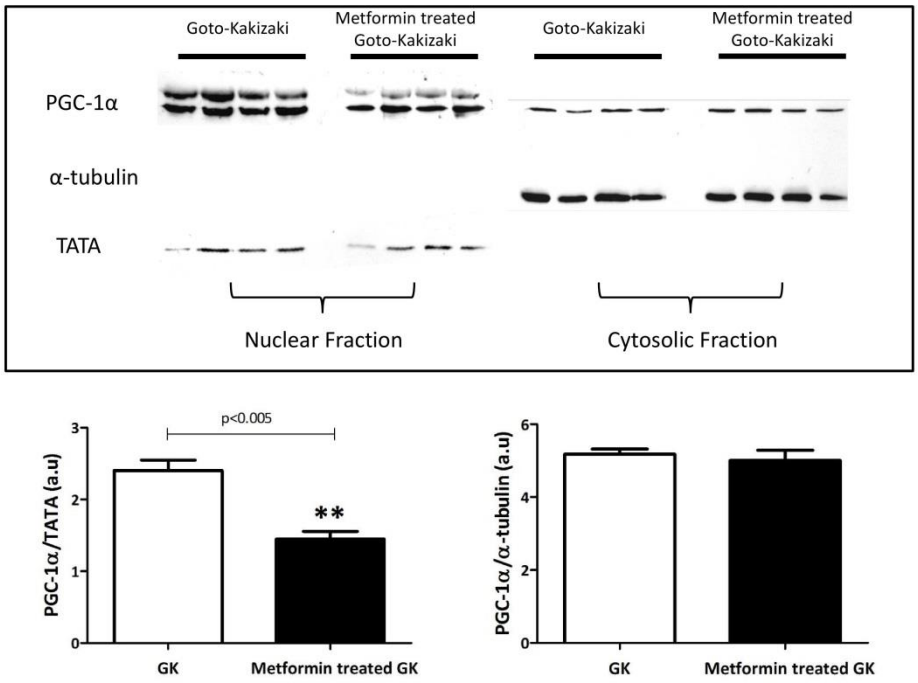

Figure 4.12: The effect of metformin treatment on the subcellular localisation of PGC-1α. Chronic metformin treatment leads to decreased nuclear accumulation of PGC-1α. Following metformin treatment, PGC-1α expression in the nuclear fragment decreased compared to that of the non-treated Goto-Kakizaki. Data is shown as mean ± S.E.M, n=4 per group, **p<0.005. PGC-1α expression is calculated by measuring both bands in the nuclear fraction and single band in the cytosolic fraction and corrected to an appropriate loading control. Student's t-test was used for statistical analysis.

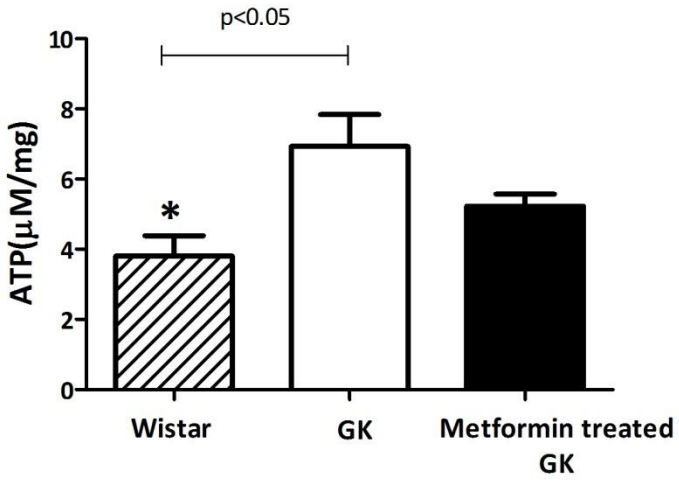

Figure 4.13: The effect of chronic metformin treatment on basal ATP levels in the diabetic Goto-Kakizaki (GK) rat heart. Basal ATP levels were significantly higher in the diabetic GK heart compared to the non-diabetic Wistar heart, metformin treatment (4 weeks) reduced the basal increase in ATP production. Data is shown as mean ± S.E.M, n=4 per group. One-way ANOVA followed by Bonferroni's multiple comparison test were used to determine statistical significance.

4.1.4.5 The up regulation of PGC-1α expression following chronic metformin treatment may require AMPK phosphorylation

To further elucidate the mechanism by which metformin restores the expression levels of PGC-1α, HL-1 cells were treated with metformin and a known activator of AMPK, AICAR, in the presence of increasing concentrations of the AMPK inhibitor Compound C. Activation of AMPK and ACC by phosphorylation was assessed using Western Blot analysis. Metformin increased the phosphorylation of both AMPK and ACC; in metformin treated cells, this increase was inhibited by 20µM and 40µM compound C however in AICAR treated cells levels were undetectable (Figure 4.14 and Figure 4.15).

Following these findings, HL-1 cells were treated with metformin in the presence and absence of 20µM Compound C, subsequently AMPK-P, PGC-1α and Mfn-2 expression were assessed. Analysis showed 20µM Compound C significantly reduced AMPK-P (Figure 4.16); furthermore metformin associated increase in expression of PGC-1α was prevented in presence of the inhibitor compound (Figure 4.17). This concentration of Compound C did not significantly prevent the metformin-associated increase in Mfn-2 expression (Figure 4.18).

Next, we assessed protein expression and activation following metformin treatment in the presence and absence of 20µM or 40µM Compound C in 12month,

diabetic GK isolated cardiomyocytes (Figure 4.19). In the previous study 20 µM Compound C did not alter the Mfn-2 levels; we hypothesised that a higher concentration of the inhibitor may be required to elicit a significant effect therefore in these studies we also used 40µM Compound C. We found metformin increased AMPK-P and both concentrations of Compound C inhibited this increase (Figure 4.20). PGC-1α expression was also increased following metformin treatment, 20 µM of Compound C decreased PGC-1α expression but this reduction did not reach significance. 40µM of Compound C significantly prevented the metformin associated increase in PGC-1α expression, however, Compound C alone also decreased PGC-1α expression at this concentration (Figure 4.21). Mfn-2 expression was not significantly affected by metformin and/or AMPK-P inhibition; however a similar trend was seen (Figure 4.22).

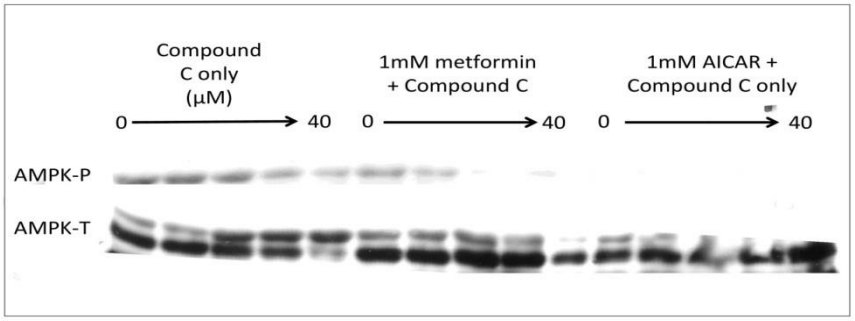

Figure 4.14: Characterisation of the effectiveness of Compound C in blocking the action of metformin on AMPK activation in HL-1 cells. HL-1 cells were treated with either increasing concentrations of Compound C only (µM: 0,5,10,20,40), treated with 1mM Metformin in the presence of Compound C or treated with 1mM AICAR + Compound C for 16 hours before protein assessment using Western Blot. Total levels of AMPK and phosphorylation at Thr172 were assessed.

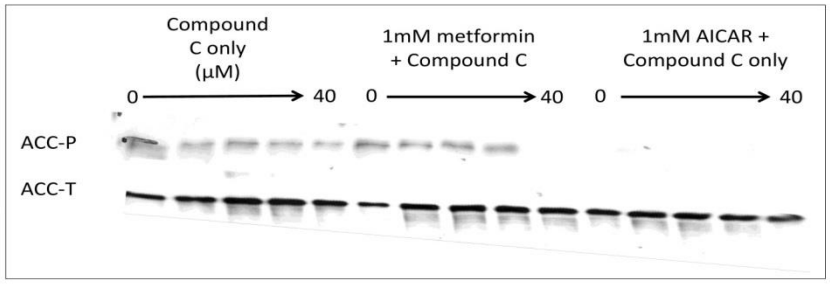

Figure 4.15: Characterisation of the effectiveness of Compound C in blocking the action of metformin on ACC activation in HL-1 cells. HL-1 cells were treated with either increasing concentrations of Compound C only (µM: 0,5,10,20,40), treated with 1mM Metformin in the presence of Compound C or treated with 1mM AICAR + Compound C for 16 hours before protein assessment using Western Blot. Total levels of ACC and phosphorylation were assessed.

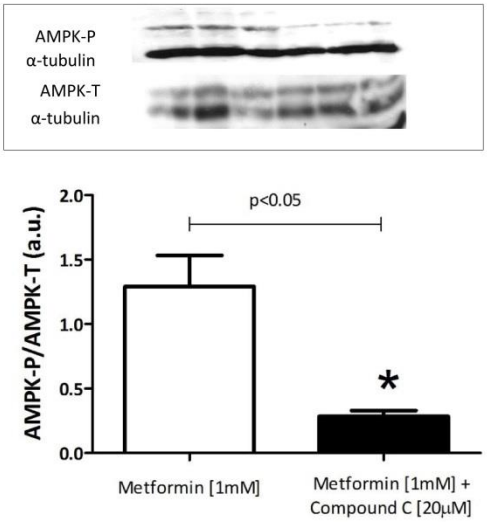

Figure 4.16: AMPK activation following 16 hours metformin treatment in HL-1 cells.: HL-1 cells were treated for 16 hours with 1mM metformin in the presence or absence of 20μM Compound C. AMPK phosphorylation was assessed using Western Blot analysis, n=3 per group, student's t test was used to determine statistical significance.

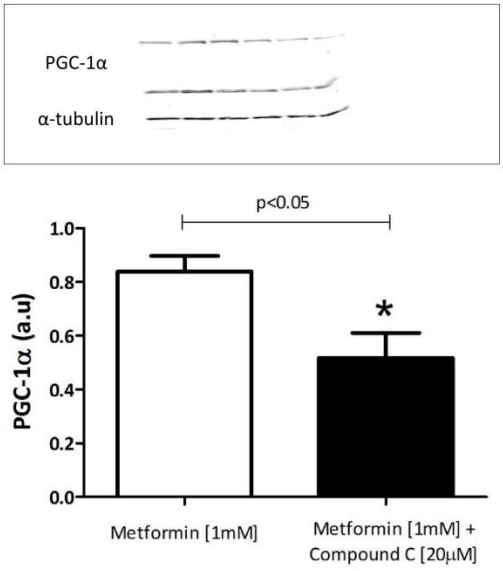

Figure 4.17: PGC-1α expression following 16 hours metformin treatment in HL-1 cells. HL-1 cells were treated for 16 hours with 1mM metformin in the presence or absence of 20μM Compound C. PGC-1α expression was assessed using Western Blot analysis, n=3 per group, student's t test was used to determine statistical significance.

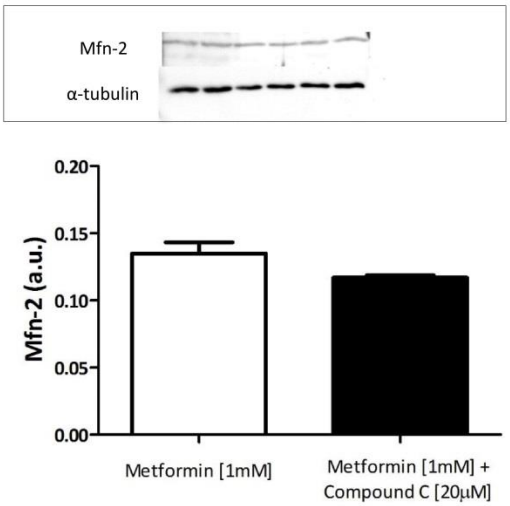

Figure 4.18: Mfn-2 expression following 16 hours metformin treatment in HL-1 cells. HL-1 cells were treated for 16 hours with 1mM metformin in the presence or absence of 20μM Compound C. Mfn-2 expression was assessed using Western Blot analysis, n=3 per group, student's t test was used to determine statistical significance.

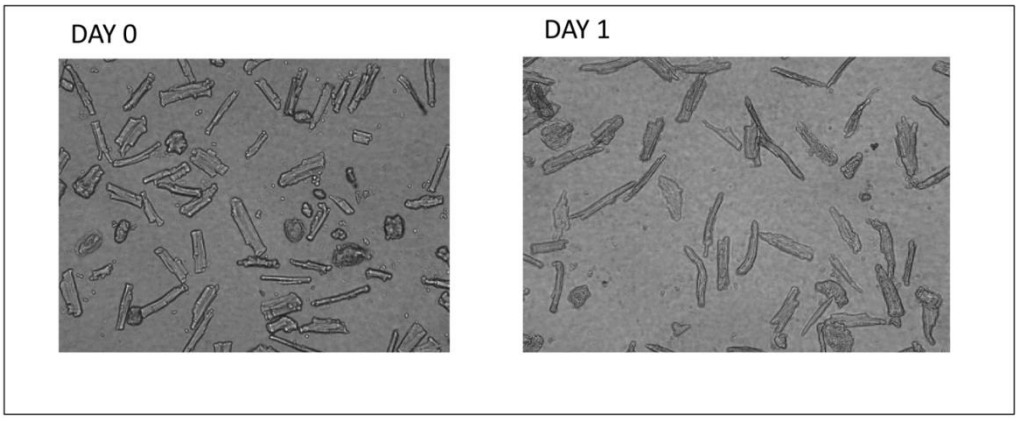

Figure 4.19: Plating of isolated cardiomyocytes. Representative pictures of isolated cardiomyocytes from 12 month GK rat hearts. Cardiomyocytes were isolated and plated for 2 hours (Day 0) and 24 hours (Day 1).

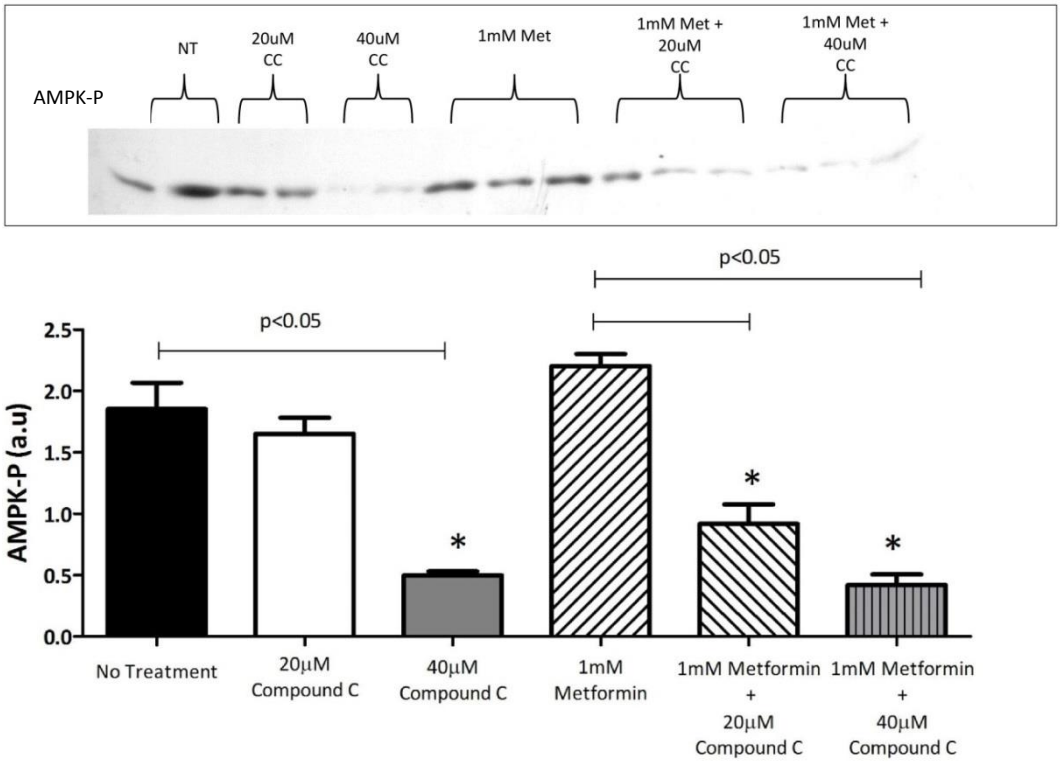

Figure 4.20: AMPK activation following 16 hours metformin treatment in isolated cardiomyocytes from the 12 month diabetic GK hearts. Following isolation, cells were treated for 16 hours with 1) no treatment 2) 20µM Compound C (CC) only 3) 40µM Compound C (CC) 4) 1mM metformin 5) 1mM metformin + 20µM Compound C 6) 1mM metformin + 40µM Compound C . AMPK phosphorylation was assessed using Western Blot analysis, n=3 per group, One-way ANOVA followed by Bonferroni's multiple comparison test was used to determine statistical significance.

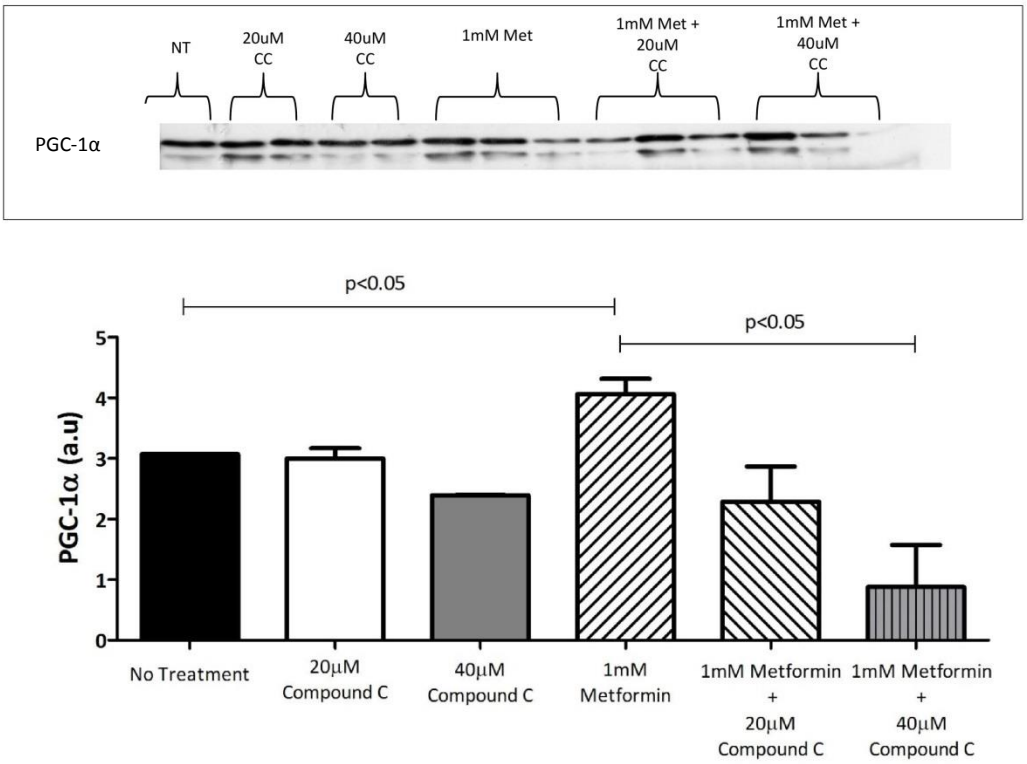

Figure 4.21: PGC-1α expression following 16 hours metformin treatment in isolated cardiomyocytes from the 12 month diabetic GK hearts. Following isolation, cells were treated for 16 hours with 1) no treatment 2) 20μM Compound C (CC) only 3) 40μM Compound C (CC) 4) 1mM metformin 5) 1mM metformin + 20μM Compound C 6) 1mM metformin + 40μM Compound C . AMPK phosphorylation was assessed using Western Blot analysis, n=3 per group, One-way ANOVA followed by Bonferroni's multiple comparison test was used to determine statistical significance.

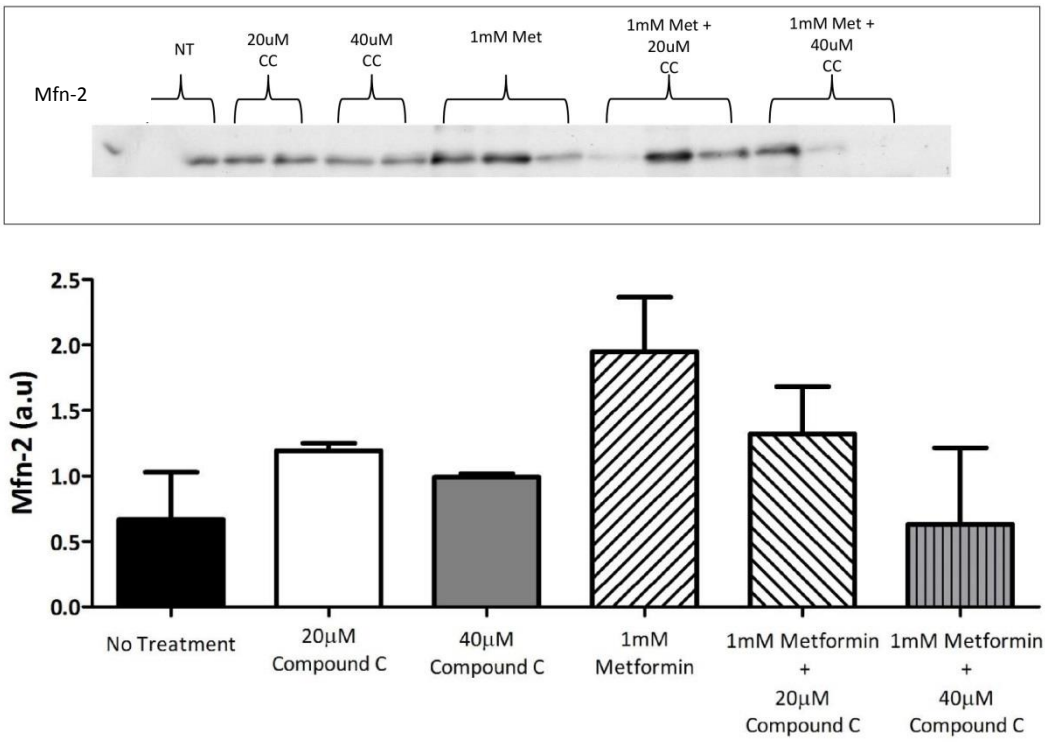

Figure 4.22: Assessment of Mfn-2 expression following 16 hours metformin treatment in isolated 12 month diabetic GK cardiomyocytes. Following isolation, cells were treated for 16 hours with 1) no treatment 2) 20μM Compound C (CC) only 3) 40μM Compound C (CC) 4) 1mM metformin 5) 1mM metformin + 20μM Compound C 6) 1mM metformin + 40μM Compound C . Mfn-2 expression was assessed using Western Blot analysis, n=3 per group, One-way ANOVA followed by Bonferroni's multiple comparison test was used to determine statistical significance.

4.1.5 Summary and Discussion

The key findings presented in this section of the chapter are:

- Chronic metformin treatment lowered blood glucose only in the GK rats but elicits a cardioprotective effect against ischaemia-reperfusion injury in both the diabetic and non-diabetic ageing heart.
- Intriguingly, this protection is more effective in the diabetic heart.
- The ageing diabetic heart has a decreased expression of PGC-1α compared to the non-diabetic heart.
- Chronic metformin treatment is associated with an increased level of phosphorylated AMPK and increased expression of PGC-1α and Mfn-2.

4.1.5.1 Chronic Metformin treatment protects the diabetic and non-diabetic heart against ischaemia-reperfusion injury

Type 2 diabetic patients taking metformin have a reduced incidence of cardiovascular events[260], moreover, experimentally this agent is proven to be cardioprotective in

different animal models of ischaemia-reperfusion injury. Patients presenting with type 2 diabetes are often middle to old aged, however the majority of experimental information collected have used young, diabetic or non-diabetic animal models. Therefore using a model which corroborates 2 co-morbidities (diabetes and age) will provide insightful information regarding metformin-related cardioprotection.

The majority of experimental studies have been performed in an acute setting, either administrating metformin for a short period before an ischaemic insult [284] or following ischaemia [281] in a postconditioning fashion. However, if a long term treatment can potentially lower the incidence of cardiovascular events, prevention is often preferable to cure. Therefore experimental investigations assessing whether long term treatment with metformin proves beneficial is essential and may aid interpretation of clinical outcome studies.

The data presented in this section demonstrated that chronic metformin treatment reduced infarct size in both aged diabetic and non-diabetic rat hearts, albeit to a lesser extent in the latter group. The fact that metformin could reduce infarct size in the non-diabetic group led us to question whether cardioprotection elicited by metformin in the diabetic heart is entirely based on a simple reduction of hyperglycaemia. Interestingly, in this model, metformin did not appear to have a significant effect on cardiac function; however the intra-ventricular balloon used in this mode of the Langendorff preparation may not be sensitive enough to register small but significant changes.

4.1.5.2 Chronic Metformin treatment enhances phosphorylation of AMPK not Akt in the ageing, diabetic heart

The molecular mechanisms underlying metformin associated protection are complex and not fully understood yet. The majority of experimental evidence in the acute setting thus far shows a strong involvement via AMPK [266, 283] and Akt [281] activation.

AMPK is a dynamic kinase molecule that acts as the major regulator of energy balance within the cell [533]. This study shows that chronic metformin treatment also causes an increased basal activation of AMPK by phosphorylation. Other studies also demonstrate this; Musi et al, 2002 [268] revealed that AMPK is still activated in skeletal muscle following 10 weeks of oral metformin treatment in type 2 diabetic patients [268]. However, in contrast, no enhancement of AMPK phosphorylation was seen in normoglycaemic rat hearts from rats treated with metformin for 2 weeks [534]. Interestingly, at a higher dose of metformin an increase in AMPK phosphorylation is

seen [534], suggesting that perhaps the cardioprotective benefits of metformin are time and/or dose-dependent [535]. In contrast, some studies oppose the necessity for AMPK activation to elicit the positive effects of metformin [536]. For instance, Foretz et al, 2010 showed that metformin administration in mice produced a reduction in hepatic gluconeogenesis and that this decrease did not require AMPK activation and instead directly decreased hepatic energy state [271]. This variability in results may be caused by the diverse effects of metformin in different organs or tissues and also potentially by the use of different experimental models. Metformin treatment has been assessed in both non-diabetic animals and diabetic animals, the latter consisting of genetically modified, chemically induced or sporadic models which all have differences in basal signalling. In this respect, the 12 month old Goto Kakizaki rat model is an important tool to investigate the chronic effect of metformin, as it more closely reflects a non-obese middle aged diabetic patient.

Apart from activation of AMPK, previous studies have shown that acute metformin treatment given at the time of reperfusion can activate the RISK pathway [281]. Bhamra et al, 2008 demonstrated that diabetic GK and non-diabetic Wistar isolated rat hearts could be protected against IRI by administering metformin during the first 15minutes of reperfusion. Acute metformin applied in this setting activated Akt by phosphorylation; moreover simultaneous administration of a PI3K inhibitor, LY294002, prevented this increase in phosphorylation and subsequently protection was lost. The authors further characterised this finding by assessing mPTP opening in isolated cardiomyocytes and demonstrated metformin induced activation of PI3K/Akt pathway led to inhibition of the mitochondrial permeability transition pore (mPTP) and therefore reduced infarct size in this model of IRI [281]. Akt phosphorylation was also assessed in this study; however, chronic treatment with metformin did not appear to chronically activate this kinase. It is likely that chronic administration of drugs may not manifest the same outcomes as acute drug administration due to the existence of inhibitory feedback regulation mechanisms [521].

4.1.5.3 Chronic metformin treatment can restore reduced PGC-1α expression and increase mitochondrial regulation in the ageing, diabetic heart

A decreased expression of PGC-1α has been previously shown in diabetic skeletal muscle [524]. In this study, we showed that PGC-1α protein expression is down-regulated in aged, diabetic rat myocardial tissue compared to the non-diabetic rat heart, a finding not yet to be reported elsewhere. Moreover, electron microscopy images suggest mitochondria to be more organised and in their favoured elongated appearance in

metformin-treated GK rat hearts; possibly as a consequence of enhanced PGC-1α expression. PGC-1α, a key regulator of energy metabolism has been extensively studied [525], with its expression finely regulated to meet the energy demands of cellular systems [506]. Interestingly, investigations in skeletal muscle suggest that increasing activation of AMPK by pharmacological activation, either by 5-aminoimidazole-4-carboxamide-1-β-d-ribofuranoside (AICAR) [271] or metformin [524] enhanced PGC-1α expression resulting in increased mitochondrial biogenesis. Yet, the mechanisms by which increasing AMPK activity can subsequently lead to increased PGC-1α expression are still not completely understood. This study suggests similarities to this scenario: following administration of metformin for 4 weeks we recorded an increase in activation of AMPK and a subsequent increase in the expression levels of PGC-1α in the heart, an effect similar to that previously seen in skeletal muscle.

Intriguingly, basal ATP levels in the aged, diabetic heart were surprisingly significantly greater than in the age matched Wistar hearts and metformin treatment decreased basal levels of ATP. ATP levels are tightly regulated in the heart by both AMPK and PGC-1α[94], and normal cardiac function is dependent on a constant supply and demand of ATP. In the young insulin resistant heart, it has been suggested that PGC-1α expression is increased in accordance with a metabolic shift[206] and dependency on fatty acid oxidation in response to a decreased availability of glucose uptake available for glycolysis[537].

As the diabetic heart ages, PGC-1α expression appears to decrease (as reported in chapter 3), therefore it could be suggested that fatty acid oxidation which is responsible for 60-90% of ATP synthesis could become inappropriately regulated and therefore production of ATP by the respiratory chain is inadequately controlled. Excessive concentrations of long-chain fatty acids including acyl CoA ester are present in the diabetic heart[538], which may lead to overproduction of ATP and favour activation of cell membrane K_{ATP} channels and a subsequent change in Ca^{2+} handling[210]. This was shown to occur in type 2 diabetic db/db mice which exhibit impaired cardiac contractility[539]. Metformin may enhance AMPK activation therefore restoring the control of AMP:ATP ratio and alongside PGC-1α ensures normal ATP regulation. However, the lipid profile of ageing GK hearts were not assessed in this investigation and some may argue that an increased level of ATP would in fact be beneficial in IRI[248].

Recent advances suggest that proteins involved in the control of mitochondrial dynamics namely Mfn-2, can also regulate mitochondrial metabolism [526]. Mfn-2 has

pleiotropic roles within the cellular system, moreover, it has emerged as a key target of the PGC-1α regulatory pathway [540]. In support of a PGC-1α/Mfn-2 interaction, Soriano et al, 2006 showed that overexpression of PGC-1α in cultured muscle cells induced both Mfn-2 mRNA and protein expression above the levels of other genes typically enhanced by PGC-1α. They also found that PGC-1α stimulates the expression of Mfn-2 through its transcriptional properties [541]. Additionally, a decreased expression of Mfn-2 has been demonstrated in skeletal muscle of type 2 diabetes patients [542].

Based on these findings reported in the literature and our data showing that chronic metformin administration can increase PGC-1α expression, and improve mitochondrial organisation and appearance in GK rat hearts, we hypothesised that Mfn-2 expression may be implemented in this pathway. We did not see a significant reduction in Mfn-2 levels in the diabetic heart compared to the non-diabetic heart, yet metformin treatment enhanced Mfn-2 expression. Mfn-2 could potentially play a role in metformin induced protection in this set up. Although we do not show any direct evidence, it is possible that metformin through phosphorylation of AMPK can up-regulate and provide an increased platform for activation of PGC-1α via either phosphorylation or deacetylation [39]. This increase in activity may then act downstream on the mitofusin protein Mfn-2 which contributes to improved mitochondrial biogenesis and renders the diabetic heart less prone to damage by IRI.

4.1.5.4 Up regulation of PGC-1α expression may require phosphorylation and activation of AMPK

In an attempt to establish whether a direct link exists between metformin associated phosphorylation of AMPK and PGC-1α expression; HL-1 cells and isolated 12 month diabetic cardiomyocytes were incubated with metformin with or without the presence of AMPK inhibitor compound C and protein expression and activation assessed. Characterisation studies using the HL-1 cell line demonstrated that metformin treatment enhanced AMPK phosphorylation and PGC-1α expression and that these changes were reduced when AMPK activation was inhibited. Furthermore, this outcome was repeated in aged, diabetic cardiomyocytes. Interestingly, inhibition of AMPK phosphorylation did not significantly affect metformin associated influence on mfn-2 expression, which may suggest that an alternative pathway other than AMPK-phosphorylation could contribute to metformin-related changes in Mfn-2 expression. Whether metformin associated up regulation of PGC-1α expression in the diabetic heart absolutely requires AMPK phosphorylation is unclear. Inhibition of AMPK using 20μM of Compound C did not significantly reduce the enhancement of PGC-1α expression due to the variability in the data. The reduction in expression reached

significance when using 40μM of the inhibitor compound, however, this concentration of Compound C also decreased the expression of PGC-1α without prior metformin administration. Therefore, one cannot exclude the possibility that Compound C has a direct inhibitory effect on PGC-1α expression or that perhaps the higher concentration produced toxic effects on the cells.

It has been demonstrated previously that there is a strong overlap in the target genes of AMPK and PGC-1α especially in those involving mitochondrial function[543]. The findings in this investigation and the potential importance of AMPK activation on subsequent PGC-1α transcription are supported by numerous studies. These include studies demonstrating that AMPK over-activation by mutational changes increase mitochondrial content *in vivo*[544] and that AMPK can directly influence PGC-1α activity through direct interaction by phosphorylation[90]. Whether AMPK phosphorylates PGC-1α in the heart is yet to be determined and would provide significant understanding into how chronic metformin treatment may lead to an improved mitochondrial function in the heart. To answer whether AMPK can directly phosphorylate PGC-1α in the heart, we attempted to immunoprecipitate (IP) out the PGC-1α protein from aged, diabetic heart tissue and to assess whether metformin phosphorylated PGC-1α. Unfortunately, this proved problematic and we were unsuccessful in isolating PGC-1α protein from our heart samples.

4.1.5.5 Metformin may alter the subcellular location of PGC-1α

The up regulation of PGC-1α expression following metformin treatment may provide a platform for post translational modifications to occur. A dynamic shift in localisation can take place in response to a change in the energy status of the cell, with the main pool localised in the cytoplasm rapidly modified by phosphorylation, de/acetylation, ubiquination, methylation or GlcNacylation[506]. Subsequently PGC-1α can be both activated and transported into a different cellular location, for example into the nucleus to co activate transcription factors for target genes, or remains in an inactive form in the cytoplasm, all depending on the cellular demands [100].

Interestingly, in the whole cell, we found that the PGC-1α protein appeared as a double band; the lower band was uniform and the upper band more differential in expression levels. This led to an overall decreased expression in diabetes, which increased in metformin treated hearts. Following subcellular fractionation, the cytoplasmic fraction displayed no difference in PGC-1α expression following metformin treatment and appeared as a single band. Intriguingly, this band was seen in the same molecular weight range as the lower band seen in the whole cell experiment. In the

nuclear extract, PGC-1α appeared once again as a double band; however the results were opposite to that seen in the whole cell investigation. PGC-1α expression was decreased in the nuclear extract following metformin treatment in the diabetic heart. Interestingly, Holloway et al, 2010 demonstrate an increased accumulation of nuclear PGC-1α expression in diabetic hearts isolated from Zucker diabetic fatty (ZDF) rats, an alternative model of type 2 diabetes [545]. However, other authors suggest that PGC-1α is active when transported into the nucleus [100], therefore creating a puzzling conclusion.

It could be suggested that the double banding that was used to calculate total PGC-1α expression levels are in fact a representation of activity and expression, Aquilano et al, 2010 suggesting that the two bands could be representative of a post-translational process[546]. Based on this, one interpretation of our results could be that the upper band, which had a reduced expression in the nuclear fraction, could be a representation of a post-translational modification. One possible modification could be acetylation, which would translate that the diabetic hearts have more PGC-1α in the acetylated (inactive) form, therefore prevented it from performing its co-transcriptional activity**.** The results are intriguing and difficult to interpret, but they definitely indicate trafficking of PGC-1α between the cell compartments. Experiments investigating the functional state of PGC-1α in different cellular compartments could provide crucial information on the acetylation and/or phosphorylation of the protein. Recent evidence also suggests mitochondrial localisation of PGC-1α [546] and upon activation target genes can be directly stimulated within the mitochondria, thereby reinforcing a possible direct link to mitochondrial biogenesis. Interestingly, metformin induced phosphorylation of AMPK in skeletal muscle improved mitochondrial biogenesis by stimulating PGC-1α transcription [524], or by direct activation of PGC-1α via phosphorylation [90], suggesting a dual effector system following metformin treatment.

4.1.6 Conclusion

Chronic administration of metformin is cardioprotective against ischaemia-reperfusion injury in both non-diabetic and type 2 diabetic rat hearts. A possible dual effect of metformin is seen in the setting of type 2 diabetes and cardioprotection, whereby glucose is lowered alongside the initiation of prosurvival signalling pathways. This results in an enhanced protection against ischaemia-reperfusion injury. The mechanism of protection elicited by metformin appears to be dependent on the duration of the treatment. Previous studies have demonstrated that acute metformin treatment activates Akt and AMPK leading to the acute closure of the mPTP. The

protection associated with **chronic** metformin treatment appears to be independent of **acute** Akt and AMPK activation. The chronic activation of AMPK by metformin may promote changes at the transcriptional level in the cardiomyocyte, resulting in an increased expression of PGC-1α and improved mitochondrial biogenesis in the diabetic heart (Figure 4.23).

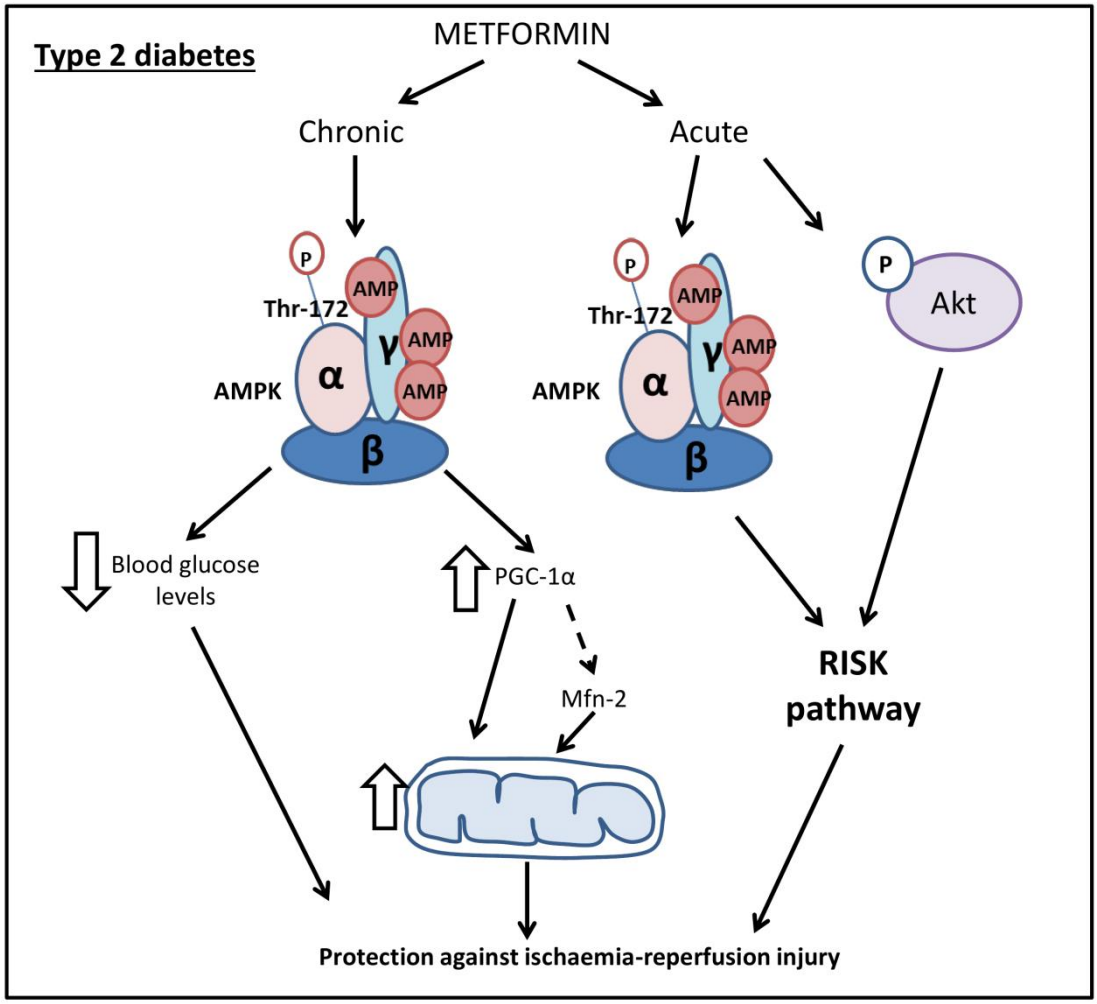

Figure 4.23: The effect of chronic metformin treatment in type 2 diabetic rats.:

4.2 Sitagliptin and cardioprotection

4.2.1 Background

Glucagon like peptide-1 (GLP-1) is an incretin hormone, secreted postprandially following an increase in blood glucose. It binds to G-protein coupled receptors in the pancreas and stimulates a G protein receptor pathway involving adenylyl cyclase and cAMP, which results in increased insulin secretion from the pancreatic β-cells and decreased glucagon release from α-cells[295]. Circulating GLP-1 is rapidly broken down into its inactive metabolite GLP-1(9-36) amide by DPP-4; therefore there is an interest in finding ways to prolong active GLP-1 in the blood stream. In this respect, two groups of drugs have emerged: GLP-1 receptor agonists, that mimic the action of GLP-1 but are resistant to DPP-4 degradation (exenatide, liraglutide) and drugs which inhibit DPP-4 itself (gliptins such as sitagliptin, vildagliptin, saxagliptin) [295].

Alongside the direct benefit of GLP-1 and its breakdown products on myocardial metabolism[547, 548], emerging evidence suggests GLP-1, GLP-1(7-36) and GLP-1(9-36) all have the ability to protect against acute IRI[302, 304, 549].

Based on this evidence, the Yellon lab hypothesised that treatment with a DPP-4 inhibitor; Sitagliptin may also confer cardioprotection against IRI. Unpublished studies demonstrated that 2 weeks oral pre-treatment with Sitagliptin, significantly reduced myocardial infarct size in the non-diabetic isolated perfused rat heart. Interestingly, it appeared that the infarct-limiting effects of 2 weeks Sitagliptin pre-treatment were glucose-sensitive. In this respect, cardioprotection was noted when hearts were perfused with 11mmol/L glucose but not 5mmol/L glucose. In addition this protection was abolished in the presence of GLP-1 receptor antagonist exendin (Figure 4.24). Similarly, cardioprotection elicited by GLP-1 treatment was also glucose-sensitive with infarct reduction observed at glucose levels of 7, 9 and 11 mmol/L but not at 5 mmol/L (Figure 4.25). Importantly, in this model, the infarct size developed in the control hearts which were perfused with different concentrations of glucose in the buffer (5, 7, 9, 11 mmol/L) but without the drug was not affected (Figure 4.26).

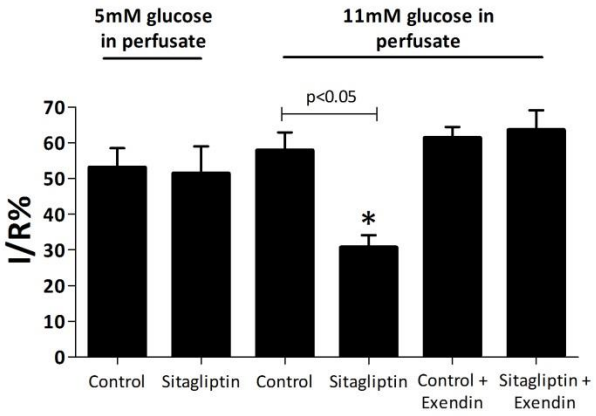

Figure 4.24: The influence of glucose levels on sitagliptin induced cardioprotection in the isolated heart. Pre-treatment for 2 weeks with Sitagliptin reduced the myocardial infarct to area at risk ratio (I/R %) in isolated rat hearts perfused with buffer containing 11 but not 5 mmol/L glucose. This infarct-limiting effect was abolished in hearts Langendorff-perfused with Exendin 9-39 (Exendin), a GLP-1 receptor antagonist. One-way ANOVA followed by Bonferroni's multiple comparison test was used to determine statistical significance (n≥6/group). Data produced by Miss Abigail Wynne.

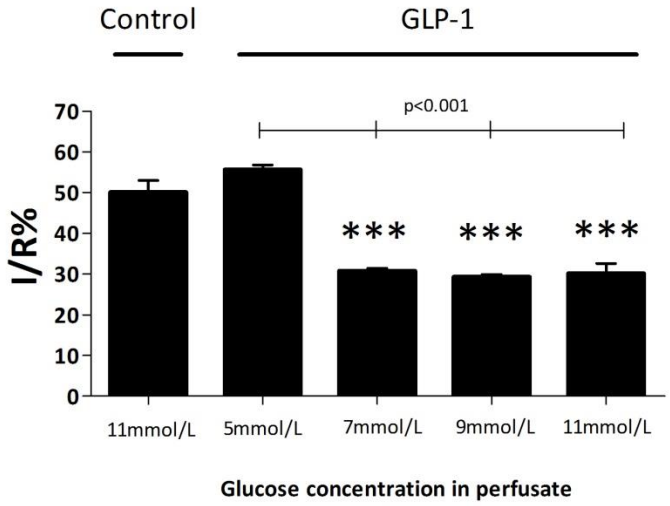

Figure 4.25: The influence of glucose levels on GLP-1 induced cardioprotection in the isolated heart..:. The effect of different concentrations of glucose on GLP-1 induced reduction in infarct size. Non-diabetic Sprague-dawley rat hearts were isolated and perfused according to Langendorff isolated heart perfusion. Perfusion of isolated rat hearts with buffer containing GLP-1 reduced myocardial infarct to area at risk ratio (I/R %) in hearts perfused with buffer containing glucose at 7, 9, or 11 mmol/L but not at 5 mmol/L. One-way ANOVA followed by Bonferroni's multiple comparison test was used to determine statistical significance (n≥6/group). Data produced by Dr Shah Begum/Miss Abigail Wynne.

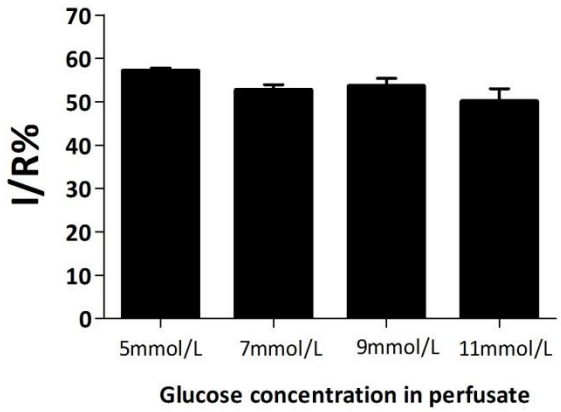

Figure 4.26: The effect of different concentrations of glucose on infarct size. Non-diabetic Sprague-dawley rat hearts were isolated and perfused according to Langendorff isolated heart perfusion, There was no difference in myocardial infarct to area at risk ratio (I/R %) in hearts perfused with buffer containing glucose at either 5, 7, 9, or 11 mmol/L. One-way ANOVA followed by Bonferroni's multiple comparison test was used to determine statistical significance (n≥6/group). Data produced by Dr Shah Begum/Miss Abigail Wynne.

4.2.2 Hypothesis

Using the aforementioned unpublished data from the Yellon lab, we hypothesised 2 weeks pre-treatment with DPP-4 inhibitor Sitagliptin may reduce infarct size *in vivo i*n a glucose dependent manner. To assess this hypothesis, diabetic and non-diabetic rat models exhibiting different basal blood glucose levels were treated with or without sitagliptin for 2 weeks and infarct size examined *in vivo.*

4.2.3 Experimental Protocols

4.2.3.1 Animals

Male Goto-Kakizaki (GK) rats (a mild, non-obese diabetic model [427] obtained from Taconic (Denmark), were kept in house until they reached 7-8 months of age; they received humane care in accordance with the United Kingdom Animal (Scientific Procedures) Act of 1986. Male Wistar rats (normoglycaemic) were obtained from Charles River UK Limited (Margate, UK) and kept in house until they reached 3-4 or 7-8 months of age.

4.2.3.2 Treatments

Rats were randomly assigned to receive 100mg/kg/day Sitagliptin (Sigma, UK) or water control orally by gavage for 2 weeks. Physiological parameters including body weight

and overnight fasting blood glucose (Accu-chek system, Roche) were collected prior to and at 10 days into treatment.

4.2.3.3 In vivo rat model of ischaemia-reperfusion injury

Left anterior descending coronary artery (LAD) occlusion and reperfusion were performed *in vivo* as described in detail in the chapter 2.2.2. Briefly, rats were anesthetised with sodium pentobarbital (20mg/kg intraperitoneally) and heparin (300IU). The rats were intubated and ventilated with a Harvard ventilator (room air, 70 strokes/min, tidal volume: 8-9ml/kg). Body temperature was maintained at 37.4±1°C by means of a rectal probe thermometer attached to a temperature control system (CMA450). A lateral thoracotomy was performed to expose the heart and a suture placed around the LAD. The suture was tightened using a loop system to create LAD ligation and regional ischaemia which was confirmed by a change in ECG profile. Following 30 minutes of ischaemia, the vessel was reperfused for 120 minutes (as described in chapter 2.2.2). At the end of reperfusion, the heart was removed from the chest, the LAD permanently occluded and the heart perfused with 0.5% Evans blue in saline to delineate the area at risk. Hearts were frozen at -20°C for several hours before infarct size determination using TTC staining, as described in chapter 2.2.4).

4.2.4 Results

4.2.4.1 Sitagliptin pre-treatment reduced myocardial infarct size in vivo in a glucose-dependent manner

Physiological parameters were recorded prior to and 10 days into control or sitagliptin treatment. In the young Wistar group, body weight increased after 10 days, however this is likely to be due to the general weight gain seen in Wistar rats over time. From the start, the middle-aged Wistars were significantly bigger than both other groups. Sitagliptin treatment was weight neutral in both middle-aged groups (Table 4.3). Blood glucose levels were in the normoglycaemic range in young (3-4 month) Wistar rats, however as Wistar rats aged to 7-8 months, their blood glucose levels significantly increased (mmol/L: 5.6±0.2 *vs* 7.5±0.3, $p<0.001$, Figure 4.27). Middle aged diabetic GK rats demonstrated a significantly greater blood glucose level than either Wistar group (9.3±1.5, $p<0.001$ *vs* both groups, Figure 4.27)**.** Interestingly**,** sitagliptin pre-treatment did not reduce blood glucose levels in any of the groups, Figure 4.28.

Weight (g)	**Control**		**Sitagliptin**	
	Baseline	*10days*	*Baseline*	*10days*
Young Wistars	305.7±12.4	355.5±9.7*	309.5±14.4	370.9±8.7*
Middle aged Wistars	557.6±9.3*	548.3±12.0	570.0±20.1*	562.4±19.7
Middle aged GKs	409.8±5.0	400±3.7	393.5±10.4	384±12.1

Table 4.3: The effect of sitagliptin treatment on body weight. Summary of body weight before and 10days into Sitagliptin or control treatment. Young (3-4 months) Wistars, middle-aged (7-8month) Wistars and middle-aged (7-8month) GKs were weighed before and 10days into 100mg/kg/day sitagliptin or control (water) treatment. Young Wistars had a significantly greater body weight 10days into treatment and middle-aged Wistars were significantly heavier than both other groups. One-way ANOVA followed by Bonferroni's multiple comparison test was used to determine statistical significance.

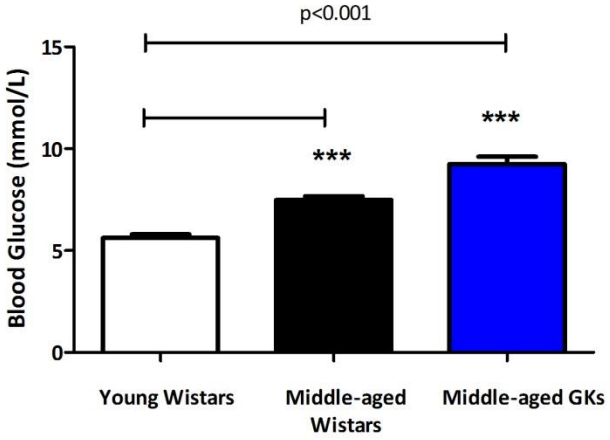

Figure 4.27: Basal blood glucose levels in non-diabetic and diabetic rats. Blood Glucose levels. Fasting blood glucose was measured before treatment in all 3 groups; young (3-4 month) Wistars, middle-aged (7-8month) Wistars and middle-aged (7-8month) GKs. Blood glucose was measured via collection of blood from the tail vein and assessed using the Accu-chek system, Roche. Data is shown as mean ± S.E.M, n≥6 per group. One-way ANOVA followed by Bonferroni's multiple comparison test was used to determine statistical significance.

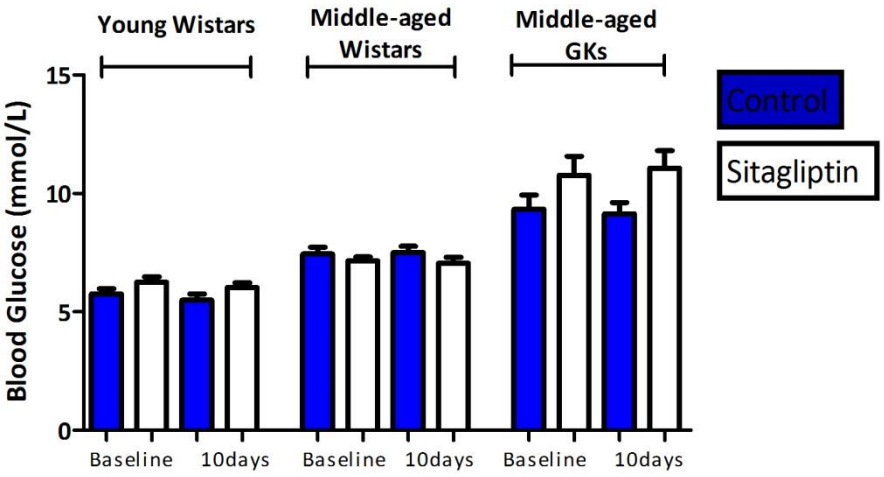

Figure 4.28: Summary of blood glucose measured before and after administration of sitagliptin or control. Fasting blood glucose was measured initially and at 10days into treatment in young (3-4 month) Wistar rats, middle-aged (7-8 month) Wistar rats and middle-aged (7-8 months) Goto-Kakizaki (GK) rats. 100mg/kg/day sitagliptin treatment for 2 weeks did not reduce blood glucose in any of the groups. Data is represented as mean ± S.E.M, n≥6. Repeated measures ANOVA was used to determine any statistical significance.

In vivo LAD occlusion/reperfusion studies showed sitagliptin pre-treatment was successful in reducing myocardial infarct size in both middle aged Wistar and GK rats (15.4±2.4% with Sitagliptin *vs.* 44.8±4.0% with control in Wistars; and 29.10±5.3% with Sitagliptin *vs.* 60.9±5.5% with control in GKs. $P<0.05$:N≥6/group). However, in the young Wistar group there was no difference in infarct size (34.5±5.9% with Sitagliptin *vs.* 33.8±3.1% with control). Moreover, young Wistars developed smaller infarcts in the control group compared to both middle aged groups (Figure 4.29).

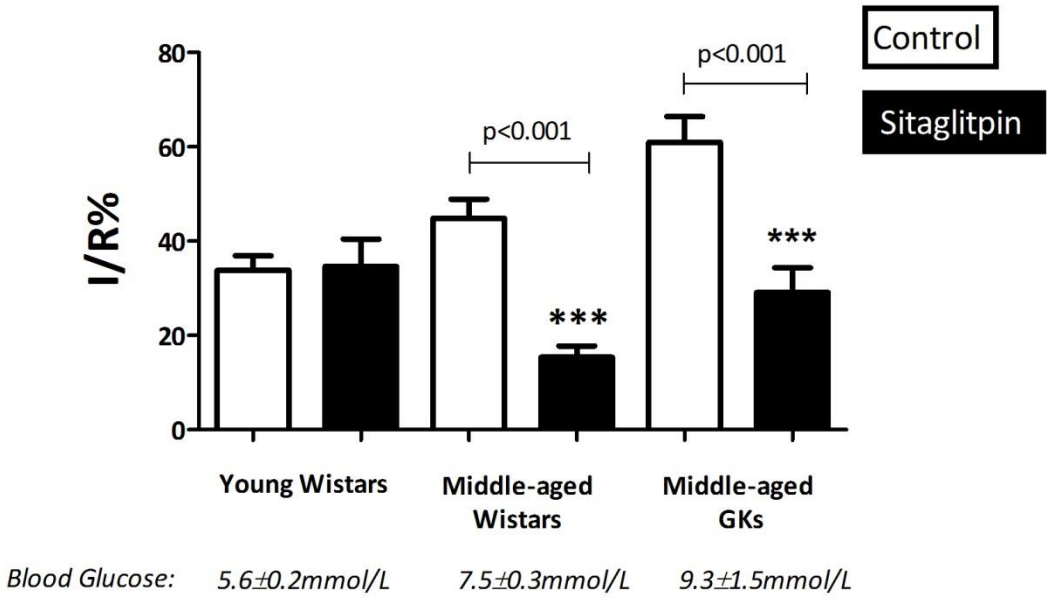

Figure 4.29: The effect of Sitagliptin treatment on infarct size in the young Wistar, and middle-aged Wistar and GK rats. Infarct size is expressed as the infarcted volume within the area at risk of the left ventricle (% I/R) in hearts either treated with sitagliptin for 2 weeks or control hearts. Sitagliptin treatment significantly reduced the infarct size compared to the control group in both the middle-aged Wistar and GK rat but not the young Wistar group. Data is shown as mean ± S.E.M, n≥6. ***p<0.001 versus respective control. One way ANOVA followed by a Tukey Post-Hoc analysis were used for statistical analysis between groups.

4.2.5 Summary and Discussion

The key findings presented in this section of the chapter are:

- Chronic sitagliptin treatment reduced infarct size *in vivo* in both middle-aged diabetic GK rats and middle-aged non-diabetic Wistar rats.
- However, this treatment is not effective in reducing this injury in the young non-diabetic Wistar rats.
- Interesingly, the blood glucose levels in the young Wistar groups were significantly lower than in the other two groups.
- This suggests a glucose-dependency of sitagliptin induced cardioprotection *in vivo*.

4.2.5.1 The cardioprotective effect of Sitagliptin is dependent on blood glucose levels

The cardioprotective effects of exogenous GLP-1, GLP-1 agonists and DPP-4 inhibitors have been well documented [549]. However, no investigations are yet to report a glucose-sensitivity of these agents. Bose et al, 2005 demonstrated, using both *ex vivo*

and *in vivo* models that the non-diabetic rat heart could be protected against IRI using exogenous GLP-1. In this study they included valine pyrrolidide (VP), a DPP-4 inhibitor that prevents the breakdown of exogenous GLP-1; however, the inhibitor alone did not reduce infarct size. Inhibition of cAMP, PI3K and p44/42 MAPK by specific inhibitors all abolished infarct-limiting effect of GLP-1[304]. Blood glucose levels were not assessed in the *in vivo* investigations, however, the data collected using the standard Langendorff isolated heart model used 11mmol/L glucose in the perfusion buffer[304], therefore reflects the outcome of the preliminary data from the Yellon lab (Figure 4.25).

Following these initial studies with exogenous GLP-1, Ye et al, 2010 demonstrated that DPP-4 inhibitors could also protect the heart against IRI[322]. 3 days oral pre-treatment with Sitagliptin successfully reduced infarct size *in vivo* in mice subjected to IR. Sitagliptin treatment increased myocardial levels of cAMP and subsequent PKA activity and inhibition of PKA by H-89 completely abolished this protection. Further studies *in vitro*, suggested a similar mode of action to that of exogenous GLP-1; p44/42 MAPK was also essential for the protective effect of sitagliptin[322]. In comparison to the previously mentioned study, the DPP-4 inhibitor was given orally for 3 day prior to IR as a pre-treatment, which could suggest short term administration of DPP-4 inhibitors, such as VP used in the previous study, is not a sufficient amount of time to stimulate cardioprotective pathways.

In accordance with the study by Ye et al, 2010[322]; our data demonstrated that chronic, 2 week sitagliptin treatment also protected the heart against IRI; moreover this protection was only seen in the middle-aged Wistar and middle-aged GK groups which exhibited blood glucose levels greater than 7 mmol/L. Interestingly, in the study performed by Ye et al, the blood glucose levels were on average 7.5 mmol/L, which in fact corresponds to the levels of glucose in which cardioprotection was observed in our study. This apparent glucose-dependency was also observed in preliminary data obtained with GLP-1, whereby GLP-1 mediated cardioprotection with infarct-limitation being observed at glucose levels of 7, 9, and 11 mmol/L but not at 5 mmol/L (Figure 4.25).

In contrast, Sauve and co-workers[324] could not demonstrate any significant infarct limitation with genetic DPP-4 knockout mice. However, it is worth noting that these results were obtained following permanent LAD ligation not ischaemia-reperfusion injury. Furthermore, 8 weeks Sitagliptin treatment (250mg/kg/day) prior to permanent LAD ligation failed to protect STZ-diabetic mice against myocardial infarction but, paradoxically significantly improved the survival

rate[324]. Interestingly, the mice used in this latter study were fed a high-fat diet (HFD) which caused basal blood glucose levels to be 10mmol/L; following induction of diabetes using STZ, mice became severely hyperglycaemic with blood glucose levels of 20-30 mmol/L. Sitagliptin treatment in HFD-STZ mice significantly reduced blood glucose levels but only to approximately 15mmol/L. In treated animals, HbA1c levels were in fact dramatically reduced from 70-80mmol/mol to approximately 30-35mmol/mol, which is in within the 'non-diabetic' threshold[550]. Interpretation of these results is difficult, and may suggest an ideal window of blood glucose is needed for sitagliptin to produce its cardioprotective effect.

4.2.5.2 Possible mechanisms for glucose dependency of cardioprotection?

The mechanisms that contribute to the postulated glucose-dependency of the cardioprotective effect of sitagliptin were not investigated in this study. Previous studies suggesting that GLP-1/PKA activation occurs during sitagliptin induced protection[322], corroborated with studies that report glucose-dependent changes in intracellular calcium and GLP-1 receptor-PKA signalling suggest that this signalling pathway could be distinctly altered in response to high blood glucose levels[551]. An alternative possibility is that the GLP-1 receptor could be differentially regulated in response to differing circulating blood glucose levels. Poornima et al, 2008 saw a significant activation of Akt and subsequent cardioprotection in GLP-1 treated Spontaneously Hypertensive Heart Failure (SHHF) rats. Interestingly, these rats had blood glucose levels of greater than 12 mmol/L. In the presence of high glucose, GLP-1 could possibly activate a G-protein coupled receptor signalling pathway involving the Akt component of the RISK pathway leading to cardioprotection, perhaps in conditions of low blood glucose this cardioprotective pathway is not activated. However this pathway is yet to be investigated in rats exhibiting low blood glucose levels [548]. Interestingly, Chai et al, recently showed that the administration of GLP-1 increased Akt-phosphorylation and PKA activity; leading to subsequent phosphorylation and activation of eNOS in bovine aortic endothelial cells[552]. Interestingly, the eNOS/NO pathway is implicated in cardioprotection against IRI[134]. In contrast, Ye and colleagues did not see a change in Akt-phosphorylation following sitagliptin treatment in mice [322]. The link between GLP-1, high glucose and Akt phosphorylation is yet to be fully investigated.

4.2.5.3 GLP-1 independent effects of sitagliptin on cardioprotection?

The data discussed so far involving GLP-1 and DPP-4 inhibitor compounds postulate a strong involvement of elevated GLP-1 levels and PKA signalling in cardioprotection. However, DPP-4 inhibition can lead to a plethora of downstream signalling effects, including modulation of other gastrointestinal hormones, neuropeptides, cytokines, and chemokines[553]. Therefore it was not completely surprising when Ku et al, 2011 demonstrated that DPP-4 deficiency protected the heart against IRI. However, administration of exendin(9-39), GLP-1 receptor antagonist did not fully abolish this protective effect, suggesting a possible GLP-1 independent mechanism of protection[554]. Zaruba et al, 2009 demonstrated that pharmacological and genetic inhibition of DPP-4 induced cardioprotective effects including reduced cardiac remodelling and improved function and survival in mice. This protective effect was attributed to stabilisation of active SDF-1α in heart lysates and preservation of the cardiac SDF-1-CXCR4 homing axis, a chemokine which is another known substrate of DPP-4[555]. In support of this, an active SDF-1α-CXCR4 axis was proven essential for protecting the myocardium from apoptotic cell death following myocardial infarction[556].

4.3 Conclusion

The signalling mechanisms by which chronic DPP-4 inhibition can result in cardioprotection against ischaemia-reperfusion injury are still unclear. The suggestion that DPP-4 inhibition can produce beneficial effects independent of GLP-1 activity raises the question whether cardioprotection is also independent of the modulation of this incretin hormone. The observation that blood glucose levels influence the cardioprotective potential of the DPP-4 inhibitors and GLP-1 therapies is an intriguing prospect. Further studies are required to delineate the importance of blood glucose levels on the cardioprotective effect of anti-diabetic agents, particularly DPP-4 inhibitors.

5. OVERALL DISCUSSIONS

5.1 General conclusions

Specific conclusions have been presented in detail at the end of each results chapter and only an overview of the most significant findings will be presented here.

In essence, one of the main novelties of the studies presented in this thesis consists in the investigation of cardioprotective strategies in more appropriate animal models. The majority of laboratory studies have used young, healthy animals to investigate the detrimental effects of myocardial ischaemia-reperfusion injury and the signalling pathways involved to elicit protection against this lethal insult[7, 410]. However, in clinical settings the patients that develop cardiovascular disease are usually at least middle aged, and also manifest a number of co-morbidities such as hypertension, hyperlipidaemia and diabetes[557, 558].

The overall aim of this thesis has been to assess the influence of two interacting co-morbidities, old age and type 2 diabetes on: (1) the susceptibility to myocardial ischaemia-reperfusion injury, (2) the ability of ischaemic preconditioning to protect against myocardial ischaemia-reperfusion injury and (3) the effificacy of potential cardioprotective anti-diabetic agents when administered chronically in the presence of these aggravating factors. In addition, investigations have been made in the attempt to elucidate the mechanisms responsible for the observed changes in the cardioprotective potential of the aged, diabetic heart.

Our data showed that:

(1) During ageing, the diabetic heart develops an increased susceptibility to ischaemia at an earlier age than the non-diabetic heart.
(2) The extent of the injury induced by ischaemia-reperfusion increases with age in all hearts but this detrimental age related phenomenon seems to appear **earlier** in the diabetic heart.
(3) The aged, diabetic heart is less amenable to cardioprotective manoeuvres (such as ischaemic preconditioning).
(4) There is an increased baseline activation of the prosurvival kinase Akt in the ageing, diabetic heart. Moreover, acute activation of Akt following IPC is not achievable, which may explain why this manoeuvre is not cardiorprotective in the aged, diabetic heart.
(5) We noticed that the expression of PGC-1α and catalase change with age and diabetes. It is possible that these alterations may be a consequence of the chronic activation of Akt. These modifications may explain the increase in

oxidative stress and the change in mitochondrial structure, which we report here as well. These changes may be responsible for the increased susceptibility to IRI.

(6) Chronic metformin treatment is cardioprotective against ischaemia-reperfusion injury in both the diabetic and non-diabetic ageing heart. However, the protection was more pronounced in the diabetic animals in which metformin had also a significant glucose lowering effect.

(7) Chronic metformin treatment is associated with mitochondrial improvements, an increased level of phosphorylated AMPK and an enhanced expression of PGC-1α and Mfn-2.

(8) Preliminary data seem to indicate that sitagliptin treatment was cardioprotective against myocardial infarction in a glucose dependent manner.

We conclude that ageing in combination with type 2 diabetes renders the diabetic heart more susceptible to ischaemia-reperfusion injury and less amenable to protection by IPC at an earlier age than in the ageing, non-diabetic heart. Therefore, we suggest that the diabetic heart may age quicker than the non-diabetic heart and this consequently could translate into an increased vulnerability to cardiovascular events at a younger age in type 2 diabetic patients.

The paradox of Akt upregulation at baseline but reduced cardioprotection in the aged, diabetic heart is intriguing and potentially extremely important when considering the translational application of conditioning strategies that target the reperfusion injury salvage kinase (RISK) pathway to elicit protection against IRI. Furthermore, the changes in the prosurvival signalling in the aged, diabetic heart may also have an effect on pharmacological protection. Chronic treatment with the oral anti-diabetic metformin elicits cardioprotection via a mechanism distinct from those previously defined following the acute application of this agent. Lastly, a different oral anti-diabetic agent sitagliptin protects the heart against infarction in a glucose-dependent manner. However, we did not investigate the influence of old age on the cardioprotective effect of this drug.

5.2 Limitations

The studies performed in this thesis had some limitations that should be considered and discussed when interpreting the findings and when planning future investigations.

In spite of the fact that the Langendorff perfused heart preparation is universally used and accepted as a means to investigate heart physiology and pathology,

including the susceptibility to ischaemia-reperfusion injury, however it has a number of limitations. Firstly, it is an ex vivo preparation in which the heart is perfused with a crystalloid buffer and is independent of the neural and endocrine regulatory influences. In addition, the crystalloid buffer we used contains only glucose as a metabolic substrate whereas metabolism in the adult and diabetic heart is very complex. The adult, non-diabetic heart relies predominantly on fatty acids as an energy substrate for ATP production but can also utilize glucose especially in times of oxygen deprivation such as ischaemia. Whereas, as diabetes progresses, the heart has an increased reliance on fatty acids. Due to technical limitations regarding the Langendorff apparatus, fatty acids were not included in the perfusate. Furthermore, both type 2 diabetes and old age cause global molecular and cellular changes throughout the entire body including the vasculature not just within the heart. Therefore, an *in vivo* model of ischaemia-reperfusion injury was used to assess the susceptibility to infarction. This model would have provided additional physiological information of the how the aged and diabetic heart responds to myocardial infarction.

We find an increased basal activation of Akt in the aged, diabetic heart and downstream changes in protective signalling pathways. However, we do not show any direct linking evidence between elevated Akt-phosphorylation and these effects. Therefore, how chronic Akt phosphorylation directly impacts on PGC-1α and subsequently how PGC-1α influences catalase levels in the myocardium need to be further explored. This could be investigated using isolated ventricular cardiomyocytes from young and old diabetic and non-diabetic rat hearts and suitable inhibitors. More importantly, time limitations did not allow for further investigations to examine the possible upstream causes of chronic Akt-phosphorylation in age and diabetes. We would have liked to have started this with the exploration of insulin receptor signalling in the aged, diabetic myocardium.

Metformin was administered *in vivo* for 4 weeks before infarct size measurement using the Langendorff isolated heart preparation. Firstly, metformin has an effect on energy metabolism through modulating AMPK activity, therefore by removing the heart from the whole body these effects may be masked due to the reasons described above regarding the use of glucose as the only metabolic substrate in this model. However, by using the isolated heart, our data revealed a direct effect of metformin on the cardiac tissue, excluding the influence of the whole body system. Depending on the aim and desired end point of this investigation, this approach may be either crucial for providing information regarding the myocardial cell but criticisable when assessing whole body physiology.

Our molecular investigations used whole heart tissue and also isolated cardiomyocytes. The use of AMPK inhibitor Compound C appeared to produce non-specific effects on PGC-1α expression. Therefore, for definite clarification of the relationship between AMPK and PGC-1α expression and activity in the heart, the studies should use cell systems in which genetic silencing or genetic ablation of AMPK had been previously induced.

Unfortunately, time constraints and animal limitations did not allow us to assess the effect of chronic metformin treatment on myocardial ischaemia-reperfusion injury in young diabetic and non-diabetic animals.

Chronic administration of sitagliptin prior to *in vivo* coronary artery ligation provided a more translational model to investigate cardioprotection in diabetes. However, this study is in the early stages and did not examine the possible signalling mechanisms behind the apparent glucose-dependency of cardioprotection with this agent. However, glucose-clamping experiments would determine the absolute requirement of hyperglycaemia for the protective effects of sitagliptin.

Another approach which can circumvent the rapid metabolism of drugs by the rodent liver, and therefore reducing the absolute effect of the treatment, could be the use of implanted osmotic pumps when investigating chronic treatments with pharmacological agents.

5.3 Future directions

In addition to the possible additional work discussed in the limitations section, which will confirm and improve the data already reported, there are some possible crucial further directions which emerged from these studies. It would be important to examine whether the findings are reproducible in an *in vivo* left coronary artery occlusion-reperfusion model. To additionally explore the detrimental effects of chronic Akt phosphorylation in respect to IRI, mitochondrial permeability transition pore (mPTP) opening in aged, diabetic cardiomyocytes needs to be investigated. Furthermore, immunoprecipitation experiments could investigate whether the PGC-1α protein is modified at the post-translational level in the aged, diabetic heart and the use of pharmacological agents or genetic manipulations could determine the importance of Akt-phosphorylation in these processes.

Of upmost interest is the investigation of the upstream cause of chronic Akt phosphorylation in the aged, diabetic myocardium and whether reducing this

phosphorylation by pharmacological inhibition would reduce the susceptibility to infarction and also restore the ability to condition the heart with ischaemic preconditioning. More importantly, human heart tissue from cardiac surgery should be assessed to verify if chronic Akt phosphorylation is also present in the human aged, diabetic myocardium

To assess whether the chronic protective effects of metformin treatment exist in the young diabetic and non-diabetic rats would also enhance this area of research. Furthermore, to evaluate whether the basal changes in PGC-1α expression are associated to age and/or diabetes as early stages of diabetes are associated with increased PGC-1α expression. To further elucidate the importance of PGC-1α in the cardioprotective benefits of metformin treatment, it would be interesting to treat PGC-1α deficient mice with metformin and determine their susceptibility to ischaemia-reperfusion injury.

The findings of the chronic sitagliptin study are preliminary but suggest a potentially translational important finding. An interesting study would be to treat long term with this agent to normalise blood glucose levels and to then determine the susceptibility to IRI. Alternatively, using glucose clamps alongside the addition of DPP-4 inhibitors and other known targets of DPP-4 degradation will help to tease out the mechanisms behind the apparent glucose dependency of this agent.

Reference List

1. **Levick JR. An Introduction to Cardiovascular Physiology. 2010.**

2. **Hanson RW. The Role of ATP in Metabolism. *Biochemical Education* 1989;17:86-92.**

3. **Lopaschuk GD, Ussher JR, Folmes CD, Jaswal JS, Stanley WC. Myocardial fatty acid metabolism in health and disease. *Physiol Rev* 2010;90:207-258.**

4. **World Health Organisation. Global atlas on cardiovascular disease prevention and control. 2011.**

5. **Bonneux L, Barendregt JJ, Meeter K, Bonsel GJ, van der Maas PJ. Estimating clinical morbidity due to ischemic heart disease and congestive heart failure: the future rise of heart failure. *Am J Public Health* 1994;84:20-28.**

6. **Keeley EC, Boura JA, Grines CL. Primary angioplasty versus intravenous thrombolytic therapy for acute myocardial infarction: a quantitative review of 23 randomised trials. *Lancet* 2003;361:13-20.**

7. **Yellon DM, Hausenloy DJ. Myocardial reperfusion injury. *N Engl J Med* 2007;357:1121-1135.**

8. **JENNINGS RB, SOMMERS HM, SMYTH GA, FLACK HA, LINN H. Myocardial necrosis induced by temporary occlusion of a coronary artery in the dog. *Arch Pathol* 1960;70:68-78.**

9. **Bolli R, Marban E. Molecular and cellular mechanisms of myocardial stunning. *Physiol Rev* 1999;79:609-634.**

10. **Ito H. No-reflow phenomenon and prognosis in patients with acute myocardial infarction. *Nat Clin Pract Cardiovasc Med* 2006;3:499-506.**

11. **Krug A, Du Mesnil dR, Korb G. Blood supply of the myocardium after temporary coronary occlusion. *Circ Res* 1966;19:57-62.**

12. **Heusch G, Kleinbongard P, Bose D, Levkau B, Haude M, Schulz R, et al. Coronary microembolization: from bedside to bench and back to bedside. *Circulation* 2009;120:1822-1836.**

13. **Manning AS, Hearse DJ. Reperfusion-induced arrhythmias: mechanisms and prevention. *J Mol Cell Cardiol* 1984;16:497-518.**

14. **Hearse DJ, Tosaki A. Free radicals and reperfusion-induced arrhythmias: protection by spin trap agent PBN in the rat heart. *Circ Res* 1987;60:375-383.**

15. **John RM, Tedrow UB, Koplan BA, Albert CM, Epstein LM, Sweeney MO, et al. Ventricular arrhythmias and sudden cardiac death. *Lancet* 2012;380:1520-1529.**

16. **Grover GJ, Atwal KS, Sleph PG, Wang FL, Monshizadegan H, Monticello T, et al. Excessive ATP hydrolysis in ischemic myocardium by mitochondrial F1F0-ATPase: effect of selective pharmacological inhibition of mitochondrial ATPase hydrolase activity. *Am J Physiol Heart Circ Physiol* 2004;287:H1747-H1755.**

17. **Murphy E, Steenbergen C. Mechanisms underlying acute protection from cardiac ischemia-reperfusion injury. *Physiol Rev* 2008;88:581-609.**

18. **Reimer KA, JENNINGS RB. The "wavefront phenomenon" of myocardial ischemic cell death. II. Transmural progression of necrosis within the framework of ischemic bed size (myocardium at risk) and collateral flow. *Lab Invest* 1979;40:633-644.**

19. **Ytrehus K, Liu Y, Tsuchida A, Miura T, Liu GS, Yang XM, et al. Rat and rabbit heart infarction: effects of anesthesia, perfusate, risk zone, and method of infarct sizing. *Am J Physiol* 1994;267:H2383-H2390.**

20. **Miki T, Liu GS, Cohen MV, Downey JM. Mild hypothermia reduces infarct size in the beating rabbit heart: a practical intervention for acute myocardial infarction? *Basic Res Cardiol* 1998;93:372-383.**

21. **Hearse DJ, Humphrey SM, Chain EB. Abrupt reoxygenation of the anoxic potassium-arrested perfused rat heart: a study of myocardial enzyme release. *J Mol Cell Cardiol* 1973;5:395-407.**

22. **Murphy MP. How mitochondria produce reactive oxygen species. *Biochem J* 2009;417:1-13.**

23. **Li JM, Shah AM. Endothelial cell superoxide generation: regulation and relevance for cardiovascular pathophysiology. *Am J Physiol Regul Integr Comp Physiol* 2004;287:R1014-R1030.**

24. **Braunersreuther V, Jaquet V. Reactive oxygen species in myocardial reperfusion injury: from physiopathology to therapeutic approaches. *Curr Pharm Biotechnol* 2012;13:97-114.**

25. **Forstermann U. Nitric oxide and oxidative stress in vascular disease. *Pflugers Arch* 2010;459:923-939.**

26. **Zweier JL, Talukder MA. The role of oxidants and free radicals in reperfusion injury. *Cardiovasc Res* 2006;70:181-190.**

27. **Inserte J, Barba I, Hernando V, Abellan A, Ruiz-Meana M, Rodriguez-Sinovas A, et al. Effect of acidic reperfusion on prolongation of intracellular acidosis and myocardial salvage. *Cardiovasc Res* 2008;77:782-790.**

28. **Ong SB, Hall AR, Hausenloy DJ. Mitochondrial Dynamics in Cardiovascular Health and Disease. *Antioxid Redox Signal* 2012.**

29. **Ong SB, Hausenloy DJ. Mitochondrial morphology and cardiovascular disease. *Cardiovasc Res* 2010;88:16-29.**

30. **Smirnova E, Griparic L, Shurland DL, van der Bliek AM. Dynamin-related protein Drp1 is required for mitochondrial division in mammalian cells. *Mol Biol Cell* 2001;12:2245-2256.**

31. **Yoon Y, Krueger EW, Oswald BJ, McNiven MA. The mitochondrial protein hFis1 regulates mitochondrial fission in mammalian cells through an interaction with the dynamin-like protein DLP1. *Mol Cell Biol* 2003;23:5409-5420.**

32. **Chen H, Detmer SA, Ewald AJ, Griffin EE, Fraser SE, Chan DC. Mitofusins Mfn1 and Mfn2 coordinately regulate mitochondrial fusion and are essential for embryonic development. *J Cell Biol* 2003;160:189-200.**

33. **Cipolat S, Martins de BO, Dal ZB, Scorrano L. OPA1 requires mitofusin 1 to promote mitochondrial fusion. *Proc Natl Acad Sci U S A* 2004;101:15927-15932.**

34. **de Brito OM, Scorrano L. Mitofusin 2 tethers endoplasmic reticulum to mitochondria. *Nature* 2008;456:605-610.**

35. **Ong SB, Subrayan S, Lim SY, Yellon DM, Davidson SM, Hausenloy DJ. Inhibiting mitochondrial fission protects the heart against ischemia/reperfusion injury. *Circulation* 2010;121:2012-2022.**

36. **Whelan RS, Konstantinidis K, Wei AC, Chen Y, Reyna DE, Jha S, et al. Bax regulates primary necrosis through mitochondrial dynamics. *Proc Natl Acad Sci U S A* 2012;109:6566-6571.**

37. **Papanicolaou KN, Khairallah RJ, Ngoh GA, Chikando A, Luptak I, O'Shea KM, et al. Mitofusin-2 maintains mitochondrial structure and contributes to stress-induced permeability transition in cardiac myocytes. *Mol Cell Biol* 2011;31:1309-1328.**

38. **Papanicolaou KN, Ngoh GA, Dabkowski ER, O'Connell KA, Ribeiro RF, Jr., Stanley WC, et al. Cardiomyocyte deletion of mitofusin-1 leads to mitochondrial fragmentation and improves tolerance to ROS-induced mitochondrial dysfunction and cell death. *Am J Physiol Heart Circ Physiol* 2012;302:H167-H179.**

39. **Ventura-Clapier R, Garnier A, Veksler V. Transcriptional control of mitochondrial biogenesis: the central role of PGC-1alpha. *Cardiovasc Res* 2008;79:208-217.**

40. **Petersen KF, Befroy D, Dufour S, Dziura J, Ariyan C, Rothman DL, et al. Mitochondrial dysfunction in the elderly: possible role in insulin resistance. *Science* 2003;300:1140-1142.**

41. **Kelly DP, Scarpulla RC. Transcriptional regulatory circuits controlling mitochondrial biogenesis and function. *Genes Dev* 2004;18:357-368.**

42. **Finck BN, Kelly DP. Peroxisome proliferator-activated receptor gamma coactivator-1 (PGC-1) regulatory cascade in cardiac physiology and disease. *Circulation* 2007;115:2540-2548.**

43. **Puigserver P, Wu Z, Park CW, Graves R, Wright M, Spiegelman BM. A cold-inducible coactivator of nuclear receptors linked to adaptive thermogenesis. *Cell* 1998;92:829-839.**

44. Wu Z, Puigserver P, Andersson U, Zhang C, Adelmant G, Mootha V, et al. Mechanisms controlling mitochondrial biogenesis and respiration through the thermogenic coactivator PGC-1. *Cell* 1999;98:115-124.

45. Manoli I, Alesci S, Blackman MR, Su YA, Rennert OM, Chrousos GP. Mitochondria as key components of the stress response. *Trends Endocrinol Metab* 2007;18:190-198.

46. Green DR, Kroemer G. The pathophysiology of mitochondrial cell death. *Science* 2004;305:626-629.

47. Vandecasteele G, Szabadkai G, Rizzuto R. Mitochondrial calcium homeostasis: mechanisms and molecules. *IUBMB Life* 2001;52:213-219.

48. Lee HC, Wei YH. Mitochondria and aging. *Adv Exp Med Biol* 2012;942:311-327.

49. Lowell BB, Shulman GI. Mitochondrial dysfunction and type 2 diabetes. *Science* 2005;307:384-387.

50. Weiss JN, Korge P, Honda HM, Ping P. Role of the mitochondrial permeability transition in myocardial disease. *Circ Res* 2003;93:292-301.

51. Krauss S, Zhang CY, Lowell BB. The mitochondrial uncoupling-protein homologues. *Nat Rev Mol Cell Biol* 2005;6:248-261.

52. Brand MD, Pakay JL, Ocloo A, Kokoszka J, Wallace DC, Brookes PS, et al. The basal proton conductance of mitochondria depends on adenine nucleotide translocase content. *Biochem J* 2005;392:353-362.

53. Kadenbach B, Huttemann M, Arnold S, Lee I, Bender E. Mitochondrial energy metabolism is regulated via nuclear-coded subunits of cytochrome c oxidase. *Free Radic Biol Med* 2000;29:211-221.

54. O'Rourke B. Mitochondrial ion channels. *Annu Rev Physiol* 2007;69:19-49.

55. Patergnani S, Suski JM, Agnoletto C, Bononi A, Bonora M, De ME, et al. Calcium signaling around Mitochondria Associated Membranes (MAMs). *Cell Commun Signal* 2011;9:19-.

56. Kirichok Y, Krapivinsky G, Clapham DE. The mitochondrial calcium uniporter is a highly selective ion channel. *Nature* 2004;427:360-364.

57. Cortassa S, Aon MA, Marban E, Winslow RL, O'Rourke B. An integrated model of cardiac mitochondrial energy metabolism and calcium dynamics. *Biophys J* 2003;84:2734-2755.

58. O'Rourke B. Evidence for mitochondrial K+ channels and their role in cardioprotection. *Circ Res* 2004;94:420-432.

59. Beavis AD, Powers M. Temperature dependence of the mitochondrial inner membrane anion channel: the relationship between

temperature and inhibition by magnesium. *J Biol Chem* 2004;279:4045-4050.

60. O'Rourke B, Cortassa S, Aon MA. Mitochondrial ion channels: gatekeepers of life and death. *Physiology (Bethesda)* 2005;20:303-315.

61. Haworth RA, Hunter DR. The Ca2+-induced membrane transition in mitochondria. II. Nature of the Ca2+ trigger site. *Arch Biochem Biophys* 1979;195:460-467.

62. Crompton M, Costi A, Hayat L. Evidence for the presence of a reversible Ca2+-dependent pore activated by oxidative stress in heart mitochondria. *Biochem J* 1987;245:915-918.

63. Halestrap AP. What is the mitochondrial permeability transition pore? *J Mol Cell Cardiol* 2009;46:821-831.

64. Siemen D, Ziemer M. What is the nature of the mitochondrial permeability transition pore and what is it not? *IUBMB Life* 2013;65:255-262.

65. Lemasters JJ, Theruvath TP, Zhong Z, Nieminen AL. Mitochondrial calcium and the permeability transition in cell death. *Biochim Biophys Acta* 2009;1787:1395-1401.

66. Kokoszka JE, Waymire KG, Levy SE, Sligh JE, Cai J, Jones DP, et al. The ADP/ATP translocator is not essential for the mitochondrial permeability transition pore. *Nature* 2004;427:461-465.

67. Baines CP, Kaiser RA, Sheiko T, Craigen WJ, Molkentin JD. Voltage-dependent anion channels are dispensable for mitochondrial-dependent cell death. *Nat Cell Biol* 2007;9:550-555.

68. Kinnally KW, Zorov DB, Antonenko YN, Snyder SH, McEnery MW, Tedeschi H. Mitochondrial benzodiazepine receptor linked to inner membrane ion channels by nanomolar actions of ligands. *Proc Natl Acad Sci U S A* 1993;90:1374-1378.

69. Giorgio V, Soriano ME, Basso E, Bisetto E, Lippe G, Forte MA, et al. Cyclophilin D in mitochondrial pathophysiology. *Biochim Biophys Acta* 2010;1797:1113-1118.

70. Rasola A, Bernardi P. Mitochondrial permeability transition in Ca(2+)-dependent apoptosis and necrosis. *Cell Calcium* 2011;50:222-233.

71. Eliseev RA, Malecki J, Lester T, Zhang Y, Humphrey J, Gunter TE. Cyclophilin D interacts with Bcl2 and exerts an anti-apoptotic effect. *J Biol Chem* 2009;284:9692-9699.

72. Vaseva AV, Marchenko ND, Ji K, Tsirka SE, Holzmann S, Moll UM. p53 opens the mitochondrial permeability transition pore to trigger necrosis. *Cell* 2012;149:1536-1548.

73. Rasola A, Sciacovelli M, Chiara F, Pantic B, Brusilow WS, Bernardi P. Activation of mitochondrial ERK protects cancer cells from death through inhibition of the permeability transition. *Proc Natl Acad Sci U S A* 2010;107:726-731.

74. **Giorgio V, Bisetto E, Soriano ME, Dabbeni-Sala F, Basso E, Petronilli V, et al. Cyclophilin D modulates mitochondrial F0F1-ATP synthase by interacting with the lateral stalk of the complex. *J Biol Chem* 2009;284:33982-33988.**

75. **Giorgio V, von SS, Antoniel M, Fabbro A, Fogolari F, Forte M, et al. Dimers of mitochondrial ATP synthase form the permeability transition pore. *Proc Natl Acad Sci U S A* 2013;110:5887-5892.**

76. **Bernardi P. The mitochondrial permeability transition pore: a mystery solved? *Front Physiol* 2013;4:95-.**

77. **Di LF, Bernardi P. Mitochondria and ischemia-reperfusion injury of the heart: fixing a hole. *Cardiovasc Res* 2006;70:191-199.**

78. **Lin J, Puigserver P, Donovan J, Tarr P, Spiegelman BM. Peroxisome proliferator-activated receptor gamma coactivator 1beta (PGC-1beta), a novel PGC-1-related transcription coactivator associated with host cell factor. *J Biol Chem* 2002;277:1645-1648.**

79. **Kressler D, Schreiber SN, Knutti D, Kralli A. The PGC-1-related protein PERC is a selective coactivator of estrogen receptor alpha. *J Biol Chem* 2002;277:13918-13925.**

80. **Andersson U, Scarpulla RC. Pgc-1-related coactivator, a novel, serum-inducible coactivator of nuclear respiratory factor 1-dependent transcription in mammalian cells. *Mol Cell Biol* 2001;21:3738-3749.**

81. **Wallberg AE, Yamamura S, Malik S, Spiegelman BM, Roeder RG. Coordination of p300-mediated chromatin remodeling and TRAP/mediator function through coactivator PGC-1alpha. *Mol Cell* 2003;12:1137-1149.**

82. **Monsalve M, Wu Z, Adelmant G, Puigserver P, Fan M, Spiegelman BM. Direct coupling of transcription and mRNA processing through the thermogenic coactivator PGC-1. *Mol Cell* 2000;6:307-316.**

83. **Lin J, Handschin C, Spiegelman BM. Metabolic control through the PGC-1 family of transcription coactivators. *Cell Metab* 2005;1:361-370.**

84. **Handschin C, Rhee J, Lin J, Tarr PT, Spiegelman BM. An autoregulatory loop controls peroxisome proliferator-activated receptor gamma coactivator 1alpha expression in muscle. *Proc Natl Acad Sci U S A* 2003;100:7111-7116.**

85. **Schaeffer PJ, Wende AR, Magee CJ, Neilson JR, Leone TC, Chen F, et al. Calcineurin and calcium/calmodulin-dependent protein kinase activate distinct metabolic gene regulatory programs in cardiac muscle. *J Biol Chem* 2004;279:39593-39603.**

86. **Zong H, Ren JM, Young LH, Pypaert M, Mu J, Birnbaum MJ, et al. AMP kinase is required for mitochondrial biogenesis in skeletal muscle in response to chronic energy deprivation. *Proc Natl Acad Sci U S A* 2002;99:15983-15987.**

87. Mihaylova MM, Shaw RJ. The AMPK signalling pathway coordinates cell growth, autophagy and metabolism. *Nat Cell Biol* 2011;13:1016-1023.

88. Jorgensen SB, Wojtaszewski JF, Viollet B, Andreelli F, Birk JB, Hellsten Y, et al. Effects of alpha-AMPK knockout on exercise-induced gene activation in mouse skeletal muscle. *FASEB J* 2005;19:1146-1148.

89. Suwa M, Nakano H, Kumagai S. Effects of chronic AICAR treatment on fiber composition, enzyme activity, UCP3, and PGC-1 in rat muscles. *J Appl Physiol* 2003;95:960-968.

90. Jager S, Handschin C, St-Pierre J, Spiegelman BM. AMP-activated protein kinase (AMPK) action in skeletal muscle via direct phosphorylation of PGC-1alpha. *Proc Natl Acad Sci U S A* 2007;104:12017-12022.

91. Irrcher I, Ljubicic V, Kirwan AF, Hood DA. AMP-activated protein kinase-regulated activation of the PGC-1alpha promoter in skeletal muscle cells. *PLoS One* 2008;3:e3614-.

92. Czubryt MP, McAnally J, Fishman GI, Olson EN. Regulation of peroxisome proliferator-activated receptor gamma coactivator 1 alpha (PGC-1 alpha) and mitochondrial function by MEF2 and HDAC5. *Proc Natl Acad Sci U S A* 2003;100:1711-1716.

93. Southgate RJ, Bruce CR, Carey AL, Steinberg GR, Walder K, Monks R, et al. PGC-1alpha gene expression is down-regulated by Akt-mediated phosphorylation and nuclear exclusion of FoxO1 in insulin-stimulated skeletal muscle. *FASEB J* 2005;19:2072-2074.

94. Fernandez-Marcos PJ, Auwerx J. Regulation of PGC-1alpha, a nodal regulator of mitochondrial biogenesis. *Am J Clin Nutr* 2011;93:884S-8890.

95. Cai R, Yu T, Huang C, Xia X, Liu X, Gu J, et al. SUMO-specific protease 1 regulates mitochondrial biogenesis through PGC-1alpha. *J Biol Chem* 2012;287:44464-44470.

96. Puigserver P, Rhee J, Lin J, Wu Z, Yoon JC, Zhang CY, et al. Cytokine stimulation of energy expenditure through p38 MAP kinase activation of PPARgamma coactivator-1. *Mol Cell* 2001;8:971-982.

97. Fan M, Rhee J, St-Pierre J, Handschin C, Puigserver P, Lin J, et al. Suppression of mitochondrial respiration through recruitment of p160 myb binding protein to PGC-1alpha: modulation by p38 MAPK. *Genes Dev* 2004;18:278-289.

98. Li X, Monks B, Ge Q, Birnbaum MJ. Akt/PKB regulates hepatic metabolism by directly inhibiting PGC-1alpha transcription coactivator. *Nature* 2007;447:1012-1016.

99. Rodgers JT, Haas W, Gygi SP, Puigserver P. Cdc2-like kinase 2 is an insulin-regulated suppressor of hepatic gluconeogenesis. *Cell Metab* 2010;11:23-34.

100. Anderson RM, Barger JL, Edwards MG, Braun KH, O'Connor CE, Prolla TA, et al. Dynamic regulation of PGC-1alpha localization and turnover implicates mitochondrial adaptation in calorie restriction and the stress response. *Aging Cell* 2008;7:101-111.

101. Canto C, Gerhart-Hines Z, Feige JN, Lagouge M, Noriega L, Milne JC, et al. AMPK regulates energy expenditure by modulating NAD+ metabolism and SIRT1 activity. *Nature* 2009;458:1056-1060.

102. Fulco M, Cen Y, Zhao P, Hoffman EP, McBurney MW, Sauve AA, et al. Glucose restriction inhibits skeletal myoblast differentiation by activating SIRT1 through AMPK-mediated regulation of Nampt. *Dev Cell* 2008;14:661-673.

103. Lehman JJ, Barger PM, Kovacs A, Saffitz JE, Medeiros DM, Kelly DP. Peroxisome proliferator-activated receptor gamma coactivator-1 promotes cardiac mitochondrial biogenesis. *J Clin Invest* 2000;106:847-856.

104. Russell LK, Mansfield CM, Lehman JJ, Kovacs A, Courtois M, Saffitz JE, et al. Cardiac-specific induction of the transcriptional coactivator peroxisome proliferator-activated receptor gamma coactivator-1alpha promotes mitochondrial biogenesis and reversible cardiomyopathy in a developmental stage-dependent manner. *Circ Res* 2004;94:525-533.

105. Arany Z, He H, Lin J, Hoyer K, Handschin C, Toka O, et al. Transcriptional coactivator PGC-1 alpha controls the energy state and contractile function of cardiac muscle. *Cell Metab* 2005;1:259-271.

106. Ventura-Clapier R, Garnier A, Veksler V. Energy metabolism in heart failure. *J Physiol* 2004;555:1-13.

107. Garnier A, Fortin D, Delomenie C, Momken I, Veksler V, Ventura-Clapier R. Depressed mitochondrial transcription factors and oxidative capacity in rat failing cardiac and skeletal muscles. *J Physiol* 2003;551:491-501.

108. Leone TC, Lehman JJ, Finck BN, Schaeffer PJ, Wende AR, Boudina S, et al. PGC-1alpha deficiency causes multi-system energy metabolic derangements: muscle dysfunction, abnormal weight control and hepatic steatosis. *PLoS Biol* 2005;3:e101-.

109. St-Pierre J, Drori S, Uldry M, Silvaggi JM, Rhee J, Jager S, et al. Suppression of reactive oxygen species and neurodegeneration by the PGC-1 transcriptional coactivators. *Cell* 2006;127:397-408.

110. Valle I, Alvarez-Barrientos A, Arza E, Lamas S, Monsalve M. PGC-1alpha regulates the mitochondrial antioxidant defense system in vascular endothelial cells. *Cardiovasc Res* 2005;66:562-573.

111. Eguchi Y, Srinivasan A, Tomaselli KJ, Shimizu S, Tsujimoto Y. ATP-dependent steps in apoptotic signal transduction. *Cancer Res* 1999;59:2174-2181.

112. Kajstura J, Cheng W, Reiss K, Clark WA, Sonnenblick EH, Krajewski S, et al. Apoptotic and necrotic myocyte cell deaths are independent contributing variables of infarct size in rats. *Lab Invest* 1996;74:86-107.

113. McCully JD, Wakiyama H, Hsieh YJ, Jones M, Levitsky S. Differential contribution of necrosis and apoptosis in myocardial ischemia-reperfusion injury. *Am J Physiol Heart Circ Physiol* 2004;286:H1923-H1935.

114. Edinger AL, Thompson CB. Death by design: apoptosis, necrosis and autophagy. *Curr Opin Cell Biol* 2004;16:663-669.

115. Lemasters JJ, Qian T, He L, Kim JS, Elmore SP, Cascio WE, et al. Role of mitochondrial inner membrane permeabilization in necrotic cell death, apoptosis, and autophagy. *Antioxid Redox Signal* 2002;4:769-781.

116. Jeremias I, Kupatt C, Martin-Villalba A, Habazettl H, Schenkel J, Boekstegers P, et al. Involvement of CD95/Apo1/Fas in cell death after myocardial ischemia. *Circulation* 2000;102:915-920.

117. Tait SW, Green DR. Mitochondria and cell death: outer membrane permeabilization and beyond. *Nat Rev Mol Cell Biol* 2010;11:621-632.

118. Levine B, Kroemer G. Autophagy in the pathogenesis of disease. *Cell* 2008;132:27-42.

119. Hariharan N, Zhai P, Sadoshima J. Oxidative stress stimulates autophagic flux during ischemia/reperfusion. *Antioxid Redox Signal* 2011;14:2179-2190.

120. Zhao T, Huang X, Han L, Wang X, Cheng H, Zhao Y, et al. Central role of mitofusin 2 in autophagosome-lysosome fusion in cardiomyocytes. *J Biol Chem* 2012;287:23615-23625.

121. Huang C, Yitzhaki S, Perry CN, Liu W, Giricz Z, Mentzer RM, Jr., et al. Autophagy induced by ischemic preconditioning is essential for cardioprotection. *J Cardiovasc Transl Res* 2010;3:365-373.

122. Lemasters JJ. V. Necrapoptosis and the mitochondrial permeability transition: shared pathways to necrosis and apoptosis. *Am J Physiol* 1999;276:G1-G6.

123. Yellon DM, Downey JM. Preconditioning the myocardium: from cellular physiology to clinical cardiology. *Physiol Rev* 2003;83:1113-1151.

124. Murry CE, Jennings RB, Reimer KA. Preconditioning with ischemia: a delay of lethal cell injury in ischemic myocardium. *Circulation* 1986;74:1124-1136.

125. Baxter GF, Marber MS, Patel VC, Yellon DM. Adenosine receptor involvement in a delayed phase of myocardial protection 24 hours after ischemic preconditioning. *Circulation* 1994;90:2993-3000.

126. Yellon DM, Baxter GF. A "second window of protection" or delayed preconditioning phenomenon: future horizons for myocardial protection? *J Mol Cell Cardiol* 1995;27:1023-1034.

127. Hausenloy DJ, Yellon DM. The therapeutic potential of ischemic conditioning: an update. *Nat Rev Cardiol* 2011.

128. Ovize M, Baxter GF, Di Lisa F, Ferdinandy P, Garcia-Dorado D, Hausenloy DJ, et al. Postconditioning and protection from reperfusion injury: where do we stand? Position paper from the Working Group of Cellular Biology of the Heart of the European Society of Cardiology. *Cardiovasc Res* 2010;87:406-423.

129. Hausenloy DJ, Yellon DM. Remote ischaemic preconditioning: underlying mechanisms and clinical application. *Cardiovasc Res* 2008;79:377-386.

130. Downey JM, Davis AM, Cohen MV. Signaling pathways in ischemic preconditioning. *Heart Fail Rev* 2007;12:181-188.

131. Liu GS, Thornton J, Van Winkle DM, Stanley AW, Olsson RA, Downey JM. Protection against infarction afforded by preconditioning is mediated by A1 adenosine receptors in rabbit heart. *Circulation* 1991;84:350-356.

132. Wall TM, Sheehy R, Hartman JC. Role of bradykinin in myocardial preconditioning. *J Pharmacol Exp Ther* 1994;270:681-689.

133. Schultz JE, Rose E, Yao Z, Gross GJ. Evidence for involvement of opioid receptors in ischemic preconditioning in rat hearts. *Am J Physiol* 1995;268:H2157-H2161.

134. Hausenloy DJ, Yellon DM. New directions for protecting the heart against ischaemia-reperfusion injury: targeting the Reperfusion Injury Salvage Kinase (RISK)-pathway. *Cardiovasc Res* 2004;61:448-460.

135. Tong H, Chen W, Steenbergen C, Murphy E. Ischemic preconditioning activates phosphatidylinositol-3-kinase upstream of protein kinase C. *Circ Res* 2000;87:309-315.

136. Mocanu MM, Bell RM, Yellon DM. PI3 kinase and not p42/p44 appears to be implicated in the protection conferred by ischemic preconditioning. *J Mol Cell Cardiol* 2002;34:661-668.

137. Andjelkovic M, Alessi DR, Meier R, Fernandez A, Lamb NJ, Frech M, et al. Role of translocation in the activation and function of protein kinase B. *J Biol Chem* 1997;272:31515-31524.

138. Hlobilkova A, Knillova J, Bartek J, Lukas J, Kolar Z. The mechanism of action of the tumour suppressor gene PTEN. *Biomed Pap Med Fac Univ Palacky Olomouc Czech Repub* 2003;147:19-25.

139. Sussman MA, Volkers M, Fischer K, Bailey B, Cottage CT, Din S, et al. Myocardial AKT: the omnipresent nexus. *Physiol Rev* 2011;91:1023-1070.

140. Costa AD, Garlid KD, West IC, Lincoln TM, Downey JM, Cohen MV, et al. Protein kinase G transmits the cardioprotective signal from cytosol to mitochondria. *Circ Res* 2005;97:329-336.

141. Murphy E, Steenbergen C. Preconditioning: the mitochondrial connection. *Annu Rev Physiol* 2007;69:51-67.

142. Aikawa R, Nawano M, Gu Y, Katagiri H, Asano T, Zhu W, et al. Insulin prevents cardiomyocytes from oxidative stress-induced apoptosis through activation of PI3 kinase/Akt. *Circulation* 2000;102:2873-2879.

143. Arokium H, Ouerfelli H, Velours G, Camougrand N, Vallette FM, Manon S. Substitutions of potentially phosphorylatable serine residues of Bax reveal how they may regulate its interaction with mitochondria. *J Biol Chem* 2007;282:35104-35112.

144. Hochhauser E, Kivity S, Offen D, Maulik N, Otani H, Barhum Y, et al. Bax ablation protects against myocardial ischemia-reperfusion injury in transgenic mice. *Am J Physiol Heart Circ Physiol* 2003;284:H2351-H2359.

145. Caporali A, Sala-Newby GB, Meloni M, Graiani G, Pani E, Cristofaro B, et al. Identification of the prosurvival activity of nerve growth factor on cardiac myocytes. *Cell Death Differ* 2008;15:299-311.

146. Nadtochiy SM, Yao H, McBurney MW, Gu W, Guarente L, Rahman I, et al. SIRT1-mediated acute cardioprotection. *Am J Physiol Heart Circ Physiol* 2011;301:H1506-H1512.

147. Hsu CP, Zhai P, Yamamoto T, Maejima Y, Matsushima S, Hariharan N, et al. Silent information regulator 1 protects the heart from ischemia/reperfusion. *Circulation* 2010;122:2170-2182.

148. Nadtochiy SM, Redman E, Rahman I, Brookes PS. Lysine deacetylation in ischaemic preconditioning: the role of SIRT1. *Cardiovasc Res* 2011;89:643-649.

149. Sciarretta S, Hariharan N, Monden Y, Zablocki D, Sadoshima J. Is autophagy in response to ischemia and reperfusion protective or detrimental for the heart? *Pediatr Cardiol* 2011;32:275-281.

150. Murry CE, JENNINGS RB, Reimer KA. New insights into potential mechanisms of ischemic preconditioning. *Circulation* 1991;84:442-445.

151. Hausenloy DJ, Tsang A, Mocanu MM, Yellon DM. Ischemic preconditioning protects by activating prosurvival kinases at reperfusion. *Am J Physiol Heart Circ Physiol* 2005;288:H971-H976.

152. Hausenloy DJ, Tsang A, Yellon DM. The reperfusion injury salvage kinase pathway: a common target for both ischemic preconditioning and postconditioning. *Trends Cardiovasc Med* 2005;15:69-75.

153. Darling CE, Jiang R, Maynard M, Whittaker P, Vinten-Johansen J, Przyklenk K. Postconditioning via stuttering reperfusion limits

myocardial infarct size in rabbit hearts: role of ERK1/2. *Am J Physiol Heart Circ Physiol* 2005;289:H1618-H1626.

154. Lacerda L, Somers S, Opie LH, Lecour S. Ischaemic postconditioning protects against reperfusion injury via the SAFE pathway. *Cardiovasc Res* 2009;84:201-208.

155. Lecour S. Activation of the protective Survivor Activating Factor Enhancement (SAFE) pathway against reperfusion injury: Does it go beyond the RISK pathway? *J Mol Cell Cardiol* 2009;47:32-40.

156. Oxman T, Arad M, Klein R, Avazov N, Rabinowitz B. Limb ischemia preconditions the heart against reperfusion tachyarrhythmia. *Am J Physiol* 1997;273:H1707-H1712.

157. Schmidt MR, Smerup M, Konstantinov IE, Shimizu M, Li J, Cheung M, et al. Intermittent peripheral tissue ischemia during coronary ischemia reduces myocardial infarction through a KATP-dependent mechanism: first demonstration of remote ischemic perconditioning. *Am J Physiol Heart Circ Physiol* 2007;292:H1883-H1890.

158. Andreka G, Vertesaljai M, Szantho G, Font G, Piroth Z, Fontos G, et al. Remote ischaemic postconditioning protects the heart during acute myocardial infarction in pigs. *Heart* 2007;93:749-752.

159. Lim SY, Hausenloy DJ. Remote ischemic conditioning: from bench to bedside. *Front Physiol* 2012;3:27-.

160. Takemoto M, Liao JK. Pleiotropic effects of 3-hydroxy-3-methylglutaryl coenzyme a reductase inhibitors. *Arterioscler Thromb Vasc Biol* 2001;21:1712-1719.

161. Liu YH, Yang XP, Sharov VG, Sigmon DH, Sabbath HN, Carretero OA. Paracrine systems in the cardioprotective effect of angiotensin-converting enzyme inhibitors on myocardial ischemia/reperfusion injury in rats. *Hypertension* 1996;27:7-13.

162. Bell RM, Yellon DM. Atorvastatin, administered at the onset of reperfusion, and independent of lipid lowering, protects the myocardium by up-regulating a pro-survival pathway. *J Am Coll Cardiol* 2003;41:508-515.

163. Hartman JC. The role of bradykinin and nitric oxide in the cardioprotective action of ACE inhibitors. *Ann Thorac Surg* 1995;60:789-792.

164. Bell RM, Yellon DM. Bradykinin limits infarction when administered as an adjunct to reperfusion in mouse heart: the role of PI3K, Akt and eNOS. *J Mol Cell Cardiol* 2003;35:185-193.

165. Bernier SG, Haldar S, Michel T. Bradykinin-regulated interactions of the mitogen-activated protein kinase pathway with the endothelial nitric-oxide synthase. *J Biol Chem* 2000;275:30707-30715.

166. Bianchi C, Miccoli R, Daniele G, Penno G, Del PS. Is there evidence that oral hypoglycemic agents reduce cardiovascular

morbidity/mortality? Yes. *Diabetes Care* 2009;32 Suppl 2:S342-S348.

167. International Diabetes Federation . In: 2009.

168. Diabetes UK. Diabetes in the UK 2010, Key statistics on diabetes. In: 2010.

169. International Diabetes Federation. In: Diabetes Atlas, Fourth Edition, 2009.

170. Notkins AL, Lernmark A. Autoimmune type 1 diabetes: resolved and unresolved issues. *J Clin Invest* 2001;108:1247-1252.

171. Goldstein BJ. Insulin resistance as the core defect in type 2 diabetes mellitus. *Am J Cardiol* 2002;90:3G-10G.

172. D'Alessio D. The role of dysregulated glucagon secretion in type 2 diabetes. *Diabetes Obes Metab* 2011;13 Suppl 1:126-132.

173. Fagot-Campagna A, Narayan KM, Imperatore G. Type 2 diabetes in children. *BMJ* 2001;322:377-378.

174. Hess K, Marx N, Lehrke M. Cardiovascular disease and diabetes: the vulnerable patient. *European Heart Journal Supplements* 2012;14 (Supplement B):B4-B13.

175. Schalkwijk CG, Stehouwer CD. Vascular complications in diabetes mellitus: the role of endothelial dysfunction. *Clin Sci (Lond)* 2005;109:143-159.

176. Kaiser N, Sasson S, Feener EP, Boukobza-Vardi N, Higashi S, Moller DE, et al. Differential regulation of glucose transport and transporters by glucose in vascular endothelial and smooth muscle cells. *Diabetes* 1993;42:80-89.

177. Dandona P, Aljada A, Chaudhuri A, Bandyopadhyay A. The potential influence of inflammation and insulin resistance on the pathogenesis and treatment of atherosclerosis-related complications in type 2 diabetes. *J Clin Endocrinol Metab* 2003;88:2422-2429.

178. Mohamed QA, Ross A, Chu CJ. Diabetic retinopathy (treatment). *Clin Evid (Online)* 2011;2011.

179. Barber AJ. A new view of diabetic retinopathy: a neurodegenerative disease of the eye. *Prog Neuropsychopharmacol Biol Psychiatry* 2003;27:283-290.

180. King GL, Brownlee M. The cellular and molecular mechanisms of diabetic complications. *Endocrinol Metab Clin North Am* 1996;25:255-270.

181. Abaci A, Oguzhan A, Kahraman S, Eryol NK, Unal S, Arinc H, et al. Effect of diabetes mellitus on formation of coronary collateral vessels. *Circulation* 1999;99:2239-2242.

182. Falanga V. Wound healing and its impairment in the diabetic foot. *Lancet* 2005;366:1736-1743.

183. Lehmann R, Schleicher ED. Molecular mechanism of diabetic nephropathy. *Clin Chim Acta* 2000;297:135-144.

184. Tan AL, Forbes JM, Cooper ME. AGE, RAGE, and ROS in diabetic nephropathy. *Semin Nephrol* 2007;27:130-143.

185. Colwell JA, Lopes-Virella M, Halushka PV. Pathogenesis of atherosclerosis in diabetes mellitus. *Diabetes Care* 1981;4:121-133.

186. Ross R. Atherosclerosis--an inflammatory disease. *N Engl J Med* 1999;340:115-126.

187. Diabetes mellitus: a major risk factor for cardiovascular disease. A joint editorial statement by the American Diabetes Association; The National Heart, Lung, and Blood Institute; The Juvenile Diabetes Foundation International; The National Institute of Diabetes and Digestive and Kidney Diseases; and The American Heart Association. *Circulation* 1999;100:1132-1133.

188. Butler R, MacDonald TM, Struthers AD, Morris AD. The clinical implications of diabetic heart disease. *Eur Heart J* 1998;19:1617-1627.

189. Marwick TH. Diabetic heart disease. *Heart* 2006;92:296-300.

190. Hayat SA, Patel B, Khattar RS, Malik RA. Diabetic cardiomyopathy: mechanisms, diagnosis and treatment. *Clin Sci (Lond)* 2004;107:539-557.

191. Chen AF, Chen DD, Daiber A, Faraci FM, Li H, Rembold CM, et al. Free radical biology of the cardiovascular system. *Clin Sci (Lond)* 2012;123:73-91.

192. Brownlee M. Biochemistry and molecular cell biology of diabetic complications. *Nature* 2001;414:813-820.

193. Giacco F, Brownlee M. Oxidative stress and diabetic complications. *Circ Res* 2010;107:1058-1070.

194. Vanhorebeek I, De VR, Mesotten D, Wouters PJ, De Wolf-Peeters C, Van den Berghe G. Protection of hepatocyte mitochondrial ultrastructure and function by strict blood glucose control with insulin in critically ill patients. *Lancet* 2005;365:53-59.

195. Kelley DE, He J, Menshikova EV, Ritov VB. Dysfunction of mitochondria in human skeletal muscle in type 2 diabetes. *Diabetes* 2002;51:2944-2950.

196. Yu T, Robotham JL, Yoon Y. Increased production of reactive oxygen species in hyperglycemic conditions requires dynamic change of mitochondrial morphology. *Proc Natl Acad Sci U S A* 2006;103:2653-2658.

197. Makino A, Suarez J, Gawlowski T, Han W, Wang H, Scott BT, et al. Regulation of mitochondrial morphology and function by O-GlcNAcylation in neonatal cardiac myocytes. *Am J Physiol Regul Integr Comp Physiol* 2011;300:R1296-R1302.

198. Hu Y, Suarez J, Fricovsky E, Wang H, Scott BT, Trauger SA, et al. Increased enzymatic O-GlcNAcylation of mitochondrial proteins impairs mitochondrial function in cardiac myocytes exposed to high glucose. *J Biol Chem* 2009;284:547-555.

199. Gawlowski T, Suarez J, Scott B, Torres-Gonzalez M, Wang H, Schwappacher R, et al. Modulation of dynamin-related protein 1 (DRP1) function by increased O-linked-beta-N-acetylglucosamine modification (O-GlcNAc) in cardiac myocytes. *J Biol Chem* 2012;287:30024-30034.

200. Hicks S, Labinskyy N, Piteo B, Laurent D, Mathew J, Gupte SA, et al. Type II diabetes increases mitochondrial DNA (mtDNA) mutations in the left ventricle of the Goto-Kakizaki diabetic rat. *Am J Physiol Heart Circ Physiol* 2013.

201. Nomiyama T, Tanaka Y, Piao L, Hattori N, Uchino H, Watada H, et al. Accumulation of somatic mutation in mitochondrial DNA and atherosclerosis in diabetic patients. *Ann N Y Acad Sci* 2004;1011:193-204.

202. Medikayala S, Piteo B, Zhao X, Edwards JG. Chronically elevated glucose compromises myocardial mitochondrial DNA integrity by alteration of mitochondrial topoisomerase function. *Am J Physiol Cell Physiol* 2011;300:C338-C348.

203. Patti ME, Butte AJ, Crunkhorn S, Cusi K, Berria R, Kashyap S, et al. Coordinated reduction of genes of oxidative metabolism in humans with insulin resistance and diabetes: Potential role of PGC1 and NRF1. *Proc Natl Acad Sci U S A* 2003;100:8466-8471.

204. Mootha VK, Lindgren CM, Eriksson KF, Subramanian A, Sihag S, Lehar J, et al. PGC-1alpha-responsive genes involved in oxidative phosphorylation are coordinately downregulated in human diabetes. *Nat Genet* 2003;34:267-273.

205. Chang LT, Sun CK, Wang CY, Youssef AA, Wu CJ, Chua S, et al. Downregulation of peroxisme proliferator activated receptor gamma co-activator 1alpha in diabetic rats. *Int Heart J* 2006;47:901-910.

206. Duncan JG, Fong JL, Medeiros DM, Finck BN, Kelly DP. Insulin-resistant heart exhibits a mitochondrial biogenic response driven by the peroxisome proliferator-activated receptor-alpha/PGC-1alpha gene regulatory pathway. *Circulation* 2007;115:909-917.

207. Sharma S, Adrogue JV, Golfman L, Uray I, Lemm J, Youker K, et al. Intramyocardial lipid accumulation in the failing human heart resembles the lipotoxic rat heart. *FASEB J* 2004;18:1692-1700.

208. **Brookheart RT, Michel CI, Schaffer JE. As a matter of fat. *Cell Metab* 2009;10:9-12.**

209. **Zhang LN, Zhou HY, Fu YY, Li YY, Wu F, Gu M, et al. Novel Small-Molecule PGC-1alpha Transcriptional Regulator With Beneficial Effects on Diabetic db/db Mice. *Diabetes* 2013;62:1297-1307.**

210. **Feuvray D. Cardiac metabolism in the diabetic patient. *Heart Metabolism* 2010;46:11-15.**

211. **Carroll R, Carley AN, Dyck JR, Severson DL. Metabolic effects of insulin on cardiomyocytes from control and diabetic db/db mouse hearts. *Am J Physiol Endocrinol Metab* 2005;288:E900-E906.**

212. **Folmes CD, Clanachan AS, Lopaschuk GD. Fatty acids attenuate insulin regulation of 5'-AMP-activated protein kinase and insulin cardioprotection after ischemia. *Circ Res* 2006;99:61-68.**

213. **Luiken JJ, Arumugam Y, Bell RC, Calles-Escandon J, Tandon NN, Glatz JF, et al. Changes in fatty acid transport and transporters are related to the severity of insulin deficiency. *Am J Physiol Endocrinol Metab* 2002;283:E612-E621.**

214. **Luiken JJ, Arumugam Y, Dyck DJ, Bell RC, Pelsers MM, Turcotte LP, et al. Increased rates of fatty acid uptake and plasmalemmal fatty acid transporters in obese Zucker rats. *J Biol Chem* 2001;276:40567-40573.**

215. **An D, Rodrigues B. Role of changes in cardiac metabolism in development of diabetic cardiomyopathy. *Am J Physiol Heart Circ Physiol* 2006;291:H1489-H1506.**

216. **Panagia M, Gibbons GF, Radda GK, Clarke K. PPARalpha activation required for decreased glucose uptake and increased susceptibility to injury during ischemia. *Am J Physiol Heart Circ Physiol* 2005;288:H2677-H2683.**

217. **Whittington HJ, Babu GG, Mocanu MM, Yellon DM, Hausenloy DJ. The diabetic heart: too sweet for its own good? *Cardiol Res Pract* 2012;2012:845698-.**

218. **Paulson DJ. The diabetic heart is more sensitive to ischemic injury. *Cardiovasc Res* 1997;34:104-112.**

219. **Marfella R, D'Amico M, Di Filippo C, Piegari E, Nappo F, Esposito K, et al. Myocardial infarction in diabetic rats: role of hyperglycaemia on infarct size and early expression of hypoxia-inducible factor 1. *Diabetologia* 2002;45:1172-1181.**

220. **Thangarajah H, Yao D, Chang EI, Shi Y, Jazayeri L, Vial IN, et al. The molecular basis for impaired hypoxia-induced VEGF expression in diabetic tissues. *Proc Natl Acad Sci U S A* 2009;106:13505-13510.**

221. **Ma G, Al Shabrawey M, Johnson JA, Datar R, Tawfik HE, Guo D, et al. Protection against myocardial ischemia/reperfusion injury by short-term diabetes: enhancement of VEGF formation, capillary**

density, and activation of cell survival signaling. *Naunyn Schmiedebergs Arch Pharmacol* 2006;373:415-427.

222. Su H, Sun X, Ma H, Zhang HF, Yu QJ, Huang C, et al. Acute hyperglycemia exacerbates myocardial ischemia/reperfusion injury and blunts cardioprotective effect of GIK. *Am J Physiol Endocrinol Metab* 2007;293:E629-E635.

223. Fiordaliso F, Leri A, Cesselli D, Limana F, Safai B, Nadal-Ginard B, et al. Hyperglycemia activates p53 and p53-regulated genes leading to myocyte cell death. *Diabetes* 2001;50:2363-2375.

224. Kersten JR, Toller WG, Gross ER, Pagel PS, Warltier DC. Diabetes abolishes ischemic preconditioning: role of glucose, insulin, and osmolality. *Am J Physiol Heart Circ Physiol* 2000;278:H1218-H1224.

225. Ebel D, Mullenheim J, Frassdorf J, Heinen A, Huhn R, Bohlen T, et al. Effect of acute hyperglycaemia and diabetes mellitus with and without short-term insulin treatment on myocardial ischaemic late preconditioning in the rabbit heart in vivo. *Pflugers Arch* 2003;446:175-182.

226. Desrois M, Clarke K, Lan C, Dalmasso C, Cole M, Portha B, et al. Upregulation of eNOS and unchanged energy metabolism in increased susceptibility of the aging type 2 diabetic GK rat heart to ischemic injury. *Am J Physiol Heart Circ Physiol* 2010;299:H1679-H1686.

227. Lefer DJ, Scalia R, Jones SP, Sharp BR, Hoffmeyer MR, Farvid AR, et al. HMG-CoA reductase inhibition protects the diabetic myocardium from ischemia-reperfusion injury. *FASEB J* 2001;15:1454-1456.

228. Jones SP, Girod WG, Granger DN, Palazzo AJ, Lefer DJ. Reperfusion injury is not affected by blockade of P-selectin in the diabetic mouse heart. *Am J Physiol* 1999;277:H763-H769.

229. Ravingerova T, Neckar J, Kolar F. Ischemic tolerance of rat hearts in acute and chronic phases of experimental diabetes. *Mol Cell Biochem* 2003;249:167-174.

230. Shi-Ting W, Mang-Hua X, Wen-Ting C, Feng-Hou G, Zhu-Ying G. Study on tolerance to ischemia-reperfusion injury and protection of ischemic preconditioning of type 1 diabetes rat heart. *Biomed Pharmacother* 2010.

231. Nawata T, Takahashi N, Ooie T, Kaneda K, Saikawa T, Sakata T. Cardioprotection by streptozotocin-induced diabetes and insulin against ischemia/reperfusion injury in rats. *J Cardiovasc Pharmacol* 2002;40:491-500.

232. Chu LM, Osipov RM, Robich MP, Feng J, Oyamada S, Bianchi C, et al. Is hyperglycemia bad for the heart during acute ischemia? *J Thorac Cardiovasc Surg* 2010;140:1345-1352.

233. Schaffer SW, Croft CB, Solodushko V. Cardioprotective effect of chronic hyperglycemia: effect on hypoxia-induced apoptosis and necrosis. *Am J Physiol Heart Circ Physiol* 2000;278:H1948-H1954.

234. Hadour G, Ferrera R, Sebbag L, Forrat R, Delaye J, de Lorgeril M. Improved myocardial tolerance to ischaemia in the diabetic rabbit. *J Mol Cell Cardiol* 1998;30:1869-1875.

235. Ooie T, Takahashi N, Nawata T, Arikawa M, Yamanaka K, Kajimoto M, et al. Ischemia-induced translocation of protein kinase C-epsilon mediates cardioprotection in the streptozotocin-induced diabetic rat. *Circ J* 2003;67:955-961.

236. Tanaka K, Kehl F, Gu W, Krolikowski JG, Pagel PS, Warltier DC, et al. Isoflurane-induced preconditioning is attenuated by diabetes. *Am J Physiol Heart Circ Physiol* 2002;282:H2018-H2023.

237. Kristiansen SB, Lofgren B, Stottrup NB, Khatir D, Nielsen-Kudsk JE, Nielsen TT, et al. Ischaemic preconditioning does not protect the heart in obese and lean animal models of type 2 diabetes. *Diabetologia* 2004;47:1716-1721.

238. Tsang A, Hausenloy DJ, Mocanu MM, Carr RD, Yellon DM. Preconditioning the diabetic heart: the importance of Akt phosphorylation. *Diabetes* 2005;54:2360-2364.

239. Oliveira PJ, Rolo AP, Seica R, Palmeira CM, Santos MS, Moreno AJ. Decreased susceptibility of heart mitochondria from diabetic GK rats to mitochondrial permeability transition induced by calcium phosphate. *Biosci Rep* 2001;21:45-53.

240. Bulhak AA, Jung C, Ostenson CG, Lundberg JO, Sjoquist PO, Pernow J. PPAR-alpha activation protects the type 2 diabetic myocardium against ischemia-reperfusion injury: involvement of the PI3-Kinase/Akt and NO pathway. *Am J Physiol Heart Circ Physiol* 2009;296:H719-H727.

241. Matsumoto S, Cho S, Tosaka S, Ureshino H, Maekawa T, Hara T, et al. Pharmacological preconditioning in type 2 diabetic rat hearts: the roles of mitochondrial ATP-sensitive potassium channels and the phosphatidylinositol 3-kinase-Akt pathway. *Cardiovasc Drugs Ther* 2009;23:263-270.

242. Yan W, Zhang H, Liu P, Wang H, Liu J, Gao C, et al. Impaired mitochondrial biogenesis due to dysfunctional adiponectin-AMPK-PGC-1alpha signaling contributing to increased vulnerability in diabetic heart. *Basic Res Cardiol* 2013;108:329-.

243. Desrois M, Sidell RJ, Gauguier D, Davey CL, Radda GK, Clarke K. Gender differences in hypertrophy, insulin resistance and ischemic injury in the aging type 2 diabetic rat heart. *J Mol Cell Cardiol* 2004;37:547-555.

244. Sivaraman V, Hausenloy DJ, Wynne AM, Yellon DM. Preconditioning the diabetic human myocardium. *J Cell Mol Med* 2010;14:1740-1746.

245. Bouchard JF, Lamontagne D. Protection afforded by preconditioning to the diabetic heart against ischaemic injury. *Cardiovasc Res* 1998;37:82-90.

246. de Jong JW, de Jonge R, Keijzer E, Bradamante S. The role of adenosine in preconditioning. *Pharmacol Ther* 2000;87:141-149.

247. Kamata K, Miyata N, Kasuya Y. Functional changes in potassium channels in aortas from rats with streptozotocin-induced diabetes. *Eur J Pharmacol* 1989;166:319-323.

248. Hausenloy DJ, Maddock HL, Baxter GF, Yellon DM. Inhibiting mitochondrial permeability transition pore opening: a new paradigm for myocardial preconditioning? *Cardiovasc Res* 2002;55:534-543.

249. Kersten JR, Montgomery MW, Ghassemi T, Gross ER, Toller WG, Pagel PS, et al. Diabetes and hyperglycemia impair activation of mitochondrial K(ATP) channels. *Am J Physiol Heart Circ Physiol* 2001;280:H1744-H1750.

250. Hotta H, Miura T, Miki T, Togashi N, Maeda T, Kim SJ, et al. Angiotensin II type 1 receptor-mediated upregulation of calcineurin activity underlies impairment of cardioprotective signaling in diabetic hearts. *Circ Res* 2010;106:129-132.

251. Gross ER, Hsu AK, Gross GJ. The JAK/STAT pathway is essential for opioid-induced cardioprotection: JAK2 as a mediator of STAT3, Akt, and GSK-3 beta. *Am J Physiol Heart Circ Physiol* 2006;291:H827-H834.

252. Baker JE. Erythropoietin mimics ischemic preconditioning. *Vascul Pharmacol* 2005;42:233-241.

253. Gooch JL, Barnes JL, Garcia S, Abboud HE. Calcineurin is activated in diabetes and is required for glomerular hypertrophy and ECM accumulation. *Am J Physiol Renal Physiol* 2003;284:F144-F154.

254. Huisamen B, Perel SJ, Friedrich SO, Salie R, Strijdom H, Lochner A. ANG II type I receptor antagonism improved nitric oxide production and enhanced eNOS and PKB/Akt expression in hearts from a rat model of insulin resistance. *Mol Cell Biochem* 2011;349:21-31.

255. Ghaboura N, Tamareille S, Ducluzeau PH, Grimaud L, Loufrani L, Croue A, et al. Diabetes mellitus abrogates erythropoietin-induced cardioprotection against ischemic-reperfusion injury by alteration of the RISK/GSK-3beta signaling. *Basic Res Cardiol* 2011;106:147-162.

256. Gross ER, Hsu AK, Gross GJ. Diabetes abolishes morphine-induced cardioprotection via multiple pathways upstream of glycogen synthase kinase-3beta. *Diabetes* 2007;56:127-136.

257. Miki T, Miura T, Hotta H, Tanno M, Yano T, Sato T, et al. Endoplasmic reticulum stress in diabetic hearts abolishes erythropoietin-induced myocardial protection by impairment of phospho-

glycogen synthase kinase-3beta-mediated suppression of mitochondrial permeability transition. *Diabetes* 2009;58:2863-2872.

258. Ajjan RA, Grant PJ. Cardiovascular disease prevention in patients with type 2 diabetes: The role of oral anti-diabetic agents. *Diab Vasc Dis Res* 2006;3:147-158.

259. Monteiro P, Goncalves L, Providencia LA. Diabetes and cardiovascular disease: the road to cardioprotection. *Heart* 2005;91:1621-1625.

260. Effect of intensive blood-glucose control with metformin on complications in overweight patients with type 2 diabetes (UKPDS 34). UK Prospective Diabetes Study (UKPDS) Group. *Lancet* 1998;352:854-865.

261. Owen MR, Doran E, Halestrap AP. Evidence that metformin exerts its anti-diabetic effects through inhibition of complex 1 of the mitochondrial respiratory chain. *Biochem J* 2000;348 Pt 3:607-614.

262. Hundal RS, Krssak M, Dufour S, Laurent D, Lebon V, Chandramouli V, et al. Mechanism by which metformin reduces glucose production in type 2 diabetes. *Diabetes* 2000;49:2063-2069.

263. Galuska D, Nolte LA, Zierath JR, Wallberg-Henriksson H. Effect of metformin on insulin-stimulated glucose transport in isolated skeletal muscle obtained from patients with NIDDM. *Diabetologia* 1994;37:826-832.

264. Zhou G, Myers R, Li Y, Chen Y, Shen X, Fenyk-Melody J, et al. Role of AMP-activated protein kinase in mechanism of metformin action. *J Clin Invest* 2001;108:1167-1174.

265. Solskov L, Lofgren B, Kristiansen SB, Jessen N, Pold R, Nielsen TT, et al. Metformin induces cardioprotection against ischaemia/reperfusion injury in the rat heart 24 hours after administration. *Basic Clin Pharmacol Toxicol* 2008;103:82-87.

266. El MS, Rongen GA, de Boer RA, Riksen NP. The cardioprotective effects of metformin. *Curr Opin Lipidol* 2011.

267. El-Mir MY, Nogueira V, Fontaine E, Averet N, Rigoulet M, Leverve X. Dimethylbiguanide inhibits cell respiration via an indirect effect targeted on the respiratory chain complex I. *J Biol Chem* 2000;275:223-228.

268. Musi N, Hirshman MF, Nygren J, Svanfeldt M, Bavenholm P, Rooyackers O, et al. Metformin increases AMP-activated protein kinase activity in skeletal muscle of subjects with type 2 diabetes. *Diabetes* 2002;51:2074-2081.

269. Caton PW, Nayuni NK, Kieswich J, Khan NQ, Yaqoob MM, Corder R. Metformin suppresses hepatic gluconeogenesis through induction of SIRT1 and GCN5. *J Endocrinol* 2010;205:97-106.

270. Ouyang J, Parakhia RA, Ochs RS. Metformin activates AMP kinase through inhibition of AMP deaminase. *J Biol Chem* 2011;286:1-11.

271. Foretz M, Hebrard S, Leclerc J, Zarrinpashneh E, Soty M, Mithieux G, et al. Metformin inhibits hepatic gluconeogenesis in mice independently of the LKB1/AMPK pathway via a decrease in hepatic energy state. *J Clin Invest* 2010;120:2355-2369.

272. Mather KJ, Verma S, Anderson TJ. Improved endothelial function with metformin in type 2 diabetes mellitus. *J Am Coll Cardiol* 2001;37:1344-1350.

273. Sena CM, Matafome P, Louro T, Nunes E, Fernandes R, Seica RM. Metformin restores endothelial function in aorta of diabetic rats. *Br J Pharmacol* 2011;163:424-437.

274. Effect of intensive blood-glucose control with metformin on complications in overweight patients with type 2 diabetes (UKPDS 34). UK Prospective Diabetes Study (UKPDS) Group. *Lancet* 1998;352:854-865.

275. Roussel R, Travert F, Pasquet B, Wilson PW, Smith SC, Jr., Goto S, et al. Metformin use and mortality among patients with diabetes and atherothrombosis. *Arch Intern Med* 2010;170:1892-1899.

276. Carlson CA, Kim KH. Regulation of hepatic acetyl coenzyme A carboxylase by phosphorylation and dephosphorylation. *J Biol Chem* 1973;248:378-380.

277. Hardie DG, Scott JW, Pan DA, Hudson ER. Management of cellular energy by the AMP-activated protein kinase system. *FEBS Lett* 2003;546:113-120.

278. Heidrich F, Schotola H, Popov AF, Sohns C, Schuenemann J, Friedrich M, et al. A. *Curr Cardiol Rev* 2010;6:337-342.

279. Suter M, Riek U, Tuerk R, Schlattner U, Wallimann T, Neumann D. Dissecting the role of 5'-AMP for allosteric stimulation, activation, and deactivation of AMP-activated protein kinase. *J Biol Chem* 2006;281:32207-32216.

280. Charlon V, Boucher F, Mouhieddine S, de Leiris J. Reduction of myocardial

infarct size by metformin in rats submitted to permanent left coronary artery

ligation. *Diabetes Metabolism* 1988;14:591-595.

281. Bhamra GS, Hausenloy DJ, Davidson SM, Carr RD, Paiva M, Wynne AM, et al. Metformin protects the ischemic heart by the Akt-mediated inhibition of mitochondrial permeability transition pore opening. *Basic Res Cardiol* 2008;103:274-284.

282. Paiva M, Riksen NP, Davidson SM, Hausenloy DJ, Monteiro P, Goncalves L, et al. Metformin prevents myocardial reperfusion injury by activating the adenosine receptor. *J Cardiovasc Pharmacol* 2009;53:373-378.

283. Paiva MA, Goncalves LM, Providencia LA, Davidson SM, Yellon DM, Mocanu MM. Transitory activation of AMPK at reperfusion protects

the ischaemic-reperfused rat myocardium against infarction. *Cardiovasc Drugs Ther* 2010;24:25-32.

284. Calvert JW, Gundewar S, Jha S, Greer JJ, Bestermann WH, Tian R, et al. Acute metformin therapy confers cardioprotection against myocardial infarction via AMPK-eNOS-mediated signaling. *Diabetes* 2008;57:696-705.

285. Lexis CP, van der Horst IC, Lipsic E, van der Harst P, van der Horst-Schrivers AN, Wolffenbuttel BH, et al. Metformin in non-diabetic patients presenting with ST elevation myocardial infarction: rationale and design of the glycometabolic intervention as adjunct to primary percutaneous intervention in ST elevation myocardial infarction (GIPS)-III trial. *Cardiovasc Drugs Ther* 2012;26:417-426.

286. Kravchuk E, Grineva E, Bairamov A, Galagudza M, Vlasov T. The effect of metformin on the myocardial tolerance to ischemia-reperfusion injury in the rat model of diabetes mellitus type II. *Exp Diabetes Res* 2011;2011:907496-.

287. Gundewar S, Calvert JW, Jha S, Toedt-Pingel I, Ji SY, Nunez D, et al. Activation of AMP-activated protein kinase by metformin improves left ventricular function and survival in heart failure. *Circ Res* 2009;104:403-411.

288. Mubagwa K, Flameng W. Adenosine, adenosine receptors and myocardial protection: an updated overview. *Cardiovasc Res* 2001;52:25-39.

289. Zhang L, He H, Balschi JA. Metformin and phenformin activate AMP-activated protein kinase in the heart by increasing cytosolic AMP concentration. *Am J Physiol Heart Circ Physiol* 2007;293:H457-H466.

290. Barreto-Torres G, Parodi-Rullan R, Javadov S. The Role of PPARalpha in Metformin-Induced Attenuation of Mitochondrial Dysfunction in Acute Cardiac Ischemia/Reperfusion in Rats. *Int J Mol Sci* 2012;13:7694-7709.

291. Xie Z, Lau K, Eby B, Lozano P, He C, Pennington B, et al. Improvement of cardiac functions by chronic metformin treatment is associated with enhanced cardiac autophagy in diabetic OVE26 mice. *Diabetes* 2011;60:1770-1778.

292. ELRICK H, STIMMLER L, HLAD CJ, Jr., ARAI Y. PLASMA INSULIN RESPONSE TO ORAL AND INTRAVENOUS GLUCOSE ADMINISTRATION. *J Clin Endocrinol Metab* 1964;24:1076-1082.

293. Chinda K, Chattipakorn S, Chattipakorn N. Cardioprotective effects of incretin during ischaemia-reperfusion. *Diab Vasc Dis Res* 2012;9:256-269.

294. Baggio LL, Drucker DJ. Biology of incretins: GLP-1 and GIP. *Gastroenterology* 2007;132:2131-2157.

295. Drucker DJ, Nauck MA. The incretin system: glucagon-like peptide-1 receptor agonists and dipeptidyl peptidase-4 inhibitors in type 2 diabetes. *Lancet* 2006;368:1696-1705.

296. Orskov C, Rabenhoj L, Wettergren A, Kofod H, Holst JJ. Tissue and plasma concentrations of amidated and glycine-extended glucagon-like peptide I in humans. *Diabetes* 1994;43:535-539.

297. Drucker DJ, Philippe J, Mojsov S, Chick WL, Habener JF. Glucagon-like peptide I stimulates insulin gene expression and increases cyclic AMP levels in a rat islet cell line. *Proc Natl Acad Sci U S A* 1987;84:3434-3438.

298. De Marinis YZ, Salehi A, Ward CE, Zhang Q, Abdulkader F, Bengtsson M, et al. GLP-1 inhibits and adrenaline stimulates glucagon release by differential modulation of N- and L-type Ca2+ channel-dependent exocytosis. *Cell Metab* 2010;11:543-553.

299. Nauck M, Stockmann F, Ebert R, Creutzfeldt W. Reduced incretin effect in type 2 (non-insulin-dependent) diabetes. *Diabetologia* 1986;29:46-52.

300. Fadini GP, Avogaro A. Cardiovascular effects of DPP-4 inhibition: beyond GLP-1. *Vascul Pharmacol* 2011;55:10-16.

301. Ban K, Noyan-Ashraf MH, Hoefer J, Bolz SS, Drucker DJ, Husain M. Cardioprotective and vasodilatory actions of glucagon-like peptide 1 receptor are mediated through both glucagon-like peptide 1 receptor-dependent and -independent pathways. *Circulation* 2008;117:2340-2350.

302. Bose AK, Mocanu MM, Carr RD, Yellon DM. Myocardial ischaemia-reperfusion injury is attenuated by intact glucagon like peptide-1 (GLP-1) in the in vitro rat heart and may involve the p70s6K pathway. *Cardiovasc Drugs Ther* 2007;21:253-256.

303. Bose AK, Mocanu MM, Carr RD, Yellon DM. Glucagon like peptide-1 is protective against myocardial ischemia/reperfusion injury when given either as a preconditioning mimetic or at reperfusion in an isolated rat heart model. *Cardiovasc Drugs Ther* 2005;19:9-11.

304. Bose AK, Mocanu MM, Carr RD, Brand CL, Yellon DM. Glucagon-like peptide 1 can directly protect the heart against ischemia/reperfusion injury. *Diabetes* 2005;54:146-151.

305. Matsubara M, Kanemoto S, Leshnower BG, Albone EF, Hinmon R, Plappert T, et al. Single dose GLP-1-Tf ameliorates myocardial ischemia/reperfusion injury. *J Surg Res* 2011;165:38-45.

306. Noyan-Ashraf MH, Momen MA, Ban K, Sadi AM, Zhou YQ, Riazi AM, et al. GLP-1R agonist liraglutide activates cytoprotective pathways and improves outcomes after experimental myocardial infarction in mice. *Diabetes* 2009;58:975-983.

307. Ossum A, van DU, Engstrom T, Jensen JS, Treiman M. The cardioprotective and inotropic components of the postconditioning

effects of GLP-1 and GLP-1(9-36)a in an isolated rat heart. *Pharmacol Res* 2009;60:411-417.

308. Sonne DP, Engstrom T, Treiman M. Protective effects of GLP-1 analogues exendin-4 and GLP-1(9-36) amide against ischemia-reperfusion injury in rat heart. *Regul Pept* 2008;146:243-249.

309. Timmers L, Henriques JP, de Kleijn DP, Devries JH, Kemperman H, Steendijk P, et al. Exenatide reduces infarct size and improves cardiac function in a porcine model of ischemia and reperfusion injury. *J Am Coll Cardiol* 2009;53:501-510.

310. Scheen AJ. Cardiovascular effects of gliptins. *Nat Rev Cardiol* 2013;10:73-84.

311. Drucker DJ. Dipeptidyl peptidase-4 inhibition and the treatment of type 2 diabetes: preclinical biology and mechanisms of action. *Diabetes Care* 2007;30:1335-1343.

312. Mannucci E, Pala L, Ciani S, Bardini G, Pezzatini A, Sposato I, et al. Hyperglycaemia increases dipeptidyl peptidase IV activity in diabetes mellitus. *Diabetologia* 2005;48:1168-1172.

313. Ryskjaer J, Deacon CF, Carr RD, Krarup T, Madsbad S, Holst J, et al. Plasma dipeptidyl peptidase-IV activity in patients with type-2 diabetes mellitus correlates positively with HbAlc levels, but is not acutely affected by food intake. *Eur J Endocrinol* 2006;155:485-493.

314. Dang DT, Chun SY, Burkitt K, Abe M, Chen S, Havre P, et al. Hypoxia-inducible factor-1 target genes as indicators of tumor vessel response to vascular endothelial growth factor inhibition. *Cancer Res* 2008;68:1872-1880.

315. Lenhard JM, Croom DK, Minnick DT. Reduced serum dipeptidyl peptidase-IV after metformin and pioglitazone treatments. *Biochem Biophys Res Commun* 2004;324:92-97.

316. Brandt I, Lambeir AM, Ketelslegers JM, Vanderheyden M, Scharpe S, De M, I. Dipeptidyl-peptidase IV converts intact B-type natriuretic peptide into its des-SerPro form. *Clin Chem* 2006;52:82-87.

317. Mentlein R, Dahms P, Grandt D, Kruger R. Proteolytic processing of neuropeptide Y and peptide YY by dipeptidyl peptidase IV. *Regul Pept* 1993;49:133-144.

318. Zaruba MM, Theiss HD, Vallaster M, Mehl U, Brunner S, David R, et al. Synergy between CD26/DPP-IV inhibition and G-CSF improves cardiac function after acute myocardial infarction. *Cell Stem Cell* 2009;4:313-323.

319. Wang LH, Ahmad S, Benter IF, Chow A, Mizutani S, Ward PE. Differential processing of substance P and neurokinin A by plasma dipeptidyl(amino)peptidase IV, aminopeptidase M and angiotensin converting enzyme. *Peptides* 1991;12:1357-1364.

320. Fadini GP, Boscaro E, Albiero M, Menegazzo L, Frison V, de KS, et al. The oral dipeptidyl peptidase-4 inhibitor sitagliptin increases circulating endothelial progenitor cells in patients with type 2 diabetes: possible role of stromal-derived factor-1alpha. *Diabetes Care* 2010;33:1607-1609.

321. Huisamen B, Genis A, Marais E, Lochner A. Pre-treatment with a DPP-4 inhibitor is infarct sparing in hearts from obese, pre-diabetic rats. *Cardiovasc Drugs Ther* 2011;25:13-20.

322. Ye Y, Keyes KT, Zhang C, Perez-Polo JR, Lin Y, Birnbaum Y. The myocardial infarct size-limiting effect of sitagliptin is PKA-dependent, whereas the protective effect of pioglitazone is partially dependent on PKA. *Am J Physiol Heart Circ Physiol* 2010;298:H1454-H1465.

323. Chinda K, Palee S, Surinkaew S, Phornphutkul M, Chattipakorn S, Chattipakorn N. Cardioprotective effect of dipeptidyl peptidase-4 inhibitor during ischemia-reperfusion injury. *Int J Cardiol* 2012.

324. Sauve M, Ban K, Momen MA, Zhou YQ, Henkelman RM, Husain M, et al. Genetic deletion or pharmacological inhibition of dipeptidyl peptidase-4 improves cardiovascular outcomes after myocardial infarction in mice. *Diabetes* 2010;59:1063-1073.

325. Conarello SL, Li Z, Ronan J, Roy RS, Zhu L, Jiang G, et al. Mice lacking dipeptidyl peptidase IV are protected against obesity and insulin resistance. *Proc Natl Acad Sci U S A* 2003;100:6825-6830.

326. Oxenham H, Sharpe N. Cardiovascular aging and heart failure. *Eur J Heart Fail* 2003;5:427-434.

327. Cecelja M, Chowienczyk P. Role of arterial stiffness in cardiovascular disease. *J R Soc Med Cardiovasc Dis* 2012;1:1-11.

328. Olsen H, Lanne T. Reduced venous compliance in lower limbs of aging humans and its importance for capacitance function. *Am J Physiol* 1998;275:H878-H886.

329. Eberhardt RT, Raffetto JD. Chronic venous insufficiency. *Circulation* 2005;111:2398-2409.

330. Ferrari AU, Radaelli A, Centola M. Invited review: aging and the cardiovascular system. *J Appl Physiol* 2003;95:2591-2597.

331. Johnson FB, Sinclair DA, Guarente L. Molecular biology of aging. *Cell* 1999;96:291-302.

332. Shih H, Lee B, Lee RJ, Boyle AJ. The aging heart and post-infarction left ventricular remodeling. *J Am Coll Cardiol* 2011;57:9-17.

333. Chaudhary KR, El-Sikhry H, Seubert JM. Mitochondria and the aging heart. *J Geriatr Cardiol* 2011;8:159-167.

334. Cheng S, Fernandes VR, Bluemke DA, McClelland RL, Kronmal RA, Lima JA. Age-related left ventricular remodeling and associated risk for

cardiovascular outcomes: the Multi-Ethnic Study of Atherosclerosis. *Circ Cardiovasc Imaging* 2009;2:191-198.

335. Olivetti G, Melissari M, Capasso JM, Anversa P. Cardiomyopathy of the aging human heart. Myocyte loss and reactive cellular hypertrophy. *Circ Res* 1991;68:1560-1568.

336. Tate CA, Taffet GE, Hudson EK, Blaylock SL, McBride RP, Michael LH. Enhanced calcium uptake of cardiac sarcoplasmic reticulum in exercise-trained old rats. *Am J Physiol* 1990;258:H431-H435.

337. Cain BS, Meldrum DR, Joo KS, Wang JF, Meng X, Cleveland JC, Jr., et al. Human SERCA2a levels correlate inversely with age in senescent human myocardium. *J Am Coll Cardiol* 1998;32:458-467.

338. Schmidt U, del MF, Miyamoto MI, Matsui T, Gwathmey JK, Rosenzweig A, et al. Restoration of diastolic function in senescent rat hearts through adenoviral gene transfer of sarcoplasmic reticulum Ca(2+)-ATPase. *Circulation* 2000;101:790-796.

339. Jovanovic S, Jovanovic A. Sarcolemmal K(ATP) channels in ageing. *Ageing Res Rev* 2004;3:199-214.

340. Gardin JM, Arnold AM, Bild DE, Smith VE, Lima JA, Klopfenstein HS, et al. Left ventricular diastolic filling in the elderly: the cardiovascular health study. *Am J Cardiol* 1998;82:345-351.

341. Moslehi J, DePinho RA, Sahin E. Telomeres and mitochondria in the aging heart. *Circ Res* 2012;110:1226-1237.

342. Leri A, Malhotra A, Liew CC, Kajstura J, Anversa P. Telomerase activity in rat cardiac myocytes is age and gender dependent. *J Mol Cell Cardiol* 2000;32:385-390.

343. Cawthon RM, Smith KR, O'Brien E, Sivatchenko A, Kerber RA. Association between telomere length in blood and mortality in people aged 60 years or older. *Lancet* 2003;361:393-395.

344. Sahin E, Colla S, Liesa M, Moslehi J, Muller FL, Guo M, et al. Telomere dysfunction induces metabolic and mitochondrial compromise. *Nature* 2011;470:359-365.

345. Volkova M, Garg R, Dick S, Boheler KR. Aging-associated changes in cardiac gene expression. *Cardiovasc Res* 2005;66:194-204.

346. Bodyak N, Kang PM, Hiromura M, Sulijoadikusumo I, Horikoshi N, Khrapko K, et al. Gene expression profiling of the aging mouse cardiac myocytes. *Nucleic Acids Res* 2002;30:3788-3794.

347. Kelly DP. Cell biology: Ageing theories unified. *Nature* 2011;470:342-343.

348. Lee CK, Allison DB, Brand J, Weindruch R, Prolla TA. Transcriptional profiles associated with aging and middle age-onset caloric restriction in mouse hearts. *Proc Natl Acad Sci U S A* 2002;99:14988-14993.

349. Luptak I, Yan J, Cui L, Jain M, Liao R, Tian R. Long-term effects of increased glucose entry on mouse hearts during normal aging and ischemic stress. *Circulation* 2007;116:901-909.

350. Abel ED. Glucose for the aging heart? *Circulation* 2007;116:884-887.

351. Fannin SW, Lesnefsky EJ, Slabe TJ, Hassan MO, Hoppel CL. Aging selectively decreases oxidative capacity in rat heart interfibrillar mitochondria. *Arch Biochem Biophys* 1999;372:399-407.

352. Lesnefsky EJ, Gudz TI, Moghaddas S, Migita CT, Ikeda-Saito M, Turkaly PJ, et al. Aging decreases electron transport complex III activity in heart interfibrillar mitochondria by alteration of the cytochrome c binding site. *J Mol Cell Cardiol* 2001;33:37-47.

353. Pfeiffer K, Gohil V, Stuart RA, Hunte C, Brandt U, Greenberg ML, et al. Cardiolipin stabilizes respiratory chain supercomplexes. *J Biol Chem* 2003;278:52873-52880.

354. Arnarez C, Marrink SJ, Periole X. Identification of cardiolipin binding sites on cytochrome c oxidase at the entrance of proton channels. *Sci Rep* 2013;3:1263-.

355. Nakagawa Y. Initiation of apoptotic signal by the peroxidation of cardiolipin of mitochondria. *Ann N Y Acad Sci* 2004;1011:177-184.

356. Pepe S, Tsuchiya N, Lakatta EG, Hansford RG. PUFA and aging modulate cardiac mitochondrial membrane lipid composition and Ca2+ activation of PDH. *Am J Physiol* 1999;276:H149-H158.

357. Petrosillo G, Ruggiero FM, Pistolese M, Paradies G. Reactive oxygen species generated from the mitochondrial electron transport chain induce cytochrome c dissociation from beef-heart submitochondrial particles via cardiolipin peroxidation. Possible role in the apoptosis. *FEBS Lett* 2001;509:435-438.

358. Lagouge M, Larsson NG. The role of mitochondrial DNA mutations and free radicals in disease and ageing. *J Intern Med* 2013.

359. HARMAN D. Aging: a theory based on free radical and radiation chemistry. *J Gerontol* 1956;11:298-300.

360. HARMAN D. The biologic clock: the mitochondria? *J Am Geriatr Soc* 1972;20:145-147.

361. Miquel J, Economos AC, Fleming J, Johnson JE, Jr. Mitochondrial role in cell aging. *Exp Gerontol* 1980;15:575-591.

362. HARMAN D. Free radical theory of aging: an update: increasing the functional life span. *Ann N Y Acad Sci* 2006;1067:10-21.

363. Brunk UT, Terman A. The mitochondrial-lysosomal axis theory of aging: accumulation of damaged mitochondria as a result of imperfect autophagocytosis. *Eur J Biochem* 2002;269:1996-2002.

364. Schriner SE, Linford NJ, Martin GM, Treuting P, Ogburn CE, Emond M, et al. Extension of murine life span by overexpression of catalase targeted to mitochondria. *Science* 2005;308:1909-1911.

365. Lebovitz RM, Zhang H, Vogel H, Cartwright J, Jr., Dionne L, Lu N, et al. Neurodegeneration, myocardial injury, and perinatal death in mitochondrial superoxide dismutase-deficient mice. *Proc Natl Acad Sci U S A* 1996;93:9782-9787.

366. Li Y, Huang TT, Carlson EJ, Melov S, Ursell PC, Olson JL, et al. Dilated cardiomyopathy and neonatal lethality in mutant mice lacking manganese superoxide dismutase. *Nat Genet* 1995;11:376-381.

367. Perez VI, Van RH, Bokov A, Epstein CJ, Vijg J, Richardson A. The overexpression of major antioxidant enzymes does not extend the lifespan of mice. *Aging Cell* 2009;8:73-75.

368. Trifunovic A, Hansson A, Wredenberg A, Rovio AT, Dufour E, Khvorostov I, et al. Somatic mtDNA mutations cause aging phenotypes without affecting reactive oxygen species production. *Proc Natl Acad Sci U S A* 2005;102:17993-17998.

369. Hekimi S, Lapointe J, Wen Y. Taking a "good" look at free radicals in the aging process. *Trends Cell Biol* 2011;21:569-576.

370. Sena LA, Chandel NS. Physiological roles of mitochondrial reactive oxygen species. *Mol Cell* 2012;48:158-167.

371. Pain T, Yang XM, Critz SD, Yue Y, Nakano A, Liu GS, et al. Opening of mitochondrial K(ATP) channels triggers the preconditioned state by generating free radicals. *Circ Res* 2000;87:460-466.

372. Muscari C, Caldarera CM, Guarnieri C. Age-dependent production of mitochondrial hydrogen peroxide, lipid peroxides and fluorescent pigments in the rat heart. *Basic Res Cardiol* 1990;85:172-178.

373. Maurel A, Hernandez C, Kunduzova O, Bompart G, Cambon C, Parini A, et al. Age-dependent increase in hydrogen peroxide production by cardiac monoamine oxidase A in rats. *Am J Physiol Heart Circ Physiol* 2003;284:H1460-H1467.

374. Cosentino F, Francia P, Camici GG, Pelicci PG, Luscher TF, Volpe M. Final common molecular pathways of aging and cardiovascular disease: role of the p66Shc protein. *Arterioscler Thromb Vasc Biol* 2008;28:622-628.

375. Migliaccio E, Giorgio M, Mele S, Pelicci G, Reboldi P, Pandolfi PP, et al. The p66shc adaptor protein controls oxidative stress response and life span in mammals. *Nature* 1999;402:309-313.

376. Francia P, delli GC, Bachschmid M, Martin-Padura I, Savoia C, Migliaccio E, et al. Deletion of p66shc gene protects against age-related endothelial dysfunction. *Circulation* 2004;110:2889-2895.

377. Carpi A, Menabo R, Kaludercic N, Pelicci P, Di LF, Giorgio M. The cardioprotective effects elicited by p66(Shc) ablation demonstrate

the crucial role of mitochondrial ROS formation in ischemia/reperfusion injury. *Biochim Biophys Acta* 2009;1787:774-780.

378. Pinton P, Rimessi A, Marchi S, Orsini F, Migliaccio E, Giorgio M, et al. Protein kinase C beta and prolyl isomerase 1 regulate mitochondrial effects of the life-span determinant p66Shc. *Science* 2007;315:659-663.

379. Giorgio M, Migliaccio E, Orsini F, Paolucci D, Moroni M, Contursi C, et al. Electron transfer between cytochrome c and p66Shc generates reactive oxygen species that trigger mitochondrial apoptosis. *Cell* 2005;122:221-233.

380. Lebiedzinska M, Duszynski J, Rizzuto R, Pinton P, Wieckowski MR. Age-related changes in levels of p66Shc and serine 36-phosphorylated p66Shc in organs and mouse tissues. *Arch Biochem Biophys* 2009;486:73-80.

381. Li SY, Du M, Dolence EK, Fang CX, Mayer GE, Ceylan-Isik AF, et al. Aging induces cardiac diastolic dysfunction, oxidative stress, accumulation of advanced glycation endproducts and protein modification. *Aging Cell* 2005;4:57-64.

382. Savitha S, Tamilselvan J, Anusuyadevi M, Panneerselvam C. Oxidative stress on mitochondrial antioxidant defense system in the aging process: role of DL-alpha-lipoic acid and L-carnitine. *Clin Chim Acta* 2005;355:173-180.

383. Sivonova M, Tatarkova Z, Durackova Z, Dobrota D, Lehotsky J, Matakova T, et al. Relationship between antioxidant potential and oxidative damage to lipids, proteins and DNA in aged rats. *Physiol Res* 2007;56:757-764.

384. Boengler K, Schulz R, Heusch G. Loss of cardioprotection with ageing. *Cardiovasc Res* 2009;83:247-261.

385. Lesnefsky EJ, Lundergan CF, Hodgson JM, Nair R, Reiner JS, Greenhouse SW, et al. Increased left ventricular dysfunction in elderly patients despite successful thrombolysis: the GUSTO-I angiographic experience. *J Am Coll Cardiol* 1996;28:331-337.

386. Lucas DT, Szweda LI. Cardiac reperfusion injury: aging, lipid peroxidation, and mitochondrial dysfunction. *Proc Natl Acad Sci U S A* 1998;95:510-514.

387. Lesnefsky EJ, Gallo DS, Ye J, Whittingham TS, Lust WD. Aging increases ischemia-reperfusion injury in the isolated, buffer-perfused heart. *J Lab Clin Med* 1994;124:843-851.

388. Jahangir A, Ozcan C, Holmuhamedov EL, Terzic A. Increased calcium vulnerability of senescent cardiac mitochondria: protective role for a mitochondrial potassium channel opener. *Mech Ageing Dev* 2001;122:1073-1086.

389. O'Brien JD, Ferguson JH, Howlett SE. Effects of ischemia and reperfusion on isolated ventricular myocytes from young adult and aged Fischer 344 rat hearts. *Am J Physiol Heart Circ Physiol* 2008;294:H2174-H2183.

390. Tani M, Suganuma Y, Hasegawa H, Shinmura K, Ebihara Y, Hayashi Y, et al. Decrease in ischemic tolerance with aging in isolated perfused Fischer 344 rat hearts: relation to increases in intracellular Na+ after ischemia. *J Mol Cell Cardiol* 1997;29:3081-3089.

391. Willems L, Zatta A, Holmgren K, Ashton KJ, Headrick JP. Age-related changes in ischemic tolerance in male and female mouse hearts. *J Mol Cell Cardiol* 2005;38:245-256.

392. Zhang H, Tao L, Jiao X, Gao E, Lopez BL, Christopher TA, et al. Nitrative thioredoxin inactivation as a cause of enhanced myocardial ischemia/reperfusion injury in the aging heart. *Free Radic Biol Med* 2007;43:39-47.

393. Azhar G, Gao W, Liu L, Wei JY. Ischemia-reperfusion in the adult mouse heart influence of age. *Exp Gerontol* 1999;34:699-714.

394. Boengler K, Konietzka I, Buechert A, Heinen Y, Garcia-Dorado D, Heusch G, et al. Loss of ischemic preconditioning's cardioprotection in aged mouse hearts is associated with reduced gap junctional and mitochondrial levels of connexin 43. *Am J Physiol Heart Circ Physiol* 2007;292:H1764-H1769.

395. Besse S, Bulteau AL, Boucher F, Riou B, Swynghedauw B, de LJ. Antioxidant treatment prevents cardiac protein oxidation after ischemia-reperfusion and improves myocardial function and coronary perfusion in senescent hearts. *J Physiol Pharmacol* 2006;57:541-552.

396. Tossios P, Bloch W, Huebner A, Raji MR, Dodos F, Klass O, et al. N-acetylcysteine prevents reactive oxygen species-mediated myocardial stress in patients undergoing cardiac surgery: results of a randomized, double-blind, placebo-controlled clinical trial. *J Thorac Cardiovasc Surg* 2003;126:1513-1520.

397. Lesnefsky EJ, He D, Moghaddas S, Hoppel CL. Reversal of mitochondrial defects before ischemia protects the aged heart. *FASEB J* 2006;20:1543-1545.

398. Wojtovich AP, Nadtochiy SM, Brookes PS, Nehrke K. Ischemic preconditioning: the role of mitochondria and aging. *Exp Gerontol* 2012;47:1-7.

399. Abete P, Ferrara N, Cioppa A, Ferrara P, Bianco S, Calabrese C, et al. Preconditioning does not prevent postischemic dysfunction in aging heart. *J Am Coll Cardiol* 1996;27:1777-1786.

400. Ebrahim Z, Yellon DM, Baxter GF. Ischemic preconditioning is lost in aging hypertensive rat heart: independent effects of aging and longstanding hypertension. *Exp Gerontol* 2007;42:807-814.

401. Schulman D, Latchman DS, Yellon DM. Effect of aging on the ability of preconditioning to protect rat hearts from ischemia-reperfusion injury. *Am J Physiol Heart Circ Physiol* 2001;281:H1630-H1636.

402. Fenton RA, Dickson EW, Meyer TE, Dobson JG, Jr. Aging reduces the cardioprotective effect of ischemic preconditioning in the rat heart. *J Mol Cell Cardiol* 2000;32:1371-1375.

403. Przyklenk K, Li G, Whittaker P. No loss in the in vivo efficacy of ischemic preconditioning in middle-aged and old rabbits. *J Am Coll Cardiol* 2001;38:1741-1747.

404. Burns PG, Krunkenkamp IB, Calderone CA, Kirvaitis RJ, Gaudette GR, Levitsky S. Is the preconditioning response conserved in senescent myocardium? *Ann Thorac Surg* 1996;61:925-929.

405. Abete P, de SD, Condorelli M, Napoli C, Rengo F. A four-year-old rabbit cannot be considered the right model for investigating cardiac senescence. *J Am Coll Cardiol* 2002;39:1701-1702.

406. McCully JD, Uematsu M, Parker RA, Levitsky S. Adenosine-enhanced ischemic preconditioning provides enhanced cardioprotection in the aged heart. *Ann Thorac Surg* 1998;66:2037-2043.

407. Willems L, Ashton KJ, Headrick JP. Adenosine-mediated cardioprotection in the aging myocardium. *Cardiovasc Res* 2005;66:245-255.

408. Peart JN, Gross ER, Headrick JP, Gross GJ. Impaired p38 MAPK/HSP27 signaling underlies aging-related failure in opioid-mediated cardioprotection. *J Mol Cell Cardiol* 2007;42:972-980.

409. Cohen MV, Downey JM. Adenosine: trigger and mediator of cardioprotection. *Basic Res Cardiol* 2008;103:203-215.

410. Ferdinandy P, Schulz R, Baxter GF. Interaction of cardiovascular risk factors with myocardial ischemia/reperfusion injury, preconditioning, and postconditioning. *Pharmacol Rev* 2007;59:418-458.

411. Hacham M, White RM, Argov S, Segal S, Apte RN. Interleukin-6 and interleukin-10 are expressed in organs of normal young and old mice. *Eur Cytokine Netw* 2004;15:37-46.

412. Leri A, Kajstura J, Li B, Sonnenblick EH, Beltrami CA, Anversa P, et al. Cardiomyocyte aging is gender-dependent: the local IGF-1-IGF-1R system. *Heart Dis* 2000;2:108-115.

413. Kintsurashvili E, Duka A, Ignjacev I, Pattakos G, Gavras I, Gavras H. Age-related changes of bradykinin B1 and B2 receptors in rat heart. *Am J Physiol Heart Circ Physiol* 2005;289:H202-H205.

414. Tani M, Honma Y, Hasegawa H, Tamaki K. Direct activation of mitochondrial K(ATP) channels mimics preconditioning but protein kinase C activation is less effective in middle-aged rat hearts. *Cardiovasc Res* 2001;49:56-68.

415. Korzick DH, Holiman DA, Boluyt MO, Laughlin MH, Lakatta EG. Diminished alpha1-adrenergic-mediated contraction and translocation of PKC in senescent rat heart. *Am J Physiol Heart Circ Physiol* 2001;281:H581-H589.

416. Krylova IB, Kachaeva EV, Rodionova OM, Negoda AE, Evdokimova NR, Balina MI, et al. The cardioprotective effect of uridine and uridine-5'-monophosphate: the role of the mitochondrial ATP-dependent potassium channel. *Exp Gerontol* 2006;41:697-703.

417. Bao L, Taskin E, Foster M, Ray B, Rosario R, Ananthakrishnan R, et al. Alterations in ventricular K(ATP) channel properties during aging. *Aging Cell* 2013;12:167-176.

418. Andrukhiv A, Costa AD, West IC, Garlid KD. Opening mitoKATP increases superoxide generation from complex I of the electron transport chain. *Am J Physiol Heart Circ Physiol* 2006;291:H2067-H2074.

419. Dost T, Cohen MV, Downey JM. Redox signaling triggers protection during the reperfusion rather than the ischemic phase of preconditioning. *Basic Res Cardiol* 2008;103:378-384.

420. Schwanke U, Konietzka I, Duschin A, Li X, Schulz R, Heusch G. No ischemic preconditioning in heterozygous connexin43-deficient mice. *Am J Physiol Heart Circ Physiol* 2002;283:H1740-H1742.

421. Rodriguez-Sinovas A, Boengler K, Cabestrero A, Gres P, Morente M, Ruiz-Meana M, et al. Translocation of connexin 43 to the inner mitochondrial membrane of cardiomyocytes through the heat shock protein 90-dependent TOM pathway and its importance for cardioprotection. *Circ Res* 2006;99:93-101.

422. Heinzel FR, Luo Y, Li X, Boengler K, Buechert A, Garcia-Dorado D, et al. Impairment of diazoxide-induced formation of reactive oxygen species and loss of cardioprotection in connexin 43 deficient mice. *Circ Res* 2005;97:583-586.

423. Boengler K, Stahlhofen S, van de Sand A, Gres P, Ruiz-Meana M, Garcia-Dorado D, et al. Presence of connexin 43 in subsarcolemmal, but not in interfibrillar cardiomyocyte mitochondria. *Basic Res Cardiol* 2009;104:141-147.

424. Braidy N, Guillemin GJ, Mansour H, Chan-Ling T, Poljak A, Grant R. Age related changes in NAD+ metabolism oxidative stress and Sirt1 activity in wistar rats. *PLoS One* 2011;6:e19194-.

425. Adam T, Sharp S, Opie LH, Lecour S. Loss of cardioprotection with ischemic preconditioning in aging hearts: role of sirtuin 1? *J Cardiovasc Pharmacol Ther* 2013;18:46-53.

426. Haq S, Choukroun G, Lim H, Tymitz KM, del MF, Gwathmey J, et al. Differential activation of signal transduction pathways in human hearts with hypertrophy versus advanced heart failure. *Circulation* 2001;103:670-677.

427. Rees DA, Alcolado JC. Animal models of diabetes mellitus. *Diabet Med* 2005;22:359-370.

428. Chatzigeorgiou A, Halapas A, Kalafatakis K, Kamper E. The use of animal models in the study of diabetes mellitus. *In Vivo* 2009;23:245-258.

429. Yoon JW, Jun HS. Cellular and molecular pathogenic mechanisms of insulin-dependent diabetes mellitus. *Ann N Y Acad Sci* 2001;928:200-211.

430. Bolzan AD, Bianchi MS. Genotoxicity of streptozotocin. *Mutat Res* 2002;512:121-134.

431. Like AA, Rossini AA. Streptozotocin-induced pancreatic insulitis: new model of diabetes mellitus. *Science* 1976;193:415-417.

432. Wilson GL, Leiter EH. Streptozotocin interactions with pancreatic beta cells and the induction of insulin-dependent diabetes. *Curr Top Microbiol Immunol* 1990;156:27-54.

433. Lenzen S. The mechanisms of alloxan- and streptozotocin-induced diabetes. *Diabetologia* 2008;51:216-226.

434. Van Belle TL, Taylor P, von Herrath MG. Mouse Models for Type 1 Diabetes. *Drug Discov Today Dis Models* 2009;6:41-45.

435. Mordes JP, Bortell R, Blankenhorn EP, Rossini AA, Greiner DL. Rat models of type 1 diabetes: genetics, environment, and autoimmunity. *ILAR J* 2004;45:278-291.

436. Knowler WC, Barrett-Connor E, Fowler SE, Hamman RF, Lachin JM, Walker EA, et al. Reduction in the incidence of type 2 diabetes with lifestyle intervention or metformin. *N Engl J Med* 2002;346:393-403.

437. Kobayashi K, Forte TM, Taniguchi S, Ishida BY, Oka K, Chan L. The db/db mouse, a model for diabetic dyslipidemia: molecular characterization and effects of Western diet feeding. *Metabolism* 2000;49:22-31.

438. Leonard BL, Watson RN, Loomes KM, Phillips AR, Cooper GJ. Insulin resistance in the Zucker diabetic fatty rat: a metabolic characterisation of obese and lean phenotypes. *Acta Diabetol* 2005;42:162-170.

439. Zhang B, Graziano MP, Doebber TW, Leibowitz MD, White-Carrington S, Szalkowski DM, et al. Down-regulation of the expression of the obese gene by an antidiabetic thiazolidinedione in Zucker diabetic fatty rats and db/db mice. *J Biol Chem* 1996;271:9455-9459.

440. Kawano K, Hirashima T, Mori S, Saitoh Y, Kurosumi M, Natori T. Spontaneous long-term hyperglycemic rat with diabetic complications. Otsuka Long-Evans Tokushima Fatty (OLETF) strain. *Diabetes* 1992;41:1422-1428.

441. Goto Y, Kakizaki M, Masaki N. Spontaneous diabetes produced by selective breeding of normal wistar rats. *Proc Jpn Acad Ser B Phys Biol Sci* 1975;51:80-85.

442. Goto Y, Kakizaki M. The spontaneous-diabetes rat-A model of non-insulin dependent diabetes-mellitus. *Proc Jpn Acad Ser B Phys Biol Sci* 1981;57:381-384.

443. Portha B, Serradas P, Bailbe D, Suzuki K, Goto Y, Giroix MH. Beta-cell insensitivity to glucose in the GK rat, a spontaneous nonobese model for type II diabetes. *Diabetes* 1991;40:486-491.

444. Desrois M, Sidell RJ, Gauguier D, King LM, Radda GK, Clarke K. Initial steps of insulin signaling and glucose transport are defective in the type 2 diabetic rat heart. *Cardiovasc Res* 2004;61:288-296.

445. Berthelier C, Kergoat M, Portha B. Lack of deterioration of insulin action with aging in the GK rat: a contrasted adaptation as compared with nondiabetic rats. *Metabolism* 1997;46:890-896.

446. Portha B, Giroix MH, Serradas P, Gangnerau MN, Movassat J, Rajas F, et al. beta-cell function and viability in the spontaneously diabetic GK rat: information from the GK/Par colony. *Diabetes* 2001;50 Suppl 1:S89-S93.

447. Srinivasan K, Ramarao P. Animal models in type 2 diabetes research: an overview. *Indian J Med Res* 2007;125:451-472.

448. Andreollo NA, Santos EF, Araujo MR, Lopes LR. Rat's age versus human's age: what is the relationship? *Arq Bras Cir Dig* 2012;25:49-51.

449. Brownlee M, Vlassara H, Cerami A. Nonenzymatic glycosylation and the pathogenesis of diabetic complications. *Ann Intern Med* 1984;101:527-537.

450. Skrzypiec-Spring M, Grotthus B, Szelag A, Schulz R. Isolated heart perfusion according to Langendorff---still viable in the new millennium. *J Pharmacol Toxicol Methods* 2007;55:113-126.

451. Zimmer HG. The Isolated Perfused Heart and Its Pioneers. *News Physiol Sci* 1998;13:203-210.

452. Bell RM, Mocanu MM, Yellon DM. Retrograde heart perfusion: the Langendorff technique of isolated heart perfusion. *J Mol Cell Cardiol* 2011;50:940-950.

453. Neely JR, Liebermeister H, Morgan HE. Effect of pressure development on membrane transport of glucose in isolated rat heart. *Am J Physiol* 1967;212:815-822.

454. Neely JR, Liebermeister H, Battersby EJ, Morgan HE. Effect of pressure development on oxygen consumption by isolated rat heart. *Am J Physiol* 1967;212:804-814.

455. Neely JR, Rovetto MJ, Whitmer JT, Morgan HE. Effects of ischemia on function and metabolism of the isolated working rat heart. *Am J Physiol* 1973;225:651-658.

456. Depre C. Isolated working heart: description of models relevant to radioisotopic and pharmacological assessments. *Nucl Med Biol* 1998;25:711-713.

457. Garcia PS, Kolesky SE, Jenkins A. General anesthetic actions on GABA(A) receptors. *Curr Neuropharmacol* 2010;8:2-9.

458. JOHNS TN, OLSON BJ. Experimental myocardial infarction. I. A method of coronary occlusion in small animals. *Ann Surg* 1954;140:675-682.

459. Ferrera R, Benhabbouche S, Bopassa JC, Li B, Ovize M. One hour reperfusion is enough to assess function and infarct size with TTC staining in Langendorff rat model. *Cardiovasc Drugs Ther* 2009;23:327-331.

460. Schwarz ER, Somoano Y, Hale SL, Kloner RA. What is the required reperfusion period for assessment of myocardial infarct size using triphenyltetrazolium chloride staining in the rat? *J Thromb Thrombolysis* 2000;10:181-187.

461. Vaughan-Jones RD, Spitzer KW, Swietach P. Intracellular pH regulation in heart. *J Mol Cell Cardiol* 2009;46:318-331.

462. Stenslokken KO, Rutkovskiy A, Kaljusto ML, Hafstad AD, Larsen TS, Vaage J. Inadvertent phosphorylation of survival kinases in isolated perfused hearts: a word of caution. *Basic Res Cardiol* 2009;104:412-423.

463. Sutherland FJ, Shattock MJ, Baker KE, Hearse DJ. Mouse isolated perfused heart: characteristics and cautions. *Clin Exp Pharmacol Physiol* 2003;30:867-878.

464. Awan MM, Taunyane C, Aitchison KA, Yellon DM, Opie LH. Normothermic transfer times up to 3 min will not precondition the isolated rat heart. *J Mol Cell Cardiol* 1999;31:503-511.

465. Minhaz U, Koide S, Shohtsu A, Fujishima M, Nakazawa H. Perfusion delay causes unintentional ischemic preconditioning in isolated heart preparation. *Basic Res Cardiol* 1995;90:418-423.

466. Fukunami M, Hearse DJ. The inotropic consequences of cooling: studies in the isolated rat heart. *Heart Vessels* 1989;5:1-9.

467. Chien GL, Wolff RA, Davis RF, Van Winkle DM. "Normothermic range" temperature affects myocardial infarct size. *Cardiovasc Res* 1994;28:1014-1017.

468. Khaliulin I, Clarke SJ, Lin H, Parker J, Suleiman MS, Halestrap AP. Temperature preconditioning of isolated rat hearts--a potent cardioprotective mechanism involving a reduction in oxidative stress and inhibition of the mitochondrial permeability transition pore. *J Physiol* 2007;581:1147-1161.

469. Yellon DM, Pasini E, Cargnoni A, Marber MS, Latchman DS, Ferrari R. The protective role of heat stress in the ischaemic and reperfused rabbit myocardium. *J Mol Cell Cardiol* 1992;24:895-907.

470. Powell T, Twist VW. A rapid technique for the isolation and purification of adult cardiac muscle cells having respiratory control and a

tolerance to calcium. *Biochem Biophys Res Commun* 1976;72:327-333.

471. Marso SP, Miller T, Rutherford BD, Gibbons RJ, Qureshi M, Kalynych A, et al. Comparison of myocardial reperfusion in patients undergoing percutaneous coronary intervention in ST-segment elevation acute myocardial infarction with versus without diabetes mellitus (from the EMERALD Trial). *Am J Cardiol* 2007;100:206-210.

472. Fazel R, Fang J, Kline-Rogers E, Smith DE, Eagle KA, Mukherjee D. Prognostic value of elevated biomarkers in diabetic and non-diabetic patients admitted for acute coronary syndromes. *Heart* 2005;91:388-390.

473. Alegria JR, Miller TD, Gibbons RJ, Yi QL, Yusuf S. Infarct size, ejection fraction, and mortality in diabetic patients with acute myocardial infarction treated with thrombolytic therapy. *Am Heart J* 2007;154:743-750.

474. Shamaei-Tousi A, Halcox JP, Henderson B. Stressing the obvious? Cell stress and cell stress proteins in cardiovascular disease. *Cardiovasc Res* 2007;74:19-28.

475. Moreyra AE, Conway RS, Wilson AC, Chen WH, Schmidling MJ, Kostis JB. Attenuation of myocardial stunning in isolated rat hearts by a 21-aminosteroid lazaroid (U74389G). *J Cardiovasc Pharmacol* 1996;28:659-664.

476. Manning BD, Cantley LC. AKT/PKB signaling: navigating downstream. *Cell* 2007;129:1261-1274.

477. Chen H, Li D, Saldeen T, Mehta JL. TGF-beta(1) modulates NOS expression and phosphorylation of Akt/PKB in rat myocytes exposed to hypoxia-reoxygenation. *Am J Physiol Heart Circ Physiol* 2001;281:H1035-H1039.

478. Wang X, McCullough KD, Franke TF, Holbrook NJ. Epidermal growth factor receptor-dependent Akt activation by oxidative stress enhances cell survival. *J Biol Chem* 2000;275:14624-14631.

479. Wang B, Shravah J, Luo H, Raedschelders K, Chen DD, Ansley DM. Propofol protects against hydrogen peroxide-induced injury in cardiac H9c2 cells via Akt activation and Bcl-2 up-regulation. *Biochem Biophys Res Commun* 2009;389:105-111.

480. Cho H, Thorvaldsen JL, Chu Q, Feng F, Birnbaum MJ. Akt1/PKBalpha is required for normal growth but dispensable for maintenance of glucose homeostasis in mice. *J Biol Chem* 2001;276:38349-38352.

481. DeBosch B, Treskov I, Lupu TS, Weinheimer C, Kovacs A, Courtois M, et al. Akt1 is required for physiological cardiac growth. *Circulation* 2006;113:2097-2104.

482. DeBosch B, Sambandam N, Weinheimer C, Courtois M, Muslin AJ. Akt2 regulates cardiac metabolism and cardiomyocyte survival. *J Biol Chem* 2006;281:32841-32851.

483. Chen WS, Xu PZ, Gottlob K, Chen ML, Sokol K, Shiyanova T, et al. Growth retardation and increased apoptosis in mice with homozygous disruption of the Akt1 gene. *Genes Dev* 2001;15:2203-2208.

484. Garofalo RS, Orena SJ, Rafidi K, Torchia AJ, Stock JL, Hildebrandt AL, et al. Severe diabetes, age-dependent loss of adipose tissue, and mild growth deficiency in mice lacking Akt2/PKB beta. *J Clin Invest* 2003;112:197-208.

485. Cho H, Mu J, Kim JK, Thorvaldsen JL, Chu Q, Crenshaw EB, III, et al. Insulin resistance and a diabetes mellitus-like syndrome in mice lacking the protein kinase Akt2 (PKB beta). *Science* 2001;292:1728-1731.

486. Gustafsson AB, Gottlieb RA. Bcl-2 family members and apoptosis, taken to heart. *Am J Physiol Cell Physiol* 2007;292:C45-C51.

487. Datta SR, Dudek H, Tao X, Masters S, Fu H, Gotoh Y, et al. Akt phosphorylation of BAD couples survival signals to the cell-intrinsic death machinery. *Cell* 1997;91:231-241.

488. Tremblay ML, Giguere V. Phosphatases at the heart of FoxO metabolic control. *Cell Metab* 2008;7:101-103.

489. Matsui T, Tao J, del MF, Lee KH, Li L, Picard M, et al. Akt activation preserves cardiac function and prevents injury after transient cardiac ischemia in vivo. *Circulation* 2001;104:330-335.

490. Krook A, Kawano Y, Song XM, Efendic S, Roth RA, Wallberg-Henriksson H, et al. Improved glucose tolerance restores insulin-stimulated Akt kinase activity and glucose transport in skeletal muscle from diabetic Goto-Kakizaki rats. *Diabetes* 1997;46:2110-2114.

491. Krook A, Roth RA, Jiang XJ, Zierath JR, Wallberg-Henriksson H. Insulin-stimulated Akt kinase activity is reduced in skeletal muscle from NIDDM subjects. *Diabetes* 1998;47:1281-1286.

492. Shay KP, Hagen TM. Age-associated impairment of Akt phosphorylation in primary rat hepatocytes is remediated by alpha-lipoic acid through PI3 kinase, PTEN, and PP2A. *Biogerontology* 2009;10:443-456.

493. Fang CX, Doser TA, Yang X, Sreejayan N, Ren J. Metallothionein antagonizes aging-induced cardiac contractile dysfunction: role of PTP1B, insulin receptor tyrosine phosphorylation and Akt. *Aging Cell* 2006;5:177-185.

494. Hunter JC, Kostyak JC, Novotny JL, Simpson AM, Korzick DH. Estrogen deficiency decreases ischemic tolerance in the aged rat heart: Roles of PKCdelta, PKCepsilon, Akt, and GSK3beta. *Am J Physiol Regul Integr Comp Physiol* 2007;292:R800-R809.

495. Ansley DM, Wang B. Oxidative stress and myocardial injury in the diabetic heart. *J Pathol* 2013;229:232-241.

496. Fonseca VA. Defining and characterizing the progression of type 2 diabetes. *Diabetes Care* 2009;32 Suppl 2:S151-S156.

497. Hausenloy DJ, Yellon DM. Survival kinases in ischemic preconditioning and postconditioning. *Cardiovasc Res* 2006;70:240-253.

498. Yano T, Miki T, Tanno M, Kuno A, Itoh T, Takada A, et al. Hypertensive hypertrophied myocardium is vulnerable to infarction and refractory to erythropoietin-induced protection. *Hypertension* 2011;57:110-115.

499. Nagoshi T, Matsui T, Aoyama T, Leri A, Anversa P, Li L, et al. PI3K rescues the detrimental effects of chronic Akt activation in the heart during ischemia/reperfusion injury. *J Clin Invest* 2005;115:2128-2138.

500. Shiojima I, Sato K, Izumiya Y, Schiekofer S, Ito M, Liao R, et al. Disruption of coordinated cardiac hypertrophy and angiogenesis contributes to the transition to heart failure. *J Clin Invest* 2005;115:2108-2118.

501. McMullen JR, Shioi T, Huang WY, Zhang L, Tarnavski O, Bisping E, et al. The insulin-like growth factor 1 receptor induces physiological heart growth via the phosphoinositide 3-kinase(p110alpha) pathway. *J Biol Chem* 2004;279:4782-4793.

502. McMullen JR, Shioi T, Zhang L, Tarnavski O, Sherwood MC, Kang PM, et al. Phosphoinositide 3-kinase(p110alpha) plays a critical role for the induction of physiological, but not pathological, cardiac hypertrophy. *Proc Natl Acad Sci U S A* 2003;100:12355-12360.

503. Boura-Halfon S, Zick Y. Phosphorylation of IRS proteins, insulin action, and insulin resistance. *Am J Physiol Endocrinol Metab* 2009;296:E581-E591.

504. Tonks KT, Ng Y, Miller S, Coster AC, Samocha-Bonet D, Iseli TJ, et al. Impaired Akt phosphorylation in insulin-resistant human muscle is accompanied by selective and heterogeneous downstream defects. *Diabetologia* 2013.

505. Cook SA, Matsui T, Li L, Rosenzweig A. Transcriptional effects of chronic Akt activation in the heart. *J Biol Chem* 2002;277:22528-22533.

506. Fernandez-Marcos PJ, Auwerx J. Regulation of PGC-1alpha, a nodal regulator of mitochondrial biogenesis. *Am J Clin Nutr* 2011;93:884S-8890.

507. McLeod CJ, Pagel I, Sack MN. The mitochondrial biogenesis regulatory program in cardiac adaptation to ischemia--a putative target for therapeutic intervention. *Trends Cardiovasc Med* 2005;15:118-123.

508. Duncan JG, Finck BN. The PPARalpha-PGC-1alpha Axis Controls Cardiac Energy Metabolism in Healthy and Diseased Myocardium. *PPAR Res* 2008;2008:253817-.

509. Schiekofer S, Shiojima I, Sato K, Galasso G, Oshima Y, Walsh K. Microarray analysis of Akt1 activation in transgenic mouse hearts reveals transcript expression profiles associated with

compensatory hypertrophy and failure. *Physiol Genomics* 2006;27:156-170.

510. Duncan JG. Peroxisome proliferator activated receptor-alpha (PPARalpha) and PPAR gamma coactivator-1alpha (PGC-1alpha) regulation of cardiac metabolism in diabetes. *Pediatr Cardiol* 2011;32:323-328.

511. Olmos Y, Valle I, Borniquel S, Tierrez A, Soria E, Lamas S, et al. Mutual dependence of Foxo3a and PGC-1alpha in the induction of oxidative stress genes. *J Biol Chem* 2009;284:14476-14484.

512. Halestrap AP, Clarke SJ, Javadov SA. Mitochondrial permeability transition pore opening during myocardial reperfusion--a target for cardioprotection. *Cardiovasc Res* 2004;61:372-385.

513. Dhalla NS, Elmoselhi AB, Hata T, Makino N. Status of myocardial antioxidants in ischemia-reperfusion injury. *Cardiovasc Res* 2000;47:446-456.

514. Qujeq D, Rezvani T. Catalase (antioxidant enzyme) activity in streptozotocin-induced diabetic rats. *International journal of diabetes and metabolism* 2007;15:22-24.

515. Hua Y, Zhang Y, Ceylan-Isik AF, Wold LE, Nunn JM, Ren J. Chronic Akt activation accentuates aging-induced cardiac hypertrophy and myocardial contractile dysfunction: role of autophagy. *Basic Res Cardiol* 2011;106:1173-1191.

516. Kunuthur SP, Mocanu MM, Hemmings BA, Hausenloy DJ, Yellon DM. The Akt1 isoform is an essential mediator of ischaemic preconditioning. *J Cell Mol Med* 2012;16:1739-1749.

517. Yin X, Zheng Y, Zhai X, Zhao X, Cai L. Diabetic inhibition of preconditioning- and postconditioning-mediated myocardial protection against ischemia/reperfusion injury. *Exp Diabetes Res* 2012;2012:198048-.

518. Haffner SM, Lehto S, Ronnemaa T, Pyorala K, Laakso M. Mortality from coronary heart disease in subjects with type 2 diabetes and in nondiabetic subjects with and without prior myocardial infarction. *N Engl J Med* 1998;339:229-234.

519. Wiernsperger NF, Bailey CJ. The antihyperglycaemic effect of metformin: therapeutic and cellular mechanisms. *Drugs* 1999;58 Suppl 1:31-39.

520. Paiva MA, Rutter-Locher Z, Goncalves LM, Providencia LA, Davidson SM, Yellon DM, et al. Enhancing AMPK activation during ischemia protects the diabetic heart against reperfusion injury. *Am J Physiol Heart Circ Physiol* 2011;300:H2123-H2134.

521. Mensah K, Mocanu MM, Yellon DM. Failure to protect the myocardium against ischemia/reperfusion injury after chronic atorvastatin treatment is recaptured by acute atorvastatin treatment: a potential role for phosphatase and tensin homolog deleted on chromosome ten? *J Am Coll Cardiol* 2005;45:1287-1291.

522. Mocanu MM, Yellon DM. PTEN, the Achilles' heel of myocardial ischaemia/reperfusion injury? *Br J Pharmacol* 2007;150:833-838.

523. Teresi RE, Shaiu CW, Chen CS, Chatterjee VK, Waite KA, Eng C. Increased PTEN expression due to transcriptional activation of PPARgamma by Lovastatin and Rosiglitazone. *Int J Cancer* 2006;118:2390-2398.

524. Suwa M, Egashira T, Nakano H, Sasaki H, Kumagai S. Metformin increases the PGC-1alpha protein and oxidative enzyme activities possibly via AMPK phosphorylation in skeletal muscle in vivo. *J Appl Physiol* 2006;101:1685-1692.

525. Liang H, Ward WF. PGC-1alpha: a key regulator of energy metabolism. *Adv Physiol Educ* 2006;30:145-151.

526. Zorzano A, Hernandez-Alvarez MI, Palacin M, Mingrone G. Alterations in the mitochondrial regulatory pathways constituted by the nuclear co-factors PGC-1alpha or PGC-1beta and mitofusin 2 in skeletal muscle in type 2 diabetes. *Biochim Biophys Acta* 2010;1797:1028-1033.

527. Jahangir A, Sagar S, Terzic A. Aging and cardioprotection. *J Appl Physiol* 2007;103:2120-2128.

528. Reznick RM, Zong H, Li J, Morino K, Moore IK, Yu HJ, et al. Aging-associated reductions in AMP-activated protein kinase activity and mitochondrial biogenesis. *Cell Metab* 2007;5:151-156.

529. Anderson R, Prolla T. PGC-1alpha in aging and anti-aging interventions. *Biochim Biophys Acta* 2009;1790:1059-1066.

530. Wenz T. Mitochondria and PGC-1alpha in Aging and Age-Associated Diseases. *J Aging Res* 2011;2011:810619-.

531. Elgebaly MM, Prakash R, Li W, Ogbi S, Johnson MH, Mezzetti EM, et al. Vascular protection in diabetic stroke: role of matrix metalloprotease-dependent vascular remodeling. *J Cereb Blood Flow Metab* 2010;30:1928-1938.

532. Claycomb WC, Lanson NA, Jr., Stallworth BS, Egeland DB, Delcarpio JB, Bahinski A, et al. HL-1 cells: a cardiac muscle cell line that contracts and retains phenotypic characteristics of the adult cardiomyocyte. *Proc Natl Acad Sci U S A* 1998;95:2979-2984.

533. Beauloye C, Bertrand L, Horman S, Hue L. AMPK activation, a preventive therapeutic target in the transition from cardiac injury to heart failure. *Cardiovasc Res* 2011;90:224-233.

534. Hauton D. Does long-term metformin treatment increase cardiac lipoprotein lipase? *Metabolism* 2011;60:32-42.

535. Scarpello JH, Howlett HC. Metformin therapy and clinical uses. *Diab Vasc Dis Res* 2008;5:157-167.

536. Miller RA, Birnbaum MJ. An energetic tale of AMPK-independent effects of metformin. *J Clin Invest* 2010;120:2267-2270.

537. Stanley WC, Lopaschuk GD, McCormack JG. Regulation of energy substrate metabolism in the diabetic heart. *Cardiovasc Res* 1997;34:25-33.

538. Feuvray D, Idell-Wenger JA, Neely JR. Effects of ischemia on rat myocardial function and metabolism in diabetes. *Circ Res* 1979;44:322-329.

539. Belke DD, Swanson EA, Dillmann WH. Decreased sarcoplasmic reticulum activity and contractility in diabetic db/db mouse heart. *Diabetes* 2004;53:3201-3208.

540. Liesa M, Palacin M, Zorzano A. Mitochondrial dynamics in mammalian health and disease. *Physiol Rev* 2009;89:799-845.

541. Soriano FX, Liesa M, Bach D, Chan DC, Palacin M, Zorzano A. Evidence for a mitochondrial regulatory pathway defined by peroxisome proliferator-activated receptor-gamma coactivator-1 alpha, estrogen-related receptor-alpha, and mitofusin 2. *Diabetes* 2006;55:1783-1791.

542. Bach D, Naon D, Pich S, Soriano FX, Vega N, Rieusset J, et al. Expression of Mfn2, the Charcot-Marie-Tooth neuropathy type 2A gene, in human skeletal muscle: effects of type 2 diabetes, obesity, weight loss, and the regulatory role of tumor necrosis factor alpha and interleukin-6. *Diabetes* 2005;54:2685-2693.

543. Canto C, Auwerx J. PGC-1alpha, SIRT1 and AMPK, an energy sensing network that controls energy expenditure. *Curr Opin Lipidol* 2009;20:98-105.

544. Garcia-Roves PM, Osler ME, Holmstrom MH, Zierath JR. Gain-of-function R225Q mutation in AMP-activated protein kinase gamma3 subunit increases mitochondrial biogenesis in glycolytic skeletal muscle. *J Biol Chem* 2008;283:35724-35734.

545. Holloway GP, Gurd BJ, Snook LA, Lally J, Bonen A. Compensatory increases in nuclear PGC1alpha protein are primarily associated with subsarcolemmal mitochondrial adaptations in ZDF rats. *Diabetes* 2010;59:819-828.

546. Aquilano K, Vigilanza P, Baldelli S, Pagliei B, Rotilio G, Ciriolo MR. Peroxisome proliferator-activated receptor gamma co-activator 1alpha (PGC-1alpha) and sirtuin 1 (SIRT1) reside in mitochondria: possible direct function in mitochondrial biogenesis. *J Biol Chem* 2010;285:21590-21599.

547. Nikolaidis LA, Elahi D, Shen YT, Shannon RP. Active metabolite of GLP-1 mediates myocardial glucose uptake and improves left ventricular performance in conscious dogs with dilated cardiomyopathy. *Am J Physiol Heart Circ Physiol* 2005;289:H2401-H2408.

548. Poornima I, Brown SB, Bhashyam S, Parikh P, Bolukoglu H, Shannon RP. Chronic glucagon-like peptide-1 infusion sustains left ventricular systolic function and prolongs survival in the spontaneously

hypertensive, heart failure-prone rat. *Circ Heart Fail* 2008;1:153-160.

549. Hausenloy DJ, Yellon DM. GLP-1 therapy: beyond glucose control. *Circ Heart Fail* 2008;1:147-149.

550. Cefalu WT. Translating "Nondiabetic" A1C levels to clinical practice: the art of medicine. *Diabetes* 2010;59:1868-1869.

551. Cullinan CA, Brady EJ, Saperstein R, Leibowitz MD. Glucose-dependent alterations of intracellular free calcium by glucagon-like peptide-1(7-36amide) in individual ob/ob mouse beta-cells. *Cell Calcium* 1994;15:391-400.

552. Chai W, Dong Z, Wang N, Wang W, Tao L, Cao W, et al. Glucagon-like peptide 1 recruits microvasculature and increases glucose use in muscle via a nitric oxide-dependent mechanism. *Diabetes* 2012;61:888-896.

553. Verspohl EJ. Novel therapeutics for type 2 diabetes: incretin hormone mimetics (glucagon-like peptide-1 receptor agonists) and dipeptidyl peptidase-4 inhibitors. *Pharmacol Ther* 2009;124:113-138.

554. Ku HC, Chen WP, Su MJ. DPP4 deficiency preserves cardiac function via GLP-1 signaling in rats subjected to myocardial ischemia/reperfusion. *Naunyn Schmiedebergs Arch Pharmacol* 2011;384:197-207.

555. Zaruba MM, Theiss HD, Vallaster M, Mehl U, Brunner S, David R, et al. Synergy between CD26/DPP-IV inhibition and G-CSF improves cardiac function after acute myocardial infarction. *Cell Stem Cell* 2009;4:313-323.

556. Dai S, Yuan F, Mu J, Li C, Chen N, Guo S, et al. Chronic AMD3100 antagonism of SDF-1alpha-CXCR4 exacerbates cardiac dysfunction and remodeling after myocardial infarction. *J Mol Cell Cardiol* 2010;49:587-597.

557. Isomaa B, Almgren P, Tuomi T, Forsen B, Lahti K, Nissen M, et al. Cardiovascular morbidity and mortality associated with the metabolic syndrome. *Diabetes Care* 2001;24:683-689.

558. Smith SC, Jr. Multiple risk factors for cardiovascular disease and diabetes mellitus. *Am J Med* 2007;120:S3-S11.